The lubrication of natural and artificial hip joints

Barbara Janet Roberts

The Lubrication of Natural and Artificial Hip Joints

by

Barbara Janet Roberts, B Sc Hons.

Thesis submitted for the degree of Doctor of Philosophy in the Faculty of Science, University of Durham.

Department of Engineering, 1982

ABSTRACT

Cadaveric hip joints and prostheses were tested in a hip function simulator which subjected the femoral head to a cycle of loading and oscillation similar to that experienced during walking, and measured the frictional torque transmitted to the acetabulum.

For natural joints, silicone fluids with viscosities from 10^{-2} Pa s to 30 Pa s were used as lubricants and full fluid film lubrication was observed above 10^{-1} Pa s. Sodium carboxymethylcellulose solutions were also tested at the lower viscosities.

Hyaluronic acid was added to one sample of synovial fluid to increase its viscosity range and other synovial fluid samples were digested enzymatically. Hyaluronidase digestion caused a significant increase in friction factor over the control samples whereas tryptic digestion had no consistent effect.

No correlation between compliance of the cartilage and frictional values was observed.

Experimental prostheses with a compliant lining in the acetabular component were manufactured from a silicone elastomer. The layers varied from 0.5 to 3 mm thick, and two different clearances were tested. The prostheses were tested with SCMC and silicone fluids. The friction factors obtained at low loads were higher than for a Charnley prosthesis.

The swelling effect of the silicone fluids on the elastomeric linings was investigated along with the effective elastic modulus of the arrangements.

ACKNOWLEDGEMENT

I should like to thank my supervisor, Dr A Unsworth, for all his help and encouragement during the past four years. My thanks also go to Prof G R Higginson for his advice and helpful discussions.

The assistance of the technicians in the Department of Engineering, particularly Mr R Mand, was invaluable. Dr N Mian of the Glycoprotein Unit gave advice and help with the biochemical work. Mr T Cross and Mr B B Porter supplied specimens and Mr P Platt and Dr S Jeffrey contributed useful suggestions. To all the above - thank you.

Financial support was received from both the Arthritis Research Council and the Science and Engineering Research Council without whom this work would not have been possible.

Finally, I'd like to thank Gill for the rapid typing service, all my other friends and my parents for their loving support and encouragement. A big hug to you all!

CONTENTS

NOTATION

a	radius of indentation
a_t	radius of indentation for slab of thickness t
a_∞	radius of indentation for slab of infinite thickness
A_{530}	absorbance at a wavelength of 530nm
A_{585}	absorbance at a wavelength of 585nm
$\Delta A/min$	rate of change of absorbance per minute
BAEE	α-N-benzoyl-l-arginine ethyl ester HCl
$CaCl_2$	calcium chloride
d	decrease in cartilage thickness $(h_o - h)$
d_t	depth of indentation on slab of thickness t
d_∞	depth of indentation on slab of infinite thickness
DMAB	4-dimethylaminobenzaldehyde
e	eccentricity
ehl	elastohydrodynamic lubrication
E	elastic modulus (Young's modulus)
E'	effective elastic modulus
E_t	elastic modulus measured on slab of thickness t
E_∞	elastic modulus calculated for slab of infinite thickness
F	normal load
h	cartilage thickness after time t
h_o	initial cartilage thickness
HCl	hydrochloric acid
J_y	component of force acting on a hip joint in a vertical direction
K	hydraulic permeability
L	load

M	molar
N	normal solution (also Newtons)
NAG	N-acetyl glucosamine
NF	National Formulary
P	load per unit width
PEO	polyethylene oxide
r	radius of joint
R	radius of curvature of indentor or reduced radius
Ra	roughness average value
rms	root mean square
SCMC	sodium carboxymethylcellulose
t	time or thickness
T	time period
T_B	bearing torque
T_J	journal torque
u	sliding speed
u_o	maximum sliding speed
UHMWPE	ultra high molecular weight polythene
ZN/P	tribological parameter
ε	logarithmic strain
η	viscosity
η_o	absolute viscosity at atmospheric pressure
$\eta u/L$	tribological parameter (viscosity x sliding speed/load)
θ	amplitude of oscillation
μ	friction factor
ν	Poisson's ratio
σ	stress

CHAPTER ONE

INTRODUCTION

The lubrication of human and other animal joints has interested engineers for nearly a century. Human bearings, although very resilient and long-lasting by engineering standards, do fail in use and can give rise to a great deal of pain and disability. Over 90% of the British population can expect to have signs of joint disease during their lifetime.

This pathology may be caused by physical injury, infection, viral or other unknown causes. A common factor in all serious arthritic conditions is the destruction of the articular cartilage - the bearing surface material in a joint. It is not known whether it is the failure of the lubrication which initiates the wear process, or whether the poor lubrication is a result of the wear and degeneration occurring in the joint. However, synovial fluid, the joint lubricant, is generally affected by the disease. It is therefore of interest to characterise the lubrication mechanisms in a joint since this may help to prevent or at least alleviate some aspects of joint disease.

When the disease is well advanced, the joint will not function at all and the bioengineer has to produce replacement joints from engineering materials. This raises another series of problems in designing a joint

with low friction which will have a life of many years without requiring maintenance. Some of the problems encountered are related to fixation and bone resorption. The friction in a joint is intimately connected with the problem of fixation since the frictional torque transmitted through the joint may contribute to the loosening mechanism.

The work reported here examined two areas of the lubrication problem; one relating to natural joints and the other to prostheses. The hip joint was chosen for this study because it is geometrically simple, being a ball and socket joint, and it is often involved in severe joint degeneration. Hip arthroplasty [replacement of the hip joint by a prosthesis] is a well established clinical procedure. Although the replacement joints are often very successful in the short term, there are still details of design which need to be studied in order to increase the expected lifetime of hip prostheses.

The investigation of lubrication mechanisms in a natural joint must be performed <u>in vitro</u> and this leads to problems in trying to reproduce the physiological conditions in the laboratory. The hip function simulator used in this work attempts to characterise the conditions of loading and motion of a hip joint which may be important to the lubrication mechanism. It subjects the specimen joint to a cycle of loading and oscillation which contains the main features of the walking cycle. No attempt was

made to reproduce the conditions of temperature and humidity found in a joint.

The effect on friction of the constituents of the synovial fluid has been investigated. Previous workers had presented conflicting evidence on the roles of the hyaluronic acid and the protein components of the synovial fluid in lubrication tests. Swann et al [1974] had shown that the protein component of synovial fluid was solely responsible for effective lubrication. An opposing view was presented by O'Kelly et al [1978]. Their tests indicated that the hyaluronic acid played an important role in joint lubrication. Further details of their work are described in Chapter 3. In the present work, synthetic lubricants were tested in human joints on the simulator to examine the effect of varying the viscosity. Synovial fluid was digested with the enzymes hyaluronidase and trypsin and lubrication tests with the resulting fluids were compared with those using undigested control samples.

In a human joint the articulating surfaces are covered by a visco-elastic layer of cartilage. Deformation of these compliant layers may help to maintain a full film of lubricant between them, thus reducing friction. Part of this work was to investigate the use of compliant layers in artificial hip joints. A commercial femoral head was used with acetabula lined with different thicknesses of silicone rubber. It was hoped that this

would lead to a greater understanding of the natural lubrication mechanisms, together with providing ideas for improving prosthesis design. The model used was not intended for medical use, merely a convenient way to examine the relevant material properties.

The objects then of this work were to study the functioning of human joints, particularly in terms of lubrication, and relate this to similar studies of artificial joints with similar mechanical properties.

CHAPTER TWO

JOINT MATERIALS: ARTICULAR CARTILAGE AND SYNOVIAL FLUID

The human hip joint is a ball and socket joint. The ends of the bone are covered with articular cartilage and the whole is enclosed by the synovial membrane, within which the synovial fluid is retained. In considering lubrication of any joint, it is the nature of the two opposing surfaces, the lubricant and the loading which are of importance. This chapter deals with the first two of these by looking first at some of the relevant properties of articular cartilage and then at the behaviour of synovial fluid. Lubrication mechanisms are discussed in the following chapter and the load cycle in Chapter 4.

2.1 Articular cartilage

Cartilage is a common connective tissue in the body. Articular cartilage, as its name suggests, lines the articulating surfaces of synovial joints. Its purpose is to act as a stress distributor and to minimize friction in a joint by providing a 'smooth' surface for lubrication. Much work has been published on articular cartilage and extensive details can be found in review articles and books [Wright et al, 1973, Freeman, 1979]. This section is therefore intended only to give a brief outline of presently accepted theories of the structure of articular cartilage and to examine those mechanical properties relevant to the work reported in this thesis.

2.1.1 Structure of Articular Cartilage

Articular cartilage consists of cells distributed throughout a three-dimensional network of collagen fibrils embedded in a ground substance (Edwards, 1967). The proportions of each of these three substances varies with depth from the articular surface.

The cells, or chondrocytes, represent 1 - 10 % of the volume of the cartilage (Hamerman and Schubert, 1962). They manufacture the ground substance intracellularly. This ground substance is the filler around the matrix of fibres and is rich in mucopolysaccharides, chondroitin sulphate and keratan sulphate. It has a very slow turnover rate compared to other human tissues. The collagen fibrils are crosslinked into a network which, except during growth and repair, is metabolically inert in adult cartilage (Libby et al, 1964). It has been shown that there is considerable variation in the composition of the cartilage between different joints, and between different sites and depths on the same joint (Muir et al, 1970, Kempson, 1979).

The fibres have been investigated with scanning electron microscopy (Minns and Stevens, 1976) and shown to increase in width from about 0.03 μm in the surface layer to 0.1 - 1.0 μm in the deeper layers.

The change in the structure of articular cartilage with depth can best be summarized by a model of four zones, used originally by Collins (1949) and later by McCall (1969):

Zone 1 Superficial - adjacent to the joint cavity. The fibres are tangential to the surface, the cells are discoidal with their long axis parallel to the surface.

Zone 2 Intermediate - where the coiled fibres form an interlacing network. The cells are spheroidal and equally spaced.

Zone 3 Deep - where the fibres form a tighter meshwork and are generally radial to the articular surface. Spheroidal cells are arranged in columnar groups of four to eight cells.

Zone 4 Calcified - adjacent to the subchondral bone. There are few cells and the matrix is heavily impregnated with crystals of calcium salts.

The proportion of each zone varies between joints but typically zones 1 and 4 each occupy 5 - 10 % and zones 2 and 3 each 40 - 45 % of the total thickness (Figure 2.1).

2.1.2 Surface contours of articular cartilage

The smoothness or otherwise of the cartilage surface is very relevant to the discussion of possible mechanisms for joint lubrication. This aspect is discussed further in Chapter 3.

The surface of healthy cartilage has been studied by scanning electron microscopy and replication techniques. Walker et al [1969a] suggested that the surface was gently undulating with a peak to valley height of 2.5 μm and a pitch of 25 μm. Clarke [1971] disputed this claim by obtaining evidence that the ridges occurred near fractured edges of the specimens and were probably artefacts due to the preparation technique. He showed that the surface had bowl shaped depressions of depth 1 - 6 μm and diameter 15 - 30 μm. He wondered whether the depressions were present in living articular cartilage or whether they were caused by the artefactual collapse of overlying tissue into the matrix lacunae during specimen preparation.

Obviously the ideal situation would be to study the surface roughness of cartilage in situ, but as this is not practicable, other methods have been used. The main problems can be summarised as follows [Swanson, 1979]:

1 Measurements under no load tend to give high values for roughness, since surface asperities

are reduced by loading.

2 Measurements on post-mortem material may involve errors due to the death and collapse of cells near the surface.

3 Measurements with an electron microscope have used dehydrated specimens.

4 Measurements on cast replicas may be subject to errors caused by the effect of water on the curing of the resin.

Gardner [1972] classified the surface contours into three groups according to the size of the variation:

Primary: the anatomical shape of the joint surface.

Secondary: a series of undulations of about 0.4 - 0.5 mm wavelength.

Tertiary: a series of undulations of about 20 - 30 μm diameter and 1.2 - 2.6 μm in height.

Sayles and Thomas [1979] rejected the previous studies of cartilage surface on the grounds of errors caused by the preparation techniques, and showed that direct surface measurement with a Talysurf stylus was practicable. They produced computer generated 'contour maps' of

cartilage surfaces and found no periodicity in their measurements. The surface profile of femoral head cartilage was examined directly with a Talysurf (Thomas et al, 1980). Their measured rms roughness was between 3 - 6 μm. From this they calculated a real area of contact in the hip - assuming all the load to be carried by contacting asperities - of 127 mm^2 at heel strike. The pressure at this point was 9.8 MPa and the mean distance between the cartilage surfaces, 60 μm.

2.1.3 Permeability of articular cartilage

Cartilage consists of solid constituents with fluid intimately dispersed within it. It can therefore be considered as a porous network to which the Darcy equation may be applied:

$$Q = K \Delta p$$

where Q = volume flow rate per unit cross sectional area of cartilage.

Δp = pressure drop per unit thickness.

K = hydraulic permeability.

The permeability varies from about 1 - 2.5 x 10^{-16} m^3 s kg^{-1} in the deep zone to 3 - 9 x 10^{-16} m^3 s kg^{-1} near the

articular surface [Maroudas, 1979]. The normal and tangential permeabilities seem to be similar to each other. Using a typical value for permeability, Maroudas showed that the deformation due to fluid flow out of the cartilage must be negligible over the time of loading involved in a walking cycle. This is a very important result, since McCutchen's theory of 'weeping' lubrication [see Chapter 3] depends on such a fluid flow existing.

Earlier work by Maroudas et al [1968] on dye penetration into cartilage under different conditions detected no difference in diffusion rates between in vivo and in vitro tests. Interestingly, a cyclic loading of the cartilage also had little effect on the rate of diffusion of the dye.

2.1.4 Mechanical properties of articular cartilage

Any test used to examine the mechanical properties of cartilage is necessarily in vitro, but even with this limitation it is possible to do some tests which are more likely to represent the physiological situation than others. Tensile tests - details of which may be found in Freeman [1979] - may be relevant to the breakdown of

cartilage, but do not lead to modulus values which can be related to the lubrication tests conducted in this thesis.

Many of the compressive tests on cartilage have used an indentor and shown the change of indentation with time of application of a load, and its subsequent recovery. Typical results are shown in Fig 2.2 (Kempson et al, 1971). These show an instantaneous deformation followed by a slower creep. On removal of the load, the cartilage recovers over a similar period of time as the application of load, and there appears to be no residual deformation.

Johnson et al (1975) found that in unconfined compression the elastic modulus of the cartilage varied with creep strain. They applied a static preload to the sample and then superimposed a sinusoidally varying load at a frequency of 1 Hz. The elastic modulus was defined as the sinusoidal stress amplitude divided by the sinusoidal strain amplitude. This modulus increased from 12 MPa to 45 MPa at 0.6 creep strain.

Cartilage in a joint is not unconfined. It exists in a thin layer covering the bone ends and any part of it

is restricted by the surrounding cartilage and by the fixed junction with the bone. In most measurements of cartilage deformation the underlying bone can be considered rigid. Higginson and Snaith [1979] studied the deformation of plugs of cartilage constrained by a metal cylinder under an oscillating load using a similar arrangement to Johnson [above]. They found much higher values of modulus [0.1 GPa] than generally reported. Oscilloscope traces of stress-strain loops showed that the stress and strain were almost in phase and therefore the cartilage was behaving like a linear elastic solid under conditions which were approximately physiological.

Video recordings of wet cartilage undergoing compression in a scanning electron microscope were used by Gore [1981] to examine the compliance of the cartilage in the different zones. She found that for normal patellar cartilage, the compliance is highest in the superficial zone, decreases to a minimum in the mid-zone and increases again slightly in the deep zone.

With her tests using plugs of patellar cartilage, Gore found a definite increase in compliance with age of

sample and also after storage at - 20°C. On the other hand, Armstrong et al (1980) found no alteration in Young's modulus with age using an indentation test on femoral heads. However, in an intact joint, the magnitude of the cartilage deformation for a given load, markedly increased with age. This was thought to be due to an increase in the fluid expressed in the first 30 s of loading. This corresponds to a reduction in Poisson's ratio, if the cartilage is modelled as an elastic material.

2.1.5 Contact areas in the hip joint

The contact area in the hip, estimated using a dyeing technique, varied from 3.83 in^2 (24.7 cm^2) to 4.38 in^2 (28.3 cm^2) (Greenwald and O'Connor, 1971). Using a casting technique, Dowson et al (1967) demonstrated a contact area of 4.5 cm^2. If the maximum force at the hip is 5 x body weight, a typical value for the maximum stress is 8 MPa. These contact areas may be higher than those obtained in vivo since the joint must be held under a compressive load for a longer time than would be normal during walking, in order to take a casting

or inject a dye. The real contact area in the hip, assuming asperity contact, was calculated by Thomas et al (1980) to be 1.27 cm^2, considerably smaller than the measured values since they estimated the proportion of the apparent contact area where asperities would actually be touching.

2.1.6 Theoretical models of cartilage

A number of workers have used theoretical models of cartilage to predict behaviour when physiological loads are applied. Deductions have been made concerning stresses and strains produced, and fluid flow between the surfaces.

Askew and Mow (1978) examined the effect of the fibrous ultrastructure of the cartilage on the stresses and strains produced under physiological loads. They suggested that degeneration of the cartilage with age is more likely to be a strain fatigue mechanism than the direct effect of tensile stress. Afoke et al (1982) used a finite element model of a hip joint to calculate stresses in the articular cartilage. They found that, in their model, cartilage was well able to distribute the applied

load.

Kenyon [1980] modelled the surface flow of fluid between two cartilage surfaces to determine the conditions under which surface flow was more favourable than flow within the cartilage. He tentatively deduced that if the viscosity of the synovial fluid was greater than 500 cP [0.5 Pa s], flow between the surfaces would be prevented. His model however did not consider the deformation of surface asperities under load.

To summarise, articular cartilage acts as a stress distributor and as a bearing surface in human joints. It has been described as a viscoelastic solid, but appears within the confines of physiological constraints to approximate to a linear elastic solid.

2.2 Synovial fluid

Synovial fluid is a pale yellow, viscous liquid found in human and animal joints. It is only found in very small quantities in human joints, typically 0.2 ml in the knee, although this may be increased many times in the diseased state. In animal joints, larger amounts may be found eg from 5 to 65 ml in the bovine ankle

joint. There is considerable variation in volume and composition of fluid between animals of the same species and between different joints in one animal [Davies, 1966 - 67]. Davies [1966 - 67] also summarises the purposes of synovial fluid. It is generally believed to be the lubricant in a joint, but is also important for the nutrition of the avascular articular cartilage and the removal of products of metabolism. The hyaluronic acid, which is believed to be secreted by the synovial membrane, is probably concerned with the maintenance of a constant pH, control of the fluid volume and its protein content, as well as its major function to the bioengineer, that of increasing the viscosity of the synovial fluid.

2.2.1 Composition of synovial fluid

Synovial fluid is a dialysate of blood plasma with the addition of hyaluronic acid. It contains many of the proteins in plasma such as albumin and globulin [Ropes et al, 1940], but has a much higher proportion of those with the lower molecular weights. The albumin/globulin ratio is higher by a factor of about 2.5 than in plasma [Davies 1966 - 67]. The total protein content of synovial fluid is around 2.0 mg/100 ml compared with

7.0 mg/100 ml for blood plasma.

The other major constituent of synovial fluid is hyaluronic acid, first isolated by Meyer et al [1939]. Meyer [1947] showed that the hyaluronate was depolymerized by the action of the enzyme hyaluronidase and he later concluded that hyaluronic acid was a long chain polymer consisting of regular repeating disaccharide units containing N-acetylglucosamine and glucuronic acid [Meyer, 1958]. The repeating molecular units are shown in Figure 2.3. Its molecular weight in synovial fluid is around 10^6 and its concentration, though very variable, averages about 3.5 mg/g.

In Rheumatoid Arthritis the hyaluronic acid is found to have the same structure but a shorter chain length than in normal fluid [Barber et al, 1964].

2.2.2 Viscosity of synovial fluid

One of the most important effects of hyaluronic acid in synovial fluid is as a viscosity-raiser. Synovial fluid exhibits non-Newtonian properties ie its viscosity decreases with increasing shear rate, but this was not recognised by many early workers. Barnett [1958] pointed

out the necessity of quoting shear rate with measurements of viscosity. He explains that the 'widespread impression that (joint) fluid ... varies from day to day in its physical properties' is due to the lack of knowledge of the non-Newtonian type of behaviour. It is necessary to use a viscometer which applies a uniform shear rate to the whole sample of fluid at any one time. The shear rate also needs to be variable over several orders of magnitude. Cone and plate viscometers fulfill these requirements and Cooke et al (1978a) used a Weissenberg rheogoniometer to study both healthy and pathological synovial fluid. Their composite graph (reproduced as Figure 2.4) shows a marked decrease in viscosity as the shear rate increases for normal fluid. For osteoarthrotic fluid the viscosities are lower and less shear dependent, while for rheumatoid fluid the shear dependence is even less. Cooke pointed out that the viscosities for normal and pathological fluids at high shear rates are quite similar and at 10^4 s^{-1} the ratio of the viscosities to that of water will only be around 4:1.

Figure 2.5, taken from Negami's work (1964), shows that the viscosity is indeed dependent on the hyaluronic acid

content of the fluid, However he found that the addition of hyaluronic acid to pooled fluid or buffer solution, did not increase the viscosity as much as expected. He attributed this to the idea that the hyaluronate forms a complex with protein in the synovial fluid, which it was unable to do in pooled fluid or buffer.

Negami used a method of measuring dynamic viscosity which also enabled him to measure the dynamic elasticity of the synovial fluid. He used a double cylindrical cup filled with fluid in which a ring was suspended concentrically. A torsional oscillation was applied to the cup and the response of the ring was measured. He found that the dynamic elasticity of synovial fluid increased with shear rate as dramatically as the dynamic viscosity decreased. Hence synovial fluid may act as an elastic material in a fast moving joint. The viscosity of synovial fluid under pressure has been investigated (Cooke et al, 1978b). Using pathological human and healthy bovine fluids, the viscosity was measured at pressures up to 104 MPa. No change in viscosity was observed. This contrasts with results obtained from

both mineral and silicone oils which display an increasing viscosity as the pressure rises.

The pH value of the fluid also affects its viscosity. Negami [1964] found that the viscosity decreased by 40% as the pH was reduced from 7.4 to 4.0 and Ropes et al [1947] also found a variation but showed that the viscosity was most stable between pH 7.0 and pH 8.0. They found a 10% reduction in relative viscosity with an increase in temperature from 25°C to 38°C. This was a reversible effect. A variation in viscosity with age was found by Jebens and Monk-Jones [1959]. The apparent viscosity in a capillary viscometer varied from 14 Poise for a boy aged 15 to 0.6 Poise for an 80-year-old woman. Fluid from joints which had experienced trauma had a viscosity of less than 1 Poise.

Since pathological fluid was found to have a lower viscosity than normal fluid, several workers have been interested in the degradation of synovial fluid. Ogston and Stanier [1953] studied the effect of hyaluronidase on ox synovial fluid and as expected found that the viscosity was decreased, since the enzyme breaks bonds in the chains

of hyaluronic acid. Later, Ogston and Sherman [1959] found that trypsin affected the protein in the fluid but not the viscosity, whereas papain produced a more generalised degradation. This confirmed earlier work by Ropes et al [1947] where they showed that complete digestion of the protein by trypsin resulted in a change of relative viscosity only from 33.1 to 31.3.

Anti-tryptic activity was observed by Holmes et al [1935] in some, but not all, of the synovial fluid samples he tested. The inhibition is non-competitive so increasing the amount of trypsin will overcome the inhibition.

In the following years much work was done on biochemical analysis of the fluid. The hyaluronate was isolated by methods such as density gradient sedimentation [Silpananta et al, 1968], ultrafiltration [Sandson et al, 1962] and ultracentrifugation [Scher and Hamerman, 1972]. The latter workers found that the hyaluronate could not be completely separated from the protein in the fluid, confirming earlier work by Ogston and Stanier [1950 and 1952].

Swann and Radin [1972] examined the lubricating ability of the fluid constituents in an arthrotripsometer and concluded that the lubricant was a macromolecule consisting of two glycopeptides and one peptide. Having decided that this macromolecule was responsible for lubrication and not the hyaluronate, Swann et al [1977] went on to isolate and characterize the major glycoprotein which they named 'Lubricating Glycopeptide - I'[LGP - I]. Details of their lubrication tests are given in the appropriate place in the next chapter.

In summary then, synovial fluid is a viscous liquid found in joints. Its main purposes are to provide nutrition for, and lubricate the joint. This work is concerned with the lubrication of joints and the viscosity of the fluid is therefore important. Synovial fluid is a non-Newtonian fluid, in the sense that its viscosity decreases with increasing shear-rate. The viscosity of the fluid is unchanged by pressure but is affected by pH, age and enzymatic digestion.

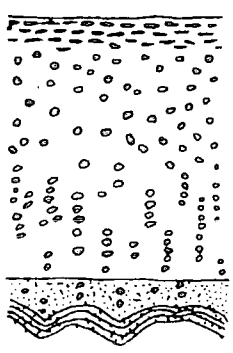

Figure 2.1

The zone model for articular cartilage.

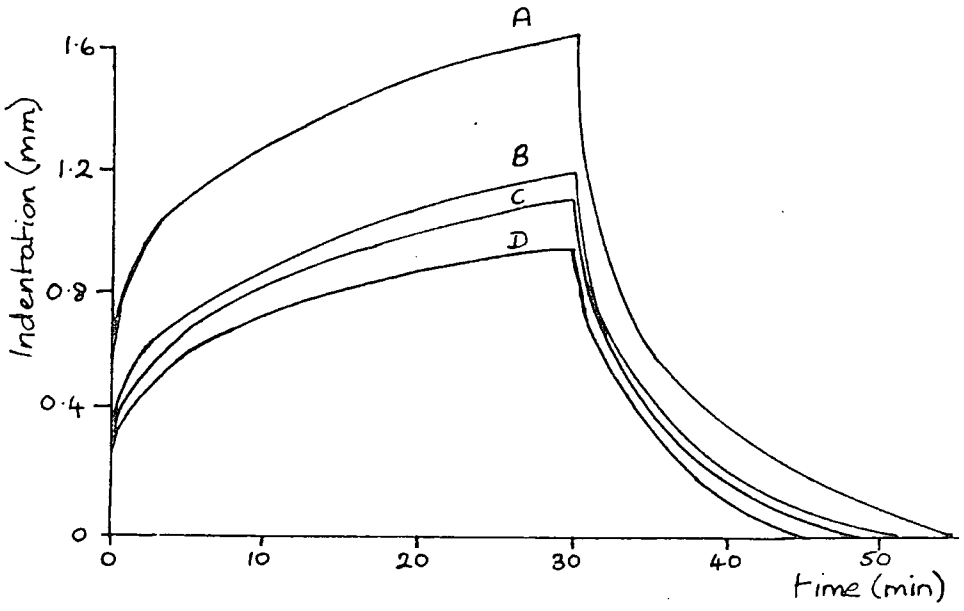

Figure 2.2

Typical results for indentation test on articular cartilage from a human femoral head. [Kempson et al, 1971]

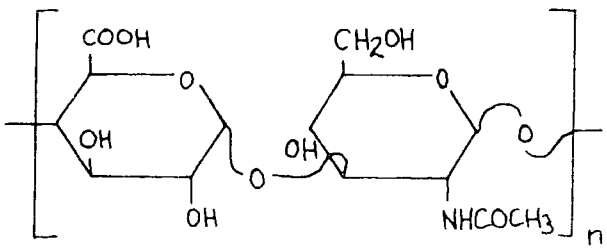

Figure 2.3

The repeating molecular unit of hyaluronic acid.
[Homsy et al, 1973]

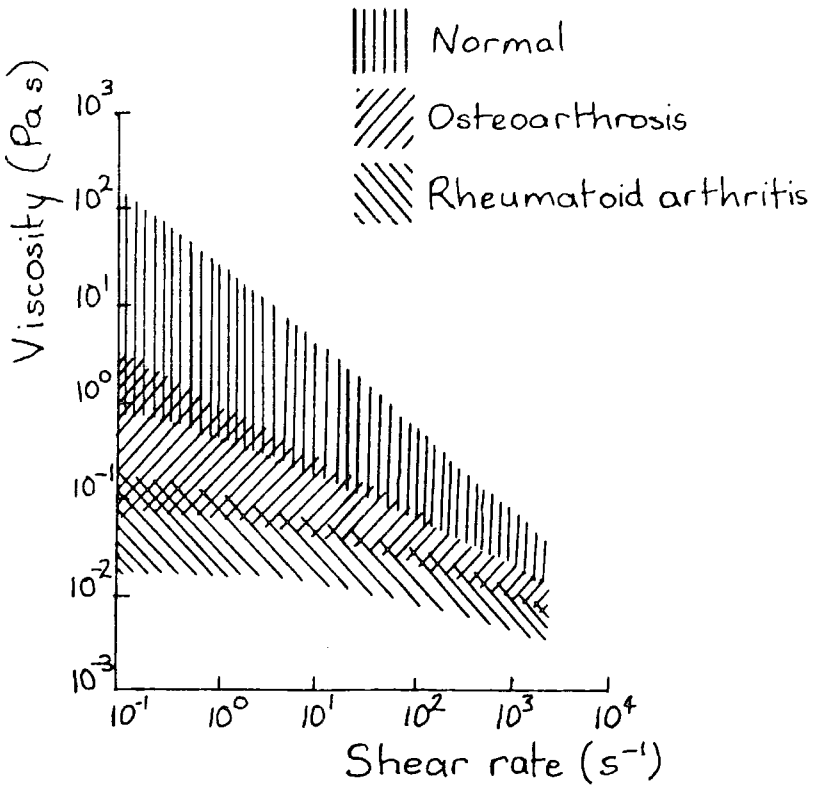

Figure 2.4

The variation of the viscosity of synovial fluid with shear rate, showing normal and arthrotic fluids. [Cooke et al, 1978a]

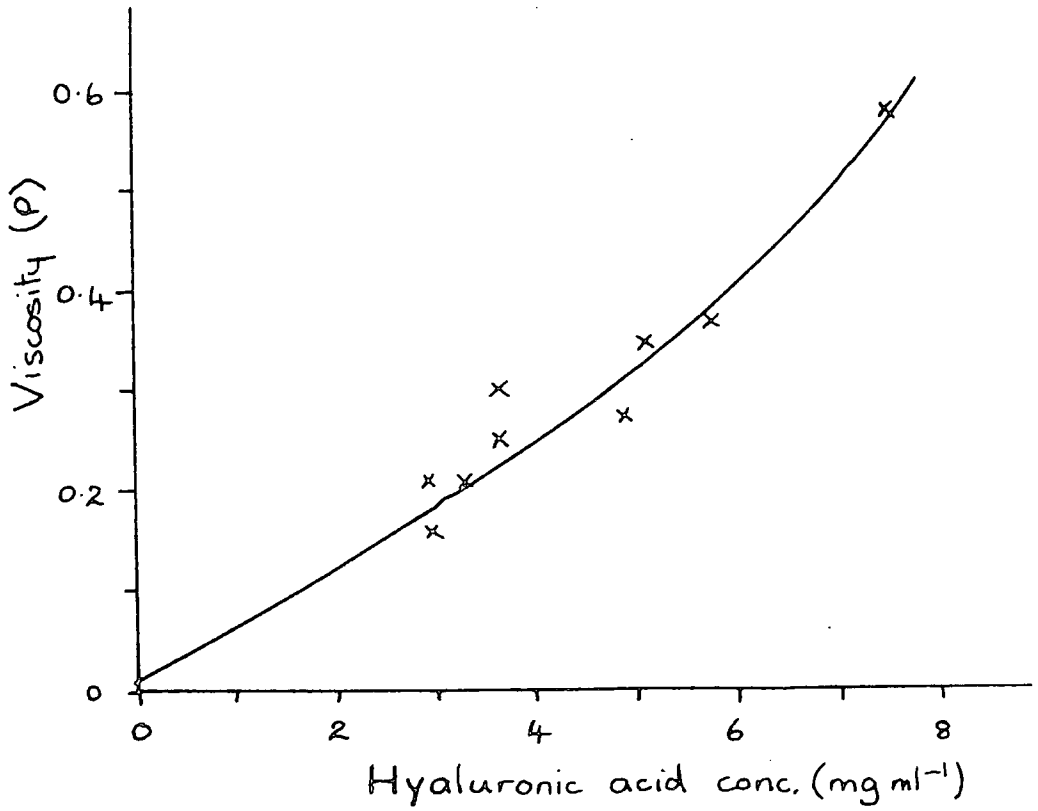

Figure 2.5

Graph showing the increase in viscosity of synovial fluid with the addition of hyaluronic acid. [Negami, 1964] (Shear rate approx. 2000s^{-1}).

CHAPTER THREE

LITERATURE REVIEW OF JOINT LUBRICATION

There is a wealth of literature on the mechanisms involved in the lubrication of joints. The matter has aroused considerable controversy and many different approaches have been made to the problem of characterising animal joint lubrication in the laboratory.

The modes of lubrication normally accepted in Tribology are illustrated in Figure 3.1. Hersey, in 1914, was the first to apply dimensional analysis to the lubrication of a journal bearing (Dowson, 1979). The coefficient of friction, μ, is plotted against the non-dimensional parameter $\eta u/p$ (viscosity x rotational speed/load per unit width). The characteristic shape of the curve can be indicative of the different lubrication modes present in the system.

In the first region, boundary lubrication occurs and there is contact between the asperities on the two bearing surfaces. The friction is not dependent on the bulk properties of the lubricant, such as viscosity, but depends on the bearing surfaces which may be covered with a layer produced by a chemical reaction, eg an oxide, or an adsorbed layer of lubricant. In the third region of the graph, the surfaces are completely separated by a film of fluid and so the viscosity of the fluid becomes

important in a hydrodynamic mechanism. Here the coefficient of friction increases with viscosity and sliding speed, but decreases with load. Between these two extremes there is a transition region, known as mixed lubrication, where boundary and hydrodynamic mechanisms are both operating. The minimum coefficient of friction occurs at the transition between mixed and full fluid film lubrication as can be seen on the graph.

In a bearing like a human joint, two further mechanisms promote the presence of a fluid film. As the bearing surfaces are compliant, they will deform under load and the possibility of obtaining a full fluid film is increased at higher loads - this is known as an elastohydrodynamic mechanism. Also, in a dynamic loading situation, a squeeze film mechanism can operate as the fluid resists being pushed out from between the surfaces on application of the load.

The literature review which follows attempts to outline the differing theories produced by various workers. Most of the authors were investigating the lubrication mechanism in natural joints though not always using biological materials to do so. On the other hand some of the later published work includes the lubrication of hip prostheses.

The earliest reference to the possible application of hydrodynamic lubrication theory to synovial joints was made by Osborne Reynolds [1886] in a well known paper

written nearly a century ago in which he proposed a theory of fluid film lubrication. Many years later MacConnail [1932] applied this theory, pointing out that the incongruence of the joint components would result in the wedge shaped gaps required by the lubrication theory.

Jones [1934] was probably the first to measure the static coefficient of friction in a joint. He used a horse's stifle joint to examine the coefficient of friction under various conditions of loading and lubrication. He found the dry coefficient of friction to be about fourteen times the lubricated value. Two years later, Jones [1936] was using a human interphalangeal finger joint as the fulcrum of a pendulum to measure friction - a method which has been used by many workers since. He deduced that a fluid film could survive a load capable of crushing bone.

Ropes et al [1947] examined the lubricating ability of synovial fluid and mucin in an artificial joint made of lucite [perspex] and found no advantage over serum. However, they were looking at a constantly loaded joint which was likely to be operating with boundary lubrication. Good boundary lubricants are adsorbed onto the bearing surfaces so the interaction of the fluid and surface needs to be carefully considered. The ineffectiveness of synovial fluid as a boundary lubricant in an artificial joint therefore tells us little about its boundary lubricating ability in a natural joint.

Charnley [1959, 1960a, 1960b] criticised the conclusions of both MacConnail and Jones. He believed that the lubrication mechanism was primarily boundary and that a hydrodynamic mechanism could not work due to the heavy loads, slow movement, and the elasticity of the cartilage which would make the surfaces conform. He tried to repeat Jones' experiments on static friction but found no difference in coefficient of friction when the synovial fluid was removed. In his pendulum experiments with ankle joints, Charnley found a linear decay of amplitude with time which he assumed must be consistent with a boundary lubrication mechanism. This led him to the conclusion that artificial joints must be designed to be boundary lubricated and he began to consider the use of polytetrafluorethylene [ptfe] in prostheses since it has a coefficient of friction against steel of around 0.04.

A 'new and interesting class of bearings' was proposed by McCutchen [1959]. He experimented with closed and open cell sponge rubbers and suggested a lubrication mechanism where fluid 'weeped' from the bearing surface under pressure, so maintaining a fluid film. Lewis and McCutchen [1959] applied the theory to animal joints and showed that fluid was exuded from articular cartilage under pressure. The low permeability of cartilage leads to doubts as to whether the transport through the cartilage can occur quickly enough for 'weeping' to be effective. Also, since the cartilage surfaces are rough the contact

areas initially will be small and pools of fluid will become trapped between opposing surfaces, without the necessity for 'weeping'.

Dintenfass [1967] in his review of the current status of joint lubrication suggested that previous workers had oversimplified the situation, in opting for either hydrodynamic or boundary lubrication. He favoured an elastohydrodynamic mechanism complicated by the time and load varying properties of the cartilage, the complexity of the synovial fluid itself and the geometry and kinematics of the joints. Tanner [1966] continued the idea of elastohydrodynamic lubrication [ehl] and calculated a film thickness for the hip joint of 10^{-7} m or more. This is rather small for fluid film lubrication since the surface roughness of the cartilage is around 10^{-6} m.

Further weight for the elastohydrodynamic theory was provided by Dowson [1966 -67] in a paper in which he comprehensively summarised the history of joint lubrication and then considered the present position. He suggested that ehl was likely to occur, helped by squeeze film effects and elastohydrostatic action where the elastic lining was also porous, but that boundary lubrication was important under certain highly loaded and slow moving conditions. He modelled a human joint in tribological terms and calculated film thicknesses at the knee and hip. For the hip the elastohydrodynamic film thickness

was about 4 - 6 x 10^{-6} m and he showed that the squeeze film time would be much greater than any oscillatory joint movement. When there is persistent loading without rolling or sliding, the flim thickness would reduce until it reached the size of the hyaluronic acid molecule, which would then act as a boundary lubricant.

Fein [1966 - 7] examined the question of a squeeze film with a model to predict film thicknesses and an experiment with a lens and an optical flat to count interference fringes as a function of time after loading. He obtained close agreement and went on to discuss the application of the theory to natural joints, concluding that they were probably squeeze film lubricated with hydrodynamic action replenishing the film. This idea was revived ten years later by Higginson's [1977] calculations of probable film thicknesses obtainable by a squeeze film mechanism.

McCutchen [1966 - 7] returned to his weeping lubrication theory with experiments using a pig's humerus rubbing against glass. The friction rose with time and was lower for synovial fluid than water. Raising the cartilage from the glass for one second then continuing the test lowered the friction briefly, a ten second interval improved the reduction. McCutchen explained this with his weeping theory in that lubricant is gradually squeezed out of the

cartilage matrix when loaded and the cartilage swells again on removal of the load. It should be noted that he used around eight minutes continuous loading which is not a situation often found under dynamic conditions in human joints. When he rubbed a thin rubber sheet on glass with synovial fluid as the lubricant, the friction again rose with time, and could be reduced by soaking the rubber in the synovial fluid. This he interpreted as a boundary mechanism where the synovial fluid takes time to be adsorbed onto the rubber surface. Again, the conditions used predispose to boundary lubrication and are not typical of the actions of human joints.

To examine the constituents of synovial fluid McCutchen used millipore filters and also digestion with hyaluronidase. From this work he concluded that the hyaluronic acid and viscosity of synovial fluid were unimportant in lubrication but there was probably some constituent in the mucin which was a good boundary lubricant. He suggested that the rheology of the synovial fluid was important for the lubrication of the soft tissue around a joint rather than the cartilage bearing surfaces.

The thickness of a film of synovial fluid which might be formed as a boundary lubricant was examined by Maroudas [1966 - 7]. At a water - air interface a film 150Å [1.5×10^{-8} m] was observed, on quartz 700Å [7×10^{-8} m]. She calculated the size of the gap between two cartilage

surfaces at which flow through the cartilage, rather than in the gap, became important as 5,000 Å [5 x 10^{-7} m]. Below this value it is likely that a concentrated film of hyaluronic acid would form on the surfaces, since the water will permeate through the cartilage. This gel may be important to the action of synovial fluid as a boundary lubricant, but it should be noted that for a stable gel to form, the water flowed through the cartilage for a period in excess of twenty hours which is an extremely long time in terms of constant joint loading.

Wilkins [1968] also examined the boundary lubricating ability of synovial fluid with a latex rubber on glass friction measuring device. He used conditions specifically designed to give good boundary lubrication, with a constant load of 330 g cm^{-2} [32 KNm^{-2}] and sliding speeds from 0 to 10^{-3} ms^{-1}. Whole synovial fluid gave friction coefficients of about 0.01 in his test system. Mild digestion of the fluid with hyaluronidase did not alter this value but exhaustive digestion increased it more than ten times. Even larger increases in friction coefficient (>0.2) were observed after proteolysis with trypsin or papain, Wilkins deduced that for boundary lubrication the protein component, destroyed by trypsin, was essential. The hyaluronic acid also seemed necessary, but its chain length could be considerably shortened before boundary lubrication was affected.

Linn produced a series of papers in which he studied joint lubrication using dogs' ankles in an arthrotripsometer. The first paper (Linn, 1967) describes the construction and use of the arthrotripsometer to measure the coefficient of friction in the joint and also the deformation of the cartilage. It was designed so that the talus rotated through 36.2^{o}, but problems arose since the centre of rotation of an ankle joint is not fixed. This meant that the line of action of the force did not always pass through the centre of rotation, so he found superposition of the torque due to the load, and the torque due to the friction. Taking an average reading from the two halves of the cycle overcame this problem. Most tests were run with a constant load varying from 9 to 64 Kg and at speeds from 10 to 200 cpm (0.17 to 3.3 Hz). He found that the coefficient of friction reduced with increased speed of oscillation, with increased load, and with bovine synovial fluid instead of saline solution as lubricant. The reduction in friction with the change in lubricant was from .0124 to .0057. He postulated shearing and ploughing components of sliding friction.

Linn's second paper (1968) discusses the lubrication mechanism in terms of the tribological parameter ZN/P and concludes that it is a mixed mode with hydrostatic (weeping), elastohydrodynamic and boundary lubrication all contributing.

Linn and Radin (1968) showed that hyaluronidase digestion of synovial fluid mucin, which reduced its viscosity to that of buffer, did not affect the friction coefficient, whereas tryptic digestion of the mucin did not alter the viscosity but increased the coefficient of friction typically from .0028 to .0054. They pointed out that the pH ahd molarity of buffer affects the frictional values. Formalin fixation of the cartilage also increased the coefficient of friction by a factor of four, presumably by making the cartilage much stiffer. Their experiments led them to the conclusion that a protein component of synovial fluid is important in lubrication and the viscosity has no effect. However, it should be noted that their experiments were carried out with the ankles constantly loaded under continuous oscillation. As previously observed, this condition is not often found in the normal range of joint actions where, if joint surfaces are in relative motion, the loading is normally dynamic, varying from nearly zero to several times body weight (see Chapter 4).

Linn's paper in the following year (1969) summarised his previous results, reiterating his conclusions that the mechanism of joint lubrication was in his belief a combination of boundary, elastohydrodynamic and self induced hydrostatic lubrication (the 'weeping' theory of McCutchen).

Radin, Paul and Pollock (1970) used a modified arthrotripsometer and bovine metatarso-phalangeal joints under increasing loads with buffer and synovial fluid. They used heavier loads than Linn (from 100 Kg to 500 Kg) and found that for synovial fluid, the coefficient of friction increased with load and at the highest loads had no advantage over buffer. This led them to conclude that a weeping type of mechanism was active, but again they were not studying friction under physiological conditions since their frictional values were recorded after two hours continuous oscillation at constant heavy loads.

In answer to the criticism that the digestion of synovial fluid may have unpredictable effects on it, Radin, Swann and Weisser (1970) used a density gradient sedimentation technique to obtain three lubricants containing respectively no hyaluronate, all the hyaluronate, and most of the protein. Using the same rig as Radin, Paul and Pollock with a load of 250 lb, they found that the fluid containing the protein was the only one which showed any advantage over buffer - concluding that it is this protein which is solely responsible for joint lubrication. Since their test conditions of constant loading predispose to boundary lubrication, it may be true that only the protein component is important in their system. This cannot be generalised to cover joint lubrication under all conditions.

A decrease in coefficient of friction with increasing speed of oscillation was noticed by Radin, Paul and Weisser (1971), also in the arthrotripsometer. This they postulated was due to the force necessary to overcome the elastic nature of the cartilage but could also have been due to a mixed lubrication regime, where an increase in sliding speed would reduce the coefficient of friction (see Figure 3.1). They also tried artificial lubricants, such as 200 cS silicone fluid, and found them to be less efficient than synovial fluid, concluding that viscosity is not important. This may be true in their system of constant loading, which is likely to require boundary lubrication. As explained in the discussion of Rope's work, the interaction of surface and lubricant is important here and may not be achieved if one component is synthetic. If however, they were operating in the mixed lubrication regime, near the minimum of the curve in Fig 3.1, increasing viscosity may have taken the system into the fluid film region. An increased viscosity here increases the coefficient of friction.

Radin et al (1971) studied the lubrication of bovine synovial membrane on a motor-driven glass slider and found here that hyaluronate was a better lubricant than buffer and that removal of hyaluronic acid from synovial fluid with hyaluronidase, removed the lubricating advantage of synovial fluid over buffer.

In their 'consolidated concept' of joint lubrication, Radin and Paul [1972] suggest that the cartilage - cartilage lubrication is boundary at low loads and squeeze - film at high loads, but this squeeze film is not dependent on the presence of hyaluronate. The hyaluronate is only important for the boundary lubrication of the synovial membrane. This squeeze film in the absence of hyaluronate does not appear to be backed up by any experimental data, and all their previous experiments involved constant loading, where the squeeze film effect is unlikely to occur.

Swann et al [1974] brought together tests on both cartilage and synovial membrane in the same series of experiments. They obtained hyaluronic acid from various sources including rooster combs and showed that the viscosity of the fluid was important in the membrane lubrication tests and that there was no reduction in lubricating ability until the hyaluronic acid content fell below 0.5 mg/ml. Human rheumatoid fluid was also tested and found to give similar results to those with bovine synovial fluid. Their tests on cartilage, carried out in the same manner as Radin, Paul and Pollock but with a load of 250 Kg, confirmed previous results - that the protein content is all important. This led them to suggest that the articular lubricating moiety is derived from the cartilage and not produced by the synovial membrane.

There are no values given for coefficient of friction, μ, in this paper: all the results are quoted as a 'lubricating ability' defined as a percentage

$$\frac{\mu[\text{buffer}] - \mu[\text{sample}]}{\mu[\text{buffer}] - \mu[\text{synovial fluid}]} \times 100\%$$

Hence if the sample lubricant is the same as the synovial fluid, the lubricating ability will be 100%, regardless of the difference between the buffer and the synovial fluid. However, if μ[sample] is different from μ[synovial fluid], the lubricating ability will be dependent on the difference between μ[synovial fluid] and μ[buffer].

Acrylic castings of the surface of cartilage taken by Dowson et al [1967] showed that it was rougher than expected. A series of papers was published following Dowson, which proposed a theory of 'boosted' lubrication [Walker et al 1968, 1969b]. Since the cartilage surface was found to contain undulations up to 200 μinch [5 x 10^{-6} m] deep, they suggested that fluid was trapped in pools between the cartilage surfaces and the viscosity of this fluid was increased as the load increased, due to water squeezing out through the pores of the cartilage. In the lightly loaded phase of a cyclic motion a full fluid film can be restored between the surfaces.

Their studies showed the contact area in the hip to be a maximum of 9.5 cm^2 with a maximum pressure of 32 Kg cm^{-2} [3.1 MPa] [Longfield et al, 1969].

Examining the film of synovial fluid deposited on the cartilage surface after sliding on glass, Walker et al [1970a] found that at light loads, the deposit showed an oriented pattern, probably representing the direction of flow. At higher loads the pattern collapsed into a continuous skin over the surface.

Dowson et al [1970] studied the concept of boosted lubrication theoretically. They assumed that the viscosity of the synovial fluid increased with decreasing film thickness, and for rigid geometries they calculated the squeeze film time to be about one minute - a long time compared with the walking cycle. They suggested that side leakage of fluid, rather than passage through the cartilage was more likely to occur.

Walker et al [1970b] examined in detail the aggregates of hyaluronic acid/protein complex formed on cartilage surfaces when sliding against glass. After freezing specimens they were viewed in a scanning electron microscope. The formation of the aggregate increased the squeeze film time and in extreme conditions, collapsed to form a protective skin acting as a boundary lubricant.

Dowson and Wright [1972] discussed the presence of both fluid film and boundary lubrication mechanisms in a joint under different conditions of loading and movement and pointed out that the full range of conditions must be carefully considered in any studies of joint lubrication.

They said that the fluid film may be prolonged by either 'boosted' or 'weeping' mechanisms, or both, but McCutchen [1972], the proponent of 'weeping' lubrication, argued that boosted and weeping theories are not compatible. Boosted theory postulates flow of fluid into the cartilage, whereas weeping theory assumes flow in the reverse direction. However, Ling [1974] used a theoretical model of the contact of two elastic porous cylindrical discs on elastic non-porous bases to show that the two theories were not exclusive. As the discs approached each other, the central portion underwent 'boosted' type of lubrication, the edges weeping whereas later in the time interval, the whole surface 'weeped'.

All the work on lubrication so far described has assumed that the synovial fluid is the joint lubricant, though the importance of the different constituents is in dispute. Little et al [1969] claimed that if the fat layer was removed from the surface of the cartilage, the coefficient of friction rose considerably and therefore this layer of lipid was acting as a boundary lubricant.

Also in 1969, Mow reviewed the present state of lubrication theories, concluding that the mechanism was elastorheodynamic - a term which includes both the elasticity of the cartilage and the non-Newtonian behaviour of synovial fluid. He posed a series of theoretical problems which needed answering to describe the mechanism in detail.

Clarke et al (1975) used a pendulum to test the friction in hip joints and found that μ = 0.0095 to 0.03 with synovial fluid present and μ = 0.028 to 0.147 when run 'dry'. After eight hours 'dry' running the cartilage began to fissure and flake in those areas normally associated with osteoarthritic damage. They were wary of specifying a lubrication mode since previous results had shown that this was difficult to predict from pendulum results.

Unsworth et al (1975a) considered the problem of both boundary and fluid film lubrication producing a linear decay in amplitude in a pendulum machine as described by Charnley (1959) and Barnett and Cobbold (1962). Barnett and Cobbold had provided a detailed criticism of Charnley's papers, confirming his experimental results showing a linear decay in amplitude but drawing opposite conclusions. They showed that a hydrostatic bearing (where a fluid film must exist) used as the fulcrum of a pendulum caused an apparently linear decay in amplitude - a situation Charnley had believed to typify boundary lubrication. Unsworth et al (1975a) concluded that the exponent of the fluid film decay was so small that the decay would appear to be linear. To overcome this problem they designed a carriage for the acetabulum which rested in hydrostatic bearings and measured the frictional torque directly. This form of carriage was also used in the hip function simulator employed in the

present work and will therefore be described in Chapter 4 of this thesis. A further modification to the pendulum was the addition of a jacking mechanism so that the load could be applied suddenly at the beginning of the test. They tested a number of natural hip joints and found that the coefficient of friction was greater at low loads than high ones, and it increased with number of swings until there was a rapid decay just before the pendulum stopped. They suggested that this decay might not be due to a sliding friction force, but that once the pendulum had come to rest, they were recording the resistance of the cartilage to shearing forces.

Artificial joints were also tested with this pendulum (Unsworth et al, 1975b) to investigate the lubricating ability of synovial fluid in prostheses. They found that under dynamic loading conditions, the coefficient of friction was reduced in the presence of synovial fluid, suggesting the operation of a squeeze film mechanism. Further investigation of the lubrication of artificial joints was reported in 1978 (Unsworth). The most significant findings were that prostheses had lower friction when lubricated than when dry and the friction depended on the viscosity of the lubricant, reducing as the viscosity increased as would be expected in mixed lubrication regimes.

O'Kelly et al [1977] described a hip joint simulator which applied dynamic loads to a joint oscillating in flexion and extension. The simulator used in the work reported in this thesis was based on this design and so a full description will be given later. They used silicone oils with a wide range of viscosities in a Charnley joint and produced a graph of μ against $\eta u/L$ which showed the classical features of mixed, and fluid film lubrication. The following year O'Kelly et al [1978] reported further work using the simulator and pendulum with human hip joints and bovine synovial fluid. They concluded that under static loading conditions with synovial fluid of viscosity 10^{-3} Pa s, the lubrication was mixed but under dynamic loading the squeeze film action gave a full fluid film. They did some work with digested synovial fluid and found that the friction increased after hyaluronidase digestion but not after tryptic digestion. However, there is little detail of the biochemical work and no control samples of the same fluid which had not been enzymatically digested were used in lubrication tests. No assays were made to ensure that digestion had taken place with either hyaluronidase or trypsin. Further work in this area was published by Roberts et al [1982], the details of which are reported in this thesis. The results of O'Kelly's work were directly opposed to that of Linn, Radin and Swann described previously.

O'Kelly *et al* [1979] also studied the lubrication of several different prostheses with silicone fluids. Above a viscosity of 0.1 Pa s full fluid film lubrication was obtained. They suggested that since the synovial fluid produced around a prosthesis after hip surgery had a viscosity less than this, consideration should be given to sealing a lubricant in with a prosthetic joint.

In America at the same time, Davis *et al* [1978] were looking specifically at the boundary lubricating ability of synovial fluid in a latex - glass system. Their conditions of constant loading and rigid surfaces were not expected to produce a fluid film so it is not surprising that they found that the friction was independent of the viscosity of the synovial fluid. They proposed a complicated theory [Davis *et al*, 1979] of the structuring of boundary water to explain the boundary lubricating ability of synovial fluid, but admit that their results are for a latex - glass system and may not relate directly to joints. The tests they tried with cartilage surfaces in their test system did not give reproducible results.

Elastohydrodynamic lubrication was suggested by Higginson [1977] with a squeeze film mechanism rather than rolling or sliding. He showed that 10^{-8} to 10^{-7} m was a reasonable estimate of the film thickness which could be obtained by rolling/sliding in the knee, whereas the Ra value of

cartilage is no better than 10^{-6} m. However when he considered squeeze film thickness after 0.5 s in the knee he arrived at a figure of 10^{-6} m (or 5×10^{-6} m for the hip). This is much more promising for the maintenance of a fluid film and depends on the elasticity of the cartilage rather than its permeability, which is probably too low to be important in the time scale of the walking cycle. He used experiments with rough and smooth rubber layers to illustrate his theories. Previous work with thin compliant layers (Bennet ahd Higginson, 1970) had demonstrated that they were beneficial to lubrication and friction in a pure sliding arrangement (rigid cylinder rotating against a plane with a compliant surface layer). In experiments examining the normal approach of a rigid sphere onto a plane with a compliant surface layer (Gaman et al, 1974) a pool of lubricant was trapped in the central region and greatly increased the squeeze film time.

Higginson and Norman (1974) looked at the lubrication of porous elastic solids, both experimentally and theoretically by again considering the normal approach of a rigid spherical surface onto a thin compliant layer on a rigid backing. The compliant layer was also either porous or perforated. Extending their theory to animal joints they proposed that the permeability of cartilage is too low to play a role in the lubrication mechanism (as required by the weeping theory for instance). The entrapment of

a squeeze film by the flexible cartilage may be important as may the filtration through surface aggregates suggested in the 'boosted' theory.

This idea that the elasticity of the cartilage was important in reducing friction led Thompson [1979] to study the effect of a compliant layer in a hip prosthesis. He found a considerable reduction in friction over a conventional Charnley joint when he used a metal acetabulum lined with silicone rubber of various thicknesses. In order to obtain a wide range of viscosities he used silicone fluid for the lubricant.

Other workers have looked at the effect of compliant layers from a theoretical viewpoint. Rybicki et al [1979] used a finite element model of a squeeze film bearing with low modulus elastic surfaces and a viscous lubricant to examine the effect of cartilage stiffness and lubricant viscosity on friction under impulse loading. They found that in their model, compliant bearings were superior to rigid ones, but that in general, changing the viscosity of the lubricant from 7 to 80 cP [7×10^{-3} to 8×10^{-2} Pa s] had a greater effect than changing the modulus of the cartilage from 4.4 MNm^{-2} to 17.6 MNm^{-2}. They did not include non-Newtonian or viscoelastic behaviour in their model. A theoretical analysis by Tandon and Rakesh [1981] of the squeeze film times for two rough cartilage surfaces approaching each other with fluid in between, showed that the time increases with

cartilage roughness and increasing concentration of hyaluronic acid molecules in the synovial fluid.

Recent work by Gore et al [1981] on another modified pendulum machine has provided further evidence of fluid film lubrication by a squeeze film mechanism in hip prostheses. They attempted to incorporate some of the advantages of testing with a simulator into the simpler pendulum motion. The load could be applied to the joint for one direction of swing and removed for the other half-cycle. This was a more physiological cycle than constant loading. They also used the method of direct friction measurement employed by Unsworth et al [1975a]. They compared friction factors with constant and on/off loading. The on/off loading gave significantly lower values of friction factor. They deduced that viscous fluid lubrication operates over at least part of the physiological range of loads and motion and the squeeze film mechanism is important.

A comprehensive review article by Chandra [1980] suggests that although the literature is extensive, the final conclusion has not yet been reached; the evidence so far pointing to various mechanisms acting under different operating conditons. The work in this thesis was planned to provide more evidence, in particular with dynamic loading, where the data has so far been limited.

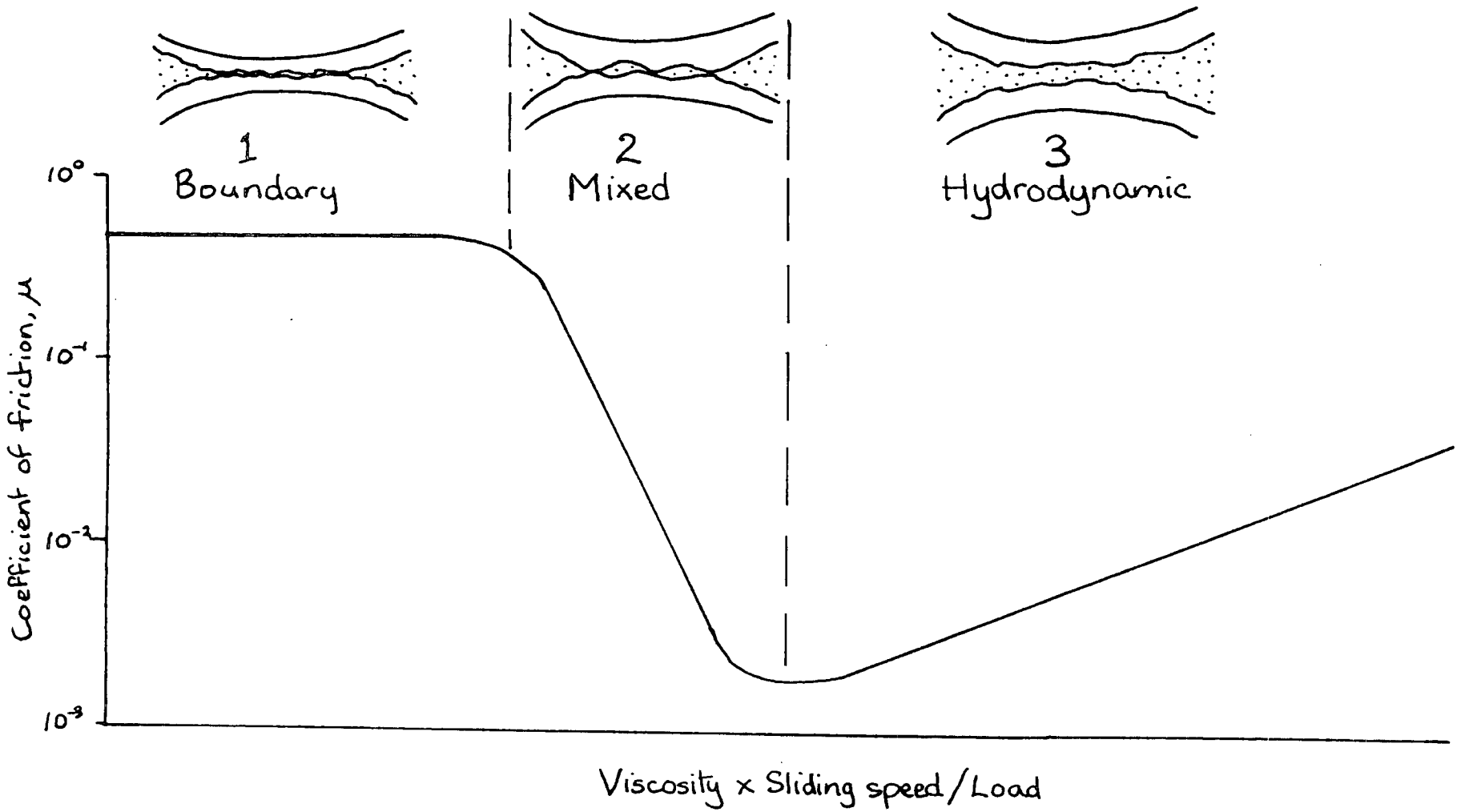

Figure 3.1

The different lubrication regimes.

CHAPTER FOUR

THE HIP FUNCTION SIMULATOR: DESCRIPTION AND USE

A hip joint function simulator similar to that described by O'Kelly et al (1977) was used for the lubrication tests (Figure 4.1). The machine was designed to give a more physiological cycle than the simple pendulum machines so frequently used, whilst not attempting completely to simulate joint conditions. The loading and motion cycles were based on the conditions experienced by the hip during walking which have been determined by various workers.

4.1 The walking cycle

Subjects were photographed with cine film as they walked over a force platform for Paul's (1966 - 7) analysis of the forces transmitted by joints. By considering the muscle groups acting and the masses and accelerations of the limb segments, he was able to deduce the forces acting on the hip joint during the walking cycle. Figure 4.2 shows the three components and the resultant force at the hip. It can be seen that the force in the vertical direction, Jy, is much larger than in the two horizontal directions and therefore the resultant closely follows Jy over much of the cycle. There are two peaks per cycle, corresponding to heel-strike and toe-off, where the force reaches three and four times body weight respectively.

English and Kilvington [1979] used a femoral prosthesis with strain gauges incorporated in its neck to record the force acting in the joint. A locally implanted transmitter emitted signals which were picked up externally and recorded against time. Figure 4.3 shows a trace taken twelve days after a hip replacement operation on a 59-year-old woman. Her body weight was 80 Kg and the vertical axis therefore shows multiples of body weight, reduced by a factor to allow for the support given by the other limb. There was a swing phase with a load of about 1.2 x body weight and a longer stance phase [61% of the cycle] with loads of 2.4 x body weight. Unlike Paul, English and Kilvington only recorded one load peak per cycle. However, their patient appears to have been walking at about half normal speed which may account for the difference. As they had no footswitches or photographic means of correlating the position in the cycle with load it is difficult to compare results.

The very rapid loading and unloading of the joint is a feature of the results obtained by both workers and is reproduced by the simulator. Figure 4.4 shows a typical load trace. In one cycle there are two similar load peaks. This similarity between the peaks enables average friction readings to be taken which, as explained later, reduces errors due to off-centre mounting. This therefore differs from Paul's work in that the load

reduces to the same value between the two peaks rather than remaining higher between heel-strike and toe-off.

The angular displacements of the hip have also been studied. Lamoreux [1971] used a complex exoskeleton with hip, knee and ankle attachments to record data on tape for computer analysis. Figure 4.5 shows typical plots for the angle of flexion-extension and axial rotation. The flexion angle has a maximum of about 30°, the extension 20°, whereas in rotation the total range of movement is only 10°. These figures were confirmed by Gore et al [1979] when they used an electrogoniometer to measure hip joint movements. The movement of the hip of a woman walking is shown in Figure 4.6. It can be seen that the total amplitude in flexion and extension was about 30°, whereas the movements about the other two axes were considerably less.

The simulator moves only in the flexion-extension direction, and from the above discussion, this appears to be a reasonable simplification of the walking cycle. The displacement is sinusoidal through the cycle. The load is always applied vertically with two maxima per cycle corresponding to heel-strike and toe-off.

4.2 Description of the simulator

The two components of a hip joint, whether natural or artificial, were mounted in separate holders [described later] which fitted into the simulator. The acetabular

holder was supported in a friction measuring carriage. The femoral holder was mounted in a frame through which hydraulic loads were applied to the joint. The femoral head rested in the acetabular cup as near to the anatomical position as possible.

4.2.1 Load application

A diagram showing the application of the hydraulic loads is shown in Figure 4.7. The cam was driven by a belt drive from a Kopp Variator variable speed gearbox and motor. The cam moved the piston in cylinder A, which transmitted the consequent increase in pressure to cylinder C, and hence through a loading frame to the joint. The Nitrogen/Air accumulator was set at a pressure of 70 psi (4.8×10^5 Nm^{-2}). This pressure governed the relationship between the maximum and minimum forces produced. The pressure in the air/oil accumulator was adjusted to balance the weight of the loading frame. Cylinder B was used to pressurise the system and replace oil loss.

A strain-gauged load cell was situated between cylinder C and the loading frame from which the load was recorded as a continuous trace. The instrumentation and calibration are described in section 4.3.

4.2.2 Oscillation

The shaft driven by the variable speed motor had the cam mounted at one end and at the other side of the loading

frame was a scotch yoke mechanism which converted the rotary motion to a vertical reciprocating motion. This drove a rack and pinion and thus oscillated the femoral head carriage sinusoidally with an amplitude determined by the adjustment of the eccentricity of the scotch yoke and a speed fixed by the motor/gearbox.

The oscillation and load application were always synchronised since they were activated by the same drive shaft.

4.2.3 Friction measuring carriage

The friction measuring carriage consisted of an aluminium tray supported on two stub shafts which were carried in externally pressurised bearings. Each bearing had two pockets at an angle of 45^{o} to the vertical, through which oil was pumped. These bearings were designed for maximum stiffness and had a very low coefficient of friction (around 10^{-4}) (Unsworth, 1978). The acetabular holder fitted in a circular hole in the base of the tray. Figure 4.8 shows an artificial joint in position. Because of the difficulty of accurately centring joints in their holders, three possible adjustments were introduced. The hydrostatic bearings could translate in the anterior-posterior direction on two hardened steel rods. This allowed the axis of rotation of the acetabulum to be lined up with that of the head even though this might vary through the cycle for a non-spherical hip joint. The total movement in this direction was 6 mm. Along

the axis of rotation a clearance was introduced between the bearing case and the carriage. This was 0.6 mm on each side and allowed the acetabulum to move until it mated exactly with the head. The third adjustment was the height of the femoral head in its mount. Washers could be used on the top of the load frame, on which the femoral head holder rested, to increase the distance between the holder and the rotational axis of the joint.

In order to facilitate the setting up, the left hand stubshaft and bearing were drilled along their axes to accommodate a steel mandril. This could be slotted through to line up the axes of the friction carriage and the femoral frame.

A mount was provided on one side of the tray for the piezo-electric transducer (Figure 4.9). The carriage was balanced with lead shot while floating freely in its bearings. The transducer was attached to a brass plate on the axis of the bearings by means of a screw which passed through an oversized hole in the plate and into the end of the transducer. There was a PTFE washer on each side of the plate. This arrangement allowed the transducer to move vertically with respect to the bearings, when the load was applied or removed, without causing bending of the transducer. The movement allowed horizontally corresponded with the axial float in the bearings

and enabled the unstrained position of the transducer to be found at the beginning of a test.

4.3 Instrumentation and measurement

The load, displacement and frictional torque were all recorded continuously throughout the cycle onto the same chart. A block diagram of the components is shown in Figure 4.10 and described under the separate headings.

4.3.1 Measurement of load

The load measurement took place at the lower piston where there was a strain-gauged load cell. This consisted of two active foil strain gauges and two passive ones connected to form a half bridge. This was in turn connected to a Wheatstone bridge (BPA transducer meter) which incorporated an analogue galvanometer to display the load. The output from the BPA meter was passed through a small amplifier (Figure 4.11) and into one channel of the chart recorder (Manarp oscillograph 150). The additional small amplifier was necessary to match the impedances of the BPA meter and the galvanometer in the recorder. The chart recorder uses a light trace on sensitised paper and has a maximum writing speed of 250 ms^{-1}. This means that its response is much faster than the changes in load and friction that it is recording.

4.3.2 Measurement of friction

Since the friction measuring carriage was supported in hydrostatic bearings it could be assumed that all the torque transmitted through the joint was measured by

the piezo-electric force transducer (KISTLER type 9203, maximum force ± 500N) which was the only constraint on the free swinging of the carriage. The output from the transducer was fed through a Kistler charge amplifier to a second channel on the chart-recorder.

4.3.3 Measurement of displacement

After conducting a number of tests, it was considered useful to have a record of the different sliding speeds through the cycle on the same chart as the load and friction measurements. Since the sliding speed was related to the displacement of the top carriage, it was decided that a measurement of displacement would be sufficient since this gives the positions of zero velocity which allows the velocity everywhere to be calculated since the variation is known to be sinusoidal (Scotch yoke characteristic).

An extension was screwed onto the end of the shaft oscillated by the pinion and a potentiometer was mounted on a bracket fixed to the rack and pinion housing. The two were connected via a flexible coupling, to allow for misalignment. The output from this was adjusted (figure 4.12) to give a third trace on the chart-recorder showing the variation of position with time. The slope of this curve gives the sliding speed.

4.3.4 Measurement of frequency of oscillation

This could be varied using the Kopp variator. The frequency for a given motor speed was calculated by counting a number of load cycles recorded on the chart and knowing the chart speed, measuring the distance taken. The cycle lengths were marked on a series of templates, one for each speed and these were used throughout the tests, showing that for a given speed setting on the variator the frequency of oscillation and chart speed were very reproducible.

4.3.5 Measurement of amplitude of oscillation

An inclinometer was used to measure the amplitude of oscillation. The femoral head carriage was rotated to the maximum inclination in one direction allowed by the scotch yoke setting and a reading taken. The position of maximum inclination during the other half cycle was also noted and the difference between the two gave twice the amplitude of oscillation.

4.4 Calibration of simulator

4.4.1 Load

In order to calibrate the load trace, a standard strain gauge transducer (BPA) was fitted in place of a hip joint. It rested on a metal plate in the friction measuring carriage and a plate bolted onto the femoral head carriage was adjusted so that contact was made when the axes of the two were coincident as determined using the mandril. The amplitude of the oscillation was reduced to zero by adjusting the scotch yoke mechanism to zero eccentricity

and the load cycle was recorded both by the load cell, and the transducer. Further points were obtained by statically loading the transducer and load cell by increasing the oil pressure in the system and recording both load readings. Two typical calibration graphs are shown in Figure 4.13. Little variation was found over the months of the tests.

4.4.2 Friction

The force transducer was calibrated *in situ* directly in terms of frictional torque. With the transducer removed a long metal bar was carefully balanced on the friction measuring carriage and then bolted into place. The transducer was replaced and a series of masses hung in turn from each end of the bar. Knowing the length of the bar, the applied torque could be calculated for the transducer both in tension and compression. A typical graph is shown in Figure 4.14. Readings were also taken on the chart for different amplification scales to check their linearity and indicated amplification ranges.

4.5 Mounting and centring joints

4.5.1 Setting-up jig

A special jig was constructed for centring the joints in their holders before fitting them into the simulator. It is pictured in Figure 4.15 and was made in two parts. The main part consisted of an annular base in which four

vertical pillars were mounted. These had stops for a given height and a rectangular plate which fitted over these pillars and rested on the stops. The plate had a rectangular hole machined out of it, into which the holder for the femoral component was a push fit. Two vertical parallels were mounted on the base, centrally between the pillars on each long side. The annular base fitted onto one of two base plates. One had a central adjustable boss with a plastic cup fitted onto it and can be seen in use with the McKee-Farrar head in Figure 4.16. The other had a frame into which the acetabular holder was bolted in a central position.

4.5.2 Method of centring a natural joint

The femoral holder was placed in the setting up jig and the femoral head was positioned inside it, resting in the plastic cup and with the greater trochanter facing a short side of the holder. The height of the cup was adjusted until the maximum diameter of the femoral head was at a distance from the top of the holder such that it would coincide with the axis of rotation when in the simulator. Four fixing screws were screwed through holes in the femoral holder until they held the joint in position. An internal micrometer was used to measure the distance between the maximum diameter of the femoral head and each of the vertical parallels. The position of the head was adjusted until these distances were equal. The bottom of the holder was sealed with tape

and plaster of paris used to fill the holder and secure the femoral head in its correct position. The base of the jig was then changed and the acetabular holder placed in position. This was partly filled with plaster, the acetabulum was mated with the femoral head and pressed into position in the wet plaster.

The cartilage surfaces of the joint were kept covered with tissues soaked in Ringer's solution throughout this procedure.

4.5.3 Method of centring an artificial joint

For the complete commercial prosthesis used the same procedure as for a natural joint was adopted, but it was easier since the components were symmetrical and the acetabulum did not have a specific orientation with respect to the femoral head.

For the conical shaped bases with compliant linings a special jig which centred the base without reference to the femoral component was constructed. The cylinder for the acetabulum was placed over the jig (Figure 4.17) and the cone placed on top. Plaster was then poured in to secure the base, the jig removed, and the remaining hole filled with plaster.

4.6 Method of aligning the mounted joint in the simulator

The joint, fixed in its holders, was fitted into the simulator and the oil supply to the hydrostatic bearings

was turned on. The frictional torque transducer was loosened and the steel mandril was used to align the two sets of bearings. The heights of the components were then adjusted if necessary to give concentricity.

The load frame was jacked up using the compressed air supply until the femoral head was just free of the acetabulum (ie the friction measuring carriage no longer followed the movement of the head when the femur was oscillated). This was taken to be the zero load position and the zero was adjusted on the BPA meter accordingly.

The air pressure was reduced to give the required base load, the friction transducer was tightened and the three zero traces on the chart recorder noted. The simulator was then ready to run lubrication tests.

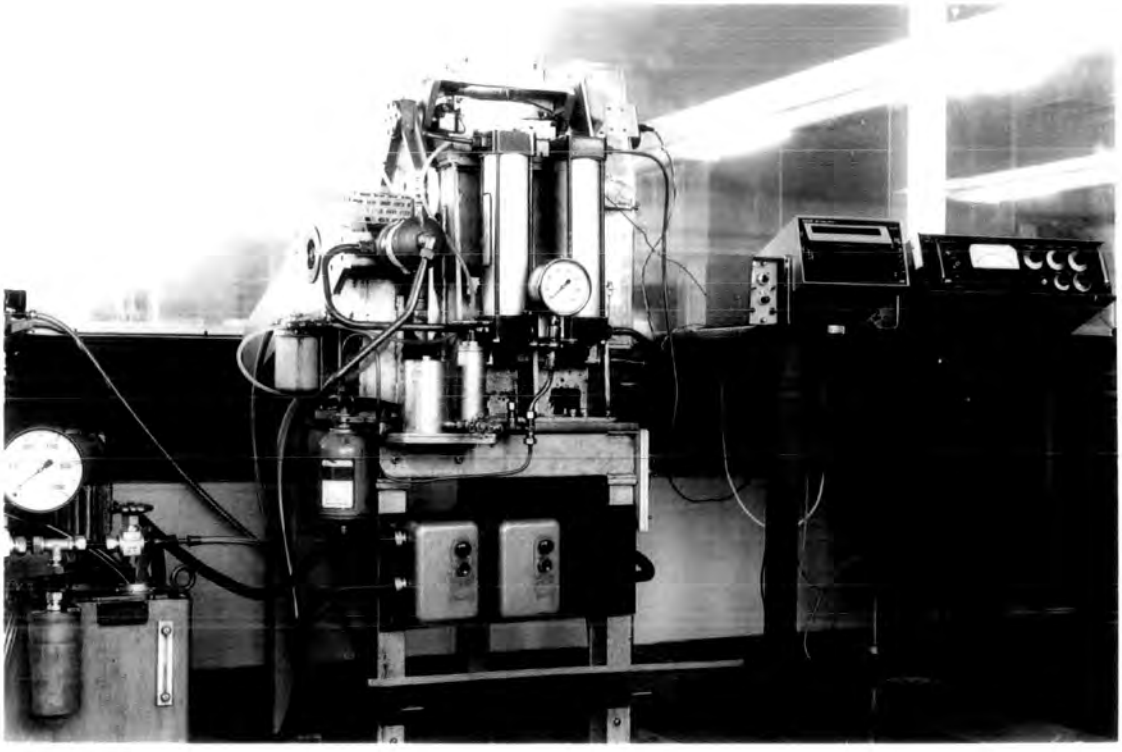

Figure 4.1

The hip function simulator and associated instrumentation

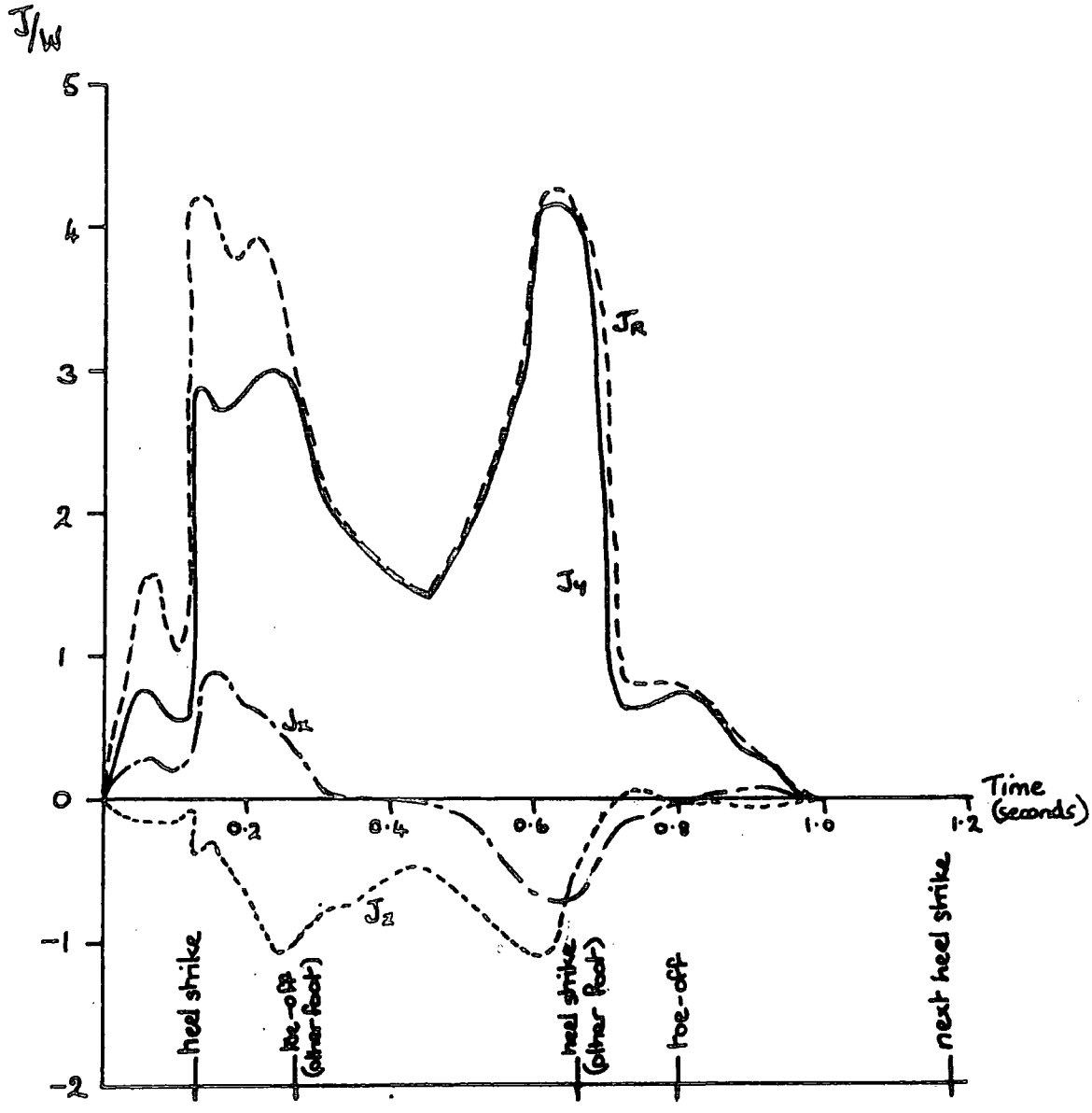

Figure 4.2

Components of force, and resultant force, acting on a hip joint during walking.
[Paul 1966 - 67]

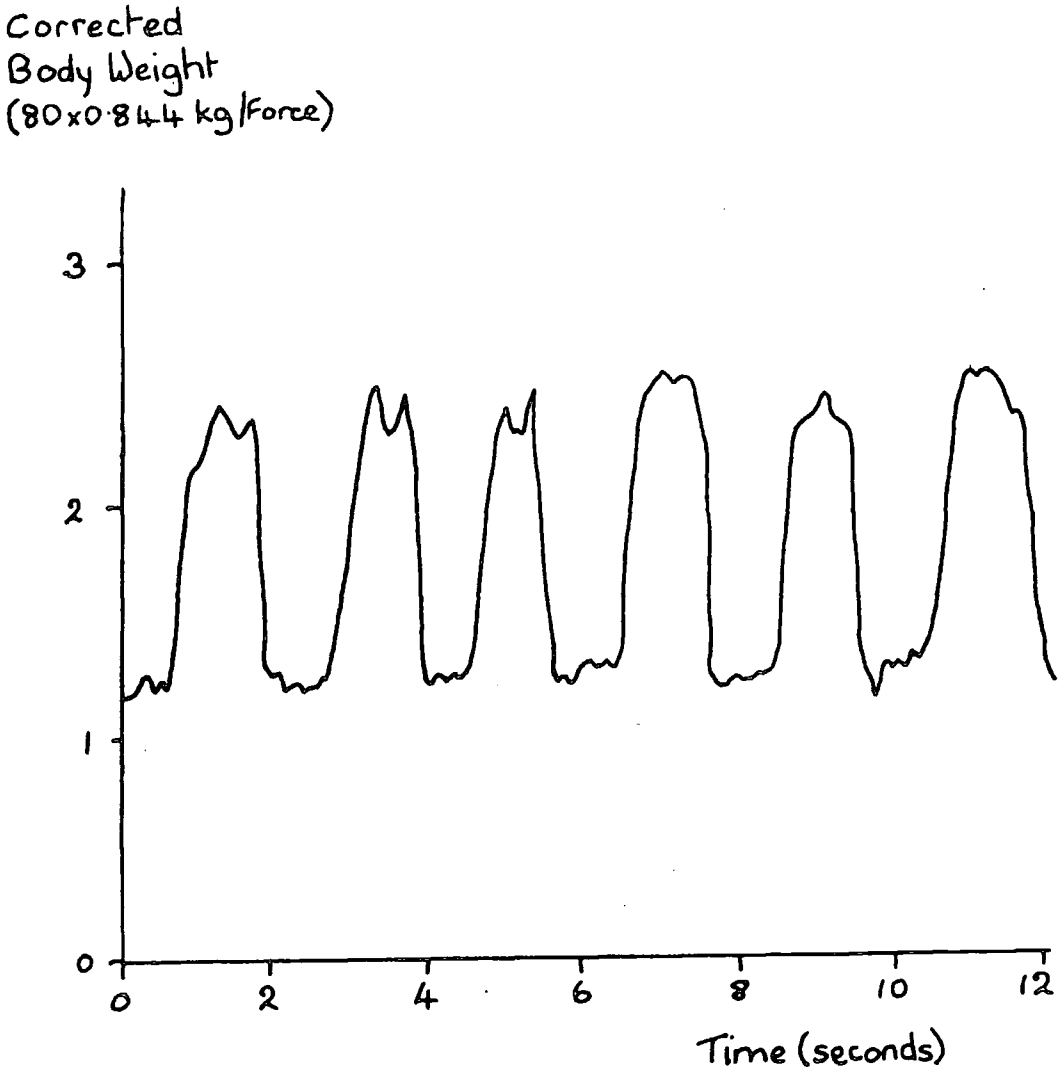

Figure 4.3

A walking trace taken twelve days after operation. Walking speed 0.44 ms^{-1}. Stance phase load is 2.42 times corrected body weight [unsupported]. [English and Kilvington, 1979]

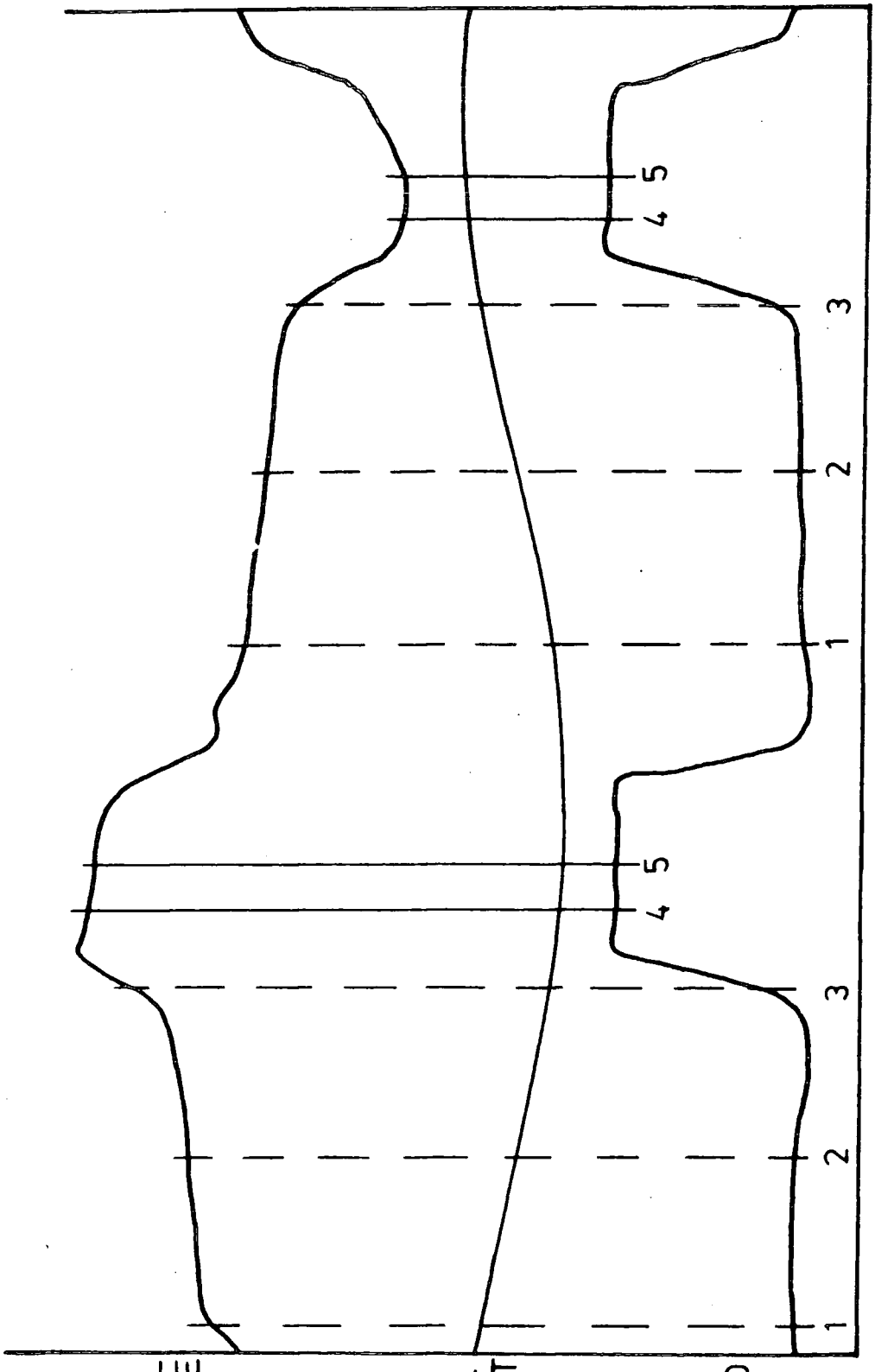

Figure 4.4

Typical traces obtained from the simulator showing load, displacement and frictional torque.

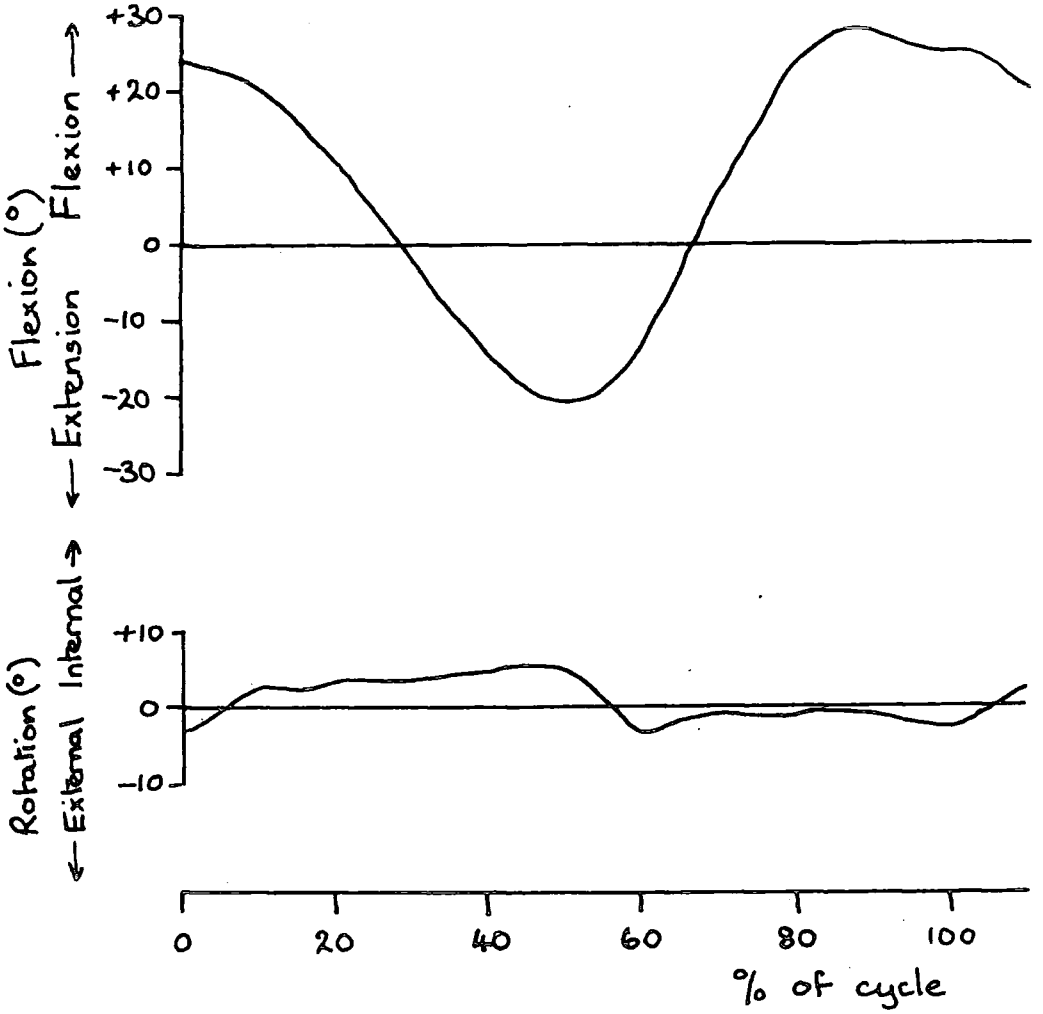

Figure 4.5

Hip angular displacements during walking. The curves are averages taken over 20 cycles.
[Lamoureux, 1971]

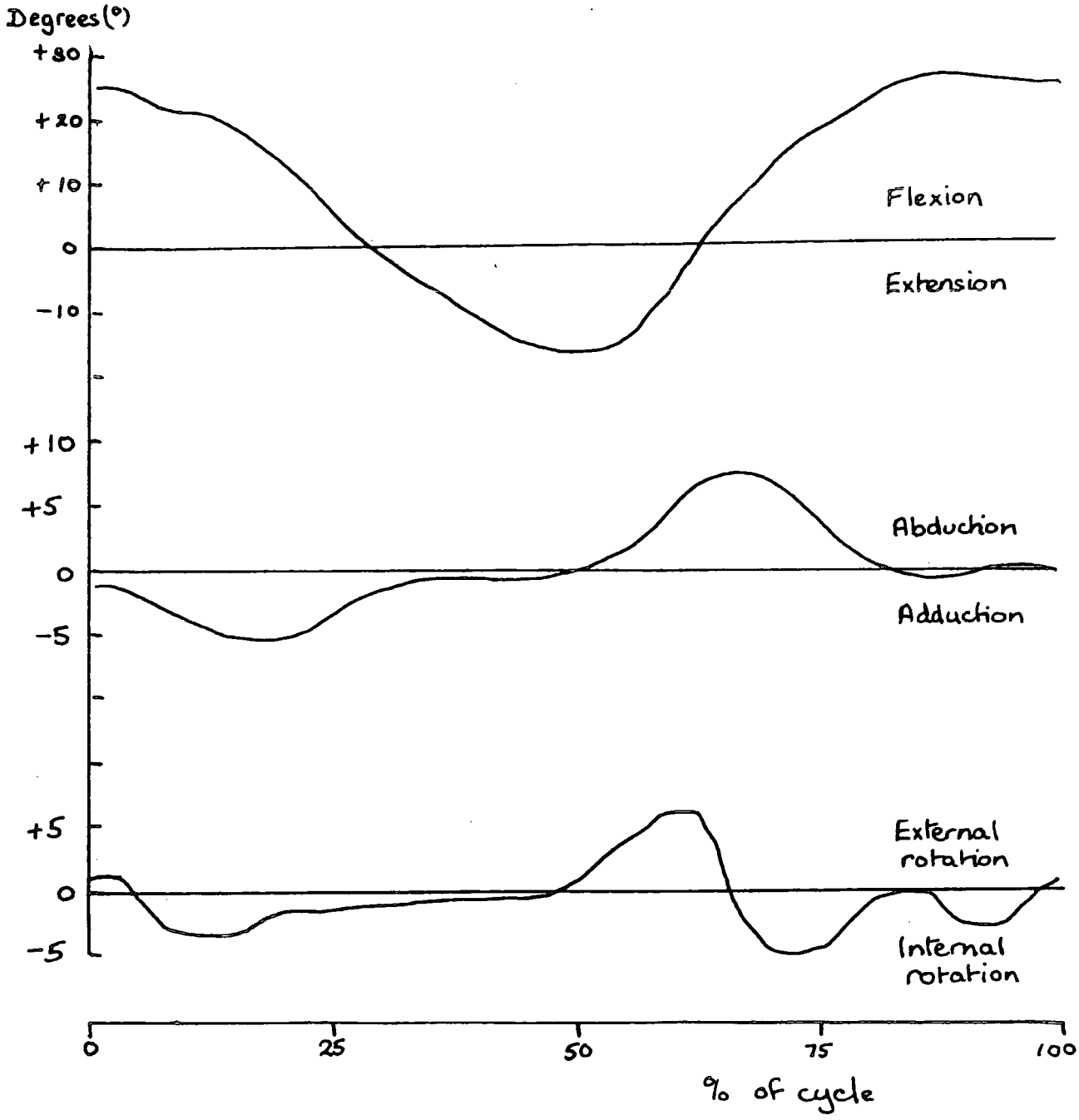

Figure 4.6

The angular displacements of a hip joint during normal female walking: average of 5 steps.
[Gore, 1980]

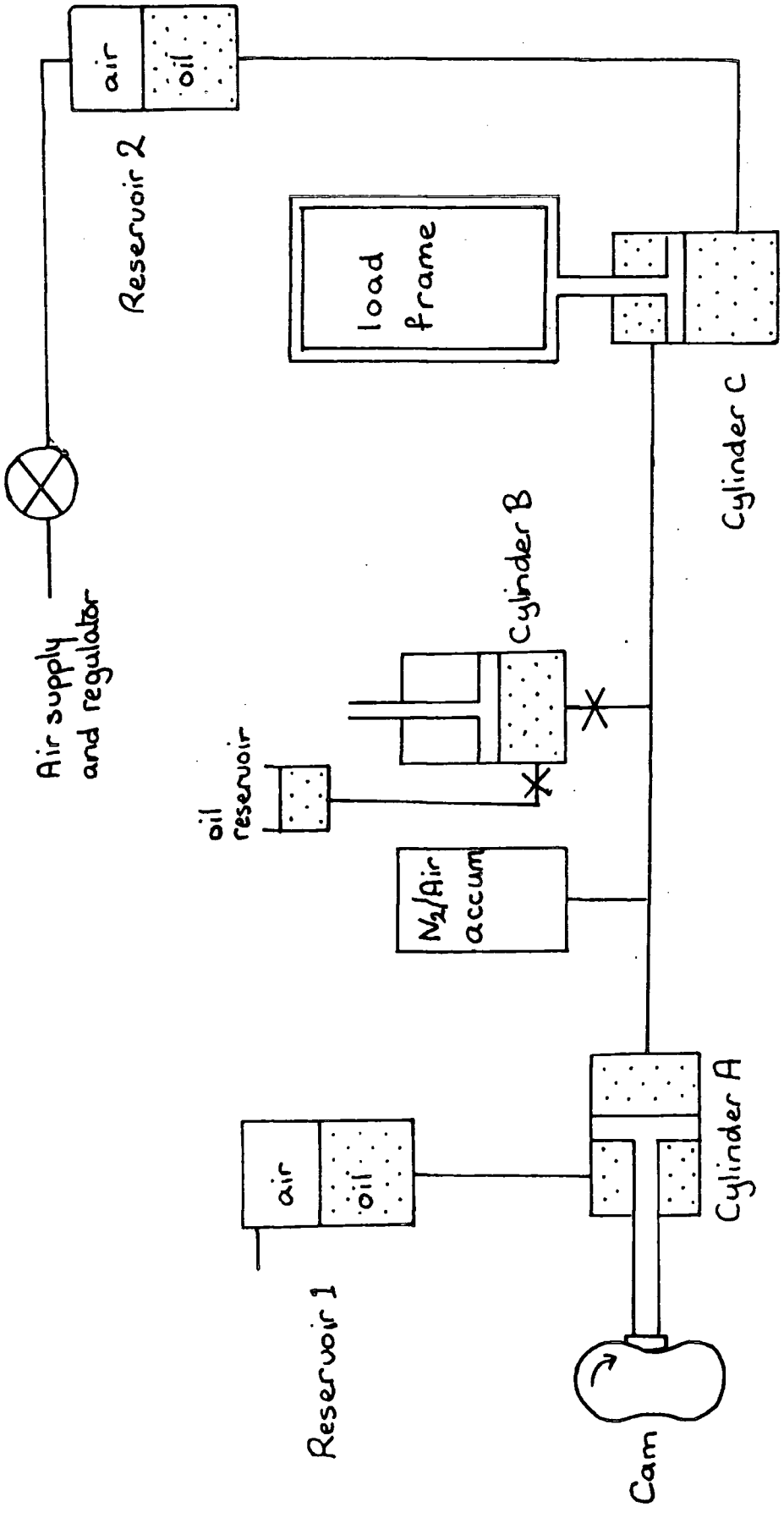

Figure 4.7

The hydraulic circuit for the hip function simulator.

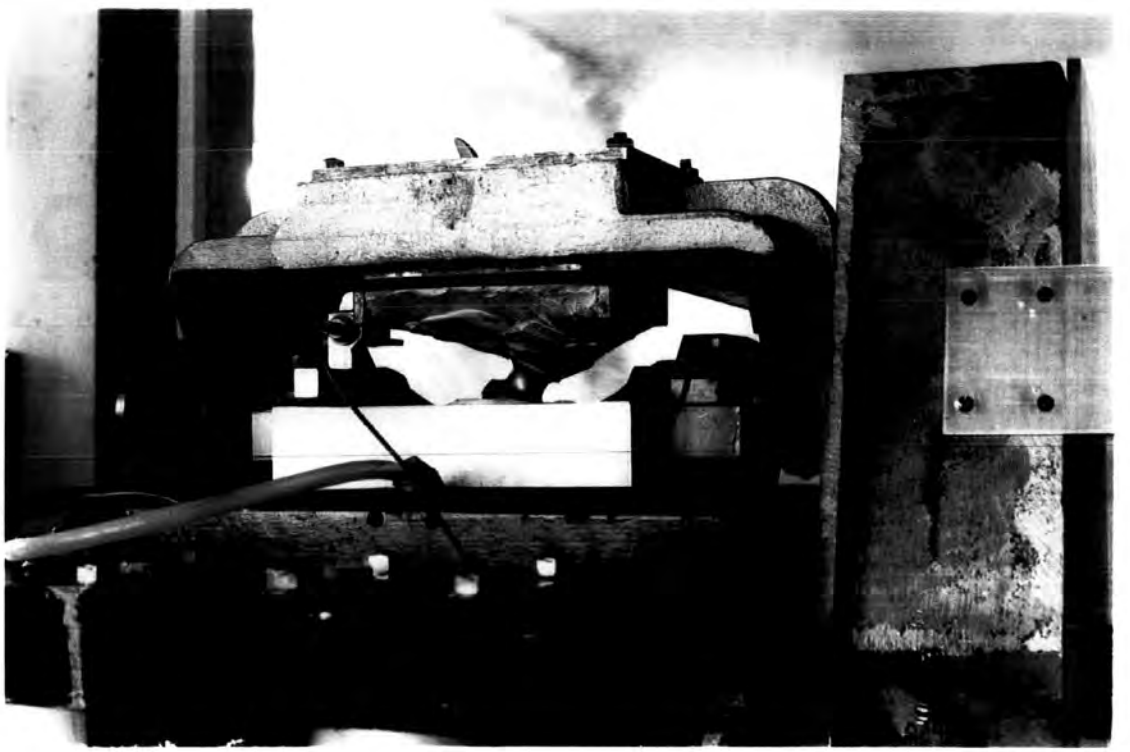

Figure 4.8

McKee-Farrar joint in the simulator, showing the friction measuring carriage

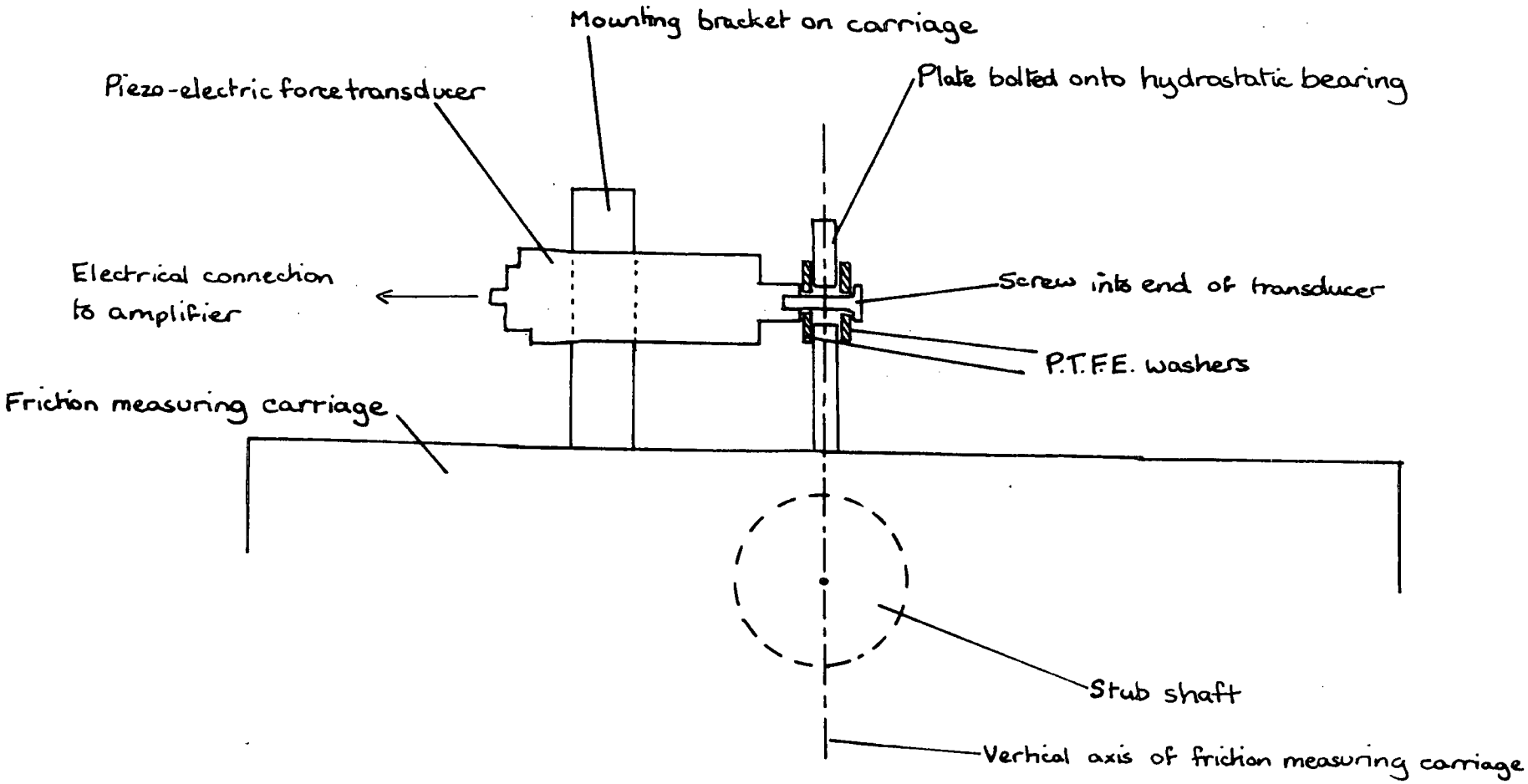

Figure 4.9

The arrangement of the mounting of the piezo electric transducer.

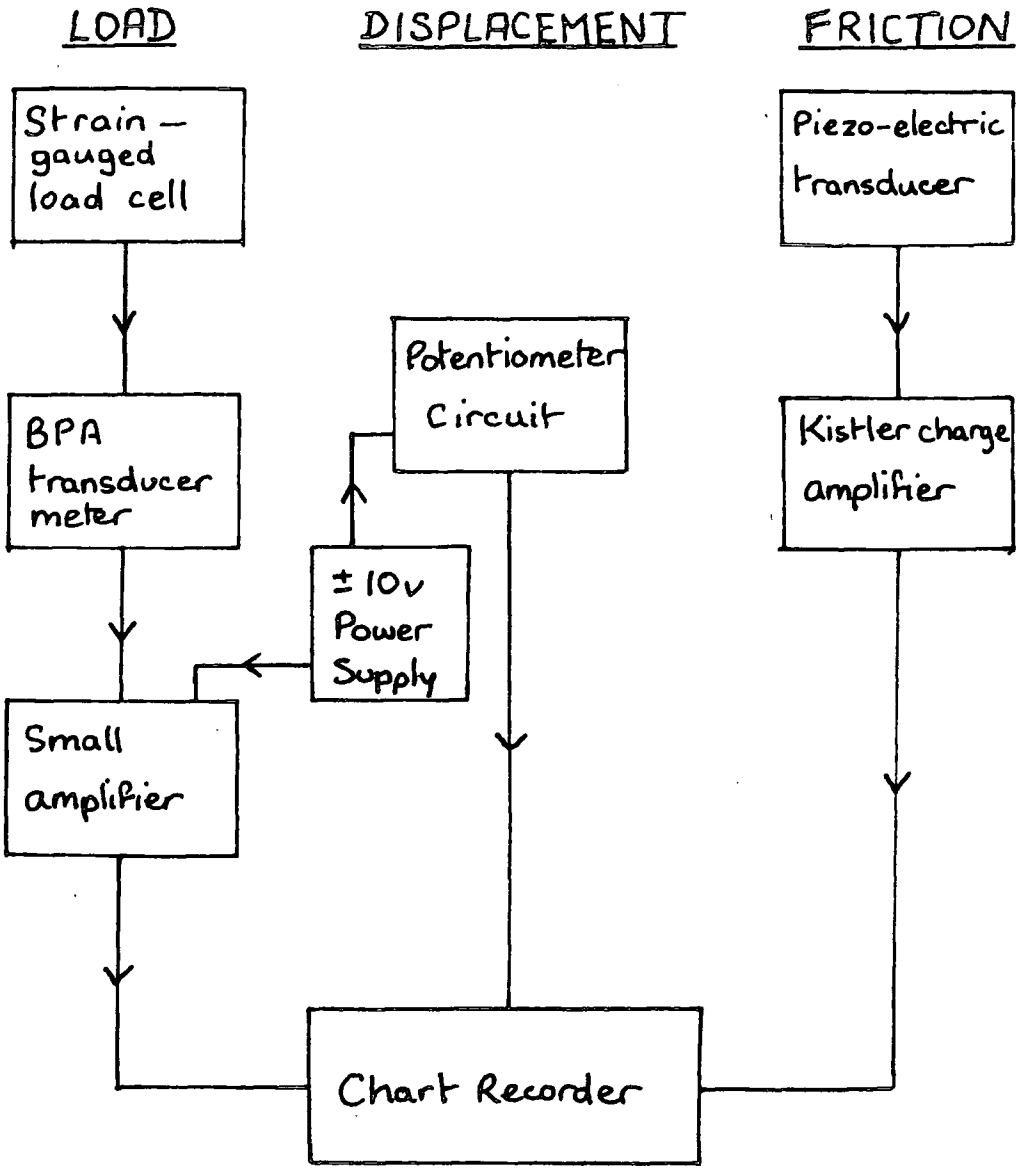

Figure 4.10

Block diagram of the instrumentation for the hip function simulator.

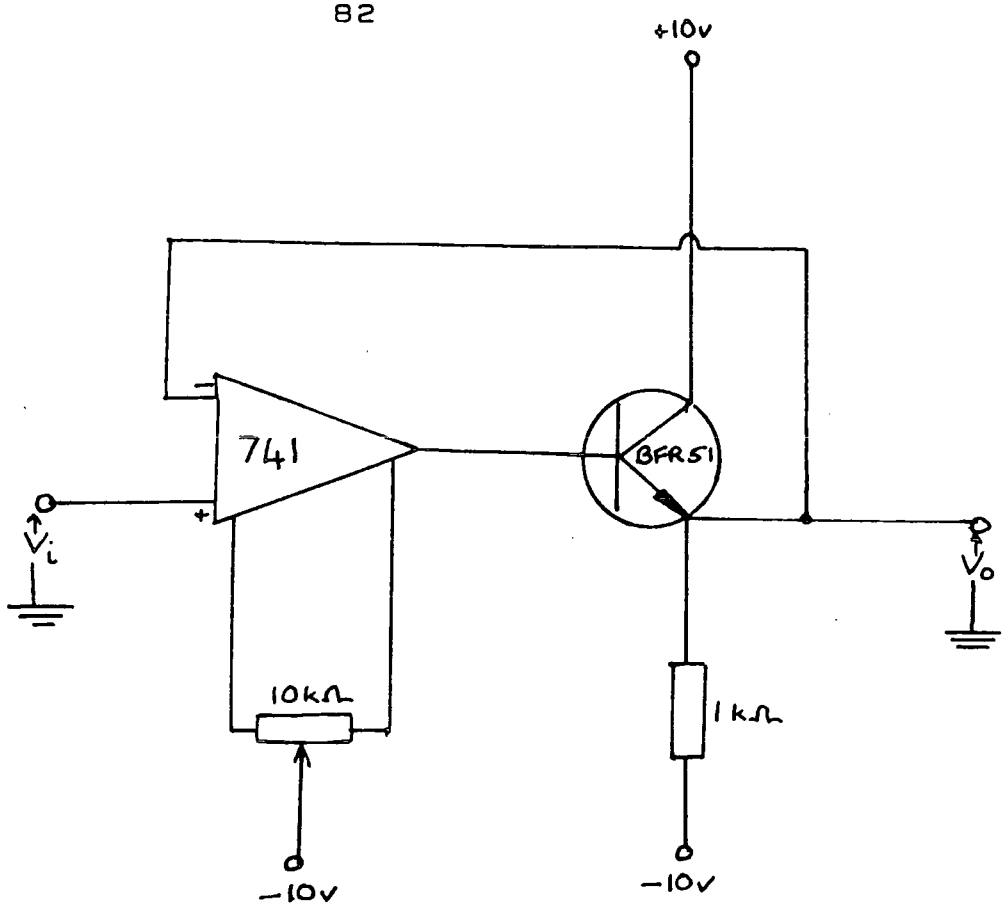

Figure 4.11

Small amplifier for impedance matching in load recording circuit.

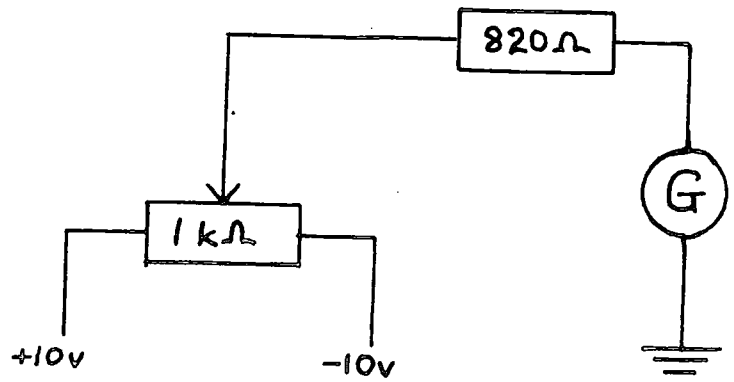

Figure 4.12

Potentiometer circuit for measuring displacement.

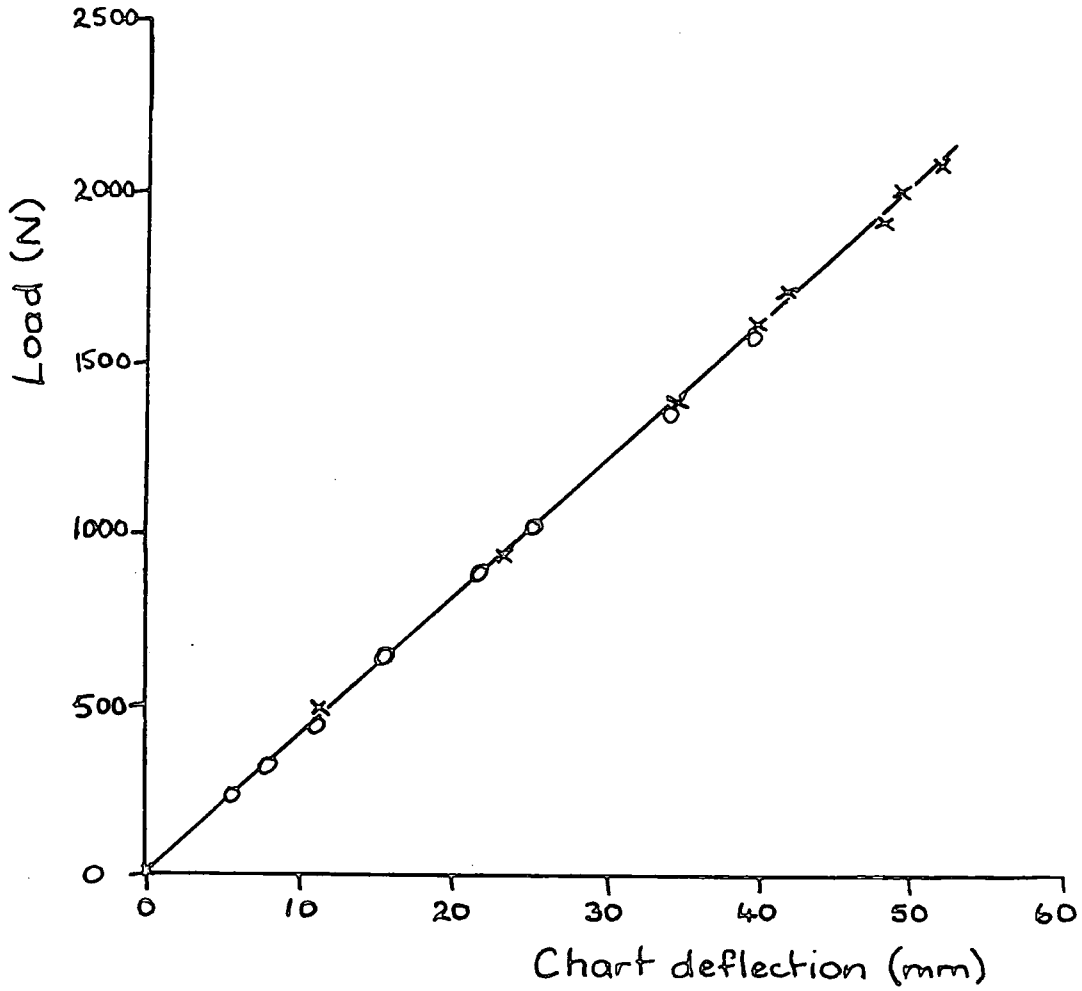

Figure 4.13

Calibration graphs for load applied by simulator.

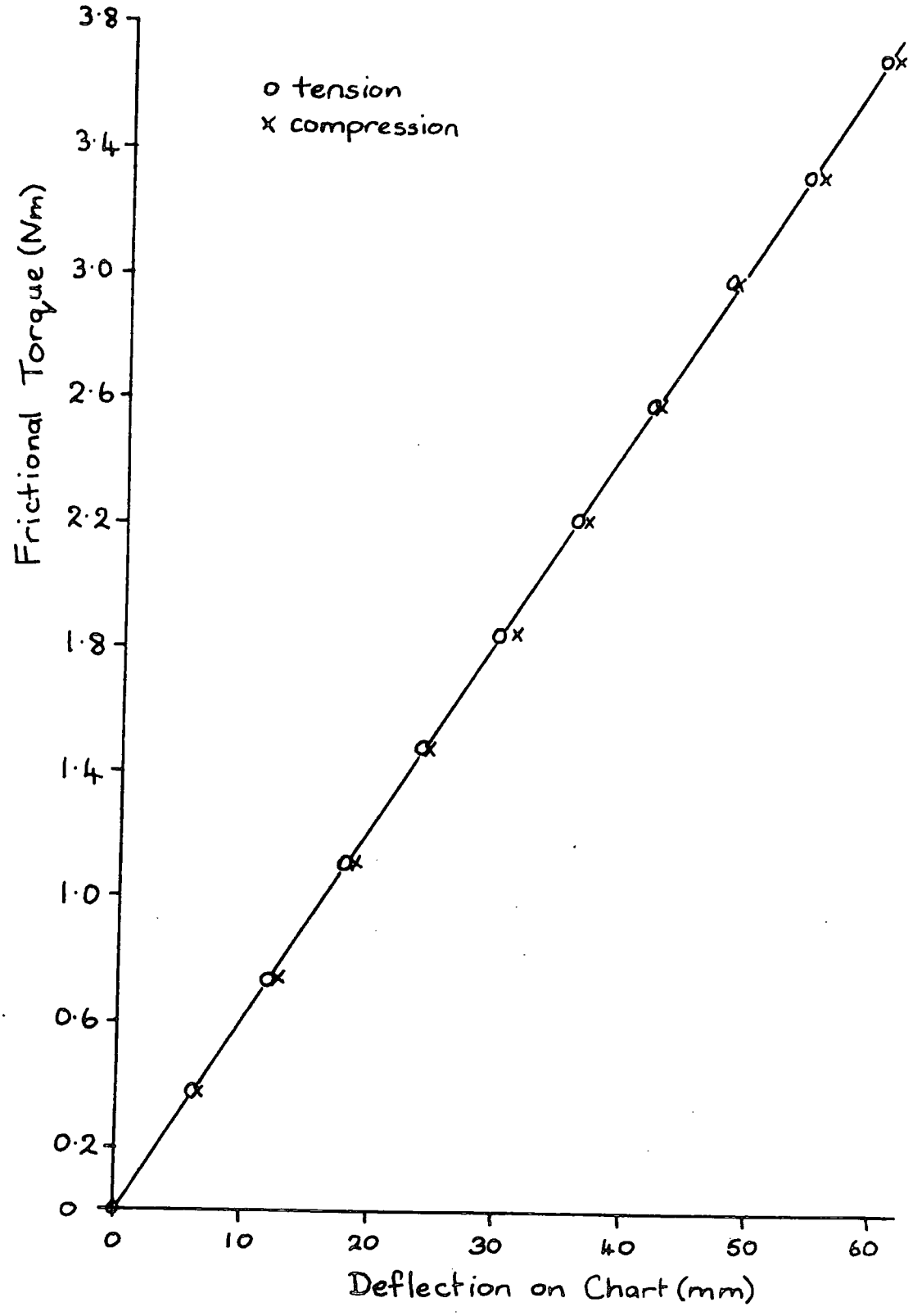

Figure 4.14

Calibration graph for frictional torque .
[Scale on charge amplifier was 0.1 Mech units/volt.]

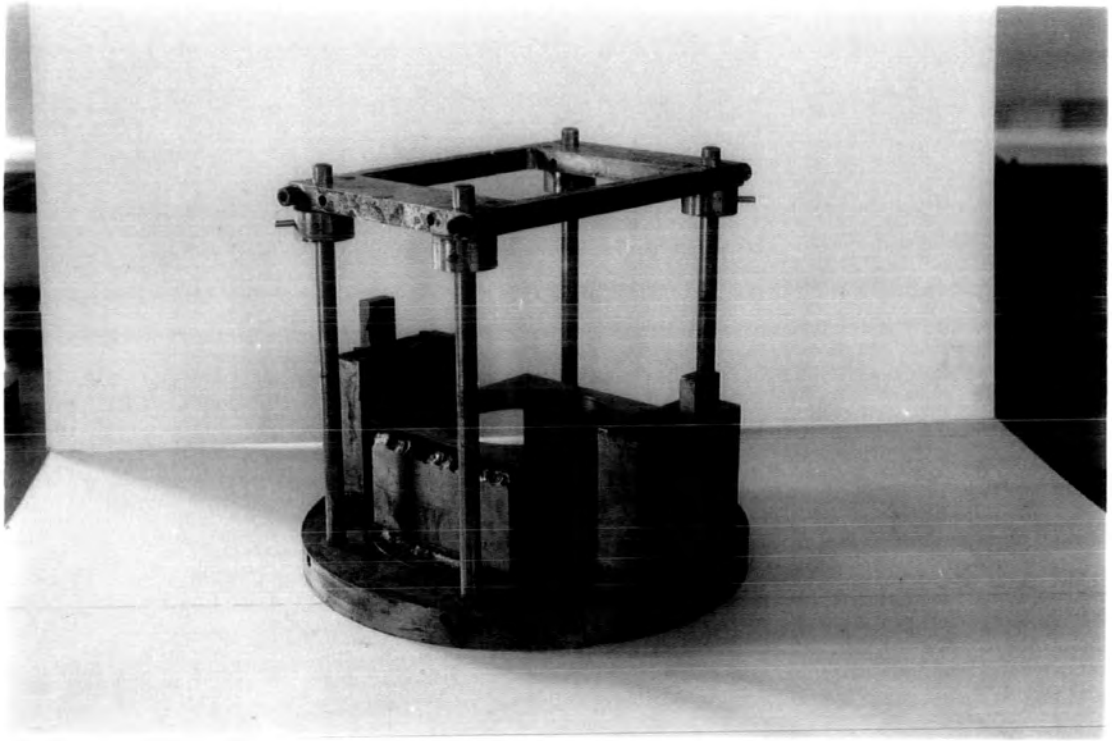

Figure 4.15

Setting-up jig

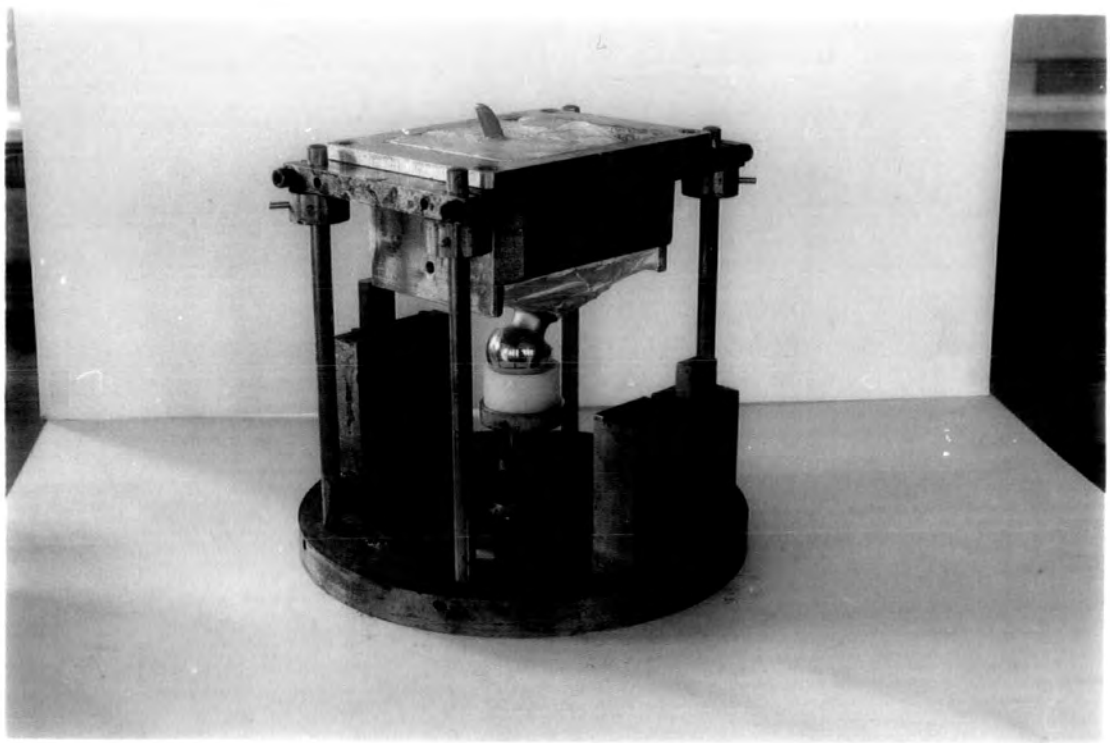

Figure 4.16

Setting-up jig using base with central cup for positioning femoral head

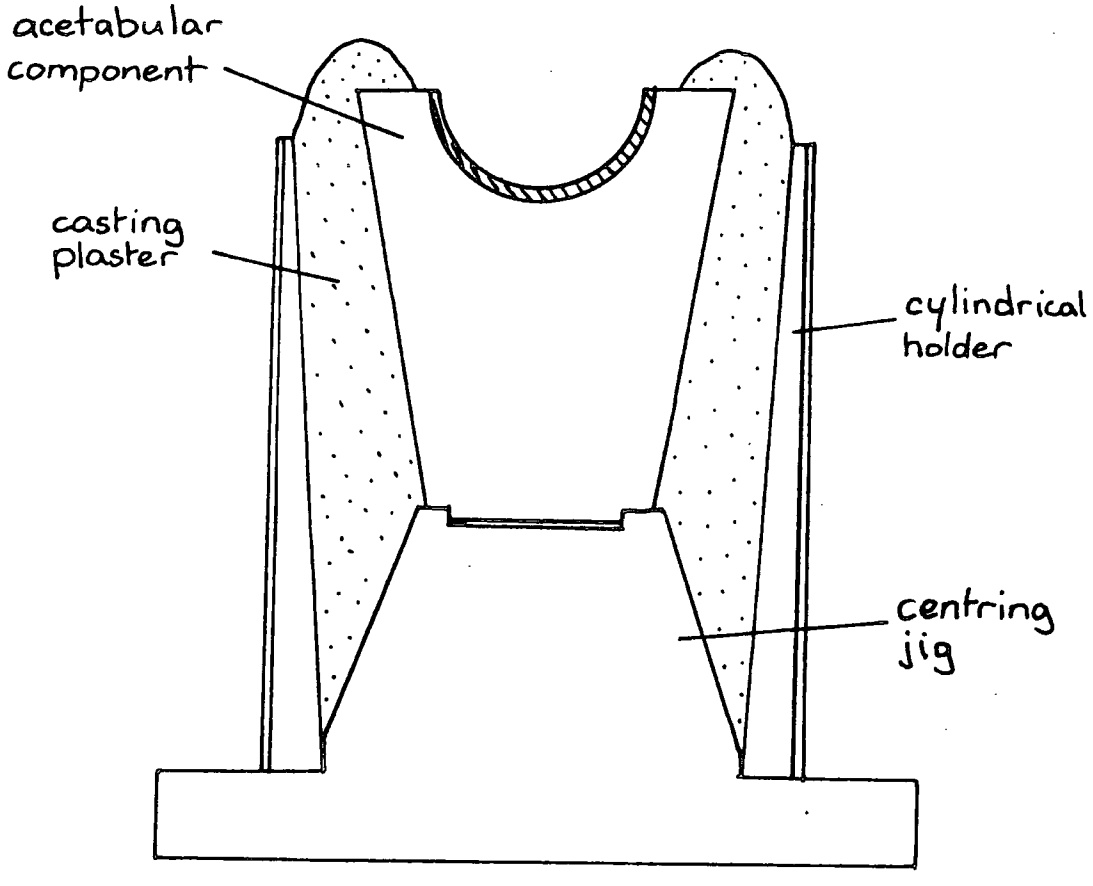

Figure 4.17

Diagram to show use of centring jig for setting up acetabulum with compliant layer.

CHAPTER FIVE

MATERIALS AND METHODS

The previous chapter has described the main apparatus used in this work - the hip function simulator. This chapter details the joints and lubricants used together with the equipment required in their preparation and testing.

5.1 Joints

Tests were run with both natural and artificial hip joints. The natural joints were as indicated in Table 5.1. Although they were all elderly, they were taken from people with no history of joint disease and were in good condition. Hip H10 was in the worst condition as it had an area of eroded cartilage on the medial side. However as this is not the main load bearing area, it was felt that it would not have a serious effect on the results, though the load bearing regions may also have been somewhat affected.

The artificial joints used ranged from commercial prostheses to joints which were specially made to study the effects of soft elastic layers on joint lubrication. This latter group were purely for laboratory use at this stage and not intended for implantation. They are listed below.

Charnley Total Hip Prosthesis

This was the commercial Charnley prosthesis consisting of a stainless steel femoral head, 22 mm in diameter and an ultra-high molecular weight polythene (UHMWPE) cup.

McKee-Farrar Femoral Head

This was a commercial femoral head, 35 mm in diameter made from cobalt chrome molybdenum alloy. It was used with a variety of acetabular cups with compliant linings, made as described in the next section. The linings varied in thickness from 0.5 mm to 3 mm and the clearance between the cup and the head was also varied. Details of the cups are given in Table 5.2.

5.2 Manufacture of compliant linings for acetabular cups

The compliant layers were moulded from Sylguard 182 silicone elastomer (Dow Corning). This is supplied as a clear viscous liquid base and separate curing agent. To prepare the rubber, one part by weight of curing agent was mixed into 10 parts base. The mixture was placed in a vacuum chamber and evacuated to a pressure of 25 mm mercury and left until all the trapped air bubbles were removed. The bubbles of air were expelled more rapidly if the vacuum was released and restored several times initially. Once all the air bubbles had disappeared (as the rubber was transparent this was easy to see), the liquid could be poured into moulds ready for curing.

A special jig was used to mould compliant layers in acetabular components, see Figure 5.1. Brass femoral plugs, with a radius equal to that of the McKee-Farrar head plus the clearance required, were machined. These could be inserted in a holder, which also held the acetabular base, and adjusted to give the required thickness of compliant layer. Several acetabular bases were machined with different cup sizes. These were made from mild steel. The radius of each cup was equal to the radius of the McKee-Farrar head plus the compliant layer thickness plus the clearance desired.

To mould a compliant layer, both components were carefully cleaned and the cup part of the base was given a thin coat of Sylguard Primer (DC 92-023) and allowed to dry for one hour. The base was placed in the holder and the oversized femoral plug lowered into it. The collar above the frame was locked in this position with a grub screw (see diagram in Figure 5.2). A feeler gauge was inserted between the collar and the frame to raise the femoral plug by the thickness of elastomer required in the cup. The large screw shown in Figure 5.2 was used to lock the femoral plug in position until its collar was repositioned. Thus a gap of known constant thickness was formed between the acetabular base and the femoral plug. The acetabular base was half filled with the liquid elastomer and the plug gently lowered into its preset position so that the elastomer filled the space between the two components. The whole assembly was

placed in an oven for four hours at 75°C to cure the elastomer. After curing, the plug was removed from the base, and any excess elastomer trimmed away, leaving a layer of known thickness bonded to the metal acetabular base.

Each time an acetabular lining was moulded, a slab of elastomer was also cured between two perspex plates separated by brass spacing bars 6.5 mm thick. This slab was used for elastic modulus measurements since it was from the same mix as the lining and had undergone the same cure cycle.

5.3 Compliance and modulus testing

There were three different tests which were used to examine the elasticity of the joints. For the natural joints plugs of cartilage were removed from the joints and tested in unconfined compression from which a value of 'compliance' could be calculated. For the artificial joints with compliant layers, two tests were performed. The first was to determine the elastic modulus of a slab of elastomer from each mix, to ensure comparability between mixes. The second was to gain some value for an 'effective' modulus of each thin elastomer layer bonded onto the steel acetabular cup. These three test methods are described more fully below.

5.3.1 Cartilage compression testing

When all the lubrication tests had been completed on a natural joint, the femoral head was sawn in half. The hemispherical portion which had been removed was placed, cartilage uppermost, in a stainless steel dish which had four pointed-end screws screwed through the walls. These were used to hold the sample firmly in place. The dish was mounted on an adjustable stand so that any area of cartilage could be made to lie horizontally. A hardened steel cutter, 5 mm in diameter, was used to obtain samples of cartilage and underlying bone. The cartilage surface was perpendicular to the sides of the specimen if the holder was correctly adjusted but the bone end needed to be machined flat in a watchmaker's lathe. Usually, five samples were taken from each femoral head.

Each cylindrical plug of cartilage and bone was stuck in the centre of a circular brass plate with cyano-acrylate adhesive. The brass plate had a circular channel into which a perspex tube fitted. The tube was filled with Ringers' solution to immerse the specimen. The assembly was positioned centrally on the base plate of an Instron 1195 universal testing machine and a brass cylinder was screwed into the cross-head so that load could be applied to the specimen.

A 500N compression load cell was used on the Instron and the sample was loaded to 120N at a strain rate of 0.3 mm s^{-1}. After testing the cartilage was sliced off the bone with a scalpel and its thickness measured with a micrometer, taking care not to compress the cartilage.

5.3.2 Elastic modulus of elastomer

The elastic modulus of each sheet of elastomer was measured using the apparatus of Clish [1979]. Figures 5.3 and 5.4 show the assembly containing a specimen. The diameter of the indentation circle caused by loading a lens in contact with the elastomer was measured for a range of weights. The elastomer was placed in intimate contact with a sheet of perspex resting on the frame. The lens and mass holder were placed on top. The whole assembly was then placed under a toolmaker's vernier microscope and illuminated from below. The diameter of the circle visible was measured with masses added in multiples of 50 g from zero to 450 g. The modulus could be found from a graph of $[\text{radius}]^3$ against additional mass.

5.3.3 Effective modulus of compliant layers

The elastic modulus of the elastomer used for compliant linings is necessary to check the comparability of the different mixes, but does not indicate the effective modulus of the thin compliant layer on steel used in the trial acetabula. To examine how this varied with thickness

of the compliant layer, tests were performed using the Instron testing machine.

A 25kN compression load cell was used in the Instron testing machine. The acetabular component was placed on the platen and a steel ball 34.9 mm in diameter [the same diameter as the McKee-Farrar head] was placed in it. The cross-head was then lowered to load the assembly up to 3kN at a speed of 10 mm/min. The load was rapidly removed. This was repeated several times to check the reproducibility of the load-displacement trace obtained.

5.4 Surface measurement of prosthetic components

A 'Talysurf 4' surface measurement device was used to estimate the surface finish of the prosthetic components used. A stylus traverses the sample and a magnified trace of the surface is produced on a chart recorder. A meter reading also gives the Ra value for the surface. The instrument normally traverses in a horizontal plane but can be used for curved surfaces by the use of a 'Datum attachment'. The insertion of a radius bar of appropriate length into this attachment ensures that the stylus traverses an arc of the same radius as the specimen.

The McKee-Farrar femoral head was measured directly. The cups with compliant layers could not be measured in this way since the elasticity of the rubber would have been a problem as well as their concavity. However

as they were moulded against brass plugs, these plugs could be measured to give an indication of the surface finish on the compliant layers.

5.5 Lubricants

Two types of synthetic lubricant, as well as human synovial fluid were used in the tests.

Several potential synthetic lubricants for use in degenerate synovial joints are discussed by Cooke [1978]. He studied their viscosity since a synthetic lubricant should have similar properties to synovial fluid. For the purposes of this work it was necessary to use lubricants which were readily available in a range of viscosities. Silicone fluid was an obvious choice for a Newtonian fluid since it is commercially available in a wide range of viscosities.

The two contenders for a non-Newtonian lubricant were polyethylene oxide [PEO] solutions and sodium carboxymethyl cellulose [SCMC] solutions. PEO exhibits a stronger variation of viscosity with shear rate but as Cooke noted, the viscosity of the fluid is very susceptible to mechanical degradation. This was borne out by Muddeman [1980] who found that PEO produced erratic results when used to lubricate prostheses. Cooke's main criticism of SCMC is that it degrades at high temperatures and therefore cannot be sterilised by autoclaving. Although this is obviously important in a lubricant

which is intended for use in the body, as a lubricant which reproduces some of the characteristics of synovial fluid in in vitro tests, it is irrelevant and so this polymer was chosen for the work reported here.

Silicone fluids were obtained with six different viscosities. Two intermediate values of viscosity were mixed using a manufacturer's chart to give the proportions of fluids required. Table 5.3 gives the Dow Corning reference number and the viscosity for the fluids used. Solutions of sodium carboxymethylcellulose (SCMC) in water were made with eight different viscosities. The reference for each fluid and its viscosity are given in Table 5.4.

The synovial fluid was collected from patients whose knee joints required aspiration. Usually 10 - 30 ml was available from each patient. The treatment of the fluid before use as a lubricant is detailed in the next section and the specific fluids used for each joint are detailed in the results section.

5.6 Biochemical analyses and estimations

Preliminary experiments were performed both to determine suitable conditions for the enzymatic digestion of the synovial fluid and to find a suitable test to check that digestion had taken place. This check was a vital part of the project since earlier work by O'Kelly et al (1978) had not checked that the fluid had been affected by the enzymatic digestion. Also, they did not use

control samples of the same fluid as that which was digested.

A veronate buffer was used throughout, except where specified otherwise. The more usual phosphate buffer was not used since Pigman and Rizvi [1959] reported that it caused degradation of synovial fluid. The veronate buffer was that used by Linn and Radin [1968] and consisted of 0.00408 M sodium 5-5 diethylbarbiturate and 0.0652 M HCl with 0.088 M NaCl, pH 7.2.

The synovial fluid samples were spun immediately after collection in an ultracentrifuge [using an 8 x 50 ml rotor in an HSE High Speed 18 centrifuge] for 30 minutes at $4^{o}C$ and 14000 x g to remove particulate matter. The supernatant was then frozen in aliquots until required.

On thawing, the pH value was measured. The pH varied from 7.2 to 8.7. The fluids were adjusted to pH 7.2 by equilibrium dialysis against six changes of veronate buffer in a cold room at $4^{o}C$ over a period of 24 hours. This was to ensure a constant pH value for all the samples since Linn and Radin [1968] found that the coefficient of friction was affected by the pH value of the lubricant used in their tests with an arthrotripsometer.

5.7 Hyaluronidase digestion of synovial fluid

Hyaluronidase splits β - [1 → 4)-N-acetylglucosaminide links in hyaluronic acid [Figure 2.3]. An assay method was required which would confirm the action of the

enzyme on each synovial fluid sample. Two possible assays were investigated: [a] uronic acid residues and [b] N-acetylglucosamine [NAG] residues. The preliminary tests for both assays are described below.

5.7.1 Chemical estimation of uronic acid residues

The modified uronic acid carbazole reaction of Bitter and Muir [1962] was used.

The sulphuric acid reagent was prepared from a 0.025 M solution of sodium tetraborate.$10H_2O$ in sulphuric acid. The carbazole reagent was a 0.125% solution of carbazole in absolute ethanol.

3.0 ml sulphuric acid reagent was placed in each tube and cooled with solid CO_2. 0.5 ml sample was carefully added and the tubes stoppered and shaken whilst remaining below room temperature. The tubes were heated for 10 minutes in a boiling water bath, then cooled to room temperature. 0.1 ml carbazole reagent was added, the tubes shaken again, then reheated for 10 minutes in the same water bath. After cooling to room temperature the absorbance at a wavelength of 530 nm was measured in a Pye-Unicam SP 18000 spectrophotometer.

A calibration curve was prepared using a range of standard solutions of glucuronolactone in water saturated with benzoic acid. 0.1 ml of the standard solution was added to 0.4 ml veronate buffer to give the required

volume for assay. The lower curve in Figure 5.5 shows the results obtained.

When the calibration assay was repeated with 0.1 ml standard glucuronolactone solution added to 0.4 ml synovial fluid, the reaction mixture was found to be very dark and discoloured, resulting in much higher and more erratic values of A_{530}. This is demonstrated by comparing the upper curve in Figure 5.5 with the lower one.

5.7.2 Chemical estimation of N-acetylglucosamine residues

The method followed was that of Barrett (1972). A borate buffer was made by adjusting an 0.80 M potassium tetraborate solution to pH 8.9 with concentrated hydrochloric acid. DMAB reagent was prepared by dissolving 1.0 g of 4-dimethylaminobenzaldehyde (DMAB) in 1.25 ml concentrated hydrochloric acid. The solution was made up to 100 ml with glacial acetic acid.

0.1 ml of the borate buffer was added to 0.5 ml sample. The mixture was heated for 3 minutes in a boiling water bath and cooled in tap water. 3.0 ml DMAB reagent were added and the colour developed for 12 minutes at 37°C. After again cooling in tap water, the absorbance at a wavelength of 585 nm (A_{585}) was measured in a Pye-Unicam SP 18000 spectrophotometer.

A calibration curve was prepared using six standard solutions of NAG in distilled water ranging from 50μg ml^{-1} to 350μg ml^{-1}. 0.1 ml of the standard solution was added to 0.4 ml veronate buffer to make the required volume for assay.

The assay was repeated using synovial fluid in place of veronate buffer to make up the required assay volume. The calibration curve in Figure 5.6 shows that the absorbance was unaffected by the presence of synovial fluid in the reaction mixture.

Since the presence of synovial fluid did not affect the results of the NAG calibration assay as happened with the uronic acid assay, it was decided to use the NAG method to examine the effectiveness of the hyaluronidase digestion.

5.8 Evaluation of optimum conditions for enzymatic digestion of synovial fluid by hyaluronidase

The hyaluronidase used was Type VI - S [SIGMA] from bovine testes, made into a solution of 10,000 NF units ml^{-1} in veronate buffer. Preliminary experiments were performed to determine suitable times, temperature and pH for the routine digestion of synovial fluid by hyaluronidase prior to lubrication tests.

5.8.1 Time of digestion

Digestion of samples of bovine and human synovial fluid and a hyaluronic acid solution were performed. Initially,

1500 NF units of hyaluronidase were added to 1.5 ml sample. An additional 1000 units were added every 3 hours. A NAG assay was performed at intervals to determine the optimum time for the digestion. Figure 5.7 shows the curves obtained and it can be seen that there was little further digestion after twelve hours for any of the samples used.

5.8.2 Incubation temperature

Three identical solutions of synovial fluid were digested for 18 hours at temperatures of 22°C, 30°C and 37°C. The solutions consisted of 0.5 ml synovial fluid and 1.5 ml veronate buffer containing 200 NF units hyaluronidase. A NAG assay was performed on the digested samples. The results in Table 5.5 show that the enzyme was more active at a raised temperature. The digestions were thus performed at 37°C.

5.8.3 Effect of pH

The effect of pH of the buffer on the digestion was investigated to ensure that reasonably exhaustive digestion would take place at pH 7.2. The veronate buffer precipitated below pH 6.8 so barbital sodium acetate buffer was used for this test with a range of seven pH values from 5.4 to 8.0.

The barbital sodium acetate buffer was made from a mixture of solutions A and B. Solution A was a 0.143 M

sodium acetate and 0.143 M barbital sodium solution. Solution B was a 0.1 N solution of hydrochloric acid. The addition of a specified volume of B to 50 ml solution A and 20 ml 8.5% NaCl, the whole then diluted to 250 ml, resulted in a buffer whose pH varied from 5.4 to 8.0.

A range of mixtures of synovial fluid, buffer and hyaluronidase, detailed in Table 5.6, were made with each of six pH values. The mixtures were incubated for 18 hours at 37°C in a shaking water bath. A NAG assay, as earlier described, was then performed on a sample from each mixture. The results are plotted in Figure 5.8. The absorbance for mixture B (synovial fluid + buffer + hyaluronidase) declines above pH 6.6, showing that above this value of pH less NAG residues are formed. At a pH of 7.2 the absorbance is 82% of its maximum for this mixture, hence it was decided that it would be reasonable, if not optimum, to perform digestion at this pH value.

5.8.4 Optimum conditions for hyaluronidase digestion

As a result of the preliminary tests, the standard conditions used for the digestion of synovial fluid with hyaluronidase were 0.01 ml enzyme solution per ml synovial fluid (ie 100 units/ml) incubated at 37°C, pH 7.2 for either 1 or 18 hours. The two times were chosen to show a difference in degree of digestion.

18 hours would result in maximum digestion whereas after one hour the sample would only be partially digested. A NAG assay was performed on the resulting fluid to ensure that digestion had taken place.

5.9 Trypsin digestion of synovial fluid

The aim of this digestion was to cause fragmentation of the protein present in the synovial fluid. Again it was necessary to ensure that digestion would take place and for this reason the inhibitory effect of synovial fluid on the action of trypsin was investigated.

5.10 Estimation of the anti-trypsin activity of synovial fluid

Synovial fluid has been reported in the literature [Holmes et al, 1935] to contain inhibitors to the action of trypsin so a check was needed to ensure that the quantity of trypsin used would be sufficient to overcome this inhibition. The synovial fluid was investigated as an inhibitor to the action of trypsin on a α-N-benzoyl-l-arginine ethyl ester HCl (BAEE) substrate and from this work, the concentration of trypsin required to overcome the inhibitory action of the synovial fluid was deduced [Burck, 1970].

An 0.00025 M solution of BAEE in 0.5 M Tris/HCl buffer (pH 8.0) was used as the substrate. The trypsin (type II-S, SIGMA) was initially used in a concentration of

1000 BAEE units/ml in 0.0025 N HCl with 0.02 M $CaCl_2$. The calcium chloride was necessary to keep the trypsin active over a prolonged period (Kassel et al, 1963).

All the solutions were kept in a water bath at 25°C. The trypsin and inhibitor solutions were mixed together in equal proportions and after a few minutes, 0.2 ml of this mixture was added to 3.0 ml BAEE solution in a quartz cuvette. The solution was quickly shaken, then the absorbance was compared with a blank of BAEE solution alone in a Pye-Unicam SP 18000 spectrophotometer. The absorbance at 253 nm was recorded on a chart against time and the rate of change of absorbance (ΔA/min) was calculated from the slope of the graph.

5.10.1 Standard inhibitor test

A standard trypsin inhibitor (Soybean, type I-S, SIGMA) was used in a range of concentrations in Tris/HCl buffer to test the system. The method was as described above. The rate of change of absorbance was plotted against the concentration of the soybean inhibitor solution. The results are shown in Figure 5.9. It can be seen that the absorbance decreases with increasing concentration of inhibitor showing that the inhibition is not complete at concentrations of less than 80 μg inhibitor in 3.0 ml BAEE substrate solution.

5.10.2 Synovial fluid inhibitor test

A range of solutions of synovial fluid in Tris/HCl buffer were then used as an inhibitor in the same way as the soybean inhibitor and Figure 5.10 plotted from the results. From this graph it can be seen that a 10% solution of synovial fluid was a powerful inhibitor of this concentration of trypsin. This is equivalent to 0.01 ml synovial fluid inhibiting the action of 100 units of trypsin.

5.10.3 Varying trypsin concentration

The test was repeated with a range of concentrations of trypsin in the enzyme solution. Three different strengths of synovial fluid solution were used as inhibitors. The results are plotted in Figure 5.11. Above a trypsin concentration of 130 μg ml^{-1} in the enzyme solution, the effect of synovial fluid as an inhibitor was rapidly lost.

5.10.4 Final test

The test was repeated with 0.1 ml undiluted synovial fluid as inhibitor and greater concentrations of trypsin, at pH 7.2. Table 5.7 shows that a concentration of trypsin of 2 mg ml^{-1} in the enzyme solution [ie 200 μg in 0.1 ml solution] was sufficient to overcome the inhibitory action of the synovial fluid, increasing the rate of change of absorbance sixfold from 0.012 to 0.075 per minute.

5.10.5 Optimum conditions for trypsin digestion

Following the above tests, it was decided that trypsin digestion should be performed at a concentration of 2 mg trypsin (20,000 BAEE units) for 1 ml synovial fluid at 22°C for either 1 or 18 hours at pH 7.2.

5.11 Viscosity measurement

There were two problems associated with the measurement of viscosity of the lubricants. Firstly, the non-Newtonian nature of some of the fluids means that it is necessary to measure viscosities at known shear rates. Secondly, only a small volume of synovial fluid was available for each measurement. For these reasons a Ferranti-Shirley cone and plate viscometer was chosen for the measurements. This only requires 1 ml samples of fluid.

The viscometer consists of a stationary flat plate and a slightly conical rotating disc driven by a variable speed motor. The cone speed, which is variable between 1 and 1000 rpm, is directly proportional to the shear rate. The viscous drag on the cone exerts a torque on a dynamometer which is directly proportional to the shearing stress. Hence the viscosity at a given shear rate can be calculated. A water jacket controls the temperature of the sample under test.

A 1 ml sample of each fluid used in the lubrication tests was kept frozen until its viscosity could be

measured. The measurements of viscosity were taken over a range of shear rates for each sample at 25°C. These measurements are given with the detailed results in the next chapter.

5.12 Test method for a series of lubricants in one joint

The instrumentation was switched on and allowed to warm up for at least 30 minutes before testing began. The alignment of the joint components was carried out as described in Chapter 4.

The femoral component was then removed, 1 ml of lubricant added to the acetabular cup and the femoral head replaced.

With the charge amplifier on its least sensitive scale, the motor was switched on and the traces observed. The sensitivity of the charge amplifier was increased until the trace of frictional torque was of a reasonable amplitude.

After a couple of minutes, a check was made to ensure that the frictional amplitude had remained constant. A trace was then run off with the chart on a speed of 125 mm s^{-1}. The speed of the motor was then altered and similar traces obtained, usually for two other speeds. The three speeds used were 0.65, 0.83 and 1.0 Hz. The speed of the motor was varied in a deliberately random order. The simulator drive motor and the oil supply to the bearings were then switched off, the femoral component

was removed and the articulating surfaces wiped dry with tissue. For natural joints, the cartilage was soaked in Ringer's solution and dried again between tests.

Another lubricant was then used and the test repeated from the point of introduction of the lubricant. The zero load position was checked periodically.

Reference	Age [yrs]	Sex	Diameter [mm]	Lubricants used		
				Synovial Fluids	Silicone Fluids	SCMC
H1	78	F	43	Yes	-	-
H2	62	M	54	Yes	-	-
H3	63	M	52	Yes	-	-
H4	60	M	53	Yes	-	-
H5	74	M	50	Yes	-	-
H6	64	M	49	Yes	-	Yes
H7	63	M	49	-	Yes	Yes
H8	54	M	45	Yes	-	-
H9	79	F	41	Yes	Yes	Yes
H10	70	F	46	Yes	-	-

Table 5.1

Human hip joints tested.

Cup Reference	Layer thickness (mm)	Radial clearance (mm)	Lubricants used		Comments
			SCMC	Silicone	
A1	1	0.25	Yes	Yes	
A2	2	0.25	Yes	Yes	
A3	3	0.25	Yes	Yes	
A0	0.5	0.25	Yes	-	Layer broke up when retested.
B0	0.5	0.25	-	-	Layer broke up on initial testing.
C0	0.5	0.25	-	-	
D0	0.5	0.25	Yes	Yes	
Y3	2.5	0.50	Yes	-	
Z1	0.5	0.50	Yes	-	

Table 5.2

Acetabular cups with compliant linings.

Reference	Viscosity [Pa s]
DC 10/200	9.4×10^{-3}
50	4.85×10^{-2}
100	9.7×10^{-2}
500	4.85×10^{-1}
1000	9.7×10^{-1}
1000 – 30000 } 3360	3.36
1000 – 30000 } 11450	11.45
30000	29.1

Table 5.3

Range of silicone fluids and their viscosities used as lubricants.

Reference	Shear rate [s^{-1}]	Viscosity [10^{-3} Pa s]
C10	1650	2.8
C50	1650	7.1
C4	1650	8.0
C100	1650	11
CC	1690	25
C8	1690	83
C17	1600	85
CD	1690	104
C6	1600	112
C5	1600	131
CA	1690	210

Table 5.4

Solutions of SCMC and their viscosities used as lubricants.

Temperature (°C)	A_{585}	NAG released (μg/ml)
22	0.260	22
30	0.325	27
37	0.318	26

Table 5.5

Effect of temperature of hyaluronidase digestion of synovial fluid on amount of NAG released.

Mixture	Synovial Fluid [ml]	Hyaluronic acid [ml]	Sodium Acetate Buffer [ml]	Hyaluronidase solution [10,000 NF units/ml] [ml]
A	0.5	-	1.5	-
B	0.5	-	1.3	0.2
C	-	0.5	1.5	-
D	-	0.5	1.3	0.2
E	0.5	0.5	1.0	-

Table 5.6

Mixtures used to investigate effect of pH on hyaluronidase digestion.

Volume of BAEE solution (ml)	Volume of synovial fluid (ml)	Mass of trypsin in 0.1 ml of solution (μg)	$\Delta A\ min^{-1}$
3.0	-	40	0.16
3.0	-	200	too fast to record
3.0	0.1	100	0.012
3.0	0.1	200	0.075

Table 5.7

Rate of change of absorbance of BAEE substrate with different concentrations of trypsin and synovial fluid.

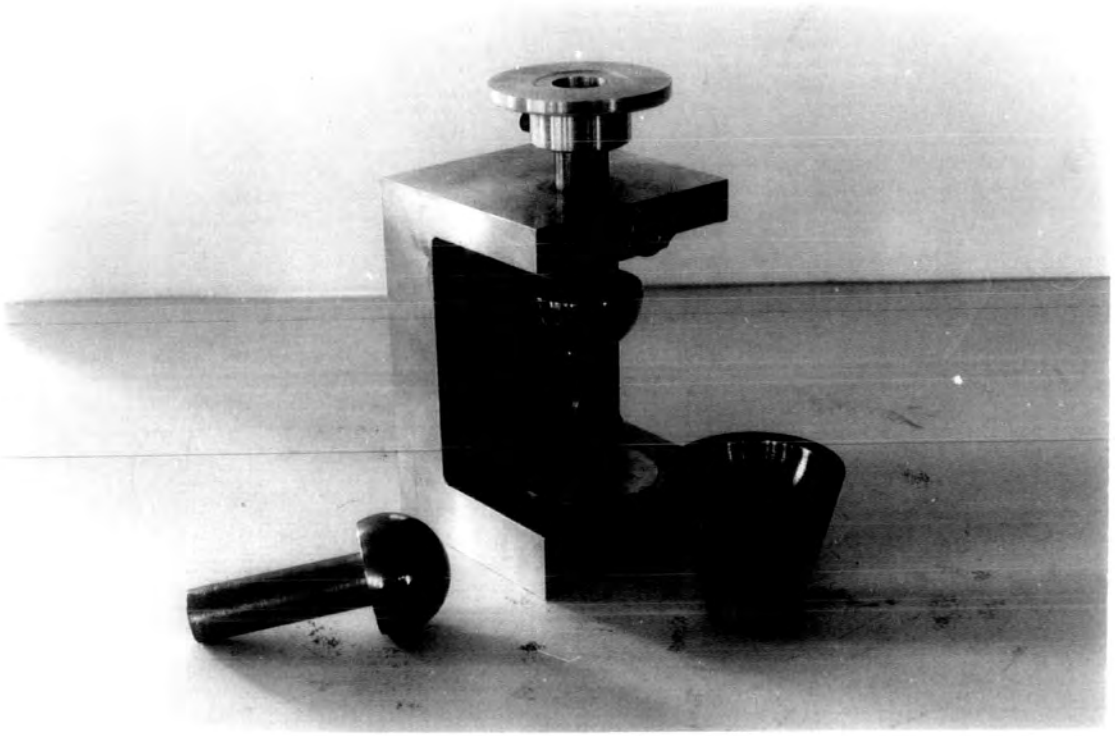

Figure 5.1

Moulding jig for compliant layers

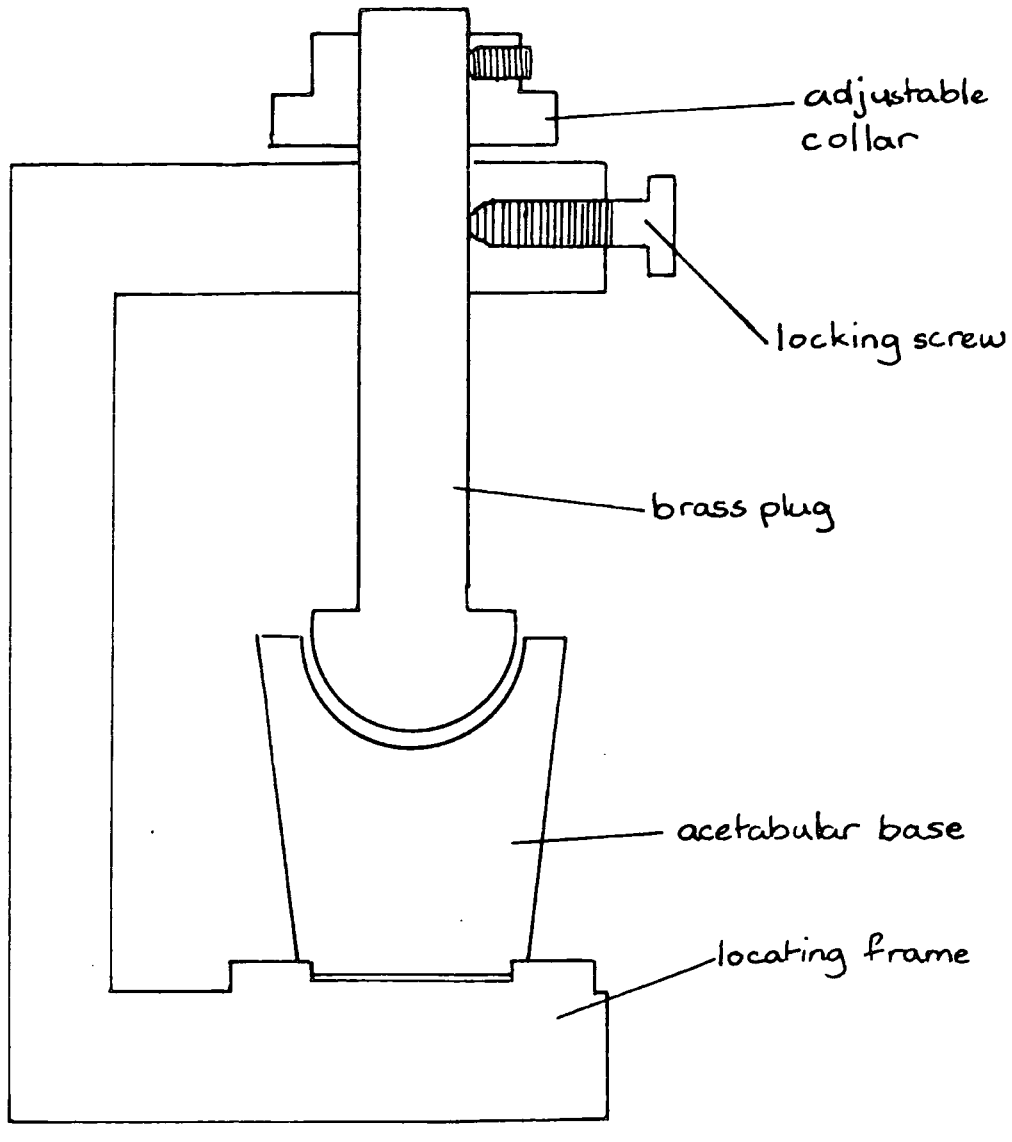

Figure 5.2

Cross section of moulding jig for compliant layers [not to scale].

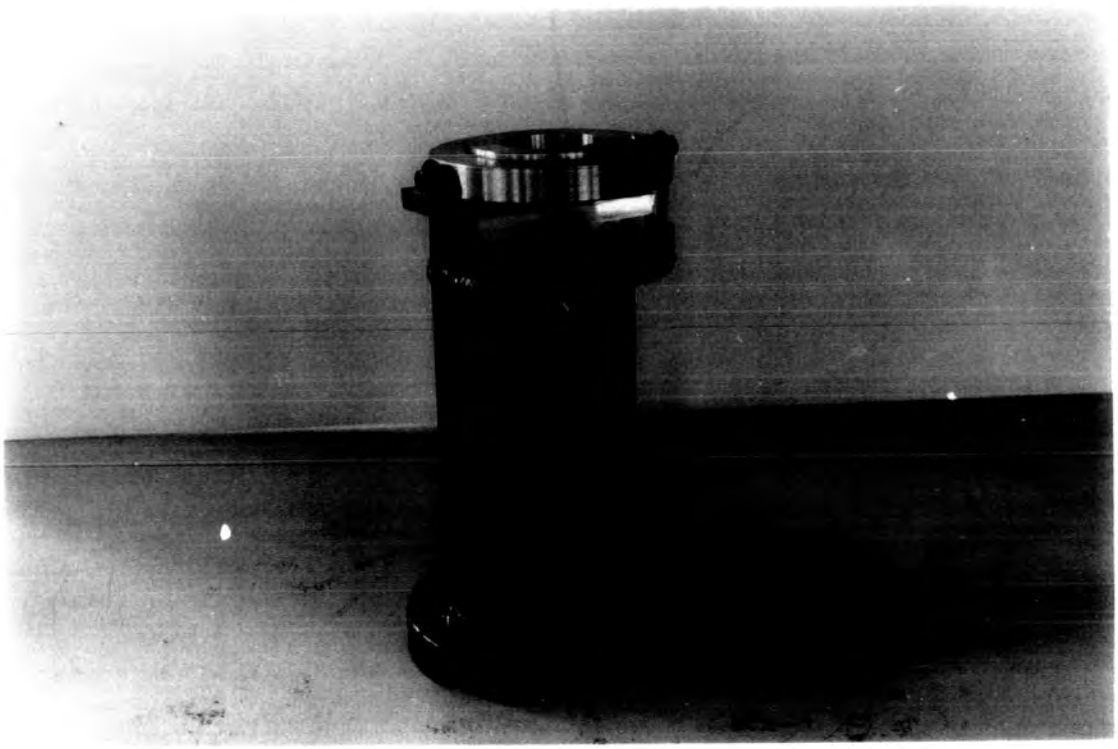

Figure 5.3

Clish's apparatus for measuring the elastic modulus of an elastomer

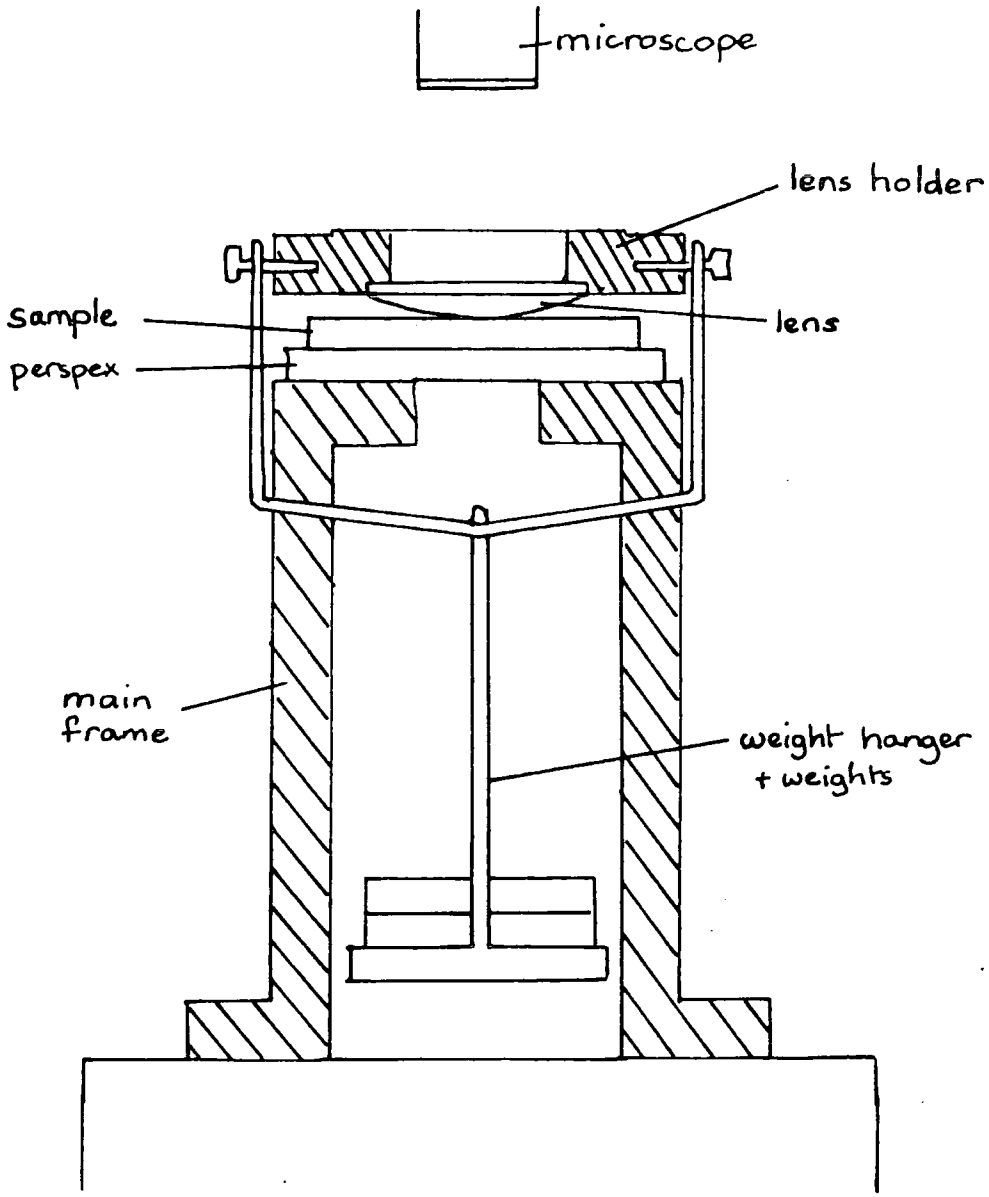

Figure 5.4

Cross-section of Clish's apparatus for measuring the elastic modulus of an elastomer.

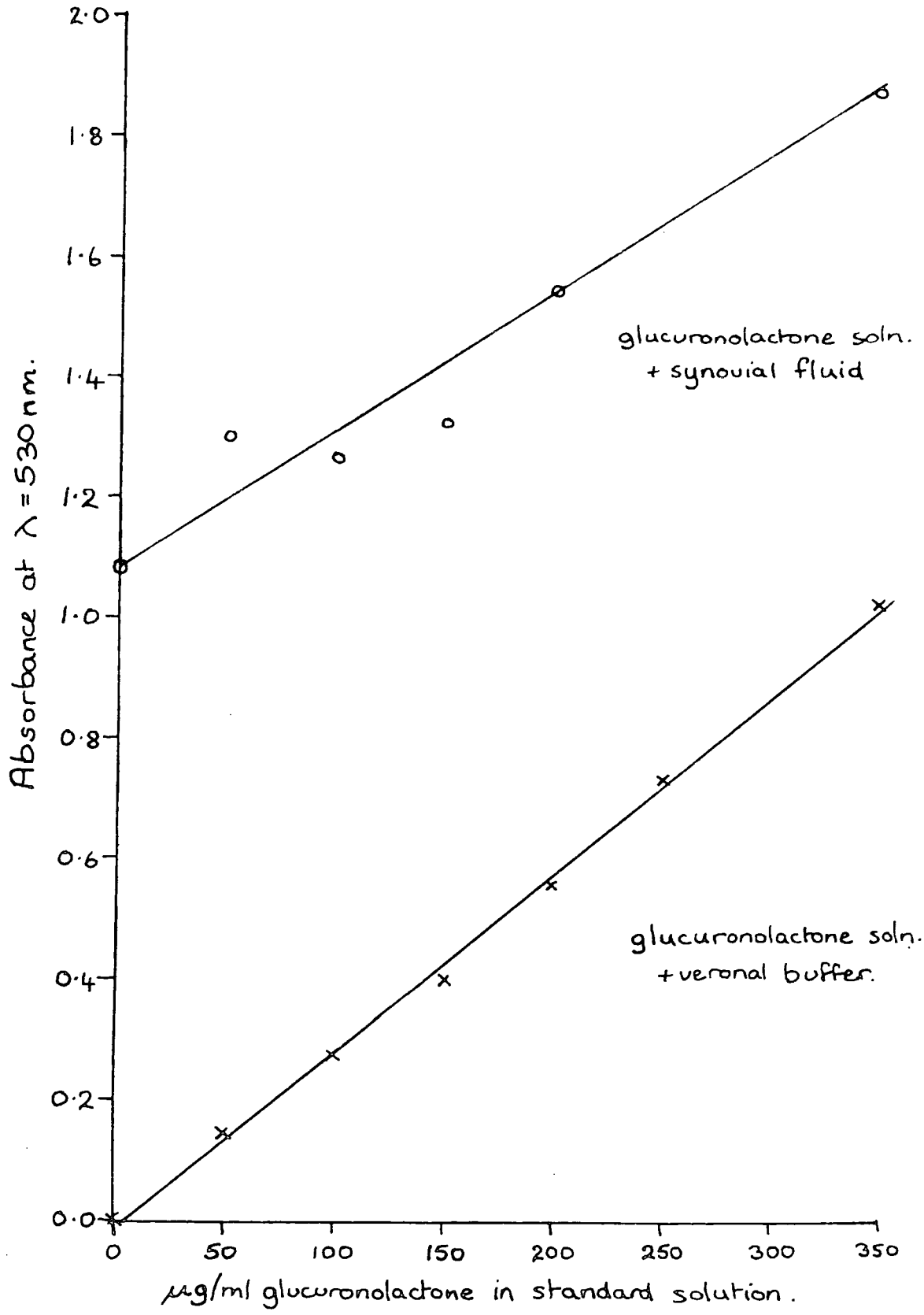

Figure 5.5

Effect of presence of synovial fluid on standards assay for uronic acid.

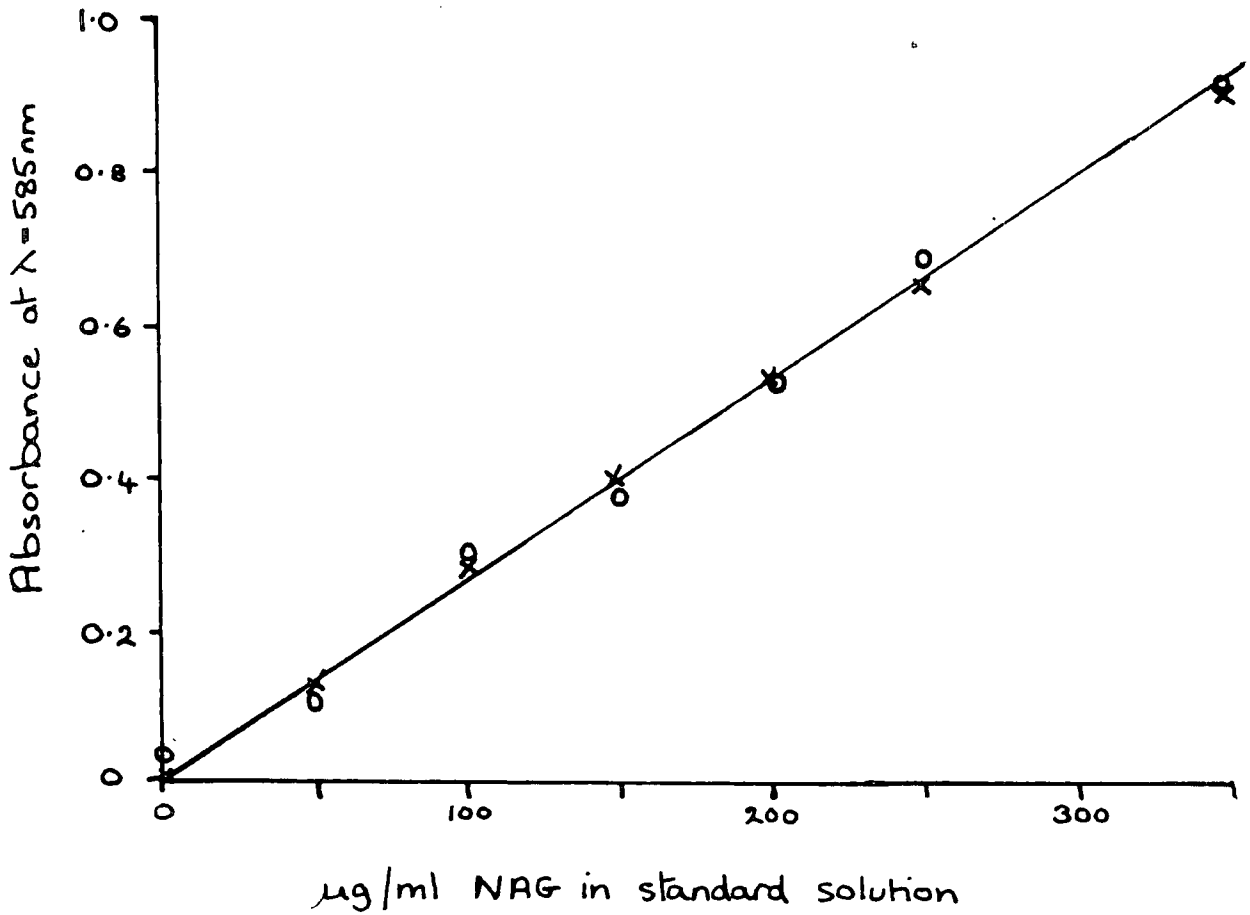

Figure 5.6

Calibration curve for NAG assay. x—x veronate buffer in reaction mixture

o—o synovial fluid in reaction mixture

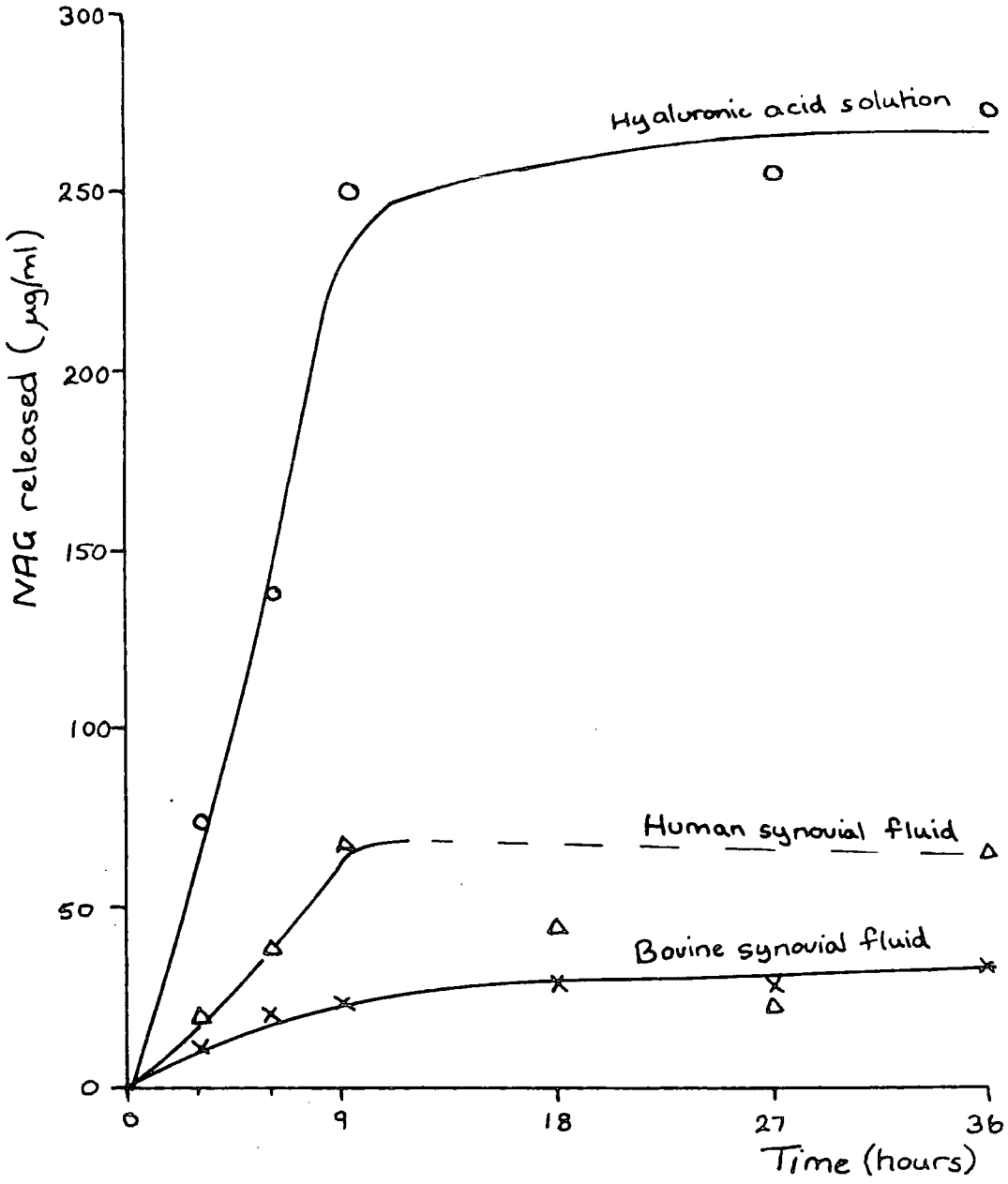

Figure 5.7

Graph showing NAG released after different times of digestion with hyaluronidase.

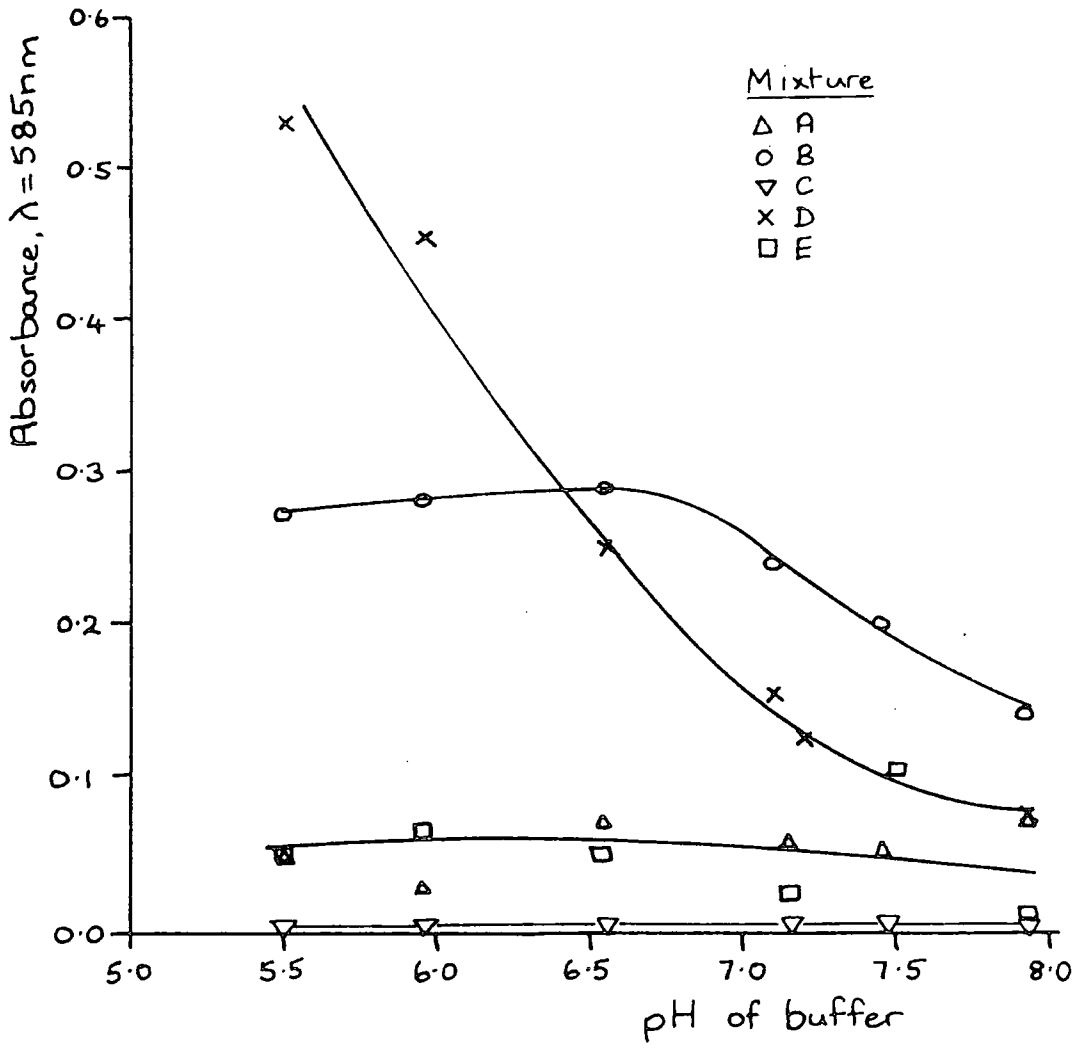

Figure 5.8

Effect of pH of solution on amount of NAG released.

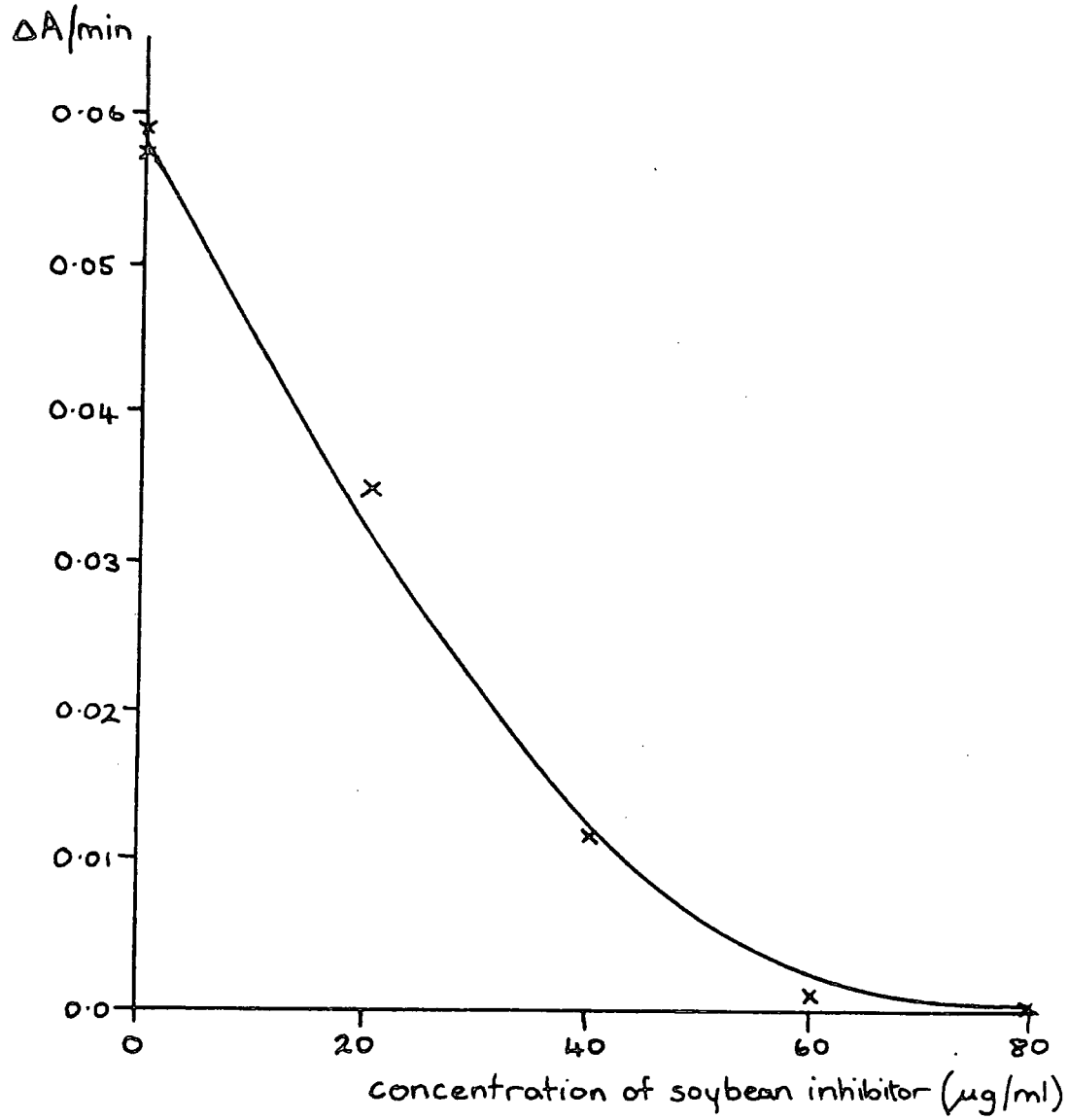

Figure 5.9

Effect of standard soybean inhibitor on trypsin digestion of BAEE.

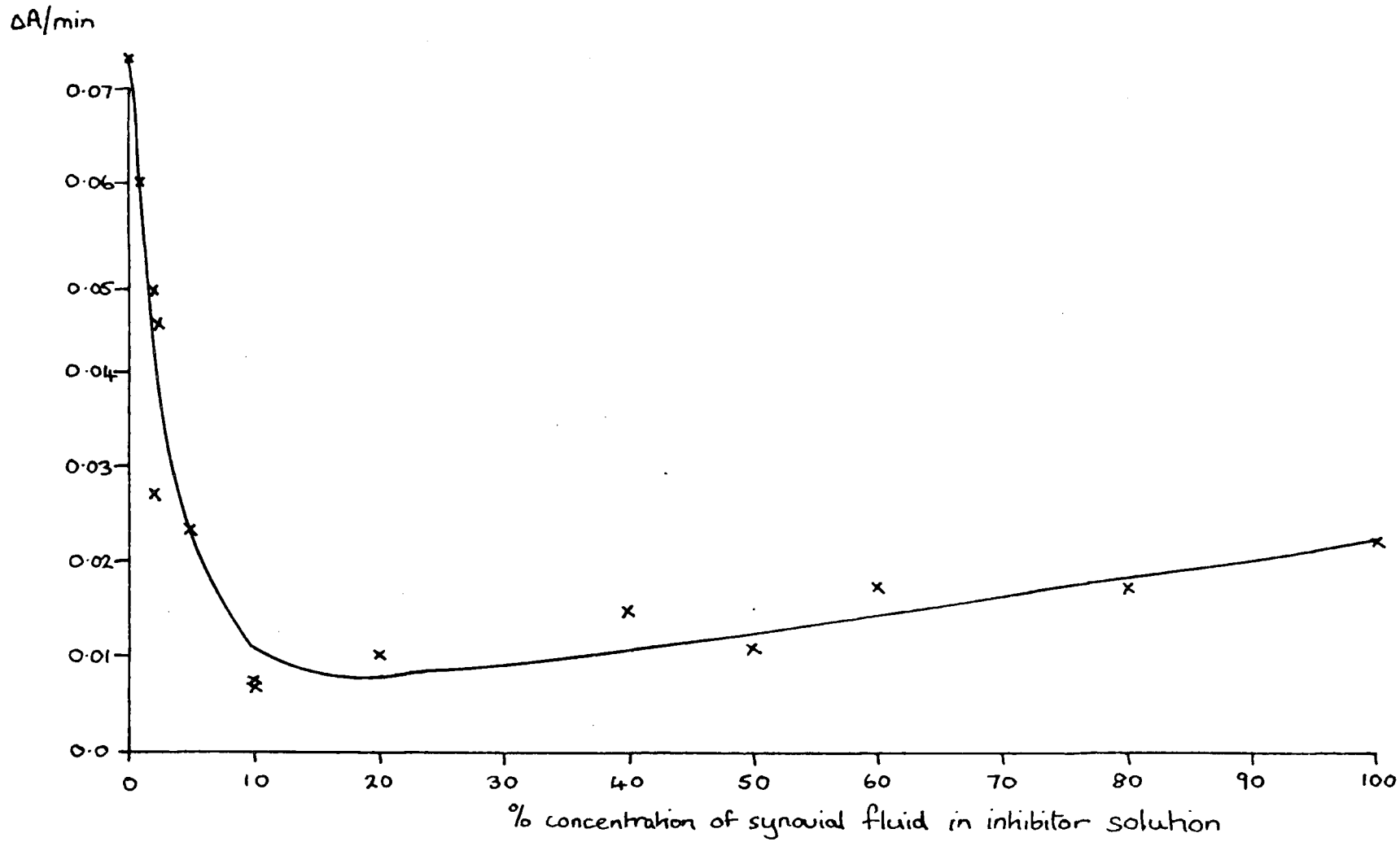

Figure 5.10

Effect of using synovial fluid as an inhibitor to the action of trypsin on BAEE.

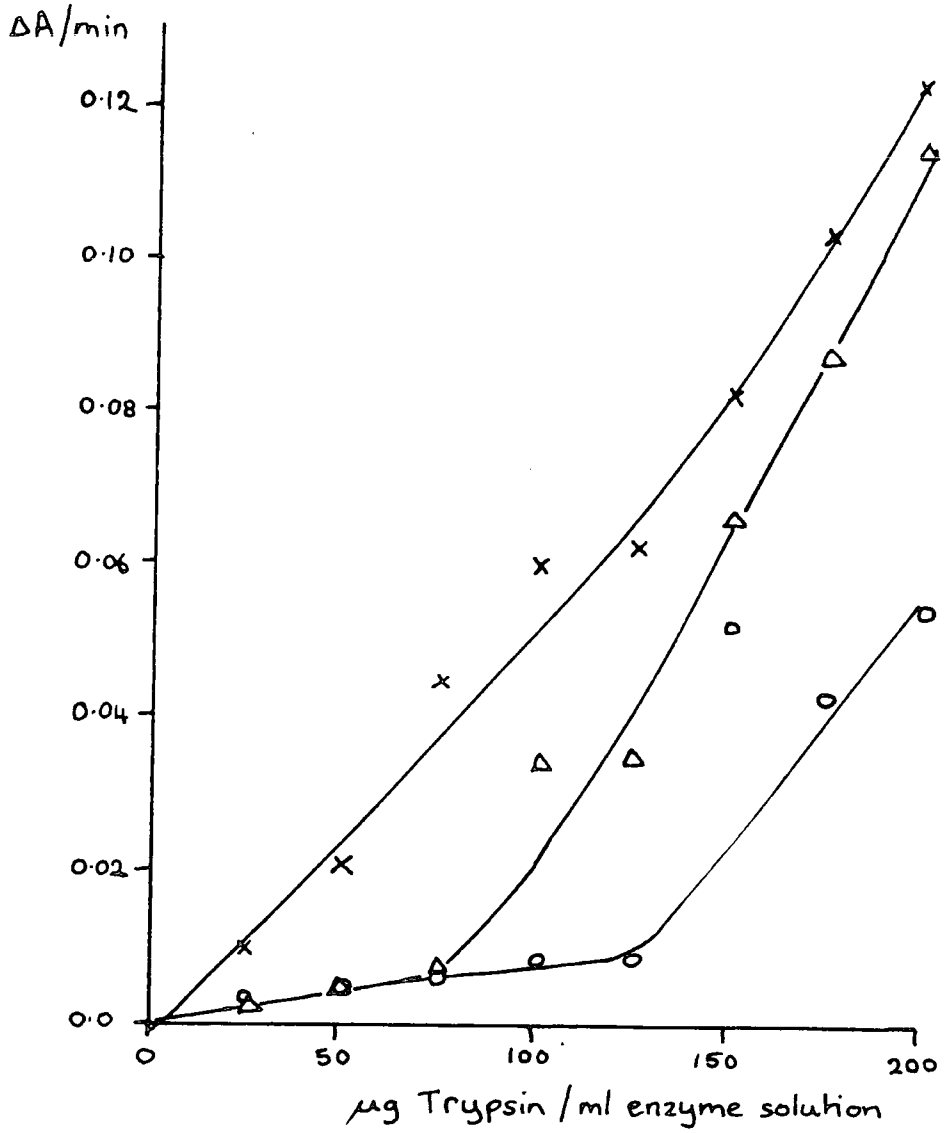

Figure 5.11

Effect of varying trypsin concentration on inhibitor action of synovial fluid.

CHAPTER SIX

RESULTS - PRELIMINARY TESTS AND NATURAL JOINTS

The main results of this work fall into two categories: those concerned with natural joints lubricated with synovial fluid, and those resulting from the work on prostheses with compliant linings. However there are also preliminary tests to check the functioning of the simulator, viscosity measurements of fluids which were used with both natural and artificial joints and elasticity tests.

The hip function simulator was used to obtain the frictional torque developed in the joint when subjected to a dynamic loading cycle and from this a friction factor was calculated. The friction factor was defined as

$$\mu = \frac{\text{Frictional Torque}}{\text{Applied load} \times \text{Radius of head}}$$

[Unsworth, 1978]

The friction factor differs from the coefficient of friction since the radius of contact is not equal to the radius of the head except under point contact conditions.

The friction factor was calculated at five points through half a cycle of loading and oscillation as shown in Figure 4.4. The values of frictional torque at a particular point for the two halves of the cycle were averaged. Since the loading cycle is almost symmetrical this averaging eliminates errors in the magnitude of frictional

torque caused by off-centre mounting of the joint.

Table 6.1 gives typical loads and sliding speeds for a natural joint 54 mm in diameter for three frequencies of oscillation. All the lubrication tests were repeated at the same three frequencies of oscillation namely 0.65, 0.83 and 1.0 Hz. Points 1, 2 and 3 were at low loads while points 4 and 5 were in the highly loaded region. The sliding speed, u , varied sinusoidally with time and could be calculated at any time, t, in the cycle as follows:

$$u = u_o \cos\left(\frac{2\pi}{T}\right) t$$

where T is the time for one complete cycle, and u_o is the maximum sliding speed. For a joint of radius r oscillating with an amplitude θ,

$$u_o = \frac{2\pi r \theta}{T}$$

therefore $$u = \frac{2\pi r \theta}{T} \cos\left(\frac{2\pi}{T}\right) t$$

Point 2 was taken at the maximum speed and points 1 and 3 are the same speed (but opposite direction) each side of the maximum. Points 4 and 5 are slower speeds.

For the lubricants which were available over a wide viscosity range the results obtained for the friction factor have been plotted against $\eta u/L$ where η is the viscosity, u the sliding speed and L the applied load. As shown in Chapter 3, this is a useful method for

demonstrating the lubrication mechanism which may be operating.

6.1 Preliminary tests with Charnley metal on UHMWPE prosthesis

Initial tests used a Charnley metal on plastic joint, of 22 mm diameter, to ensure that the results obtained were consistent with previous work in this field [O'Kelly, 1977]. Figures 6.1 and 6.2 show the results obtained using the full range of silicone fluids available [see Table 5.3] as lubricants. Figure 6.1 are the results taken at point 2 in the cycle, where the load was 50N and the sliding speed 7.3 mm s^{-1}. The data in Figure 6.2 was taken from point 5 in the cycle, where the load was 1470N and the sliding speed 1.5 mm s^{-1}. The frequency of oscillation was 0.83 Hz and the amplitude of oscillation was 8^{o}.

The tests were repeated with a larger amplitude of 13.5^{o}, and these results are shown in Figure 6.3. The load for point 2 was 50N and for point 5, 1500N. As the angle through which the joint oscillated was larger for the second set of tests, the sliding speeds were correspondingly greater, 12.2 and 2.6 mm s^{-1} respectively.

In all these graphs, the friction factor decreased as the viscosity of the lubricant increased. The friction factors for the lower loads and faster sliding speeds [point 2] were more than double the values for point 5.

When the amplitude of oscillation was increased from 8^{o} to 13.5^{o}, the friction factor also increased except for the low load and low viscosity points where the friction factor retained its already high value (up to 0.14). These curves are similar to those obtained by O'Kelly [1977] with the maximum values of friction factor about the same but the lowest friction factor around half the value she obtained.

Since there was an obvious difference between the results obtained for the friction factor at different sampling points, it was decided to evaluate results obtained with a constant load throughout the cycle of oscillation so that the only variable through a cycle would be the sliding speed. To achieve this the cam was removed from the simulator and oil added to the loading system through cylinder B [Figure 4.7] until the required value of load was reached. Three values of load were used with each lubricant: these were approximately 500N, 1000N and 1500N; the exact values were recorded each time. The tests were run with the same eight silicone fluids that were used previously and 0.83 Hz frequency of oscillation.

The friction factor was calculated for the 5 points through the cycle. Points 3, 4 and 5 gave very similar curves [Figures 6.6, 6.7, 6.8], with point 2 [Figure 6.5] reaching lower values of μ and point 1 [Figure 6.4] lower

still. The curves all decreased initially as viscosity increased then showed an almost constant value for the friction factor, except for point 1 which displayed erratic behaviour. The three different loads led to separate curves at low values of $\eta u/L$, with the lowest load giving the highest value of friction factor, but the curves coalesced as the viscosity of the lubricant increased. The friction factors measured were generally higher than for the corresponding $\eta u/L$ values with dynamic loading.

6.2 Lubrication tests with human hip joints

The results obtained from tests with synovial fluid and synthetic lubricants in conjunction with human hip joints will be described in this section. Details of each of the nine hip joints used will be given together with all the tests performed with that particular joint.

Hip joint H1

H1 was a female, 78 year old joint in good condition with a mean diameter of 43 mm. When first mounted and tested in the simulator, it was found to be sufficiently off-centre for the trace of frictional torque to remain on one side of the zero line, instead of reversing with the changing direction of motion. The hip joint was then removed from its holders and frozen whilst the setting up rig was checked and eventually modified to the form described in Chapter 4 by the addition of vertical parallels which could be used in conjunction with an internal micrometer for accurate centring.

H1 was thawed and reset successfully. It was tested with Ringer's solution and a sample of synovial fluid at each of the three different frequencies of oscillation and an amplitude of 14^{o}. The friction factor was calculated at points 2 and 5 through the cycle and plotted against u/L since the viscosities of the fluids were not known.(Figure 6.9). The cluster of points on the left of the graph correspond to the highly loaded data (point 5) whilst the higher friction factors were obtained from the lower loaded parts of the cycle.

Hip joint H2

A male, 62 year old hip with traces of cartilage fibrillation. Its diameter was 54 mm. This joint was also used on a trial basis to perfect the setting up and testing technique. Some preliminary tests were run with treated synovial fluid but the digestion conditions had not been completely determined by this time. The hyaluronidase digestion was carried out by adding 0.3 ml enzyme solution (containing 1000 NF units per ml veronate buffer) to 3.0 ml synovial fluid. Both this and the control sample of synovial fluid were incubated for 18 hours at $37^{o}C$.

The results (Figures 6.10, 6.11) show that the friction factor varied from 0.035 to 0.105, the lower values occurring with higher loads. There was a slightly increasing trend in friction factor as u/L increased. Again, viscosity measurements were not available. At high loads (Figure 6.12) all the results for the friction

factor were in the range μ = 0.06 to 0.08 and it was not possible to distinguish between fluids. At low loads, the results for point 1 were obviously lower than those for points 2 and 3. Comparing each point separately between lubricants, the friction factor was lowest for untreated synovial fluid, slightly higher for synovial fluid digested with hyaluronidase and higher still for Ringer's solution. The effect of hyaluronidase digestion is shown more clearly in Figure 6.13 for a low loaded point and a highly loaded point in the cycle.

Hip joint H3

This was a 63 year old male hip joint of diameter 52.2 mm. It was in good condition.

A range of eleven lubricants were prepared for testing with this joint. All the synovial fluid used came from one sample. The lubricant solutions are detailed in Table 6.2. Also shown in this table are the viscosity values used. These are the viscosities measured at a shear rate of 1100 s^{-1} with the Ferranti-Shirley cone and plate viscometer. The use of the viscosity measurement at a high shear rate is discussed in Chapter 8. The viscosity reduced considerably after digestion with hyaluronidase - from 6.3 x 10^{-3} Pa s down to 1.4 x 10^{-3} or 1.6 x 10^{-3} Pa s. Those samples digested with trypsin [D, H] retained a high value of viscosity.

The results obtained from the lubrication tests are illustrated by Figure 6.14 which shows the data from

lubricants J (untreated synovial fluid) and K (Ringer's solution). The highly loaded part of the cycle (points 4 and 5) produced friction factors in the range 0.02 to 0.03 for all the lubricants. The more lightly loaded region (points 1, 2 and 3) gave values for the friction factor ranging from 0.01 up to 0.04, the values increasing as $\eta\omega/L$ increased. The graph shows Ringer's solution to be an inferior lubricant to synovial fluid. A noticeable feature on all the curves for this joint is the discontinuity in friction factor between the high and low loaded regions. The effect of enzymatic digestion on friction factor is shown by the histograms in Figure 6.15. There was an increase in friction factor for point 2 (lightly loaded) after digestion with hyaluronidase but no consistent change for point 4 (heavy load). Trypsin digestion resulted in a change in friction factor which was either an increase or a decrease for both points 2 and 4.

An N-acetyl-glucosamine assay was performed on samples of fluids A - H and those samples treated with hyaluronidase (B and F) showed an increase in A_{585} over the blanks.

Hip joint H4

This male, 60 year old joint was in good condition. A full range of lubricants was prepared and tested with this joint and it was not until the NAG assay revealed

no change in the fluid after digestion that it was realised that the synovial fluid had a pH of 8.7 which was too alkaline for the enzyme to be very active. After this point in the project, all the fluids were dialysed to a constant pH of 7.2 before use. The results for this joint are included to show that repeated testing of the same joint produces consistent results if the lubricant is unchanged. Figure 6.16 is a composite graph for all 5 points and all lubricants used. The shape of the curve is very consistent between fluids. The friction factors are high, starting at around 0.06 for the high loads and increasing to 0.3 at low loads and high sliding speeds.

Hip joint H5

A 74 year old male joint in good condition.

A full range of lubricants was prepared as detailed in Table 6.3. A NAG assay was performed on samples of all the fluids and the amount of NAG released was calculated for fluids C - F, which showed an increase in absorbance over the other fluids. These four fluids, which had been digested with hyaluronidase showed a decrease in viscosity to around one quarter of the value for undigested fluids. After 1 hour the digestion was not complete, although most of the reduction in viscosity had already occurred. It made little difference to the digestion if the amount of hyaluronidase used was increased from 0.01 ml per ml synovial fluid (C and D) to 0.04 ml (E and F).

The lubrication tests in the hip function simulator were run as usual with the lubricants used in a random order. However the values for the friction factor when calculated appeared to decrease as the tests progressed. The zero load position when measured at the end of the series of tests was considerably higher than at the commencement. This resulted in the recorded load readings towards the end of the series being greater than the actual values of load. Hence the calculated friction factor was less than the true value. For this reason only those lubricants which were tested adjacent to each other could be sensibly compared. Figure 6.17 shows the results from fluids B5 and C5. B5 is the control sample incubated without enzyme whilst C5 had hyaluronidase added and produced higher values of friction factor at point 2 (low load).

Hip joint H6

H6, of diameter 49 mm, was a male 64 year old joint in good condition. The range of natural lubricants prepared and tested with this joint are detailed in Table 6.4. Again the action of hyaluronidase reduced the viscosity by a factor of four. This was achieved after only one hour's incubation, even though the quantity of NAG released increased with an extended incubation time.

The results obtained by comparing enzymatically treated and untreated fluids are shown in Figure 6.18. Once more, the friction factors for hyaluronidase treated fluids

(C6, D6) were consistently higher (for point 2) than the controls (A6, I6). The corresponding results for trypsin show considerable differences in friction factor with enzymatic treatment (for example μ may increase from 0.014 to 0.058) but they show no consistent pattern - sometimes the friction factor is increased sometimes decreased by a similar amount.

Joint H6 was also tested with a series of synthetic lubricants. These were 5 solutions of sodium carboxy-methylcellulose (SCMC) in water, chosen as they exhibit non-Newtonian properties similar to synovial fluid. Their viscosities are given in Table 5.4. The fluids used were C10, C50, C100, C4 and C5. Figures 6.19 and 6.20 show the results for friction factor plotted against $\eta u/L$. Each lubricant was tested at each of the three speeds used previously. Figure 6.19 shows the results for the low load part of the cycle. The data for point 1 has been separately identified as again it gave much lower values for friction factor than points 2 and 3. The data shows a decreasing trend as the viscosity of the lubricant increases.

Figure 6.20 shows the results for the highly loaded part of the cycle (points 4 and 5). These friction factors are almost constant around $\mu = 0.02$, though there is a slight decrease as the viscosity increases. Their values lie between those of point 1 and points 2 and 3.

Hip joint H7

This joint came from a 63 year old male and had a diameter of 49 mm. It was in good condition but one week old when used in the simulator as it had previously been used by another student. It was only tested with synthetic lubricants.

The same five SCMC lubricants were used as for H6 and the results again plotted as friction factor against $\eta u/L$ on a logarithmic scale. Considering Figure 6.21, which shows the results for the low loading, the data for point 1 is again lower than points 2 and 3 but there is more overlap in the results for this joint. The friction factor decreases from around 0.055 to 0.01 as $\eta u/L$ increases from 5×10^{-7} to 10^{-4} m^{-1}.

The highly loaded results (points 4 and 5) are displayed in Figure 6.22. These show an almost constant friction factor of around 0.02 for point 4 and slightly lower - around 0.01 - for point 5.

H7 was also tested with a range of silicone fluids as lubricant. These are Newtonian in character and their viscosities are given in Table 5.3. A total of seven fluids were used with viscosities ranging from 9.4×10^{-3} to 29.1 Pa s. All the results are shown in Figure 6.23. The low load points (1, 2 and 3) all lie in the same band which increases from $\mu = 0.02$ to $\mu = 0.13$ as the viscosity increases. The increase in friction factor above a viscosity of 1 Pa s is very marked. The high

load points (4 and 5) produce lower values of friction factor (0.007 to 0.04) and do not exhibit the sharp increase with viscosity of the low load points.

Hip joint H8

This male, 54 year old joint had a diameter of 45 mm and was in good condition.

Table 6.5 shows the range of lubricants prepared from synovial fluid, together with their viscosities. This sample of synovial fluid had a higher viscosity than the previous samples used - around 9×10^{-3} Pa s - which was reduced to 2×10^{-3} Pa s by hyaluronidase action. The histograms in Figure 6.24 show the friction factor which varies from 0.06 up to 0.10. Once again the friction factor was increased after hyaluronidase digestion for the low loads, and also for four out of the six high load readings. Trypsin digestion of the fluids had no consistent effect on the friction factor.

Hip joint H9

This 79 year old female hip joint had a diameter of 41 mm and was in good condition. Both natural and synthetic lubricants were tested with this joint.

The natural lubricants are detailed in Table 6.6. The usual range of fluids treated with hyaluronidase, and their corresponding controls were used. In addition powdered hyaluronic acid was added to several samples of

synovial fluid to attempt to obtain an increased viscosity range. The viscosity was increased from 5.2×10^{-3} Pa s up to 0.373 Pa s by the addition of 10 mg hyaluronic acid to 1 ml synovial fluid.

Figure 6.25 shows the histograms for the change in friction factor with hyaluronidase action. The results from point 2 (low load) showed a very substantial increase in friction factor after digestion. The results from point 4 (high load) showed no significant change.

The data for lubricants P9, Q9, R9 and S9 (synovial fluid with added hyaluronic acid) were plotted in the familiar form of friction factor, μ against $\eta u/L$ (Figure 6.26). Point 1 produced results sufficiently low as to coincide with the high load results (points 4 and 5). These produced an almost constant friction factor of around 0.03. Points 2 and 3 produced friction factors which were mostly in the range 0.06 to 0.08 and which had a slight minimum at $\eta u/L = 3 \times 10^{-6}$ m^{-1}. This corresponds to a viscosity of 0.025 - 0.1 Pa s.

Figure 6.27 shows that the results for SCMC are very similar to those for synovial fluid with hyaluronic acid added. The main difference is that the friction factor at point 1 has increased and the data for points 2 and 3 became more obviously separated. The minimum in friction factor at low loads is not so pronounced.

When silicone fluid was used as a lubricant for joint H9 the friction factor at the low load points increased with viscosity of the lubricant (Figure 6.28). The viscosities of the silicone fluids reached much higher values (up to 29.1 Pa s) than either synovial fluid or SCMC solutions. The high load data produced a constant friction factor around 0.026.

6.4 Cartilage tests

When the lubrication testing had been completed on any particular joint, plugs of cartilage and bone were removed from the femoral head for elasticity testing as described in section 5.3.1. A typical trace obtained on the Instron chart is shown in Figure 6.29. Since the crosshead speed was constant at 20 mm min^{-1}, it took about 0.9 s to apply a load of 120N. From the load against compression trace obtained on the Instron, a new graph was plotted of stress against logarithmic strain. The stress was defined as load divided by the original cross-sectional area. The logarithmic strain, used since the strains involved are large, was defined as:

$$\varepsilon = -\int_{h_o}^{h} \frac{dh}{h} = \ln\left(\frac{h_o}{h}\right) = \ln\left(\frac{h_o}{h_o - d}\right)$$

where h_o is the initial thickness of cartilage, h the thickness at any given time, and d the decrease in thickness at that time. The curves obtained by replotting the data in this form for several plugs of cartilage from the femoral head of joint H6 are shown in Figure 6.30.

The inverse slope of the stress strain curve at any given point gives the compliance of the cartilage at that stress [Gore, 1981]. For these samples, the stress chosen was 3 M Pa since the curve is linear here. Table 6.7 gives the average values of compliance obtained for each of the joints tested, together with the thickness of the cartilage specimens.

Point	Frequency of Oscillation [Hz]	Load [N]	Sliding speed $[mms^{-1}]$
1	0.65	204	17.1
1	0.83	204	21.9
1	1.00	143	26.8
2	0.65	239	24.3
2	0.83	224	31.0
2	1.00	367	37.9
3	0.65	265	17.1
3	0.83	245	21.9
3	1.00	204	26.8
4	0.65	1325	9.8
4	0.83	1385	12.6
4	1.00	1467	15.4
5	0.65	1284	5.0
5	0.83	1365	6.5
5	1.00	1182	7.8

Table 6.1

Loads and sliding speeds for joint 54 mm in diameter.

Reference	Enzyme		Incubation		NAG assay		Viscosity at $1100s^{-1}$ [10^{-3} Pa s]
	H - hyaluronidase T - trypsin	Volume added to 3.0 ml synovial fluid [ml]	Temperature [°C]	Time [hours]	A_{585}	µg NAG released per ml synovial fluid	
A3	—	—	37	18	0.0	—	6.3
B3	H	0.03	37	18	0.049	20	1.6
C3	—	—	22	18	0.0	—	6.3
D3	T	0.1	22	18	0.0	—	7.5
E3	—	—	37	1	0.0	—	6.3
F3	H	0.03	37	1	0.033	14	1.4
G3	—	—	22	1	0.0	—	6.1
H3	T	0.1	22	1	0.0	—	5.7
I3	T	0.1	—	—	0.0	—	6.3
J3	—	—	—	—	0.0	—	6.3

Table 6.2

Joint H3: lubricants used for friction testing.

Reference	Enzyme		Incubation		NAG assay		Viscosity at 1290 s^{-1} [10^{-3} Pa s]
	H - hyaluronidase T - trypsin	Volume added to 3 ml synovial fluid [ml]	Temperature [°C]	Time [hours]	A_{585}	µg NAG released per ml synovial fluid	
A5	—	—	—	—	0.01	—	4.4
B5	—	—	37	1	0.0	—	4.2
C5	H	0.03	37	1	0.10	25	1.2
D5	H	0.03	37	18	0.24	62	1.0
E5	H	0.12	37	1	0.11	27	1.1
F5	H	0.12	37	18	0.28	72	1.0
I5	—	—	37	18	0.01	—	3.1
J5	—	—	22	1	0.01	—	4.0
K5	—	—	22	18	0.0	—	4.0
L5	T	0.1	22	1	0.0	—	4.0
M5	T	0.1	22	18	0.02	—	3.9
N5	T	0.1	22	0	0.0	—	4.0

Table 6.3

Joint H5: lubricants used for friction testing.

Reference	Enzyme		Incubation		NAG assay		Viscosity at 1290 s^{-1} [10^{-3} Pa s]
	H - hyaluronidase T - trypsin	Volume added to 3 ml synovial fluid [ml]	Temperature [°C]	Time [hours]	A_{585}	µg NAG released per ml synovial fluid	
A6	–	–	–	–	0.0	–	4.0
B6	–	–	37	1	0.0	–	4.1
C6	H	0.03	37	1	0.21	57	1.1
D6	H	0.03	37	18	0.37	98	1.1
I6	–	–	37	18	0.01	–	3.7
J6	–	0.1	22	1	0.0	–	4.1
K6	–	0.1	22	18	0.0	–	4.1
L6	T	0.1	22	1	0.0	–	3.7
M6	T	0.1	22	18	0.0	–	3.6
N6	T	0.1	–	–	0.0	–	4.1

Table 6.4

Joint H6: lubricants used for friction testing.

Reference	Enzyme		Incubation		NAG assay		Viscosity at 1290 s^{-1} (10^{-3} Pa s)
	H - hyaluronidase T - trypsin	Volume added to 3 ml synovial fluid (ml)	Temperature (^{o}C)	Time (hours)	A_{585}	µg NAG released per ml synovial fluid	
A8	—	—	—	—	0.01	—	8.7
B8	—	—	37	1	0.02	—	8.9
C8	H	0.03	37	1	0.29	61	2.0
D8	H	0.03	37	18	0.61	140	2.2
I8	—	—	37	18	0.01	—	8.3
J8	—	—	22	1	0.01	—	9.2
K8	—	—	22	18	0.01	—	9.0
L8	T	0.1	22	1	0.01	—	—
M8	T	0.1	22	18	0.0	—	9.1
N8	T	0.1	—	—	0.0	—	—

Table 6.5

Joint H8: lubricants used for testing.

Reference	Units of hyaluronidase added per ml synovial fluid	Incubation		Added hyaluronic acid (mg per ml synovial fluid)	Viscosity at 1290 s^{-1} (10^{-3} Pa s)
		Temperature (^{o}C)	Time (hours)		
A9	—	—	—	—	5.6
B9	—	37	1	—	5.2
C9	100	37	1	—	2.0
D9	100	37	18	—	1.9
I9	—	37	18	—	5.3
P9	—	—	—	—	5.2
Q9	—	—	—	2.5	26.0
R9	—	—	—	5	92.7
S9	—	—	—	10	373

Table 6.6

Joint H9: natural lubricants used for friction testing.

Joint Reference	Average thickness (mm)	Average compliance (10^{-8} m^2 N^{-1})
H2	1.86	5.9
H3	2.36	9.1
H4	2.32	4.6
H5	2.06	5.1
H6	1.93	4.5
H7	2.04	6.0
H8	2.27	5.4

Table 6.7

Human hip joints. Values of compliance and cartilage thickness.

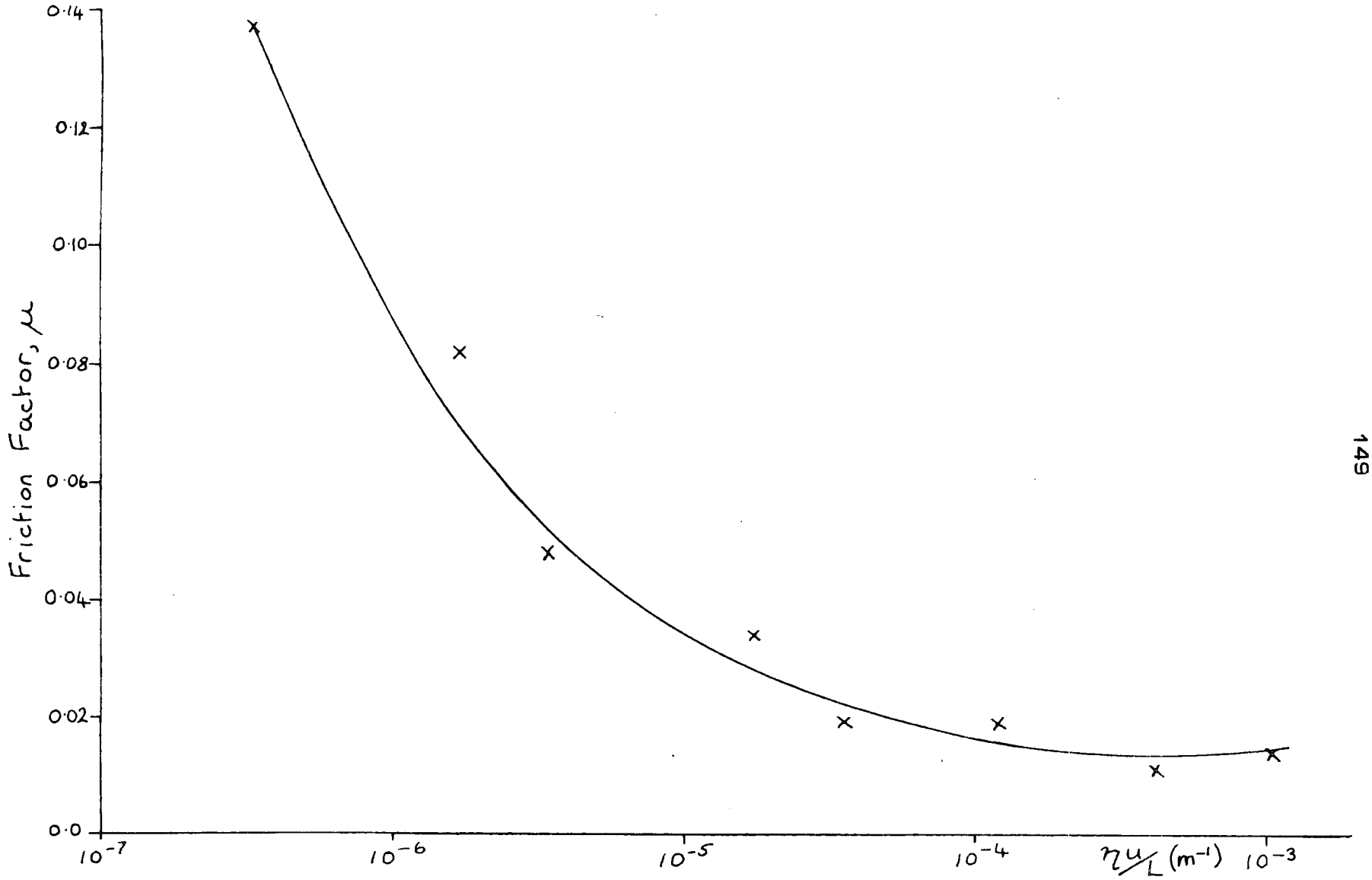

Figure 6.1

Charnley prosthesis lubricated with silicone fluids. Data From point 2 (low load).

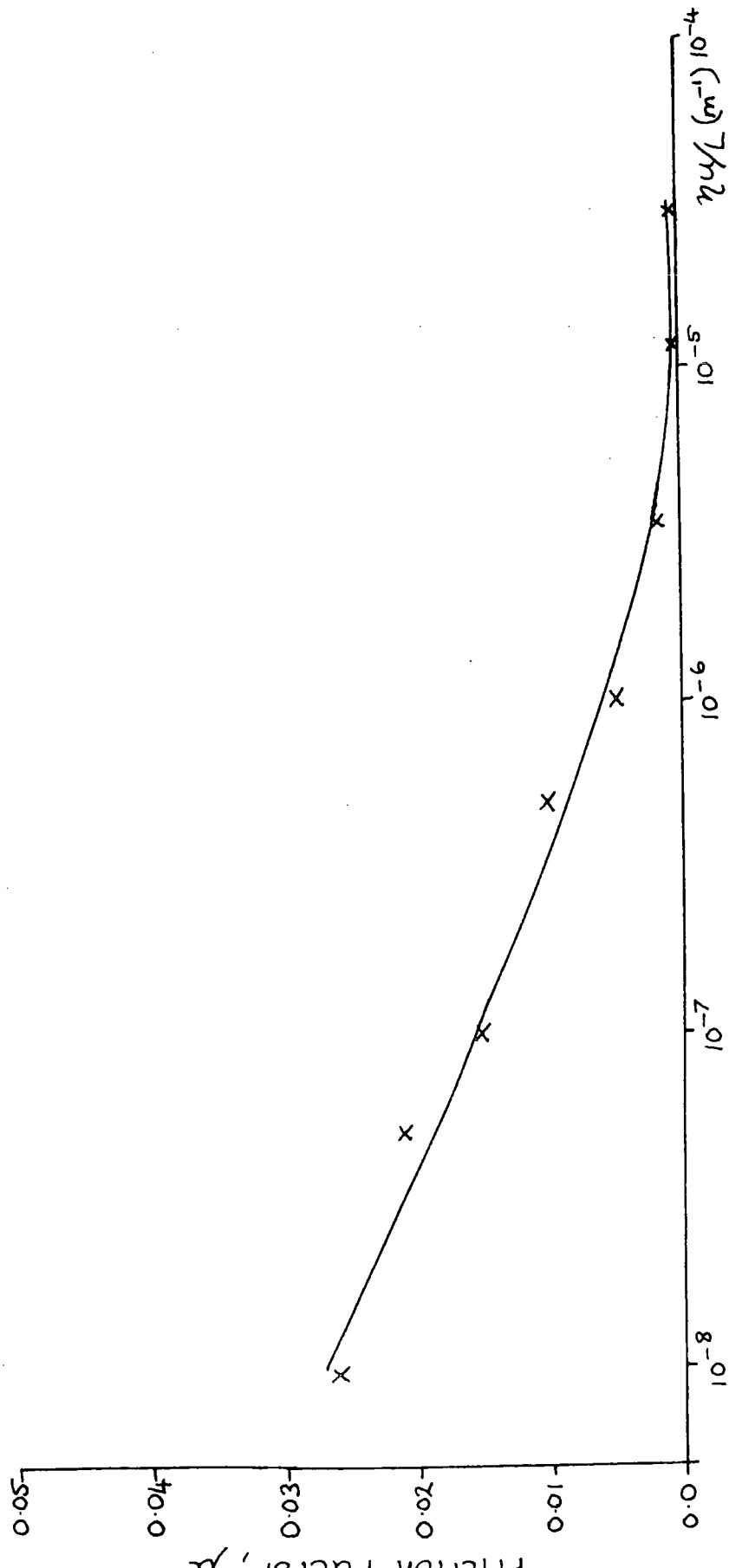

Figure 6.2

Charnley prosthesis lubricated with silicone fluids. Data from point 5 (high load).

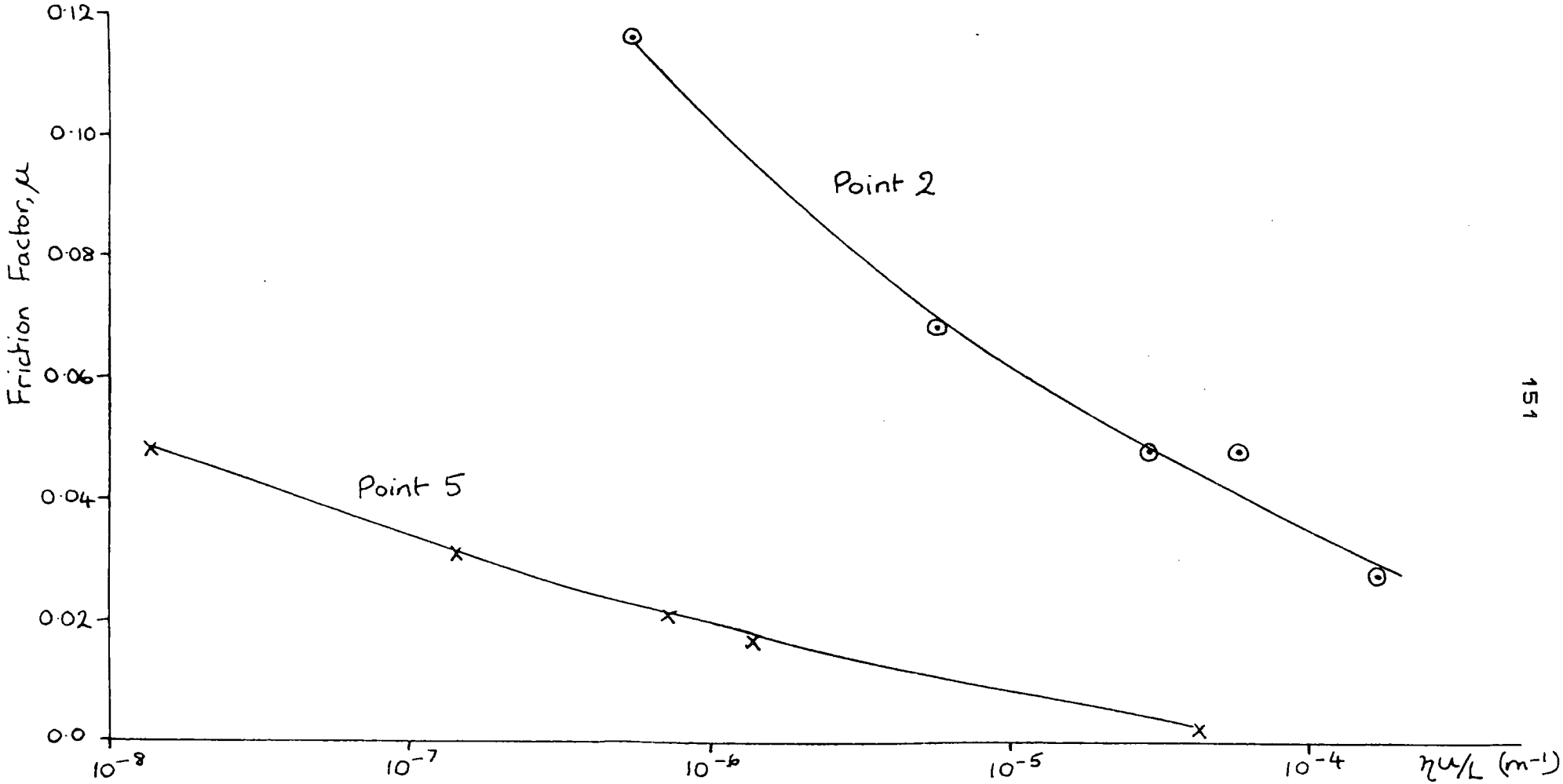

Figure 6.3

Charnley prosthesis lubricated with silicone fluids. Data from points 2 and 5, amplitude 13.5°.

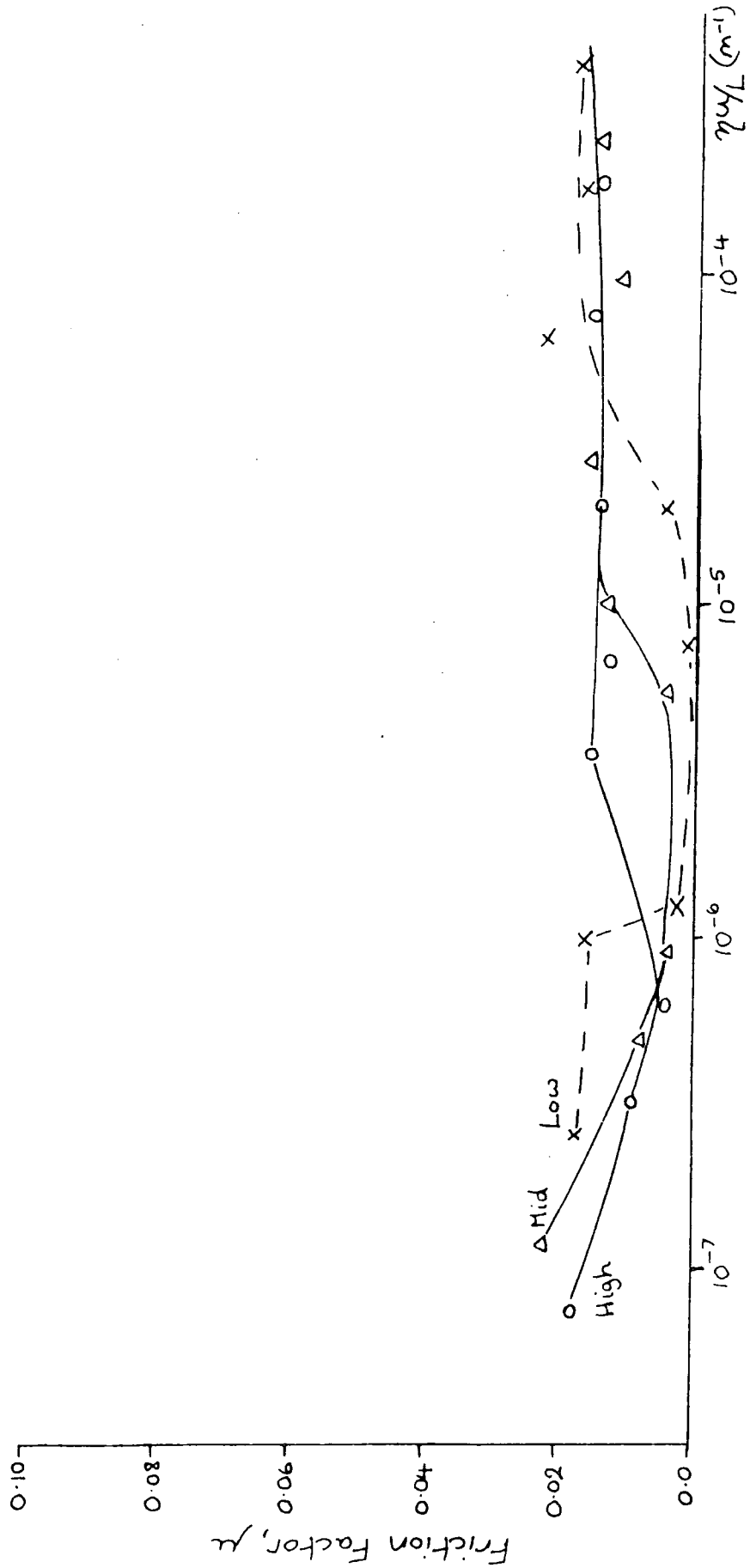

Figure 6.4

Charnley prosthesis lubricated with silicone fluids. Constant loading throughout cycle - point 1.

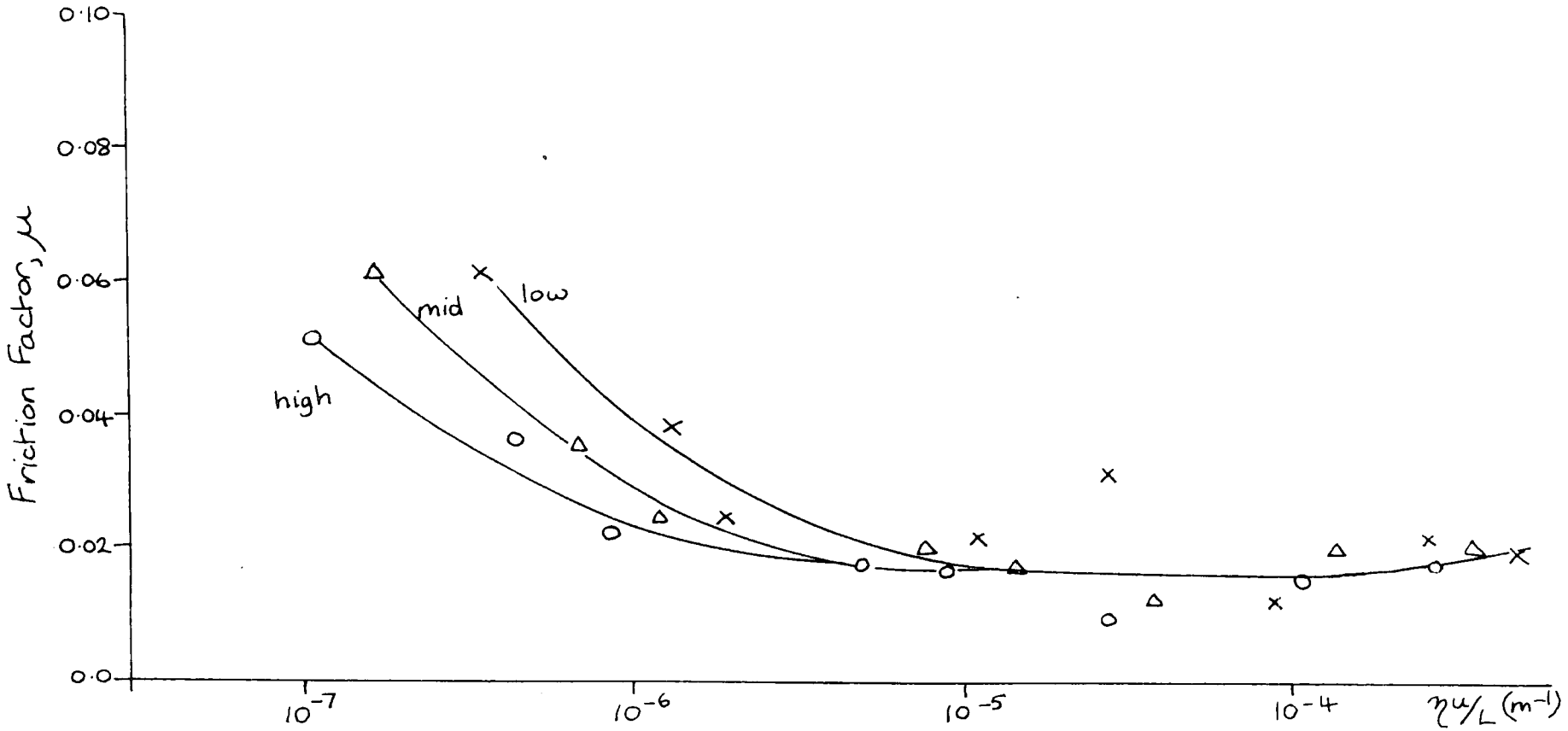

Figure 6.5

Charnley prosthesis lubricated with silicone fluids. Constant loading throughout cycle - point 2.

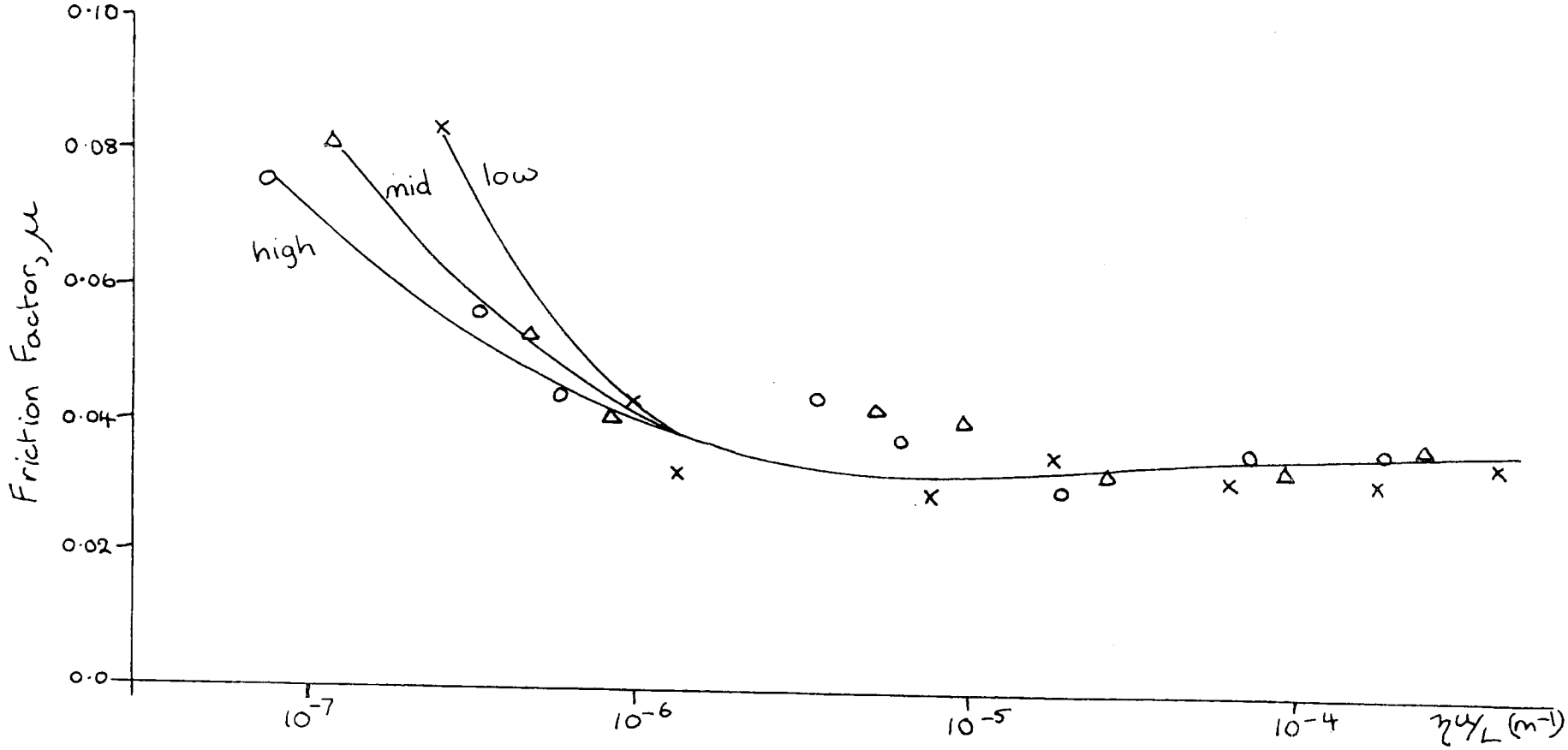

Figure 6.6

Charnley prosthesis lubricated with silicone fluids. Constant loading throughout cycle - point 3.

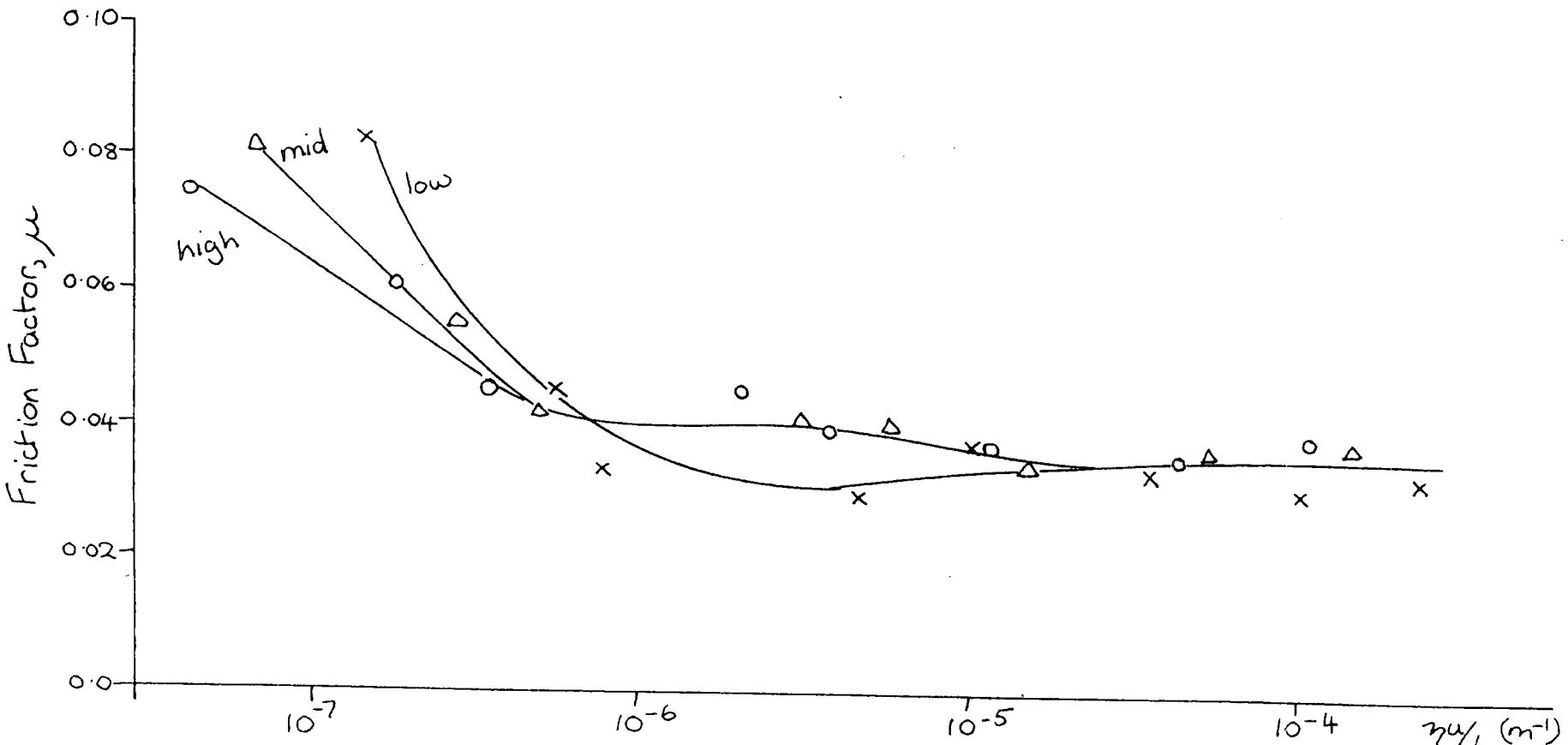

Figure 6.7

Charnley prosthesis lubricated with silicone fluids. Constant loading throughout cycle - point 4.

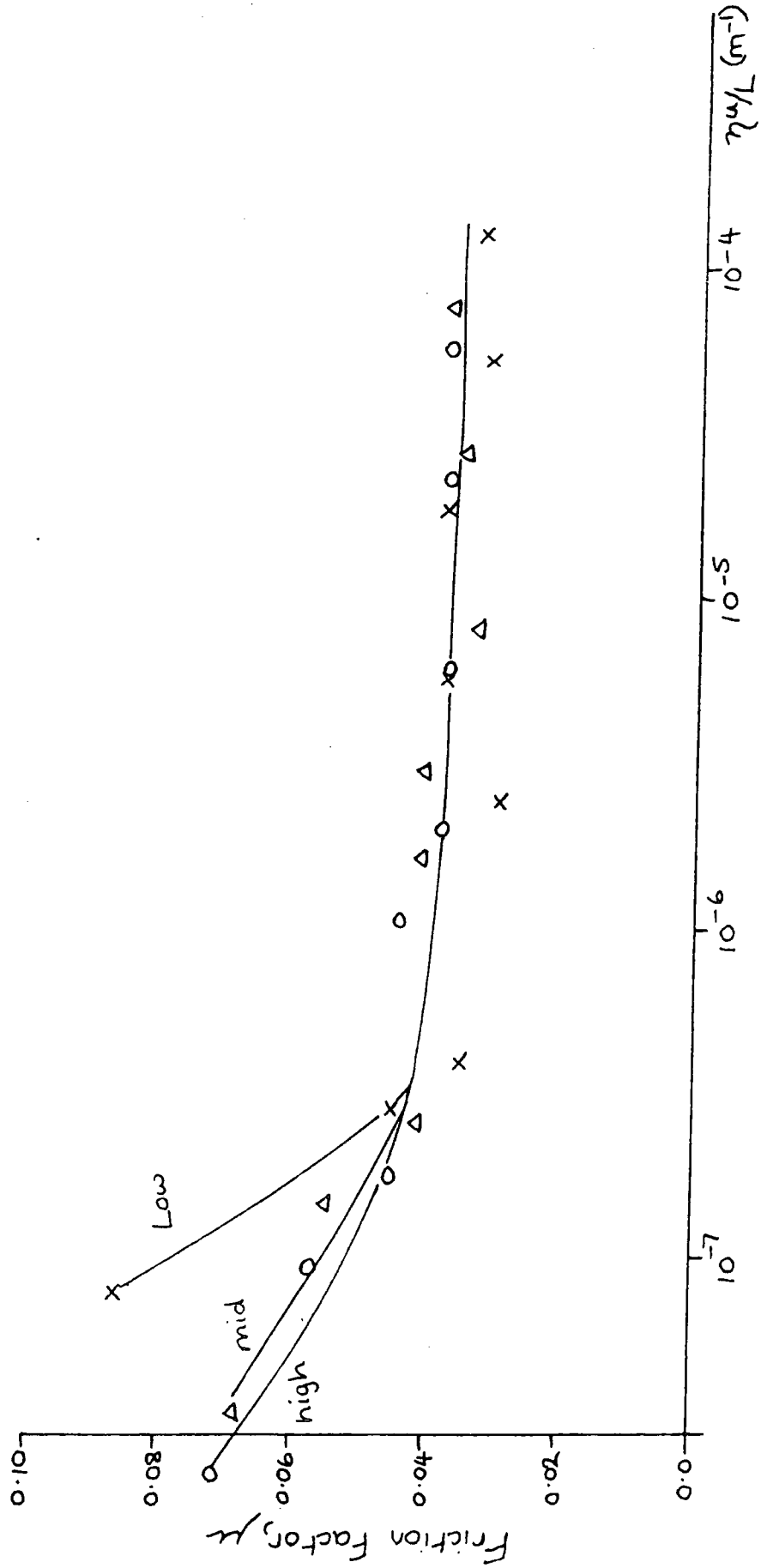

Figure 6.8

Charnley prosthesis lubricated with silicone fluids. Constant loading throughout cycle - point 5.

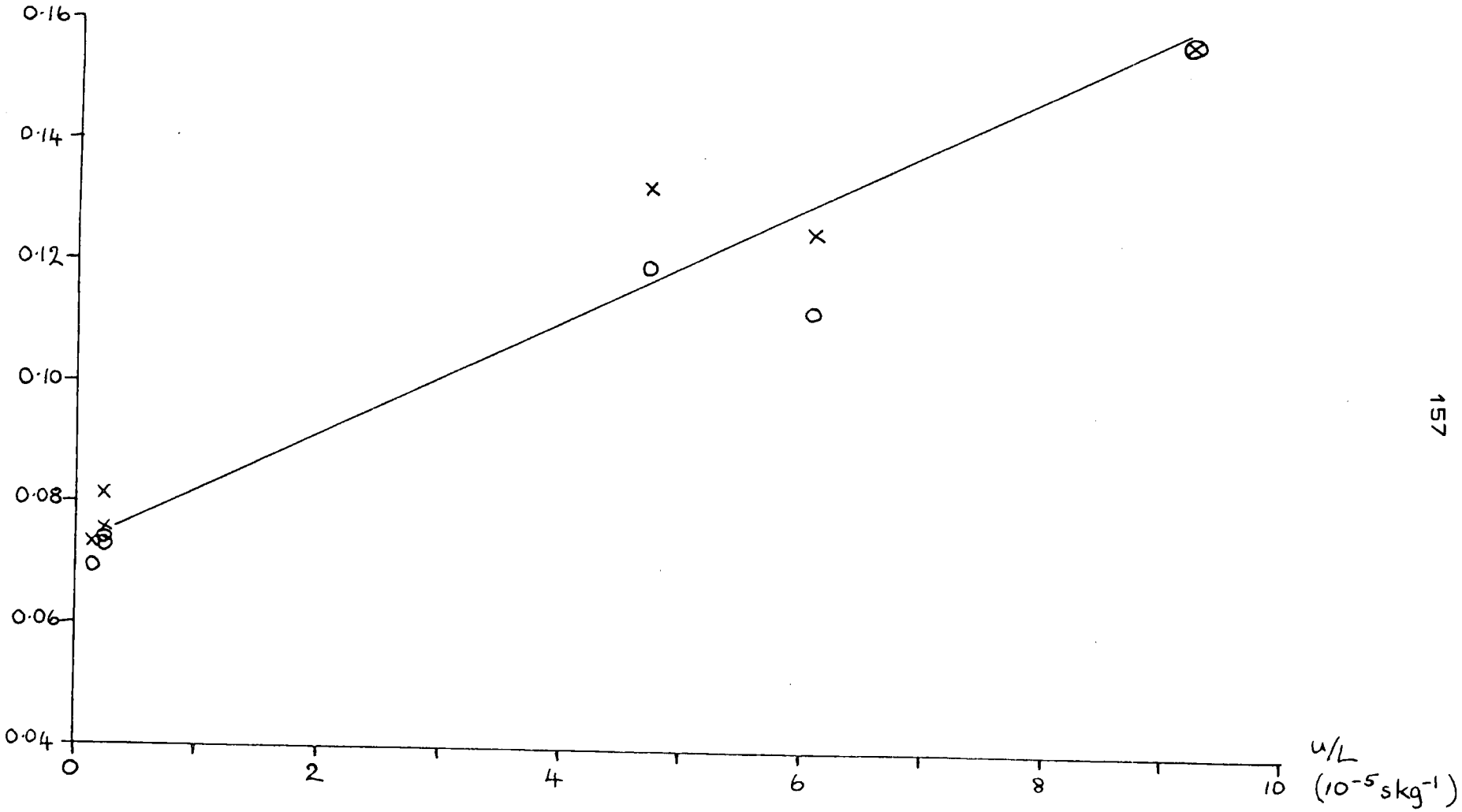

Figure 6.9

Natural hip joint, H1: initial trial.

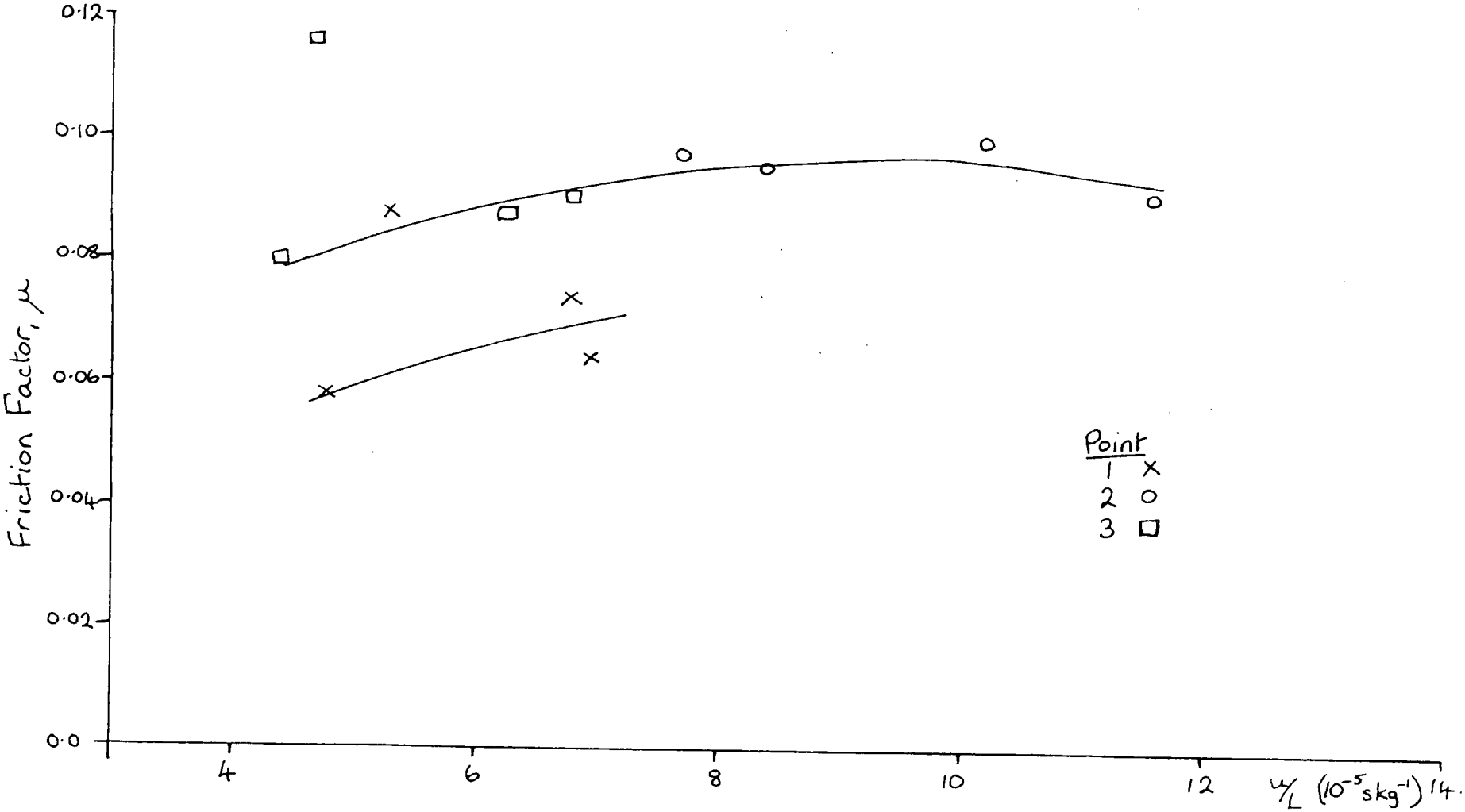

Figure 6.10

Natural hip joint, H2: lubricated with Ringer's solution - low loads.

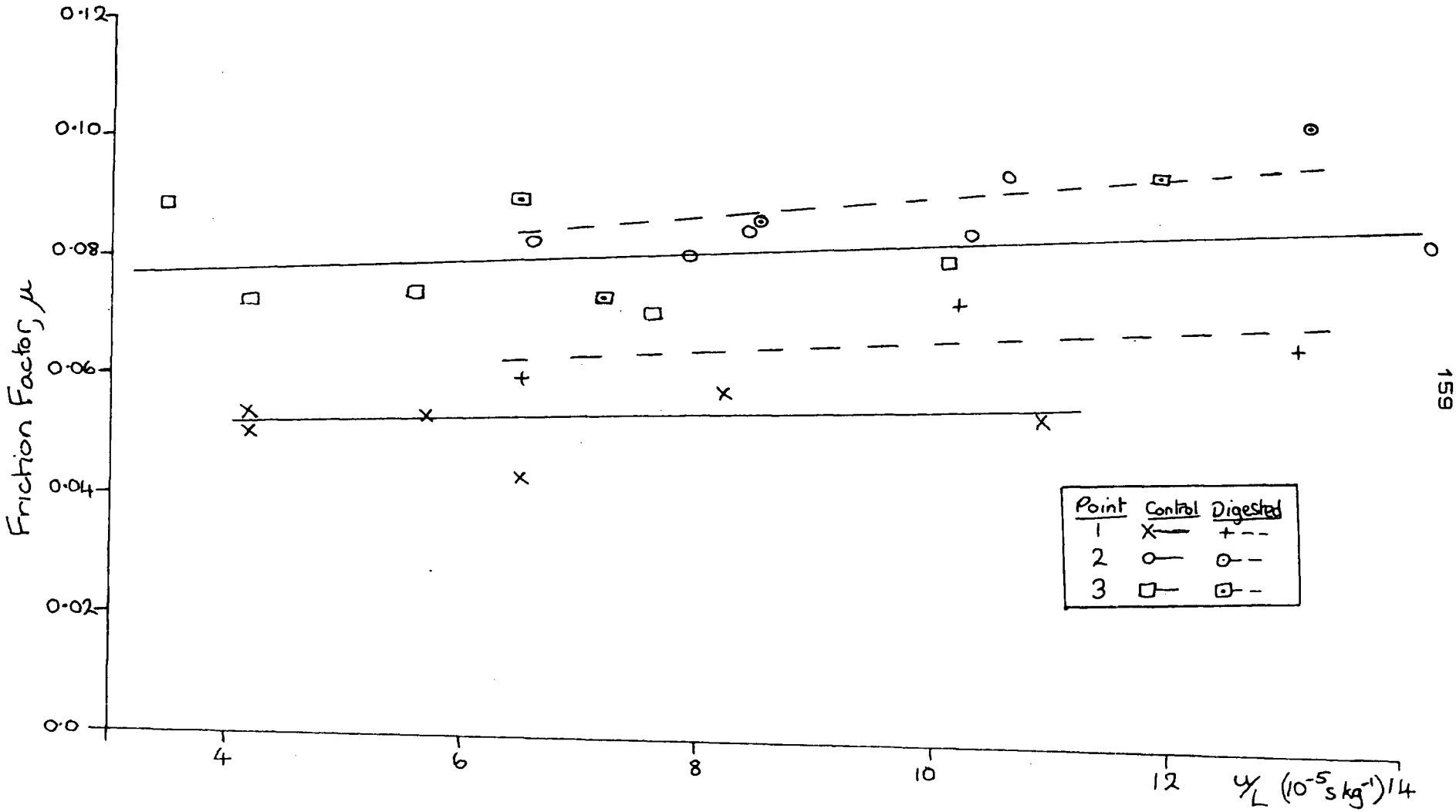

Figure 6.11

Natural hip joint, H2: lubricated with synovial fluid untreated and digested with hyaluronidase - low loads.

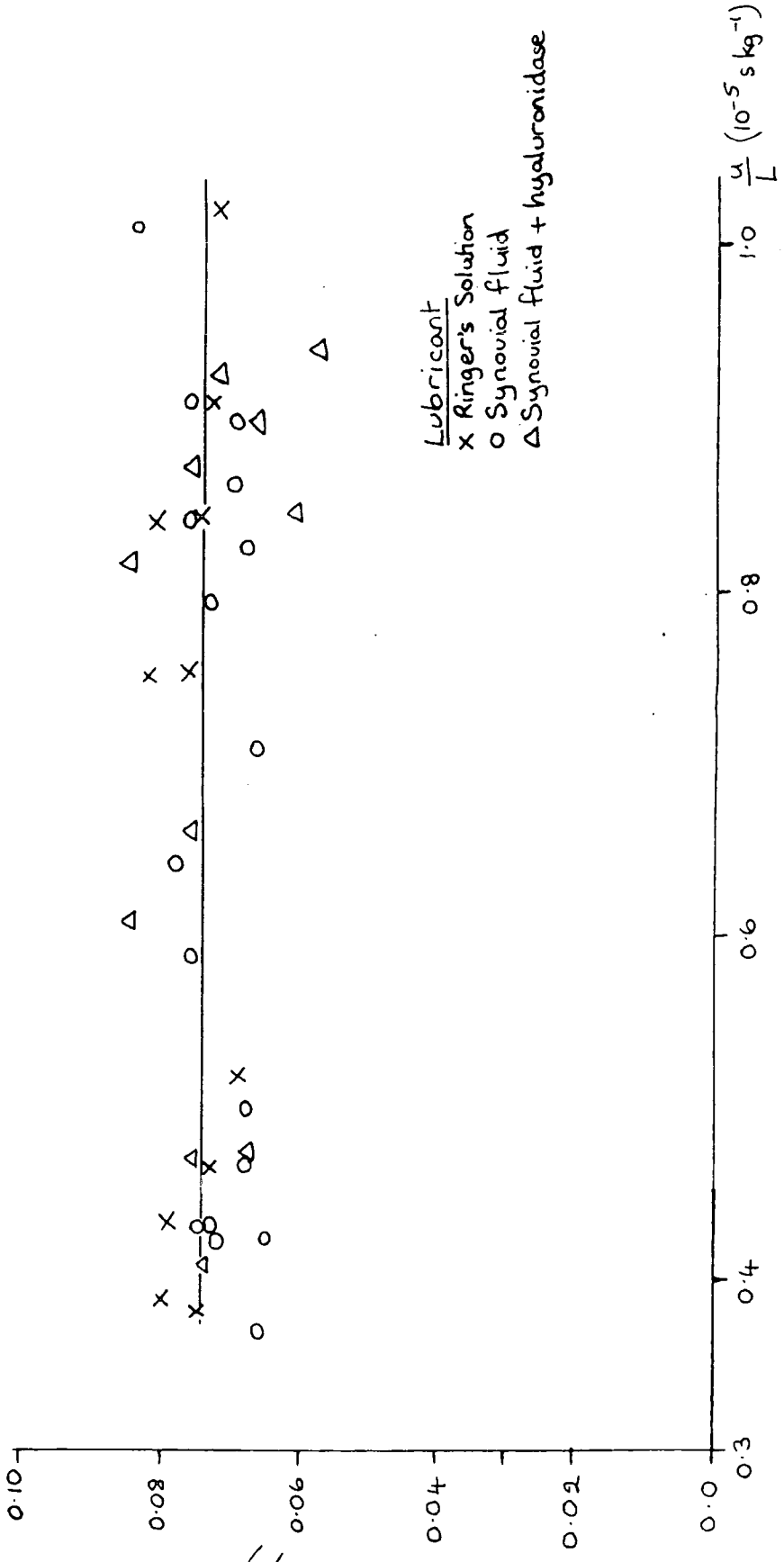

Figure 6.12

Natural hip joint, H2: lubricated with various fluids - high loads.

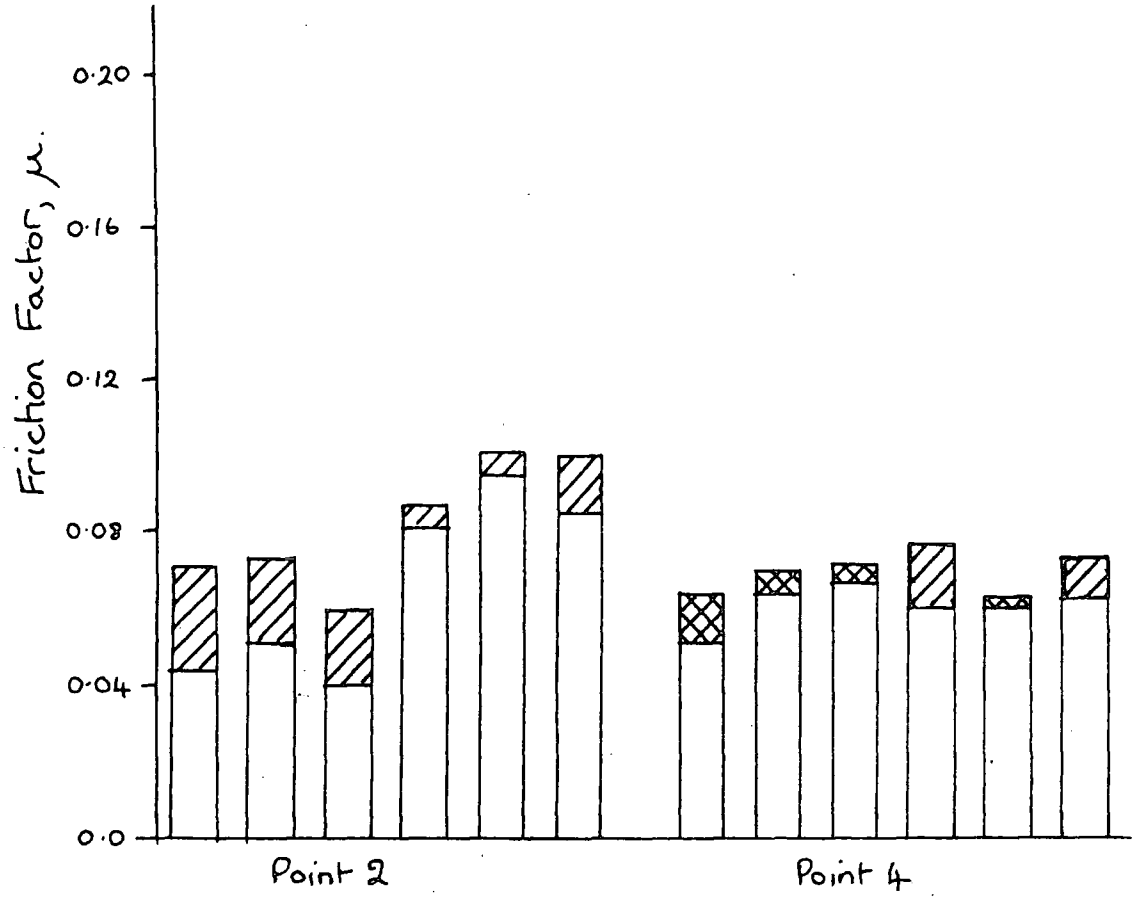

Figure 6.13

Natural hip joint, H2: effect of hyaluronidase digestion on friction factor.

Single hatching shows increase in friction factor after treatment, cross hatching shows decrease.

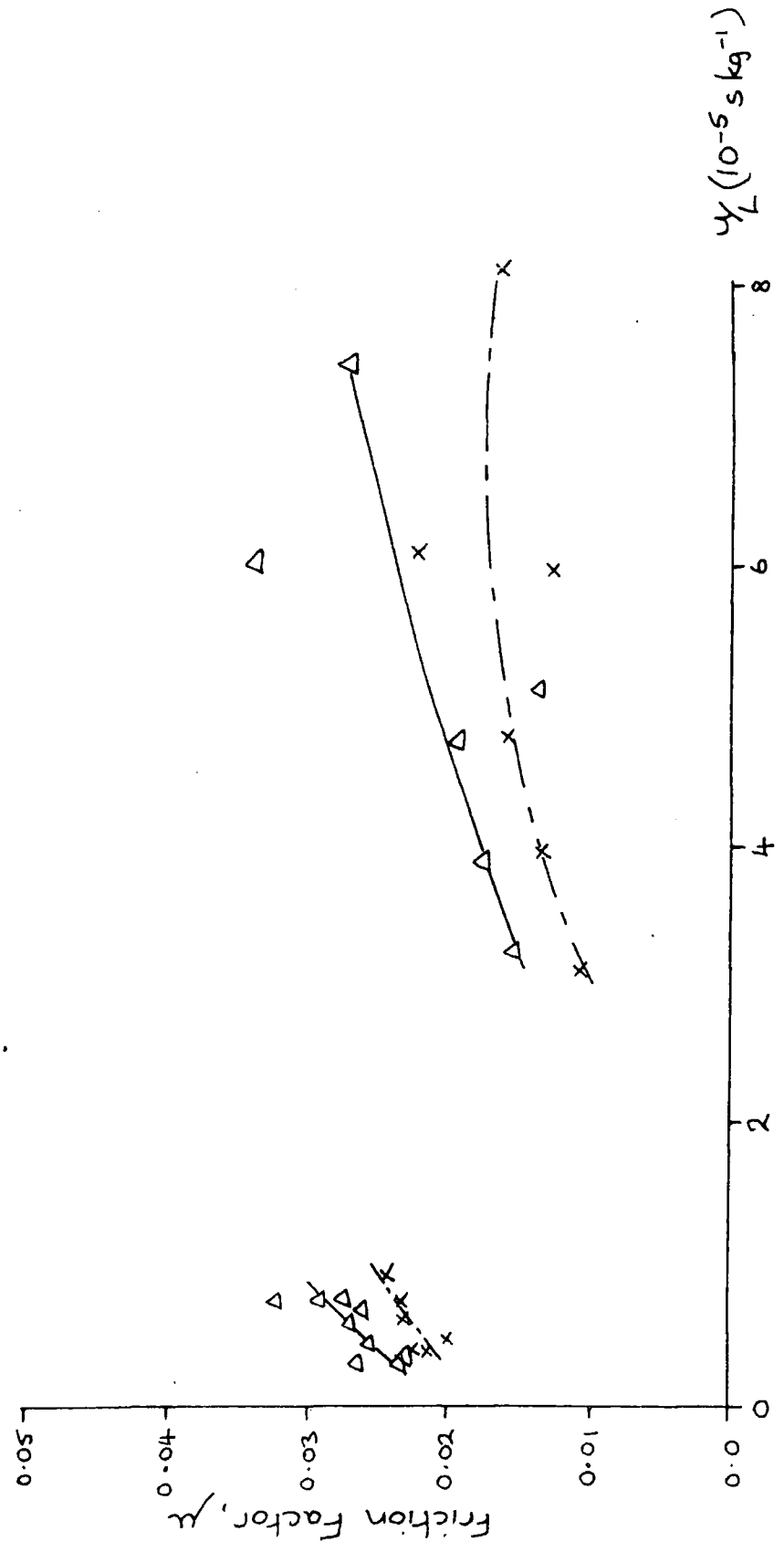

Figure 6.14

Natural hip joint H3: variation of friction factor for Ringer's solution (Δ–Δ) and untreated synovial fluid [x–x].

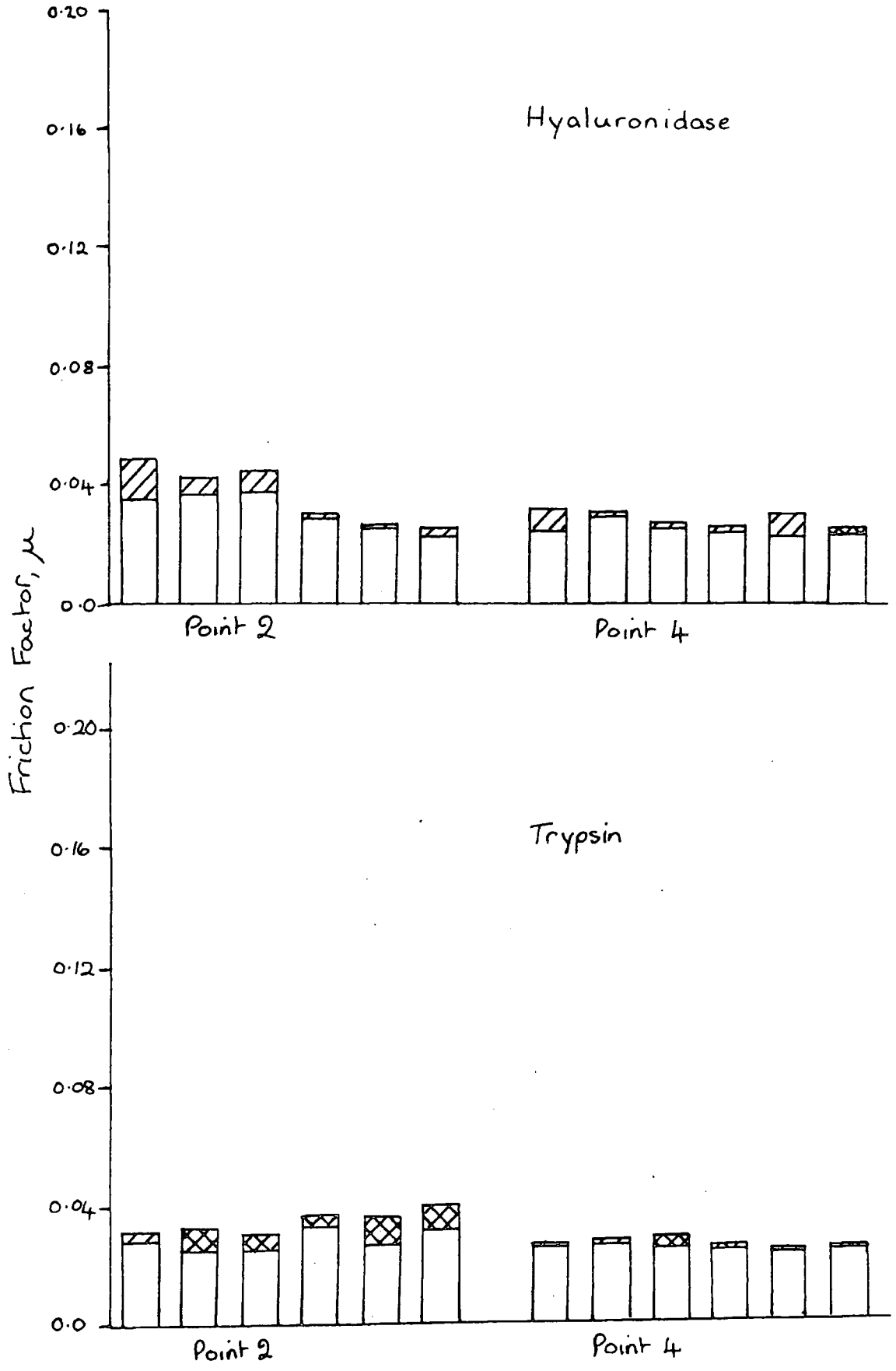

Figure 6.15

Natural hip joint H3: effect of enzymatic digestion on friction factor.

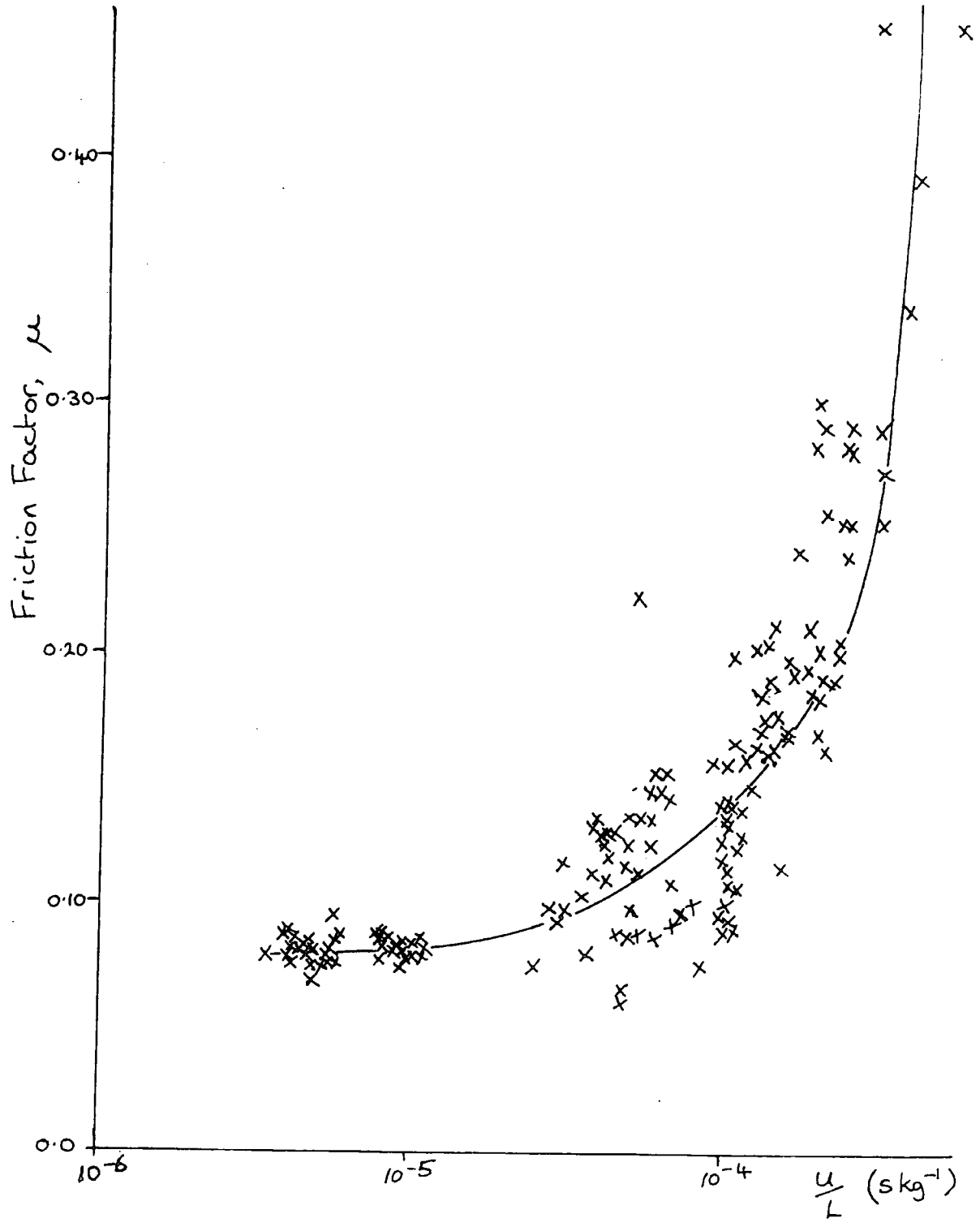

Figure 6.16

Natural hip joint, H4: graph of all results obtained for friction factor with synovial fluid.

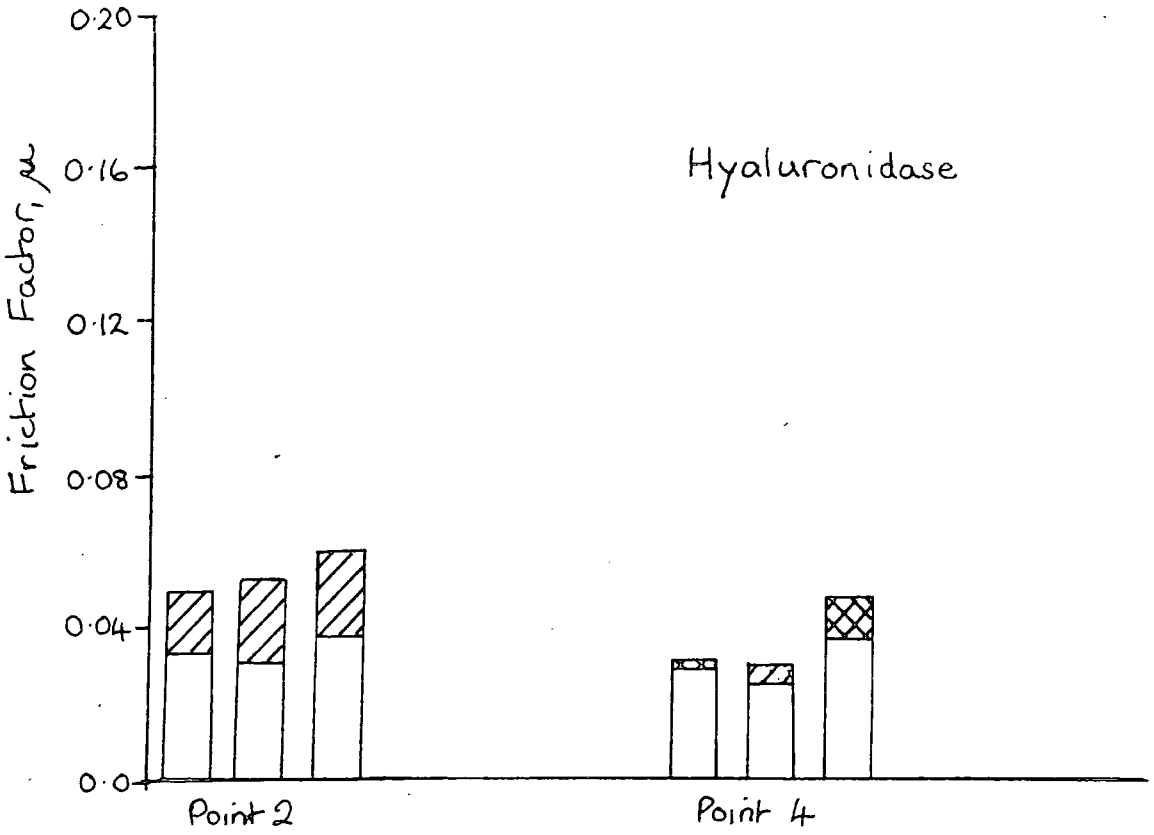

Figure 6.17

Natural hip joint, H5: effect of hyaluronidase digestion on friction factor.

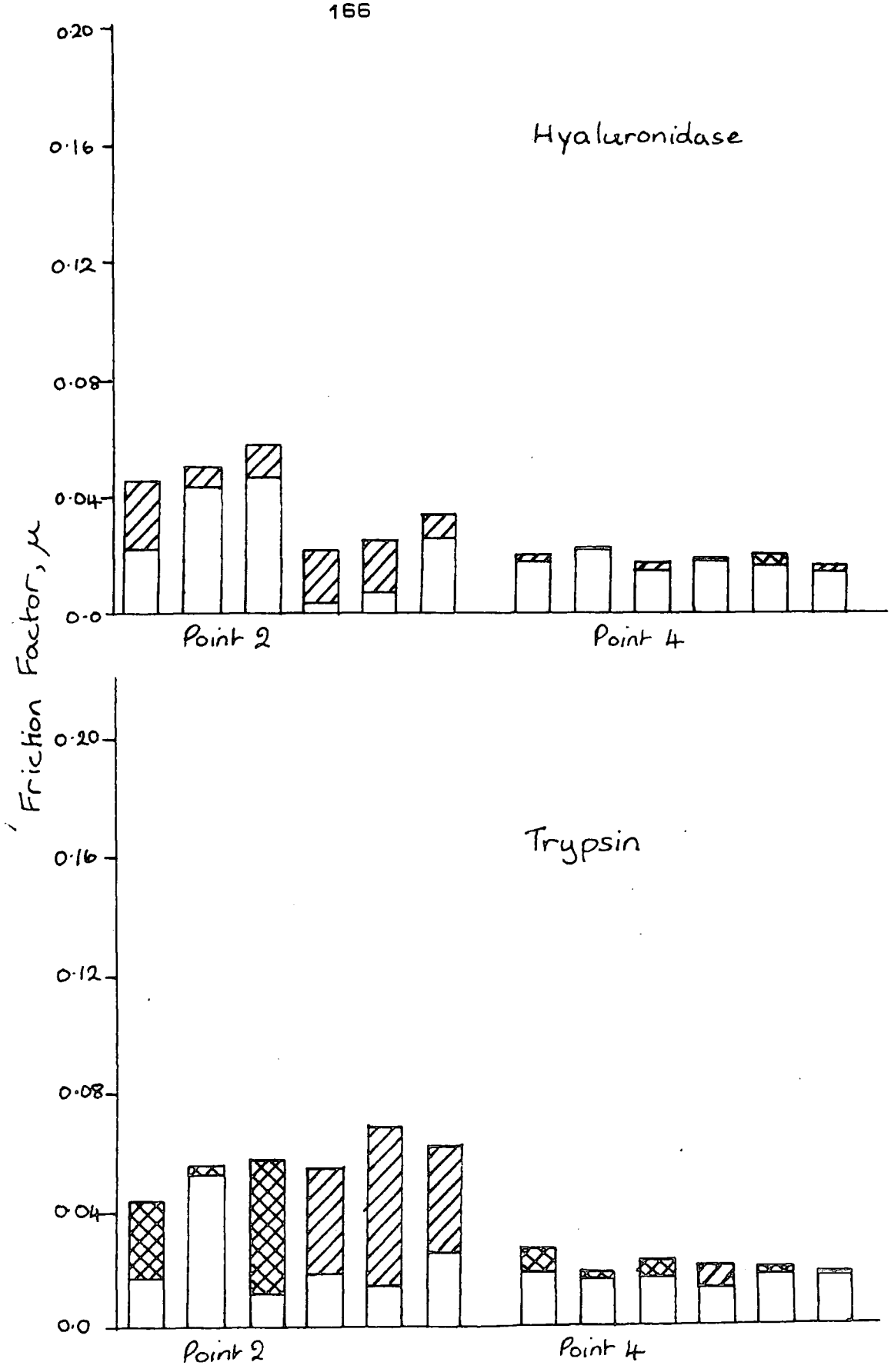

Figure 6.18

Natural hip joint H6: effect of enzymatic digestion on friction factor.

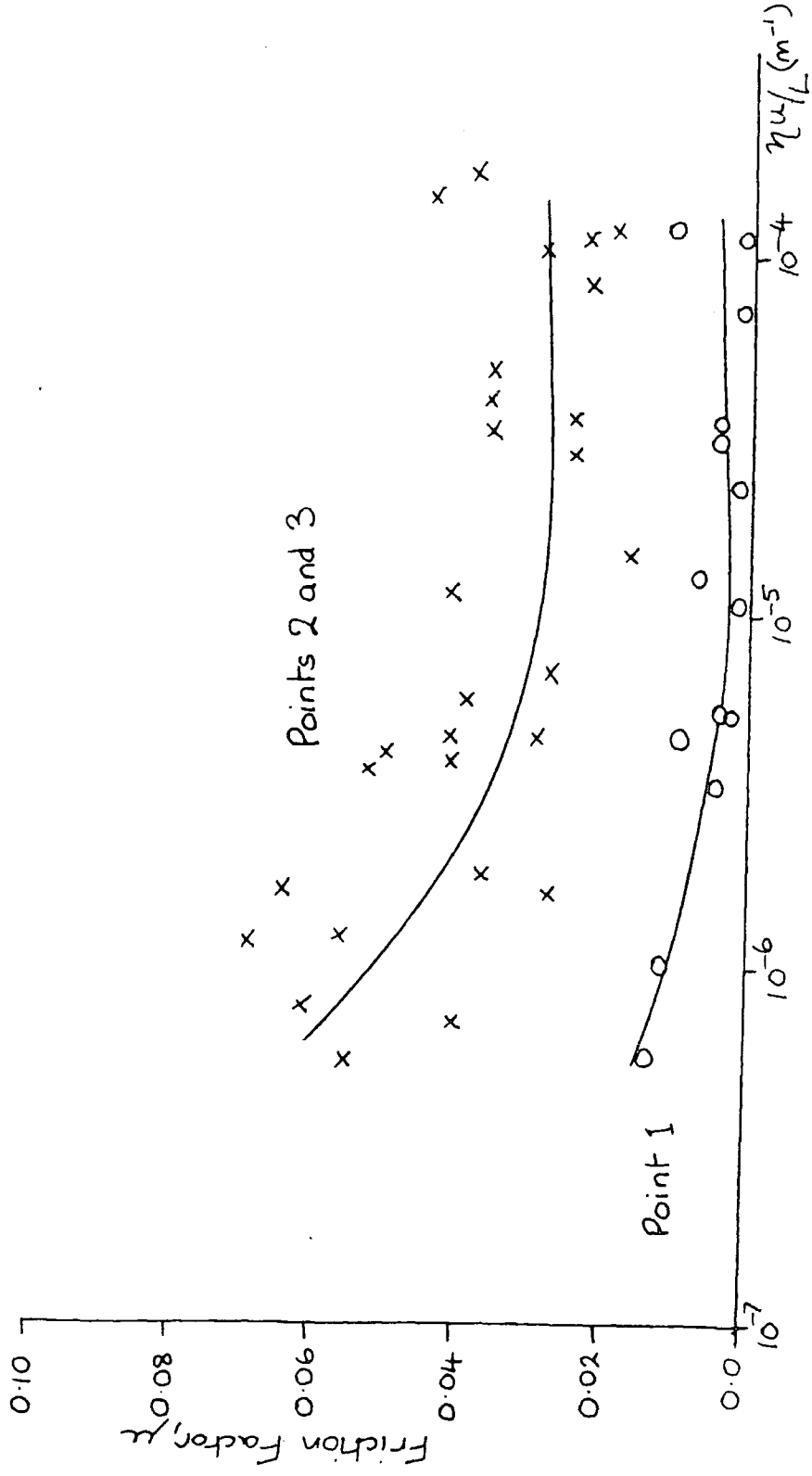

Figure 6.19

Natural hip joint, H6: lubricated with SCMC - low loads.

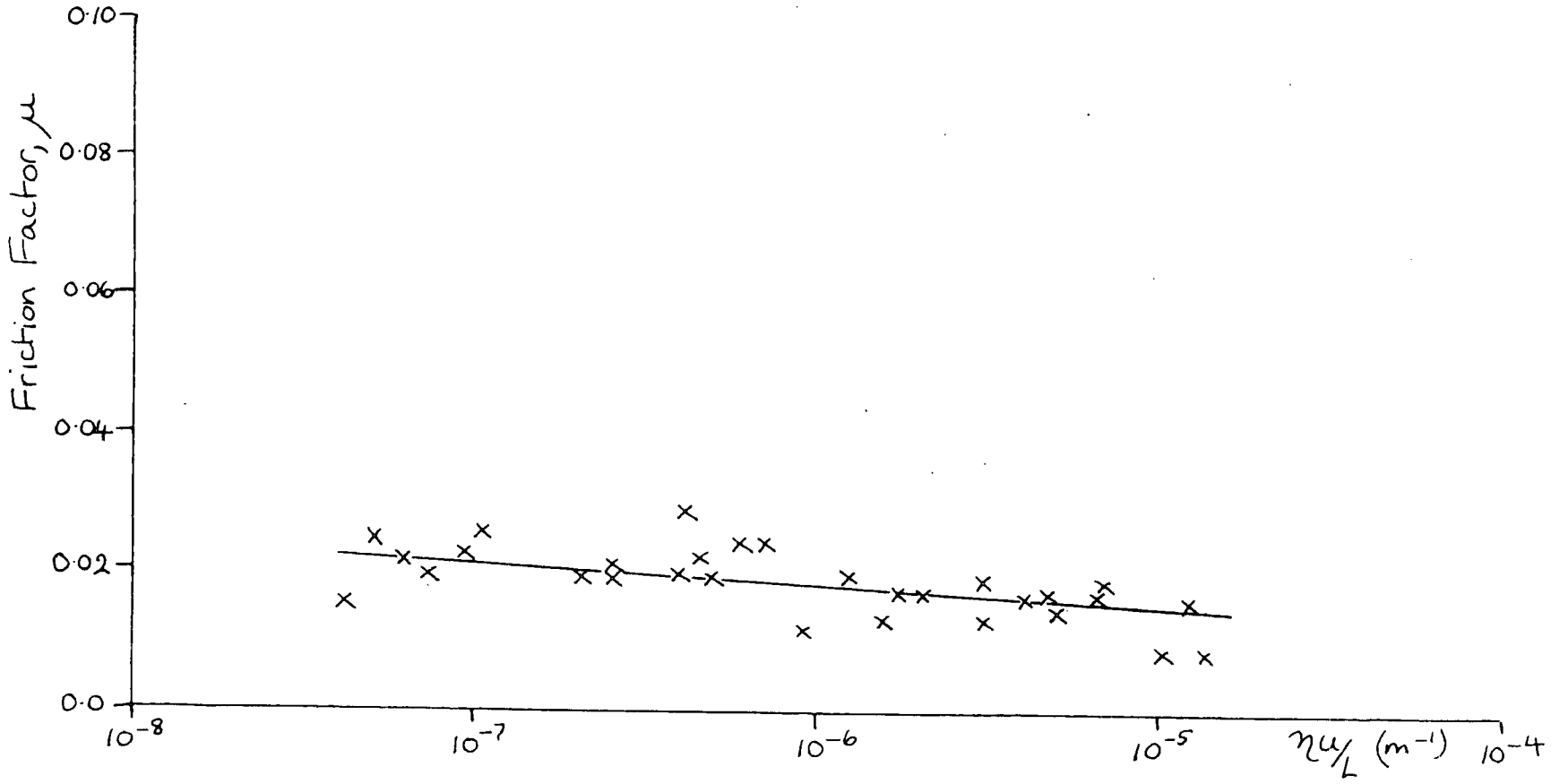

Figure 6.20

Natural hip joint, H6: lubricated with SCMC - high loads.

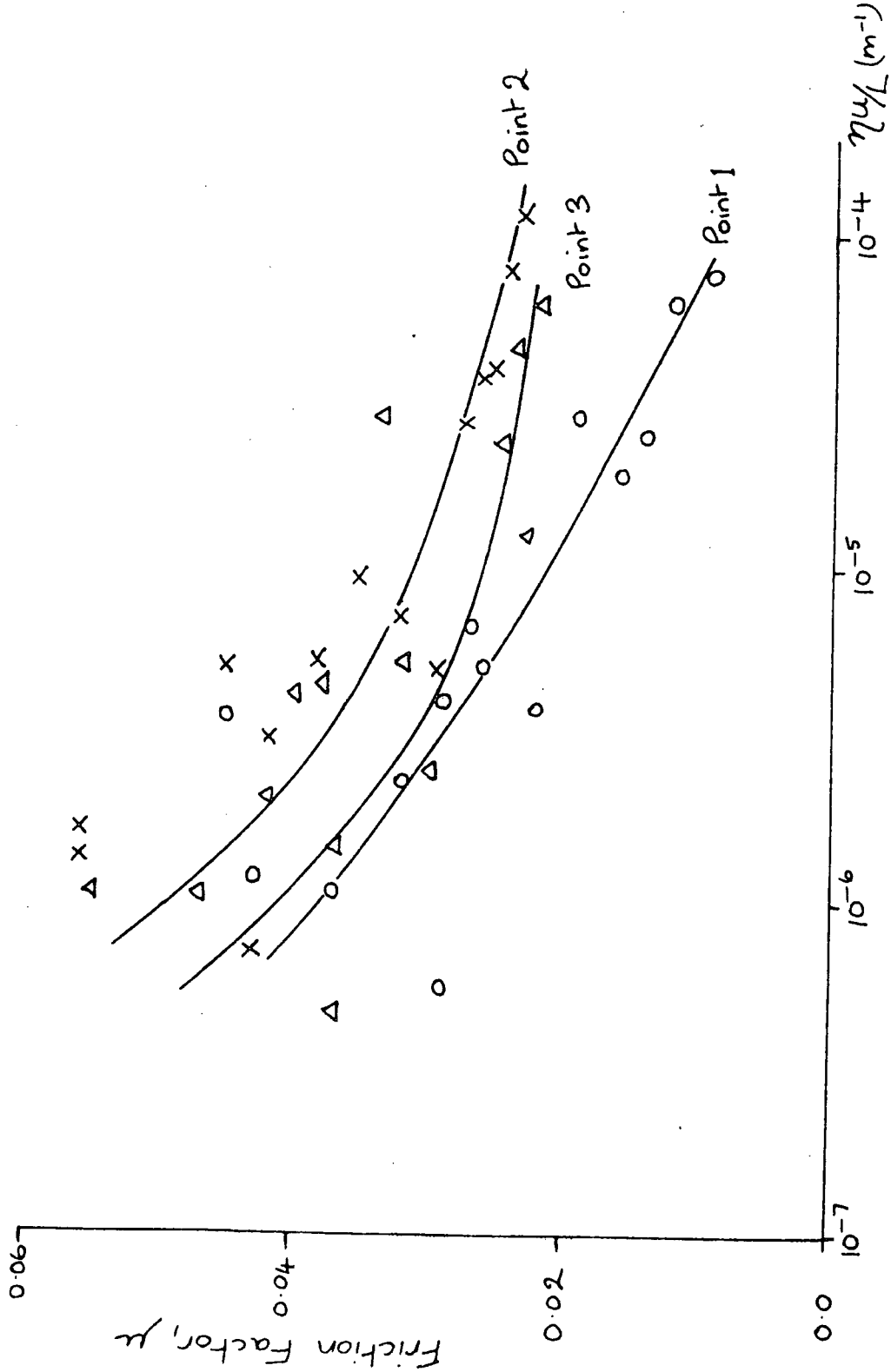

Figure 6.21

Natural hip joint, H7: lubricated with SCMC - low loads.

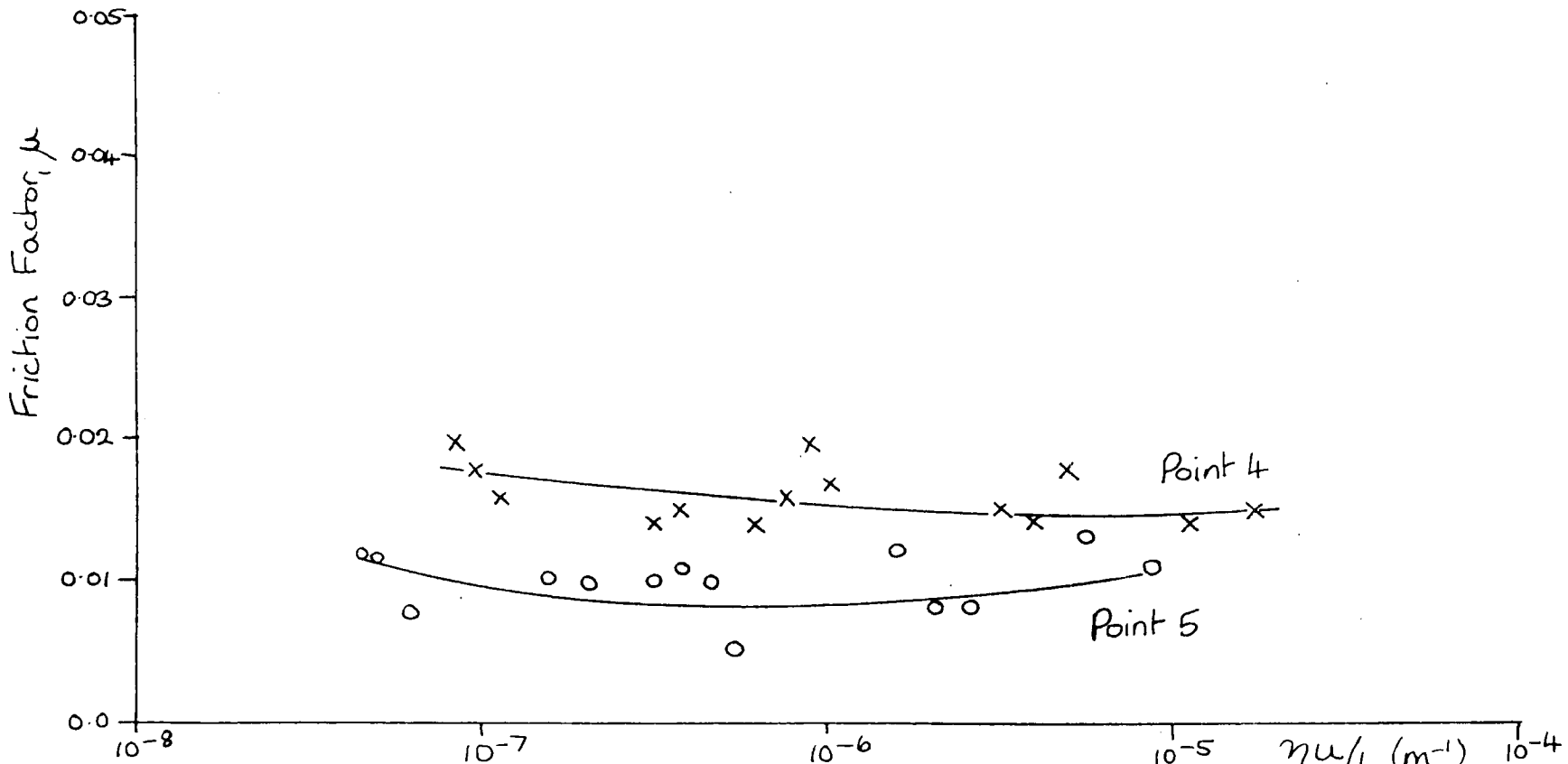

Figure 6.22

Natural hip joint, H7: lubricated with SCMC - high loads.

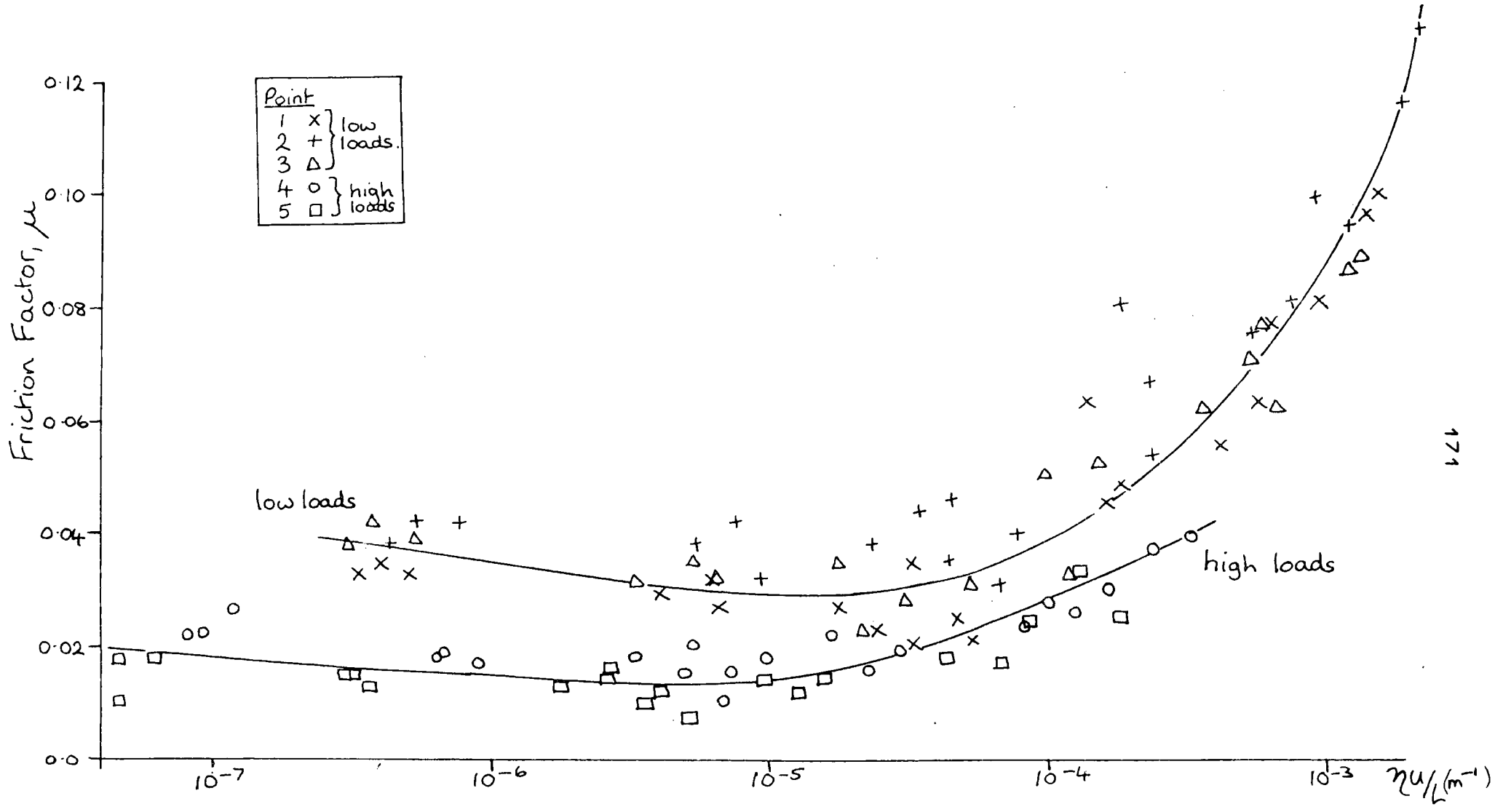

Figure 6.23

Natural hip joint, H7: lubricated with silicone fluids.

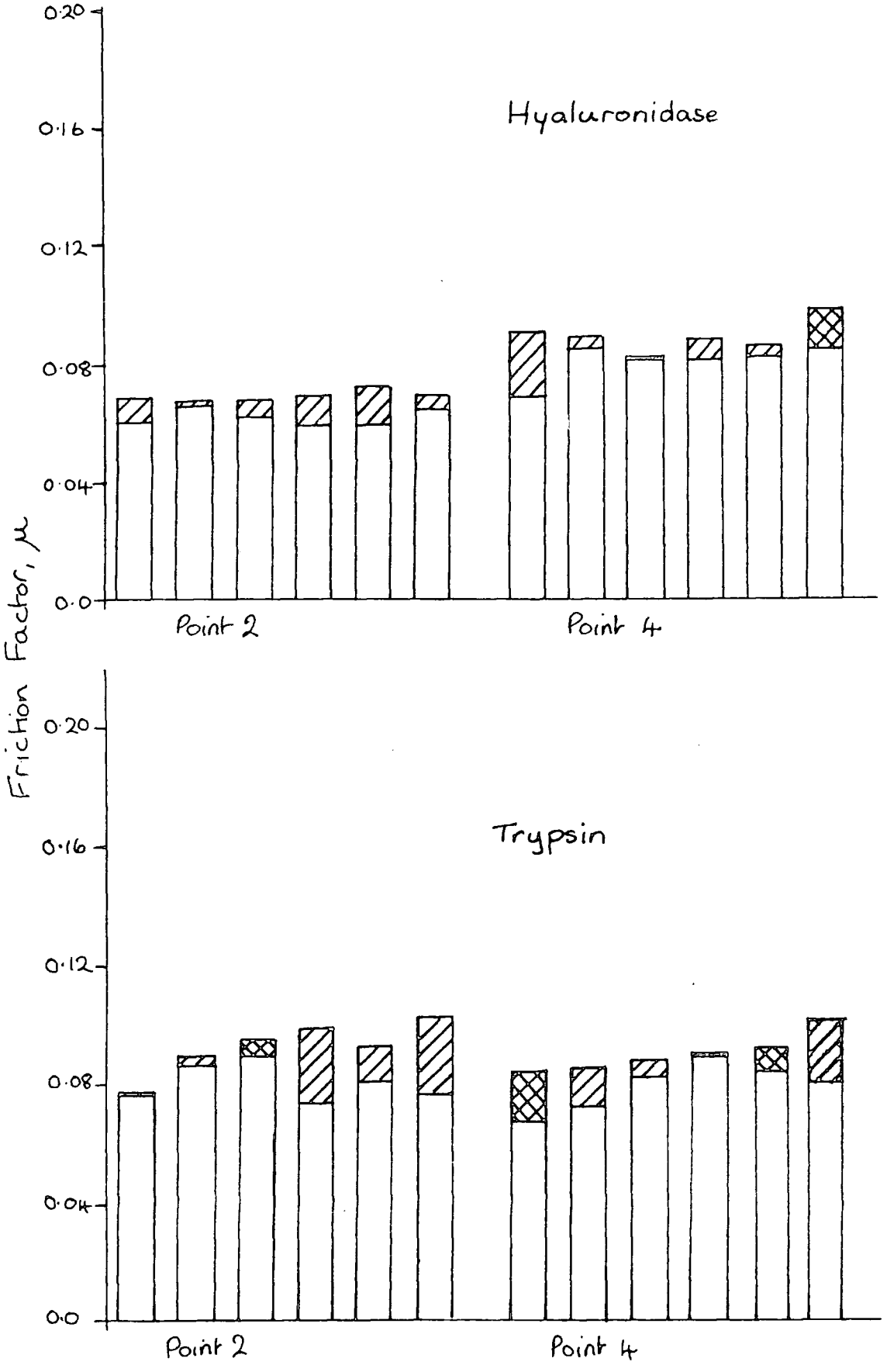

Figure 6.24

Natural hip joint, H8: effect of enzymatic digestion on friction factor.

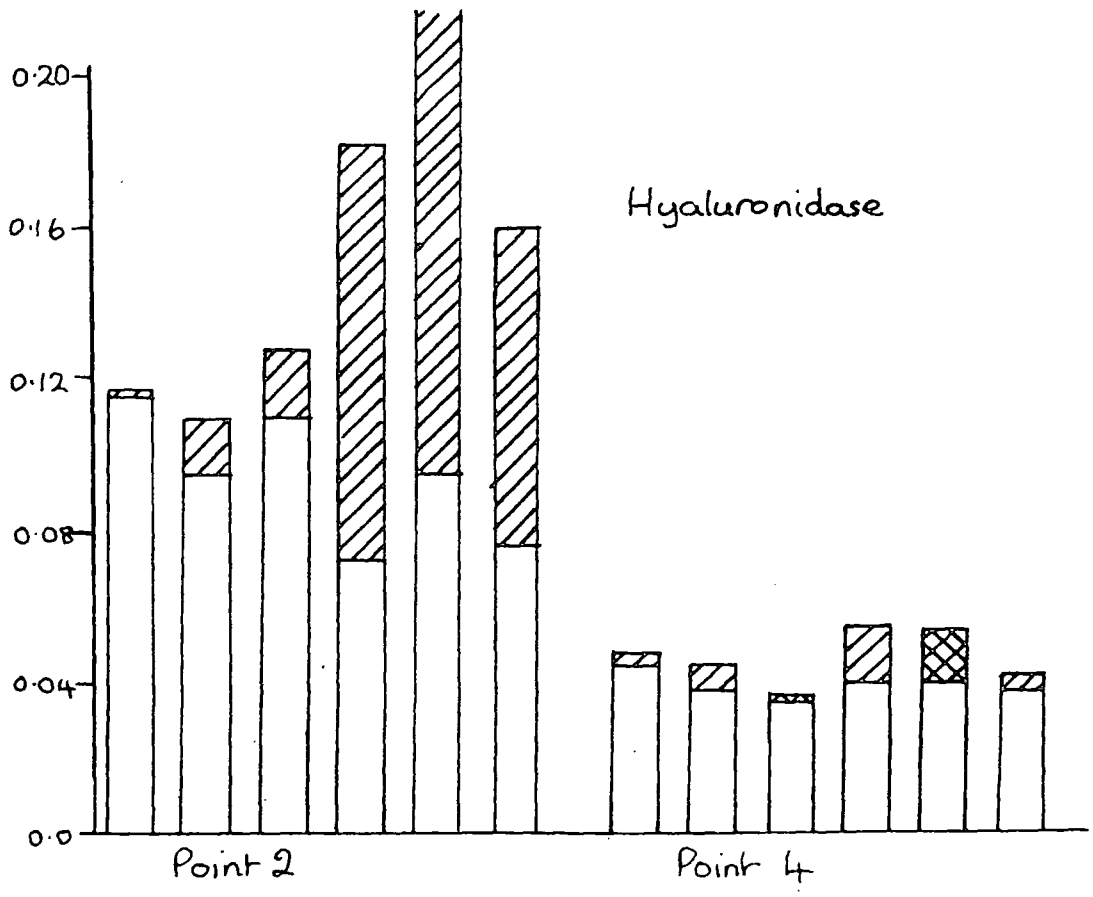

Figure 6.25

Natural hip joint, H9: effect of hyaluronidase digestion on friction factor.

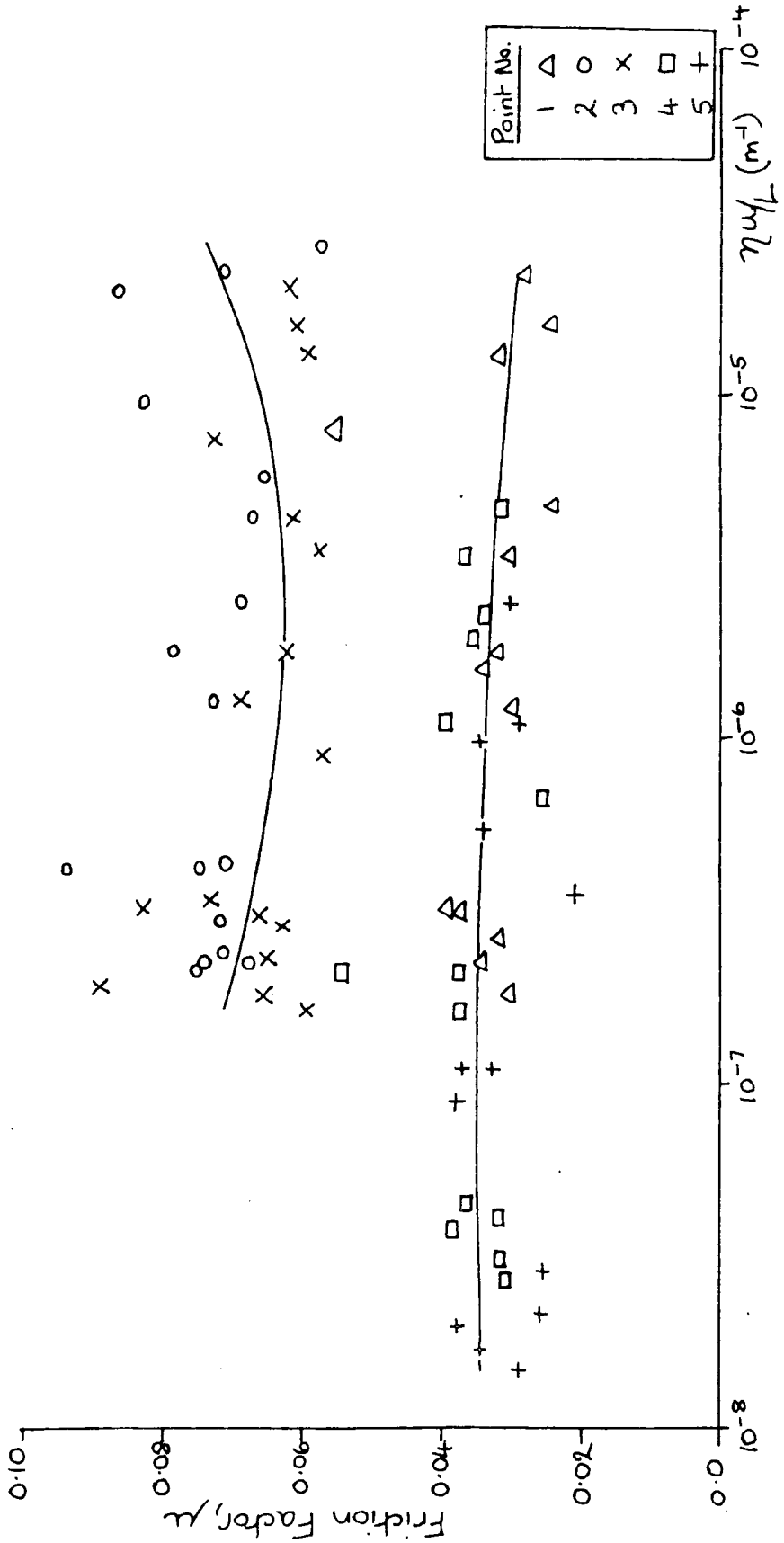

Figure 6.26

Natural hip joint, H9: lubricated with synovial fluid enhanced with hyaluronic acid.

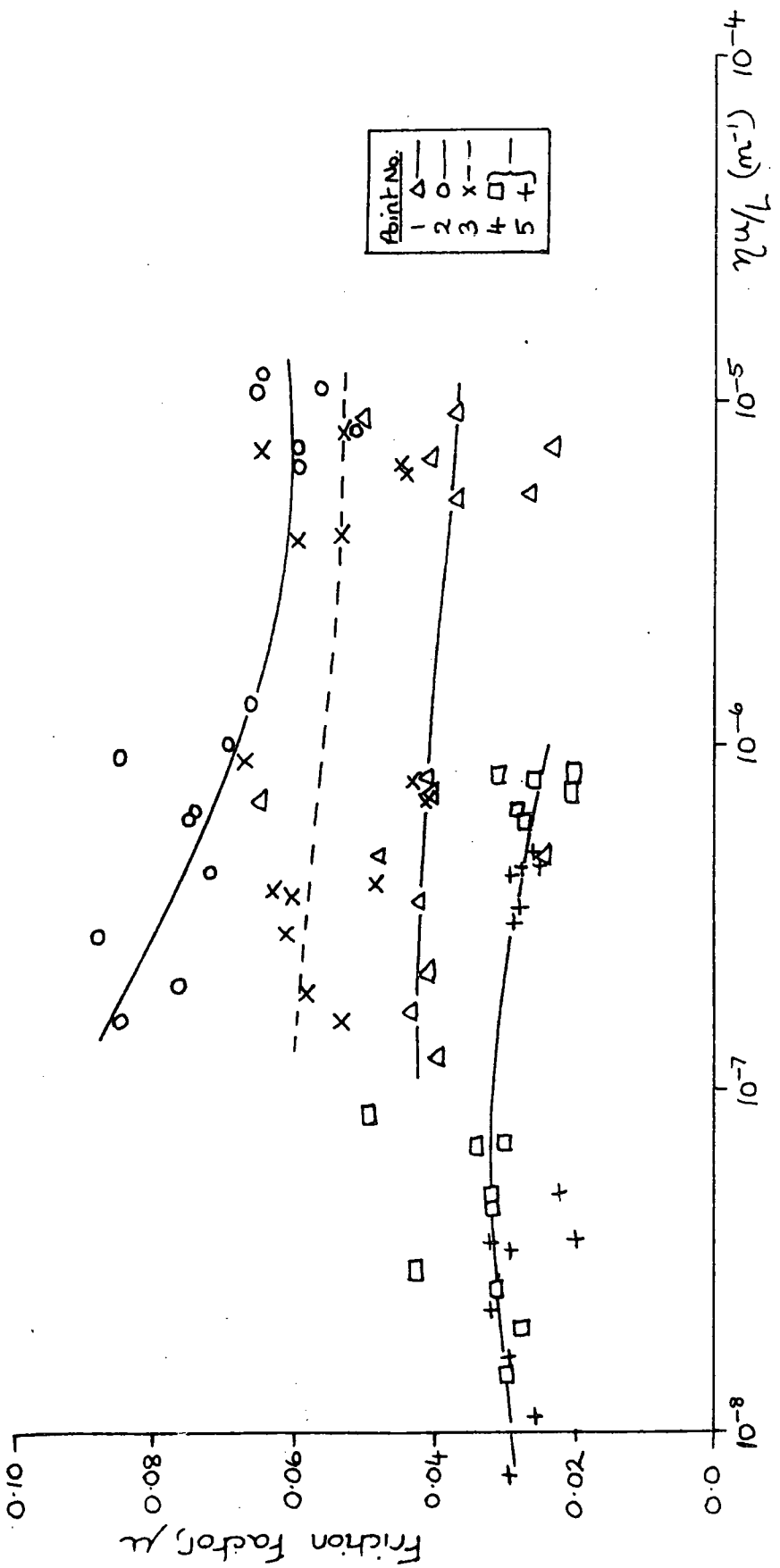

Figure 6.27

Natural hip joint, H9: lubricated with SCMC.

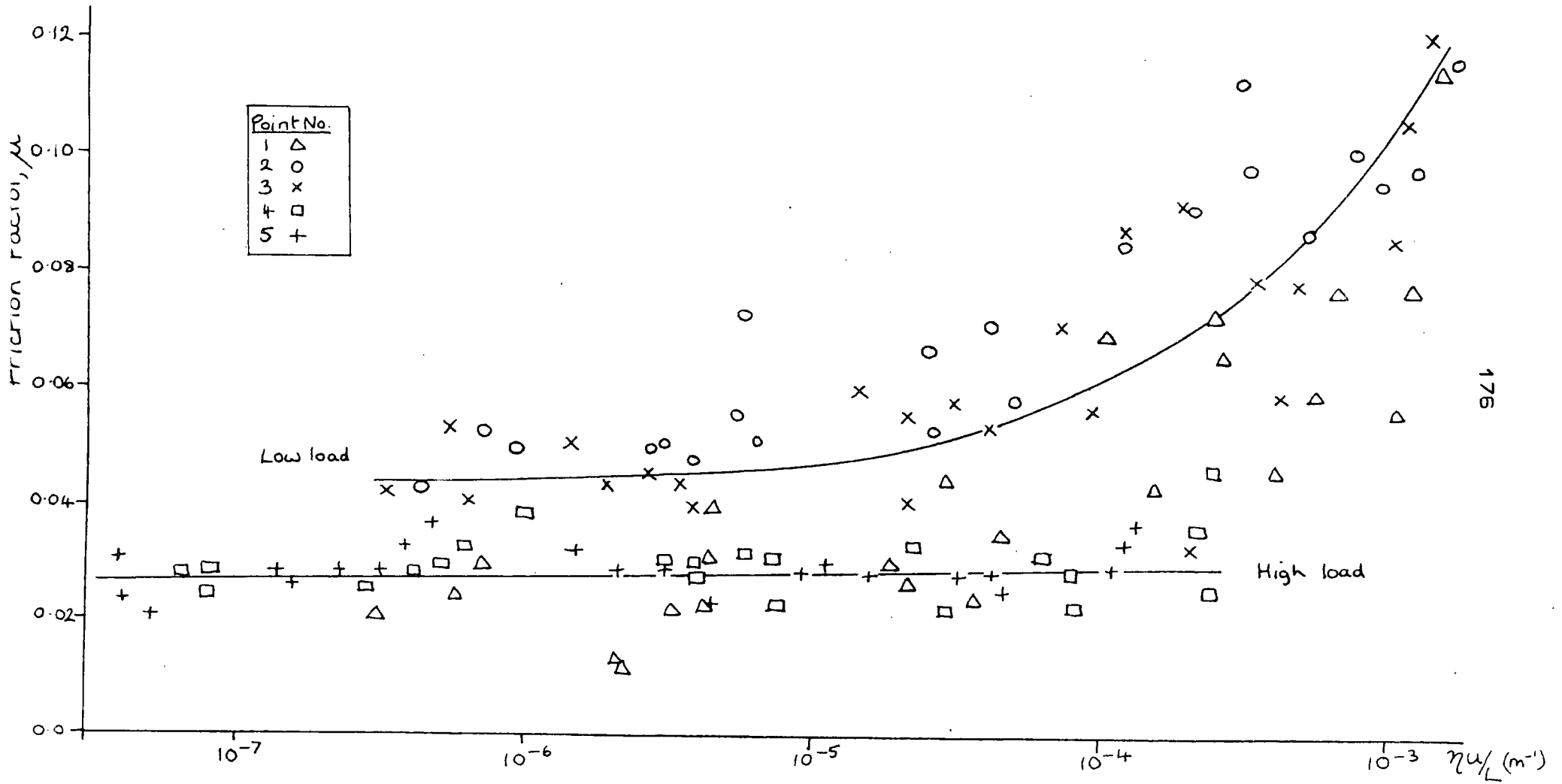

Figure 6.28

Natural hip joint, H9: lubricated with silicone fluids.

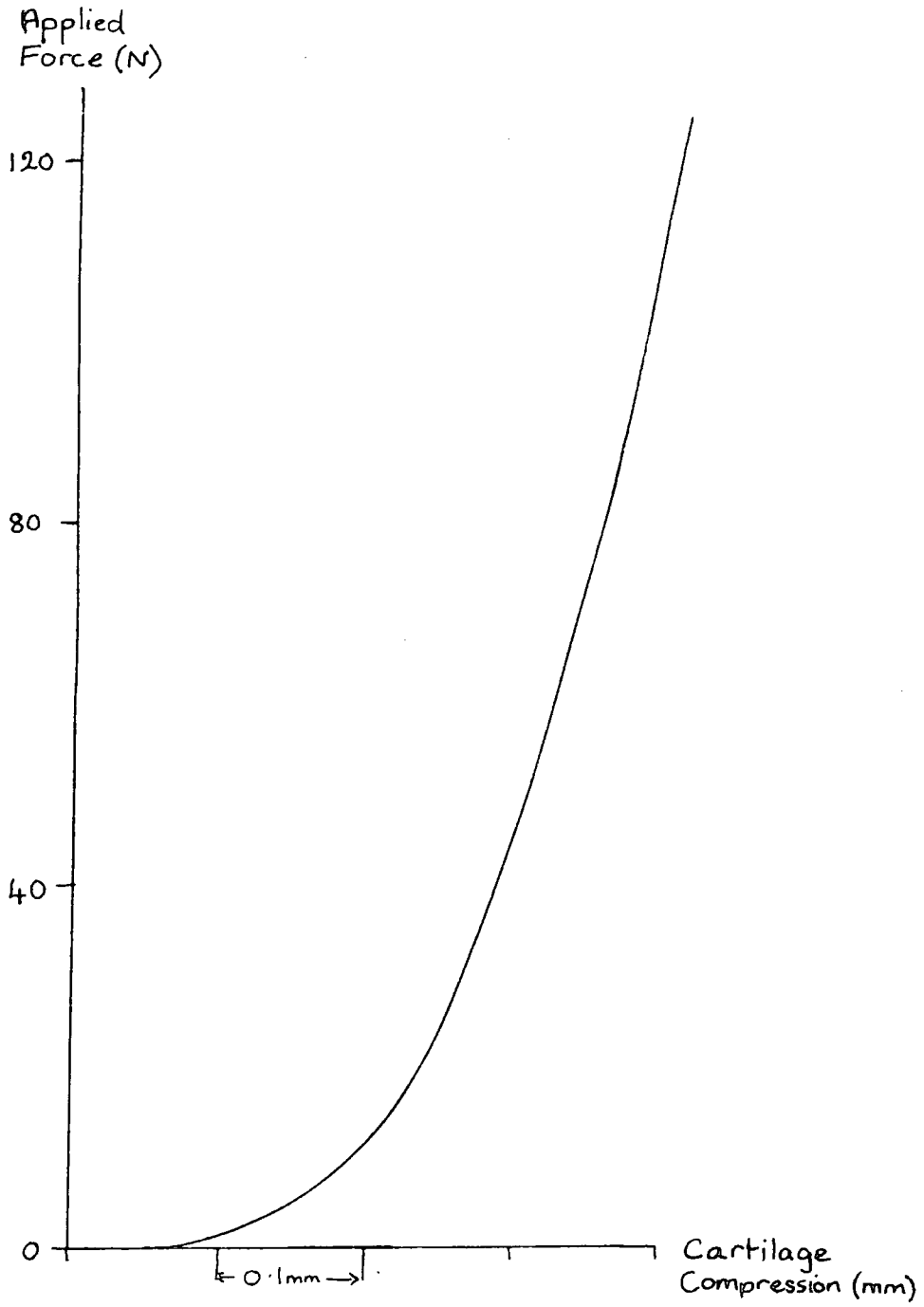

Figure 6.29

Typical trace obtained on the Instron for compression of cartilage at 20 mm min^{-1} [joint H5].

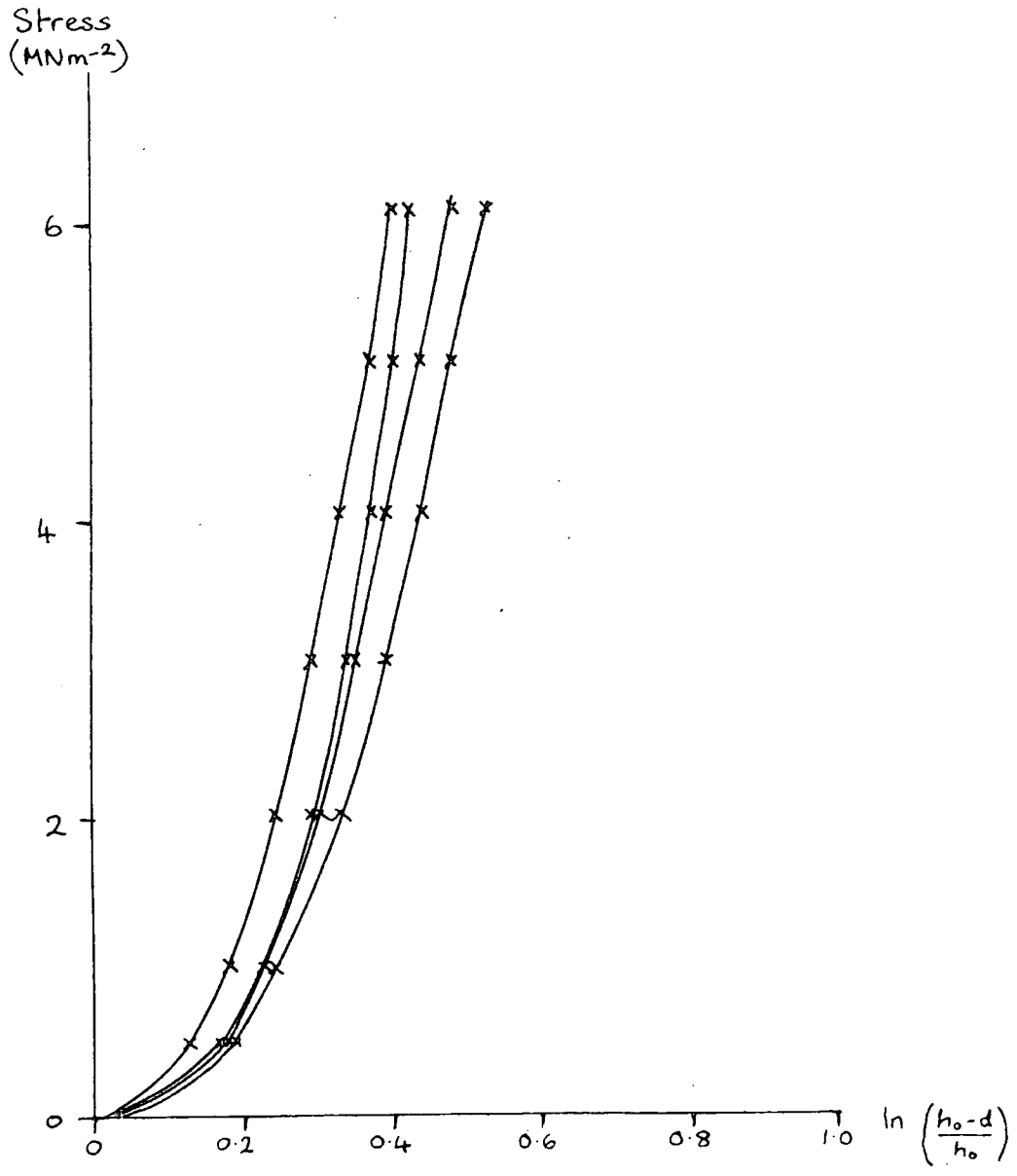

Figure 6.30

Stress/strain graph for four cartilage samples from one femoral head [joint H6].

CHAPTER SEVEN

RESULTS - ARTIFICIAL JOINTS WITH COMPLIANT LININGS

Experiments were performed on acetabular components that had compliant linings cast onto the articular surfaces. These components, produced with different thicknesses of lining, were tested in the hip function simulator. Two clearances and a range of lubricants (SCMC and silicone fluids) were also used. The elasticity and the effects of the lubricants on the linings were also examined.

7.1 Absorption tests

Thompson (1979) showed that silicone elastomer swells when soaked in silicone fluid. In order to investigate the possibility of the absorption of the lubricant by the Sylguard silicone elastomer, used for manufacturing the compliant linings, soaking tests were carried out.

Small pieces of cured elastomer weighing 1 - 2 g were soaked in lubricant and repeatedly weighed at various time intervals. Sample A was weighed initially then soaked in DC 200/10 silicone fluid and removed at intervals, dried with tissue and reweighed. The % increase in weight was calculated and plotted.

In order to check whether the increase in weight was due to surface absorbed silicone, sample B was dipped in fluid and dried before its initial weighing, then treated as A.

Sample C was soaked in an SCMC solution [C10] and similarly weighed.

The results obtained are shown in Figure 7.1. The two samples soaked in silicone reached equilibrium after absorbing 65% of their own weight of fluid. This was achieved after 100 hours of soaking. Approximately 1 g of fluid was absorbed by a sample initially weighing 1.5 g. Neither SCMC nor water were absorbed by the elastomer.

7.2 Reproducibility of elastomer between mixes

It was necessary to mould the acetabular linings from several different batches of elastomer since there was only one moulding rig, and the mix would begin to cure at room temperature if stored. A slab of elastomer was cured, along with each acetabular lining. The modulus of each slab was measured and compared with the others.

Using Clish's apparatus described in section 5.3, the radius of the indentation formed in the elastomer by a loaded lens was measured for a range of applied loads. A graph of $[\text{radius of indentation}]^3$ against applied load gives a straight line from which the modulus can be found. The Hertzian theory for the contact radius of a rigid spherical indentor on an elastic layer gives:

$$a^3 = \frac{3PR\,[1 - \nu^2]}{4E}$$

where

a is the contact radius

P the normal load

R radius of curvature of indentor

ν Poisson's ratio

E Young's modulus

Therefore, for an elastomer where ν can be assumed to be 0.5, the elastic modulus, E, can be expressed as:

$$E = \frac{9R}{16}\frac{P}{a^3} = \frac{9R}{16}\,\frac{1}{\text{gradient}}$$

Typical graphs obtained are shown in Figure 7.2, and the moduli for the different mixes are detailed in Table 7.1, together with the thickness of sample tested.

7.3 Effective elastic modulus of acetabula with compliant linings

The modulus measured above is not the true elastic modulus of the elastomer since the Hertzian theory assumes an infinite thickness of material. This explains the results for the first three samples, which were only 3.5 mm thick, and gave higher modulus values than the later, thicker samples. A theoretical approach to the effect of thin elastomer layers on effective elastic modulus is given in Appendix 2. The effective elastic modulus of the compliant linings is further complicated by their bonding to the metal substrate, and by other restrictions on movement caused by their geometry.

For these reasons it was decided to try to measure the stress v strain relationship directly by loading the acetabula using the Instron 1195 universal testing machine used earlier for the cartilage tests.

The detail of the method of Instron testing of acetabula is given in section 5.3. A typical set of traces obtained from the Instron for one acetabulum repeatedly loaded is shown in Figure 7.3. In all cases, the first application of the load led to a slower increase in load than repeated applications. When the loading was repeated the contact between the Instron's top platen and the metal sphere was broken, ie load on the metal sphere dropped to zero but the sphere was not physically removed from the cup. This slower initial increase in load with distance may therefore have been due to the sphere attaining intimate contact with the compliant layer. As the joint is subjected to repeated loading during friction testing in the simulator, the consistent results obtained after the initial loading were the ones analysed.

Since the aim of these tests was to obtain a comparison between the effective moduli of the acetabula with different layer thicknesses, a value was needed which would reflect the relationship between them. Now the

$$\text{Effective elastic modulus, } E' = \frac{\text{Apparent stress}}{\text{Apparent strain}}$$

But stress is load divided by the area over which it is applied. This area would initially be less than the maximum cross-sectional area of the sphere, but it would have increased to this value as the compliant layer was compressed. It was considered constant for all the samples. The strain is the decrease in thickness divided by the total thickness. The total thickness in these tests was constant since it was the elastic layer in conjunction with the metal base which was being investigated. Hence,

$$\text{Effective elastic modulus, } E' = [\text{constant}] \frac{\text{load}}{\text{compression}}$$

where the constant is the same for all samples. This means that the slope of the trace obtained on the Instron gives a value which is proportional to the elastic modulus and therefore can be used to rank the joints in order of 'stiffness'. Table 7.2 gives details of the joints and values of load/compression for both low and high load parts of the graphs. The table shows that for all the joints the 'stiffness' is less at 250N than at 1500N - this is also demonstrated by the shape of the curves in Figure 7.3. The 'stiffness' also decreases with increasing thickness of elastomer layer, apart from DD which displays anomalous results. Joints Z1 and Y3, which had a larger radial clearance, were less stiff than their counterparts with 'normal' clearance. This was expected since the elastomer will be less confined in these acetabula.

7.4 Analysis of friction results with compliant layers

Following the experience of analysing the results obtained from human joints, it was decided to use a computer to analyse the results of the lubrication tests on compliant layers. Two programs were written, the first, MU2.FTN, processed the data obtained from measurements on the traces, together with viscosities and speeds to produce a table of friction factor with corresponding $\eta u/L$ values. The second, GA4.FTN, used the tabulated results to plot graphs of friction factor against $\eta u/L$ for each of the five points analysed for any particular joint. Details of the data collection and analysis are given in Appendix 3. Each of the five points through the cycle could be plotted on a separate graph. As the tests with any one lubricant were run at three different speeds of oscillation, there are three points for each lubricant on each graph. These are represented by different symbols as follows:

O	0.65 Hz
*	0.83 Hz
+	1.0 Hz

7.5 Friction tests on prostheses with compliant linings, lubricated with SCMC

All eight successfully manufactured acetabula with compliant linings were tested with a range of solutions of SCMC as lubricants. The SCMC solutions were shear thinning, like synovial fluid. The viscosities of all the

SCMC solutions used throughout the work are given in Table 5.4. Eight of the solutions (C10, C50, C100, C170, CA, CB, CC, CD) were used in the present study to give adequate coverage of the viscosity range.

Results for 1 mm layer (A1 and D1)

Three of the SCMC lubricants, C50, CC and CA were used with joint A1 which had a 1 mm layer of sylguard elastomer lining the acetabulum with 0.25 mm radial clearance. The results obtained (Figures 7.4 - 7.8) seemed particularly high and rather than extend the range of lubricants, the tests were repeated on another day with the same three lubricants. Some of the results from this second test were even higher than the first.

The low load friction factors, as illustrated by the data from point 2 (Figure 7.5) varied from 0.6 to 0.3 and those at high loads (see point 4, Figure 7.7) from 0.085 to 0.045. For the low loads, the results from the two runs overlapped, but for the high loads the second set of results was higher than the first.

Later in the series of tests, a new 1 mm layer was made (D1) which was tested with the full range of eight SCMC lubricants. The results are shown in Figures 7.9 - 7.13. The friction factor decreases with increasing viscosity of lubricant, but again the friction factors are high. At low loads (point 2) they range from almost 0.9 down to 0.25. At high loads (point 4) the maximum friction factor is 0.17 and they decrease to 0.05 as the $\eta u/L$

increases. There is no obvious relationship between speed of oscillation and friction factor ie the three symbols on the graphs do not form separate sets of results.

Results for 2 mm layer [A2]

The data from joint A2, which had a 2 mm thick elastomer lining and 0.25 mm radial clearance, is shown in Figures 7.14 - 7.18. Once again, the friction factor consistently decreases with increasing $\eta u/L$. At points 4 and 5, which are highly loaded, the friction factors are less than those for the same lubricant with a 1 mm layer - ranging from 0.077 to 0.025. At low loads, the results are more widely scattered and the maximum friction factor is just over 0.5.

Results for 3 mm layer [A3]

Figures 7.19 - 7.23 show the results from joint A3 which had a 3 mm compliant layer lining the acetabular component with 0.25 mm radial clearance. The results from point 1 were almost constant but the remaining points show the decreasing trend of friction factor with viscosity. The friction factor at point 2 decreases from a maximum of 0.58 to 0.17. At point 4 the values range from 0.15 to 0.05. These friction factors are higher than those obtained with the 2 mm layer.

Results for 0.5 mm layer (A0)

After the tests had been completed on the 1, 2 and 3 mm layers, it was decided to manufacture a 0.5 mm layer, to extend the range of results. The radial clearance was again 0.25 mm. The decreasing trend of friction factor with increasing viscosity is again noticeable for all 5 points (Figures 7.24 - 7. 28). The highest friction factors were obtained from point 2 and ranged from 0.20 down to 0.05. At point 4 the values varied from 0.042 down to 0.02. These are considerably lower than for all the thicker layers.

7.5.1 Comparison of friction factor for different thicknesses of lining

In order to compare the effect of thickness of compliant layer on friction factor more directly, graphs of friction factor against thickness of lining were plotted for fixed conditions. For each viscosity of lubricant, a graph was drawn using the average value of friction factor at a given point for each joint. As there was no consistent variation of friction factor with speed of oscillation, the average of the three values seemed the most sensible value to use. Data from points 2 and 4 were used, representing both low and high load conditions (Figure 7.29). The data from point 4, clearly shows the increasing trend of friction factor with thickness. The data from point 2 is less convincing due to the very high values of friction factor from the 1 mm layer.

7.5.2 Compliant layers with increased clearance

Since increasing thickness of the elastomer layer increased the friction, particularly at low loads, it was decided to investigate the effect of increased clearance between the femoral head and the acetabulum. To do this a larger brass plug was made against which the cups could be moulded giving 0.5 mm radial clearance. The radial clearance on the previous prostheses was 0.25 mm. Two new cups were moulded in the original metal bases. A 0.5 mm layer was made using the 1 mm base and a 2.5 mm layer using the 3 mm base.

Results for 0.5 mm layer with increased clearance (Z1)

This joint was tested with the eight SCMC lubricants and the results plotted as before. In general the friction factor decreased as the viscosity of the lubricant increased (Figures 7.30 - 7.34). The data however, showed a very wide spread. The friction factor was increased in comparison with the results for an 0.5 mm layer with normal clearance.

Results for 2.5 mm layer with increased clearance (Y3)

The eight SCMC lubricants were used with joint Y3 which was a 2.5 mm layer with 0.5 mm radial clearance. The results were again more widely spread (Figures 7.35 - 7.39), which suggests that this is an effect of the increased clearance rather than a particular moulding. The friction factors are higher than for both the 2 and 3 mm layers with normal clearance.

7.6 Compliant layers lubricated with silicone fluids

Since the results for the compliant layers lubricated with SCMC produced higher values of friction factor than had been expected from Thompson's work with elastic layers [1979], it was decided to try lubrication with silicone fluids. As silicone fluid causes the elastomer to swell, the elastomer was originally soaked by filling the cups with DC 200/10 silicone fluid and leaving them for over 100 hours. Since none of the layers of elastomer lining the bases was as thick as the sample used for the absorption tests, it was assumed that they would be in equilibrium with the fluid after this time. Four cups were used with 0.5, 1, 2 and 3 mm layers.

7.6.1 Effective elastic modulus after soaking in silicone fluid

The Instron loading tests were performed on the four acetabular cups after they had been soaked in silicone. The results in Table 7.3 show that the load/compression ratio is less than for the unsoaked specimens. It must however be remembered that the geometry of the soaked specimens was different from the unsoaked, so care must be taken in discussing changes in stiffness.

The four cups were tested with the full range of eight silicone fluids, at each of the three standard speeds of oscillation.

Results for 0.5 mm layer (E0)

Figures 7.40 and 7.41 show the friction factors obtained with a 0.5 mm layer (E0). The low load points (1, 2 and 3) show a minimum in friction factor around $\eta u/L$ = 5×10^{-5} m^{-1} and the friction factor increases on either side to a maximum of about 0.2.

The high load points (4 and 5) are almost constant and their average value is about 0.015.

Results for 1 mm layer (C1)

Two graphs have been plotted to illustrate these results. Figure 7.42 shows the low load points (1, 2 and 3) and has values of friction factor below 0.1 until the viscosity of the lubricant is a maximum ie 29.1 Pa s. Figure 7.43 demonstrates again the low almost constant values of friction factor seen for E0 at high loads.

Results for 2 mm layer (C2)

Again low values of friction factor were recorded for most viscosities. The only exception with this joint was the lowest viscosity fluid (9.4×10^{-3} Pa s) which gave a much higher friction factor, around 0.26 for the low loads (see Figure 7.44) and 0.03 for the high loads (Figure 7.45).

Results for 3 mm layer (B3)

The 9.4×10^{-3} Pa s viscosity fluid gave high values of friction factor, as with the 2 mm layer above, compared with the rest of the results. All the other friction

factors were about 0.05 for points 1, 2 and 3 and 0.01 for the high loads [points 4 and 5] [Figures 7.46 and 7.47].

7.6.2 Comparison of friction factor for different thicknesses of lining

For each viscosity of silicone fluid used, a graph of average friction factor against original thickness of lining was plotted in a similar manner to the SCMC results. These showed less variation in friction factor than the SCMC but the change that did occur was generally a decrease in friction factor with increasing thickness of lining [Figure 7.48]. The 9.4×10^{-3} Pa s viscosity fluid was an exception to this, showing a rather erratic but nevertheless increasing trend of friction factor with thickness.

7.7 Results for 2 mm layer soaked in silicone fluid but lubricated with SCMC [D2]

As the prostheses lubricated with silicone fluids had given much lower friction factors than when lubricated with SCMC, an experiment was done to find the effect of lubricating a joint previously soaked with silicone, with SCMC. Since the joint had been soaked in silicone fluid there was some doubt as to how much this might be expressed into the joint cavity and mix with the SCMC during testing. The joint was originally tested with C50, CA and CC in that order and the results when

plotted showed an increase then decrease in friction factor (Figures 7.49 and 7.50) - a shape not seen before. More tests were then done, repeating lubricant C50 and also including CB. These results then combined with the original CA and CC results to form a decreasing friction factor with increasing viscosity, as now expected for SCMC. It would seem that the original test with C50 (ie C50(1) on the graphs), being the first one, was contaminated with silicone fluid which produced lower friction values than expected. The swelling of the joint alone does not appear to reduce the friction factor.

7.8 Investigation of swelling effects on clearance in the prostheses

It was noticed that the clearance between the femoral head and the elastomeric lining in the acetabulum appeared to have completely disappeared after they had been soaked in silicone fluid. The clearance was not easy to measure experimentally but a method was devised which appeared to give sensible results though its accuracy was only about 20% on the smaller clearances.

A steel ball bearing, 34.92 mm in diameter, was placed in the acetabulum which was clamped onto a measuring table. The maximum total horizontal displacement of the ball in the cup was measured using a dial gauge; this was taken to be the diametral clearance in the joint.

The ball was 0.03 mm larger in diameter than the McKee-Farrar head used in the friction tests. The acetabulum Y3, which had not been soaked was found to have a diametral clearance of 1.01 mm by this method compared with its nominal value of 1.0 mm. The two thinner layers which had been soaked in silicone [00 - 0.5 mm layer and A1 - 1 mm layer] both had a clearance of 0.15 mm by this method. Their initial clearance was nominally 0.5 mm, ie it had reduced by 70%. However, with the 2 and 3 mm layers [A2, A3] no clearance was discernable at the edges of the acetabulum.

A2 and A3 after soaking in silicone fluid appeared to make an 'interference fit'. This was confirmed by the use of engineer's blue smeared onto the ball, which was only transferred to the rim of the acetabulum. By attempting to press the ball down into the base of the acetabulum it was deduced that the clearance at the pole was greater than 0.20 mm for A2 and greater than 0.42 mm for A3. These values are, of course, for radial clearance. Considering the results from the Instron tests, it was deduced that for a load of 1500N, the crosshead and hence the steel ball moved down a distance of 0.27 mm for the 3 mm layer. According to the above results, this would mean that there was no contact at the pole of the joint during a typical loading cycle. However it must be remembered that the Instron test took place more slowly than the impulse loading of the walking cycle in the simulator.

Reference	Thickness of sample	Elastic modulus (M Pa)
A0	3.5	2.63
A1	3.5	2.61
A2	3.5	2.90
A3	6.5	1.94
B2	6.5	1.72
00	6.5	2.00
Y3	6.5	2.08
Z1	6.5	2.14
D1	6.5	1.33

Table 7.1

Elastic modulus of slabs of elastomer made from the same mixes as the linings specified.

Reference	Thickness of compliant layer [mm]	Radial clearance [mm]	Load/compression [10^3 N mm^{-1}]	
			At load of 250N	At load of 1500N
A0	0.5	'normal' 0.25	12.4	18.8
D0	0.5		10.0	15.2
A1	1.0		10.4	16.8
A2	2.0		9.2	11.2
A3	3.0		7.2	9.6
Z1	0.5	'large' 0.5	7.6	13.2
Y3	2.5		6.4	8.8

Table 7.2

Acetabula with compliant linings and their 'stiffness' ranking from Instron tests.

Reference after soaking	Reference before soaking	Thickness of compliant layer [mm]	Load/compression [10^3 N mm^{-1}]	
			At load of 250N	At load of 1500N
E0	D0	0.5	8.4	14.4
C1	A1	1.0	6.4	14.4
C2	A2	2.0	7.6	10.0
B3	A3	3.0	4.0	7.6

Table 7.3

The 'stiffness' of acetabular cups with compliant linings after soaking in silicone fluid.

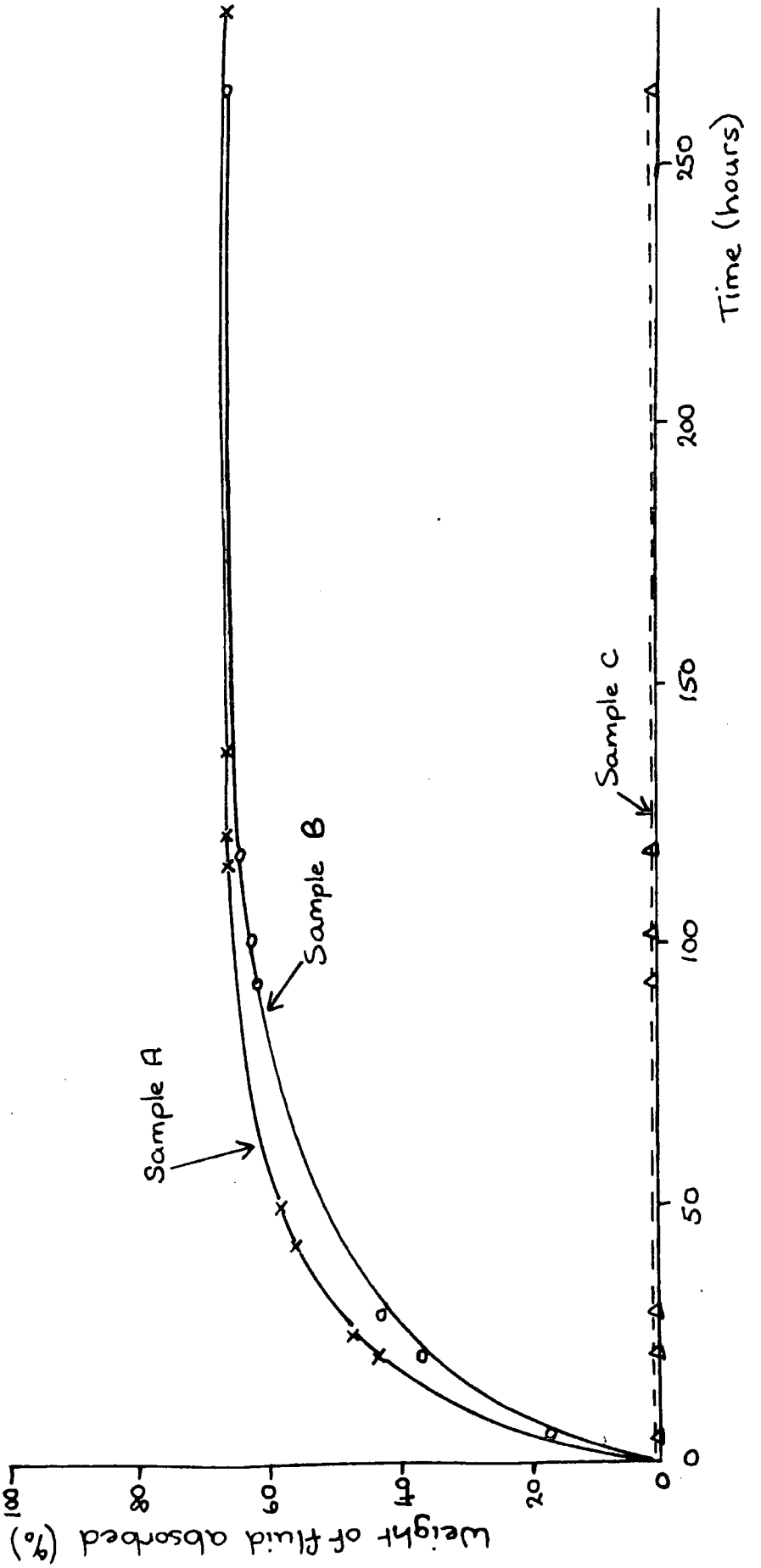

Figure 7.1

Absorption tests on silicone elastomer. Samples A and B were soaked in silicone fluid. Sample C was soaked in SCMC.

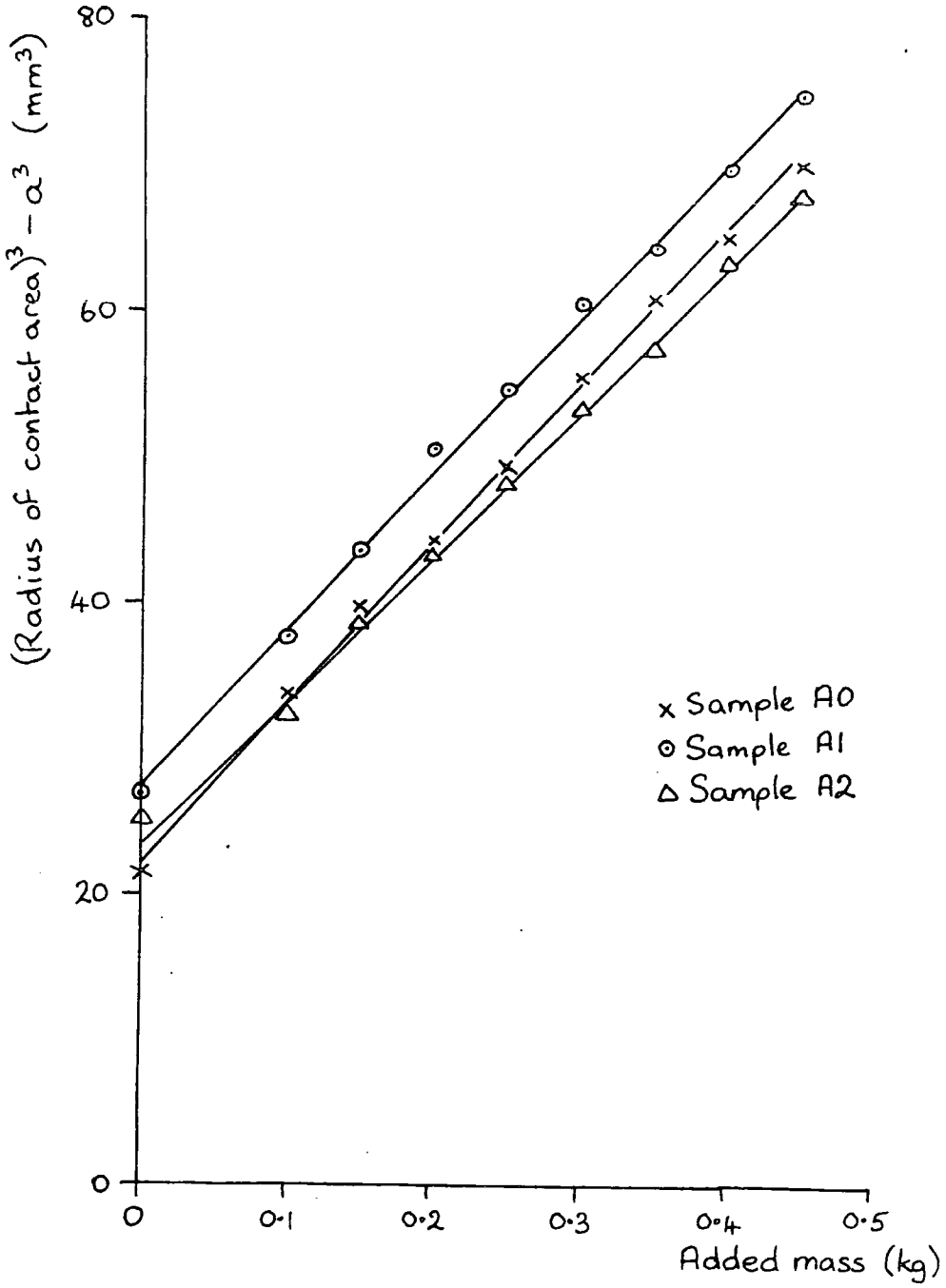

Figure 7.2

Graphs for determination of elastic modulus for elastomer mixes.

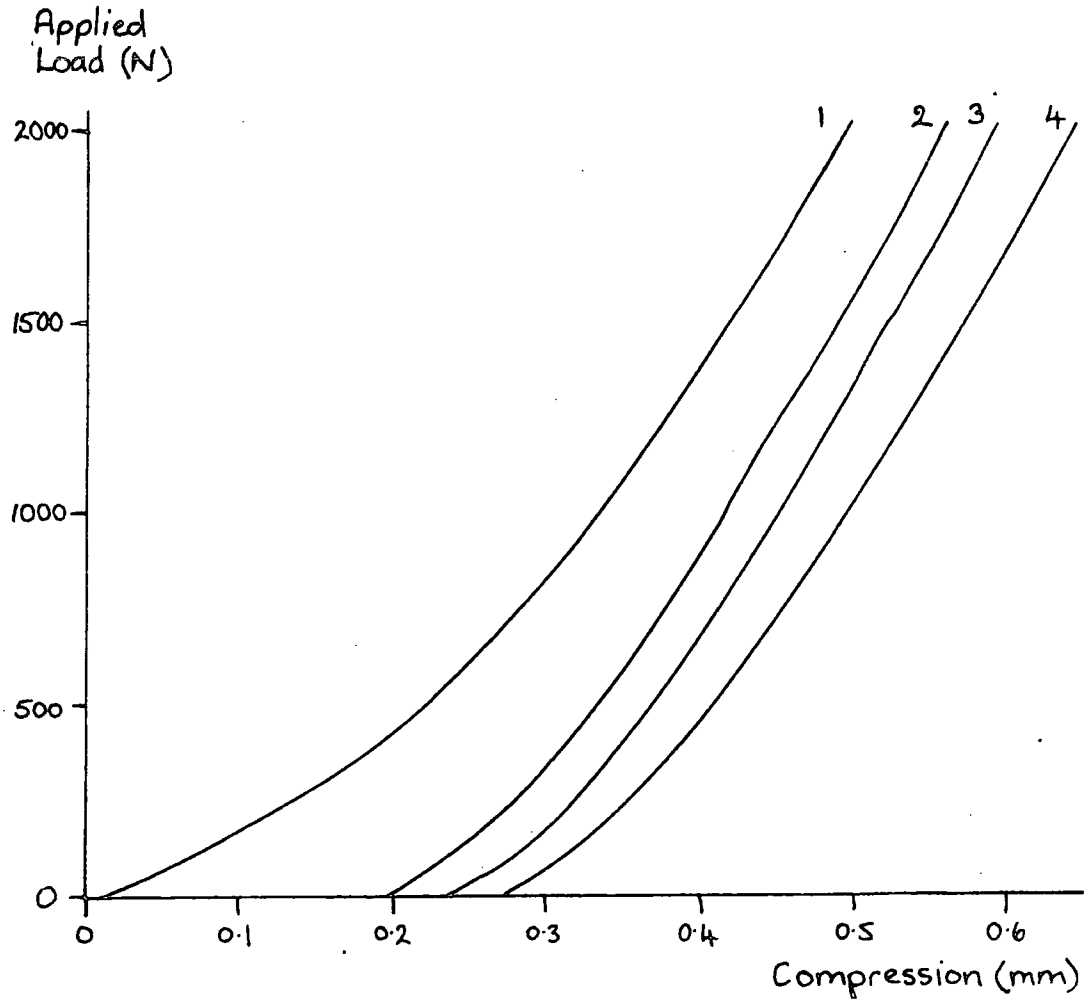

Figure 7.3

Instron traces for joint A2 loaded repeatedly at 10 mm min^{-1}.

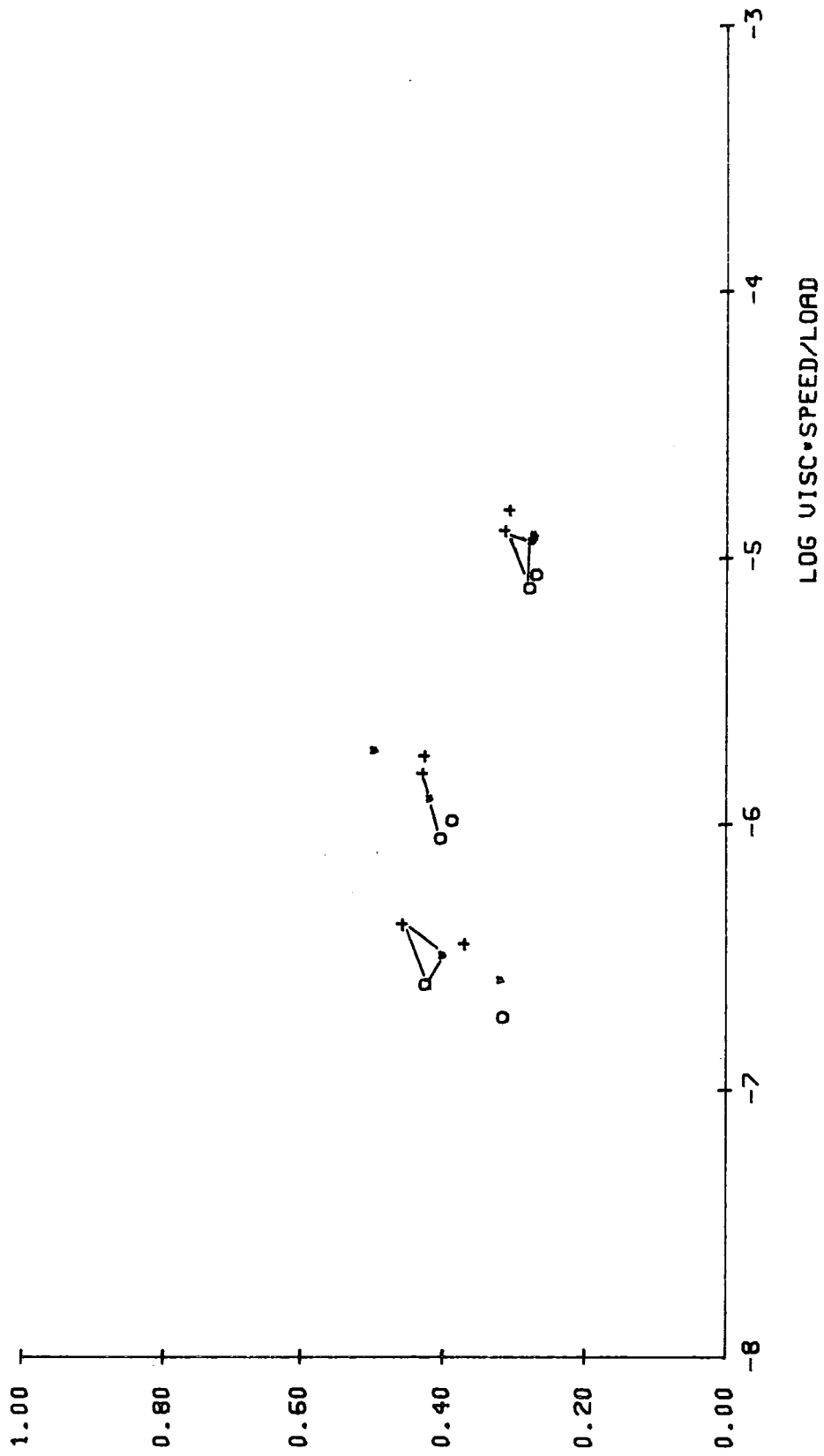

Figure 7.4

Joint A1: 1 mm layer lubricated with SCMC - point 1. (Joined points are repeat run.)

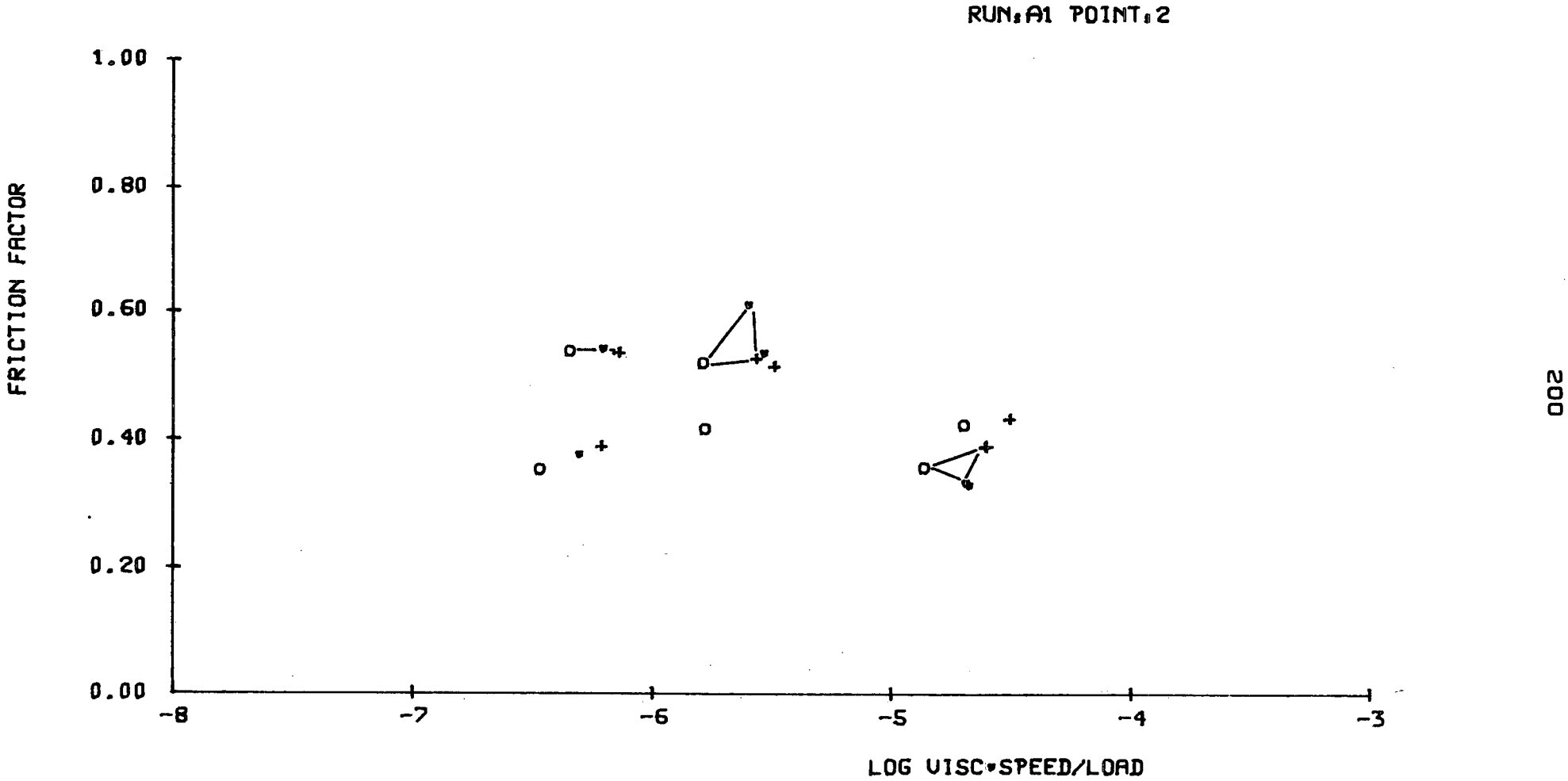

Figure 7.5

Joint A1: 1 mm layer lubricated with SCMC - point 2. [Joined points are repeat run.]

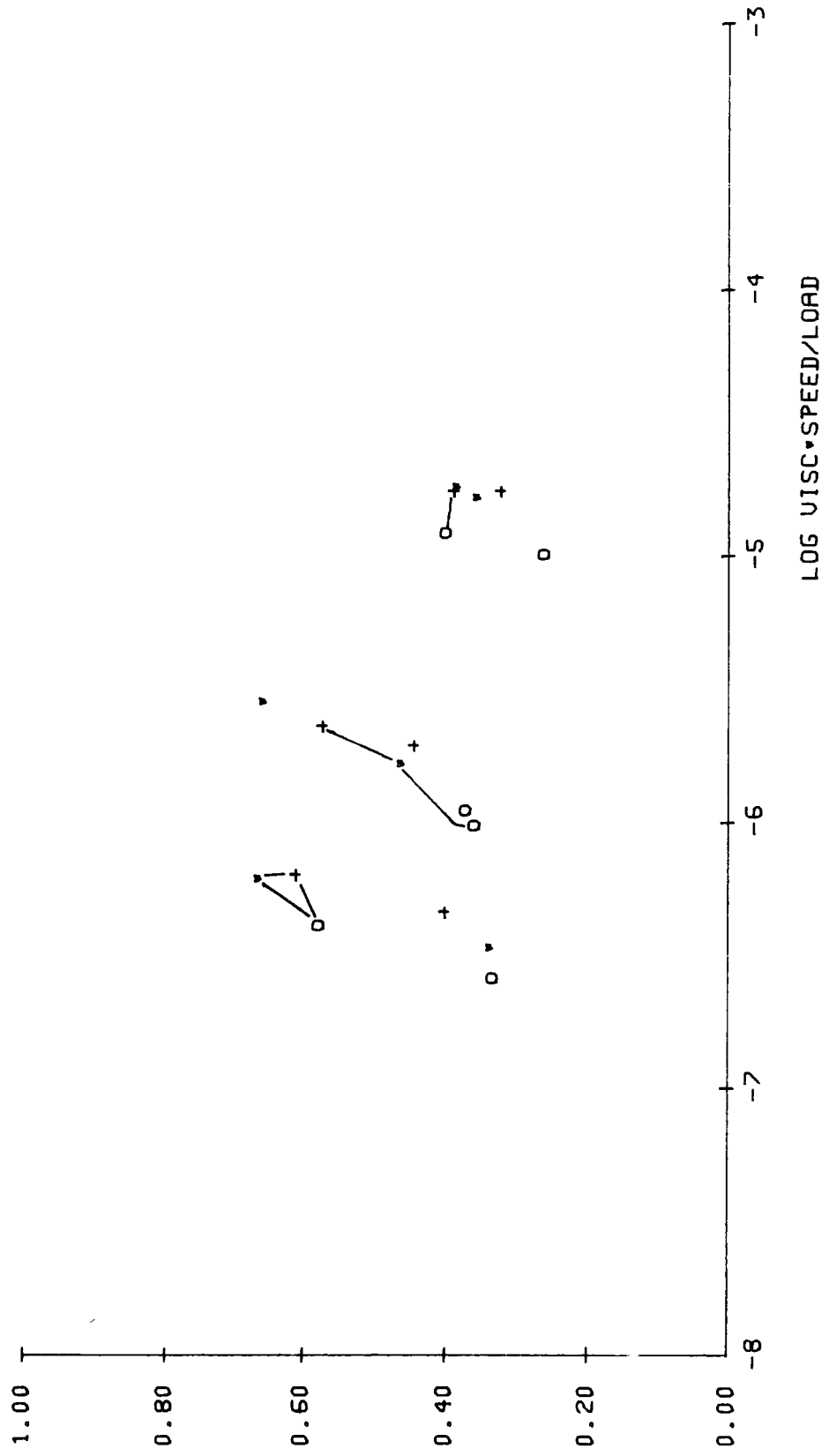

Figure 7.6

Joint A1: 1 mm layer lubricated with SCMC - point 3. (Joined points are repeat run.)

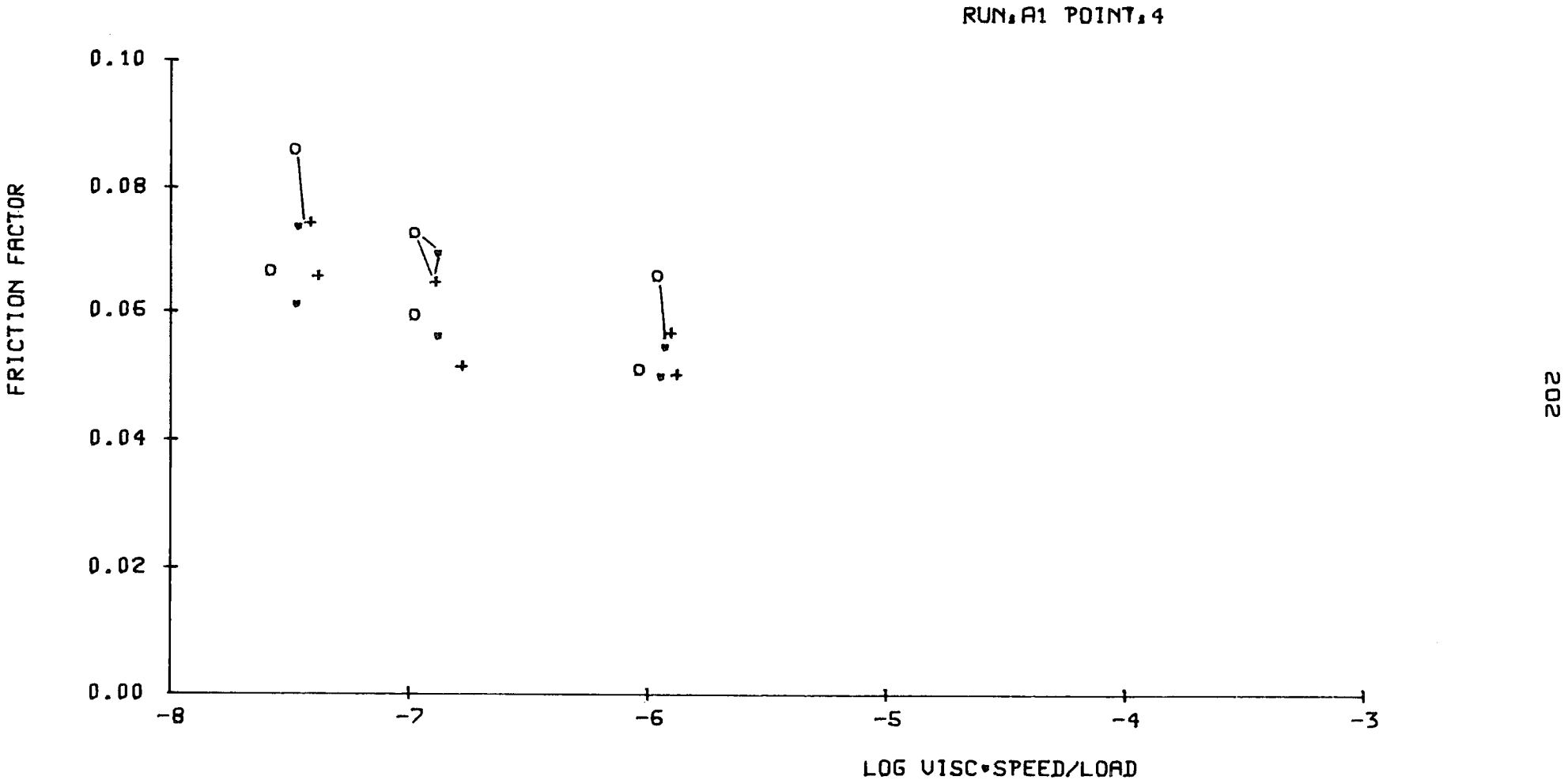

Figure 7.7

Joint A1: 1 mm layer lubricated with SCMC - point 4. [Joined points are repeat run.]

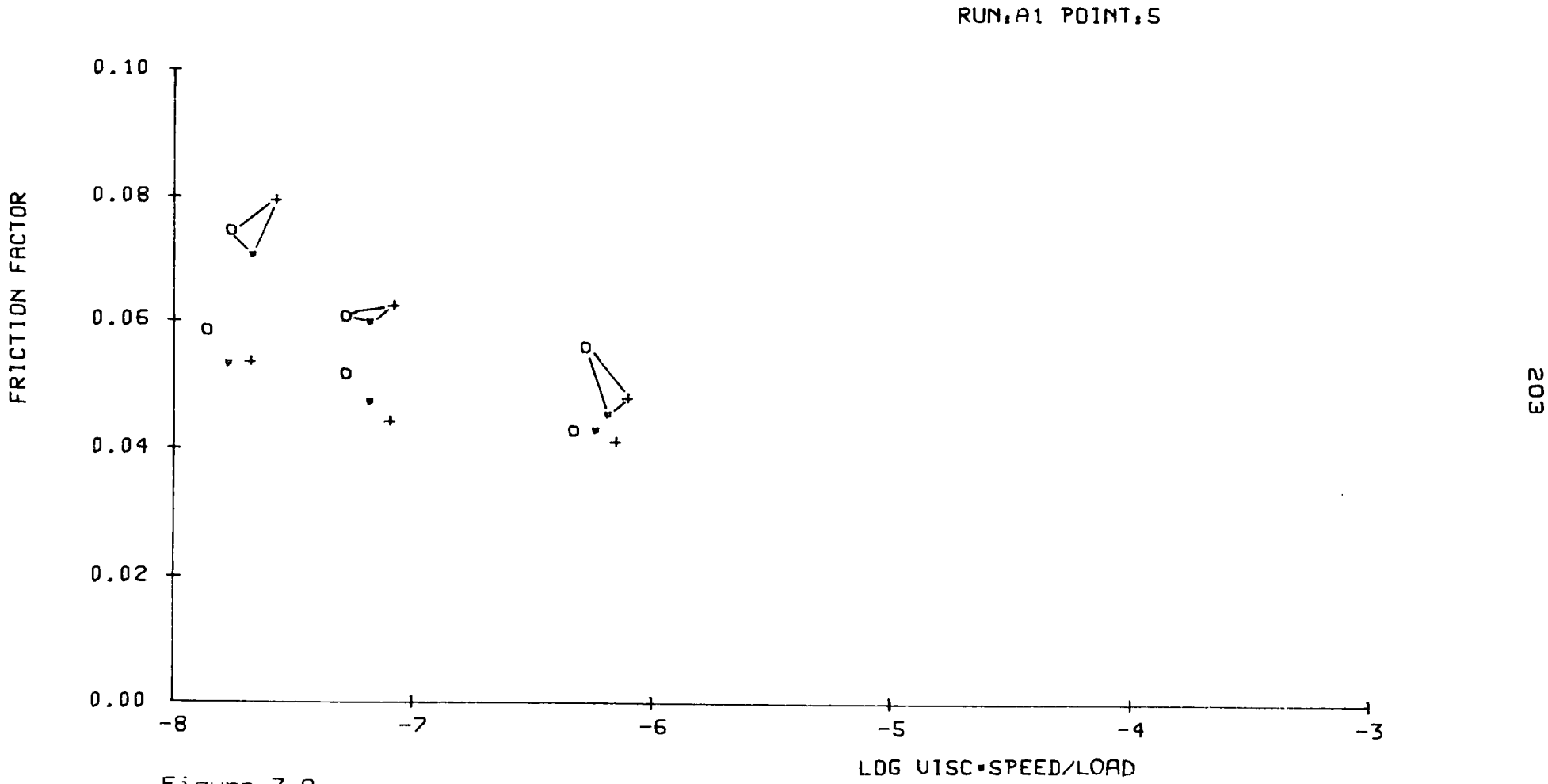

Figure 7.8

Joint A1: 1 mm layer lubricated with SCMC - point 5. (Joined points are repeat run.)

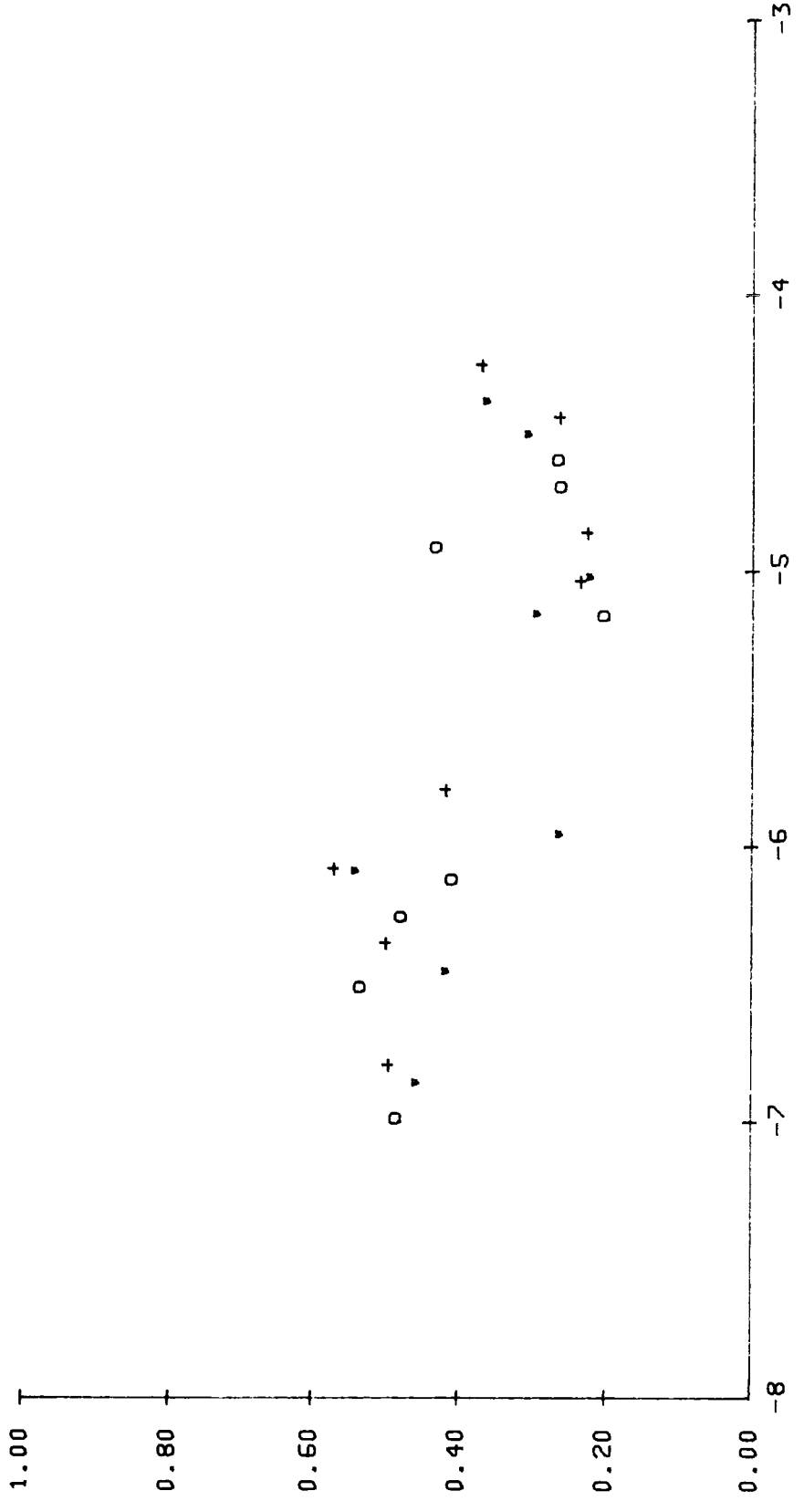

Figure 7.9

Joint D1: 1 mm layer lubricated with SCMC - point 1.

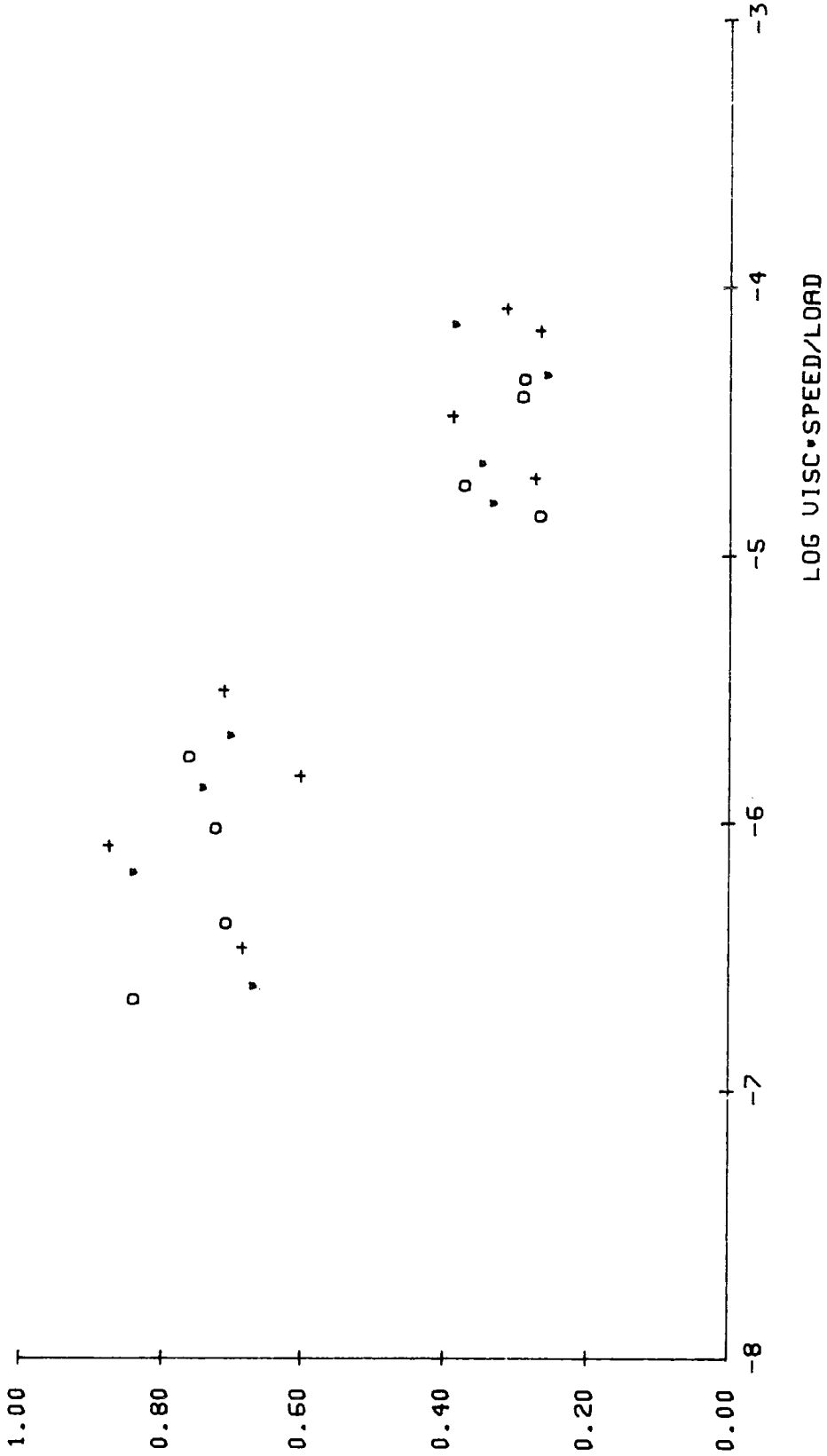

Figure 7.10

Joint D1: 1 mm layer lubricated with SCMC - point 2.

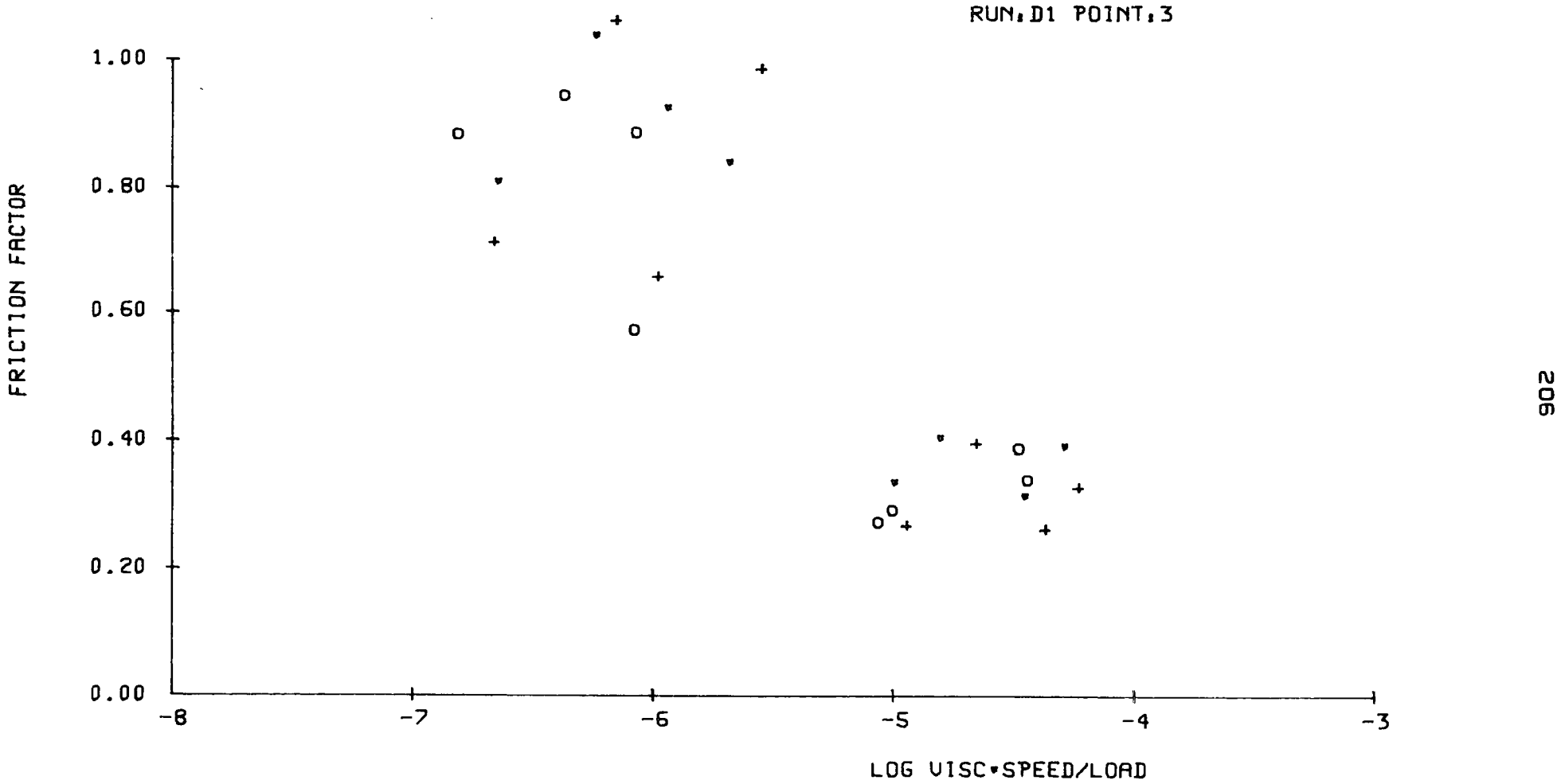

Figure 7.11

Joint D1: 1 mm layer lubricated with SCMC - point 3.

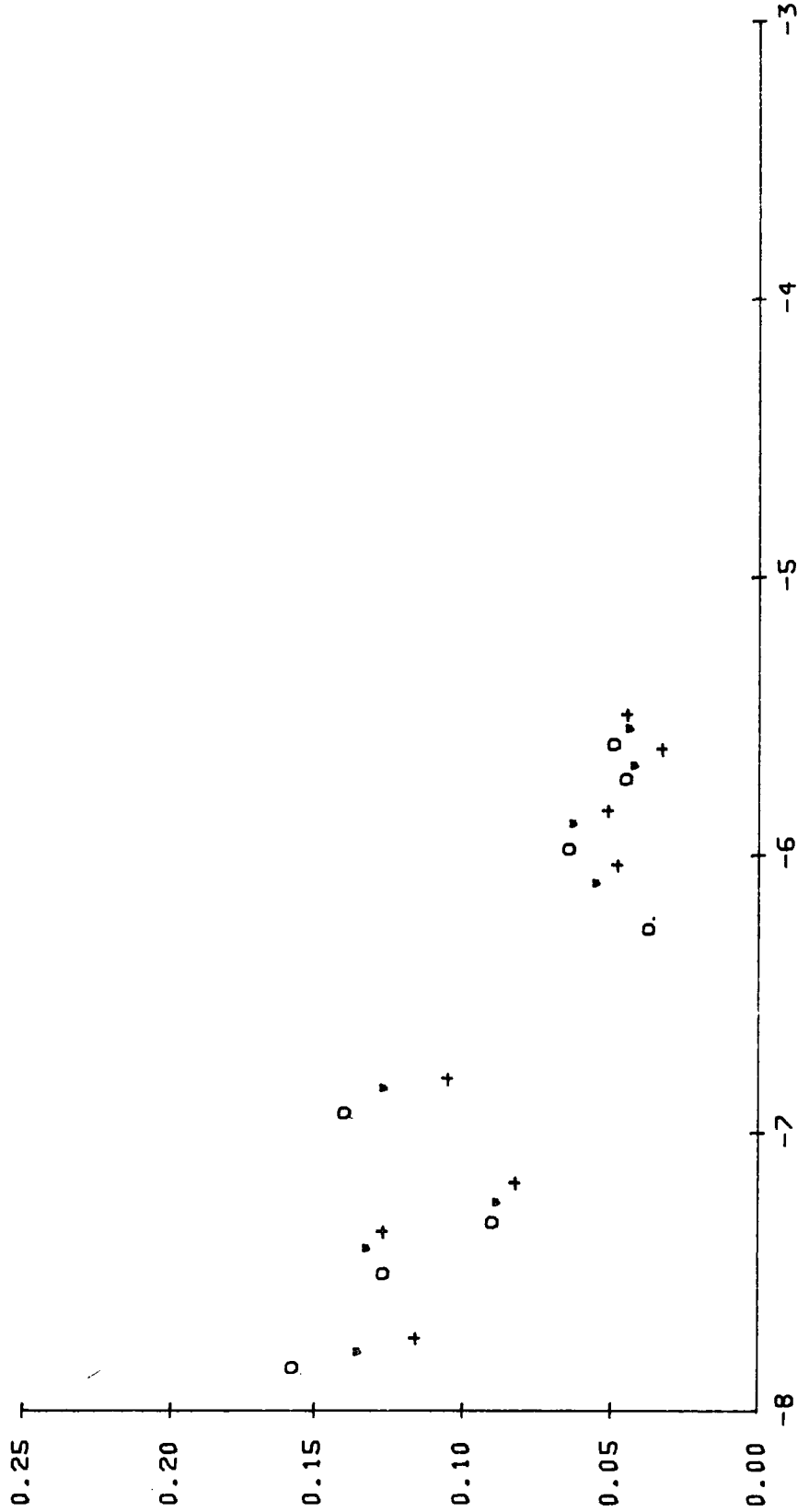

Figure 7.12

Joint D1: 1 mm layer lubricated with SCMC - point 4.

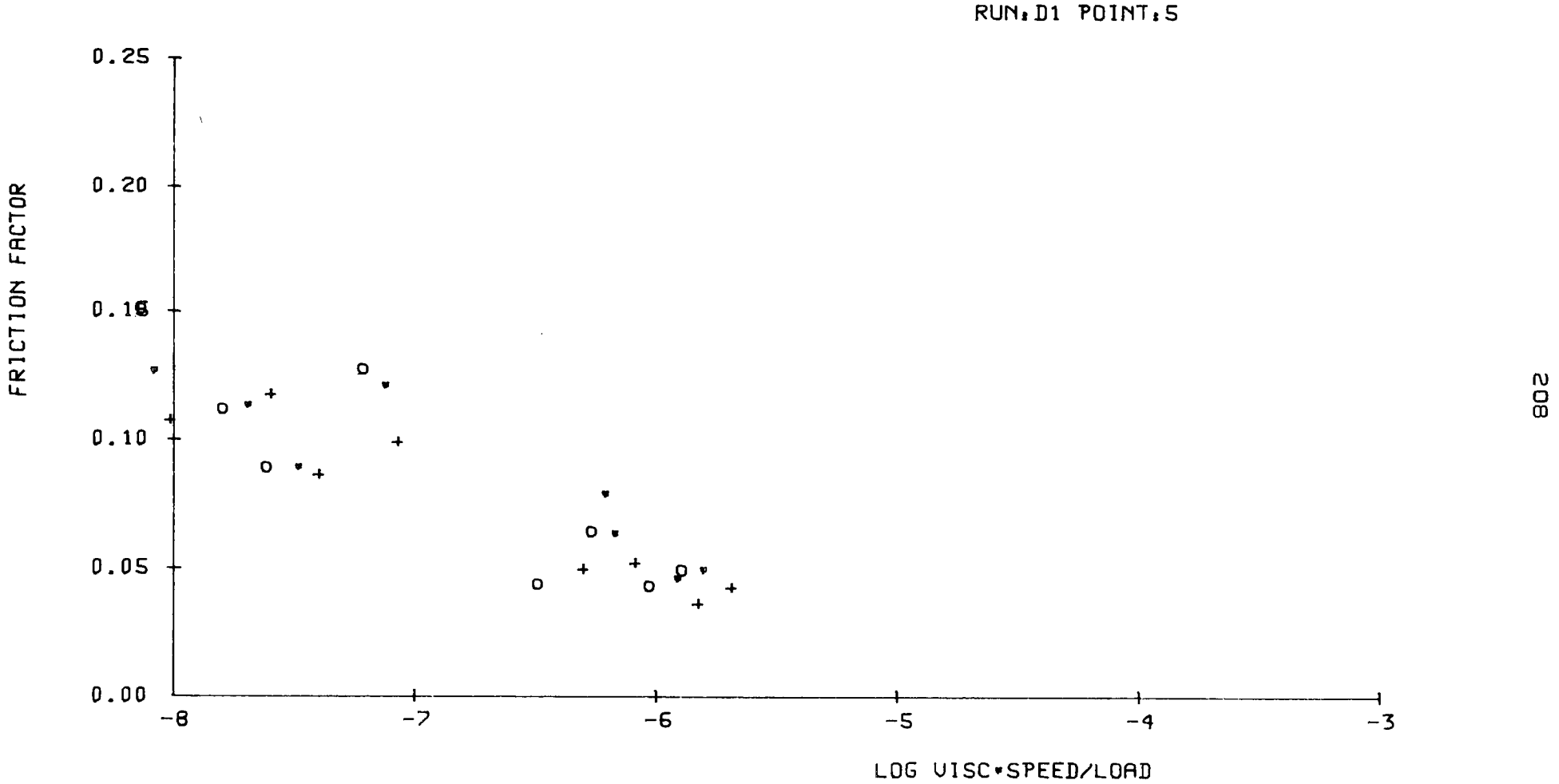

Figure 7.13

Joint D1: 1 mm layer lubricated with SCMC - point 5.

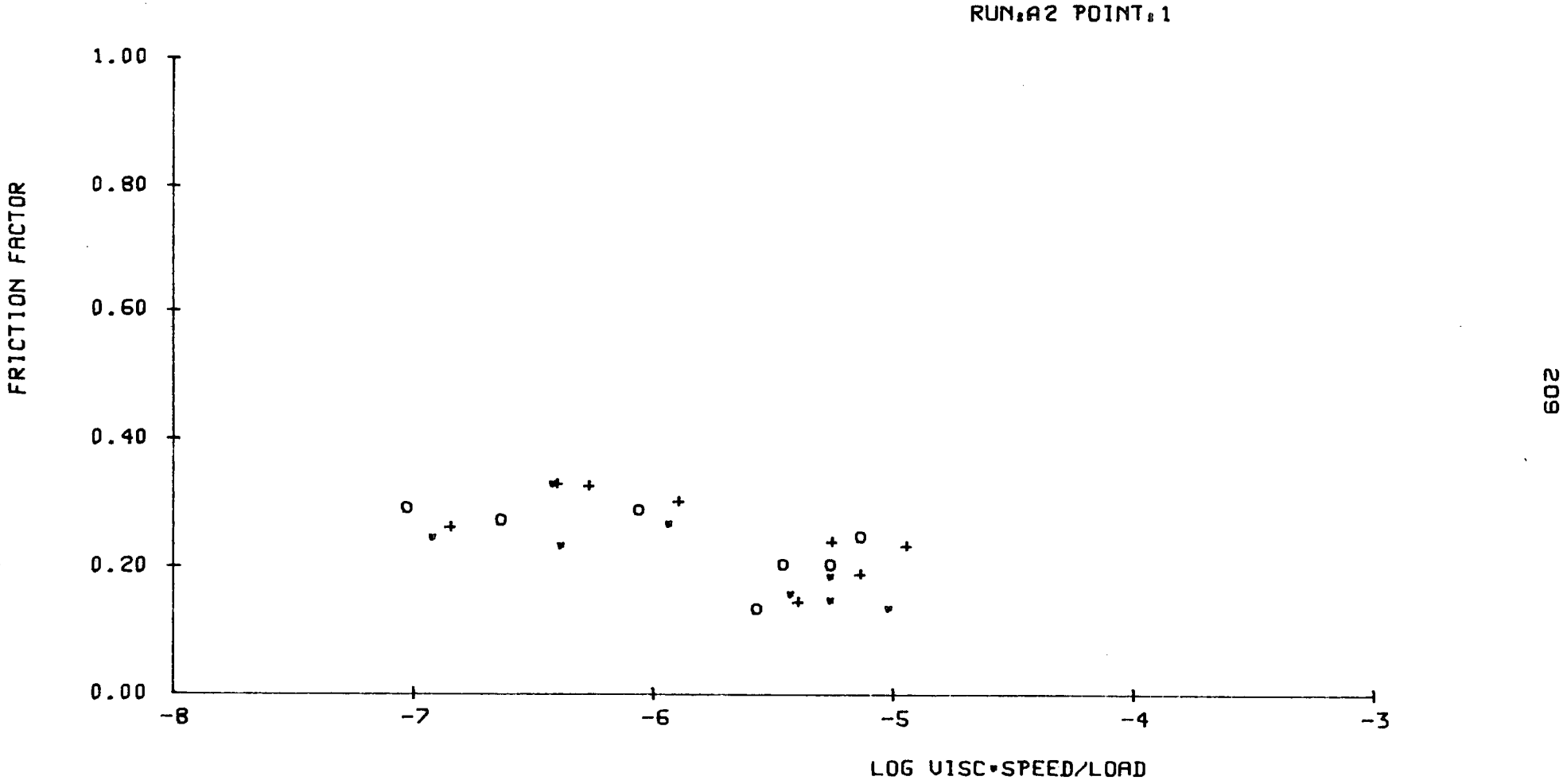

Figure 7.14

Joint A2: 2 mm layer lubricated with SCMC - point 1.

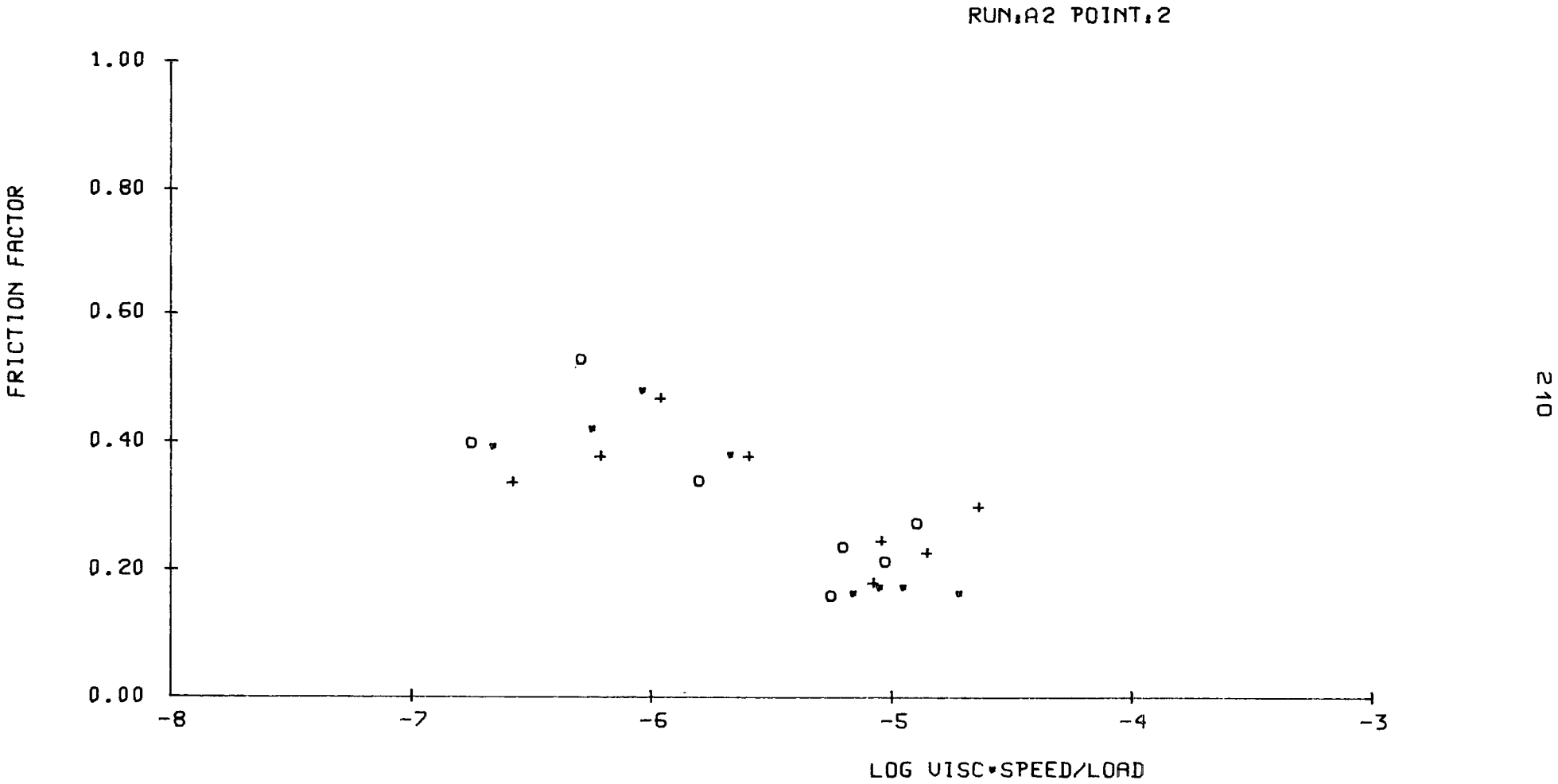

Figure 7.15

Joint A2: 2 mm layer lubricated with SCMC - point 2.

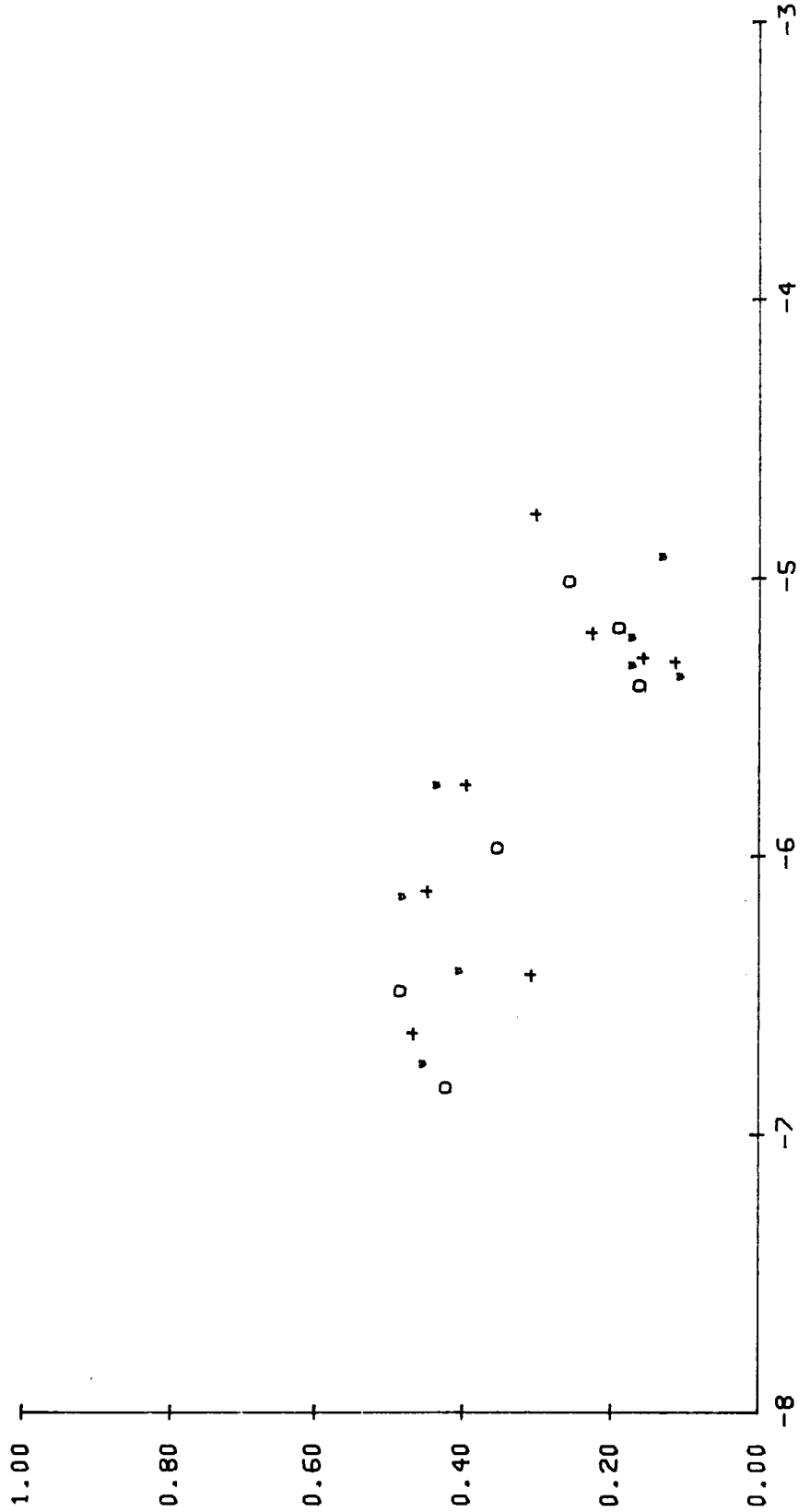

Figure 7.16

Joint A2: 2 mm layer lubricated with SCMC - point 3.

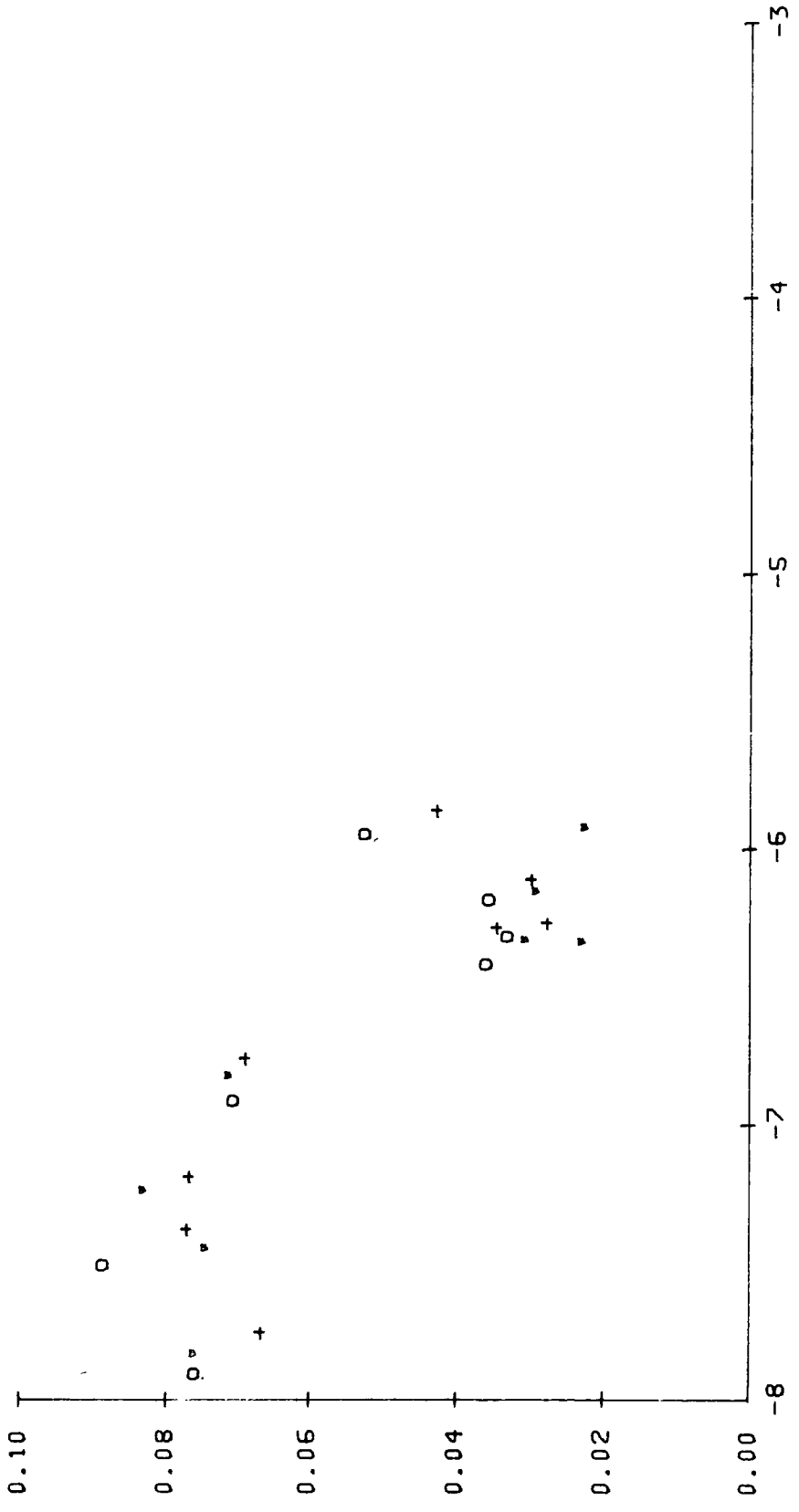

Figure 7.17

Joint A2: 2 mm layer lubricated with SCMC - point 4.

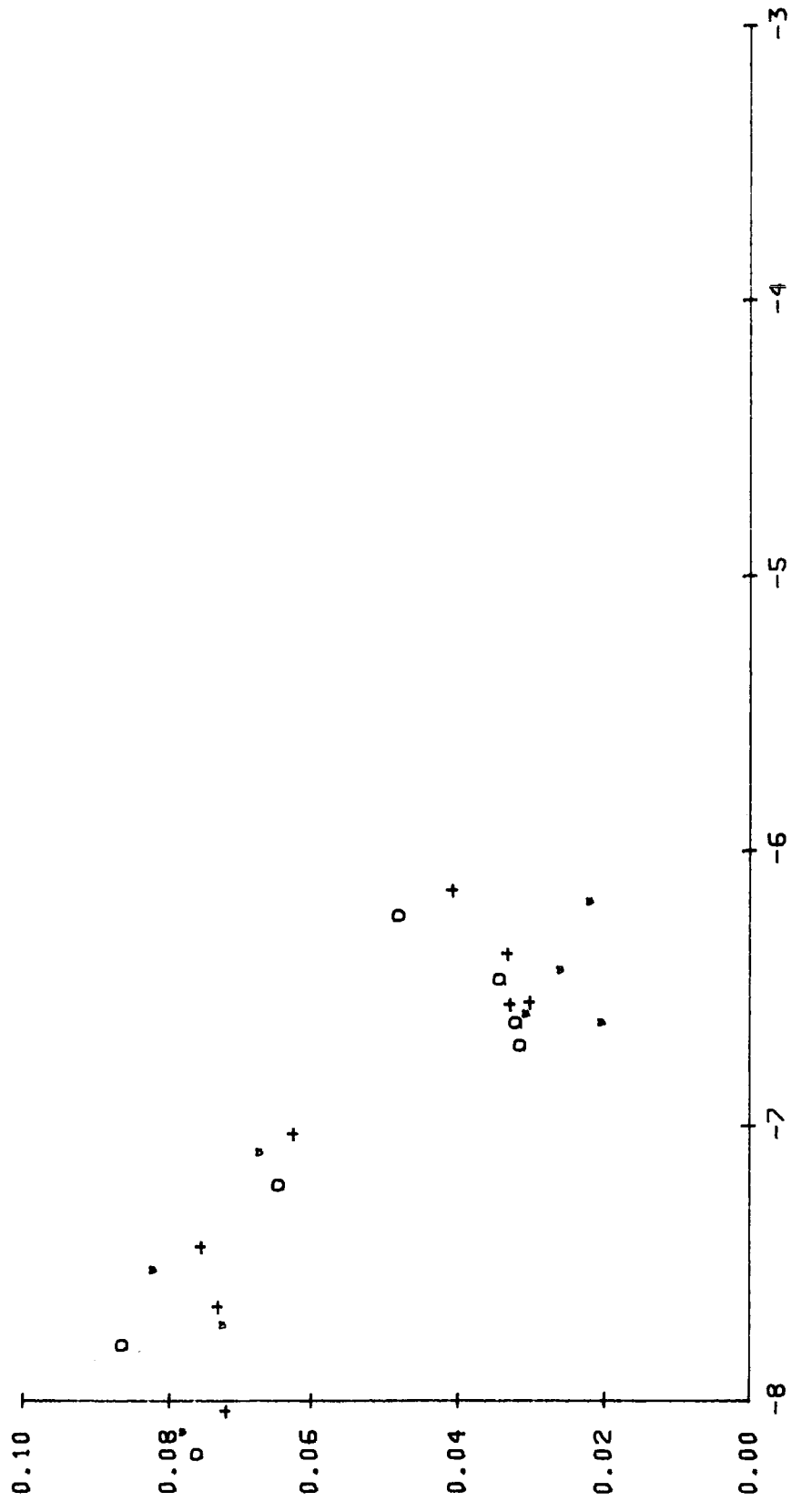

Figure 7.18

Joint A2: 2 mm layer lubricated with SCMC - point 5.

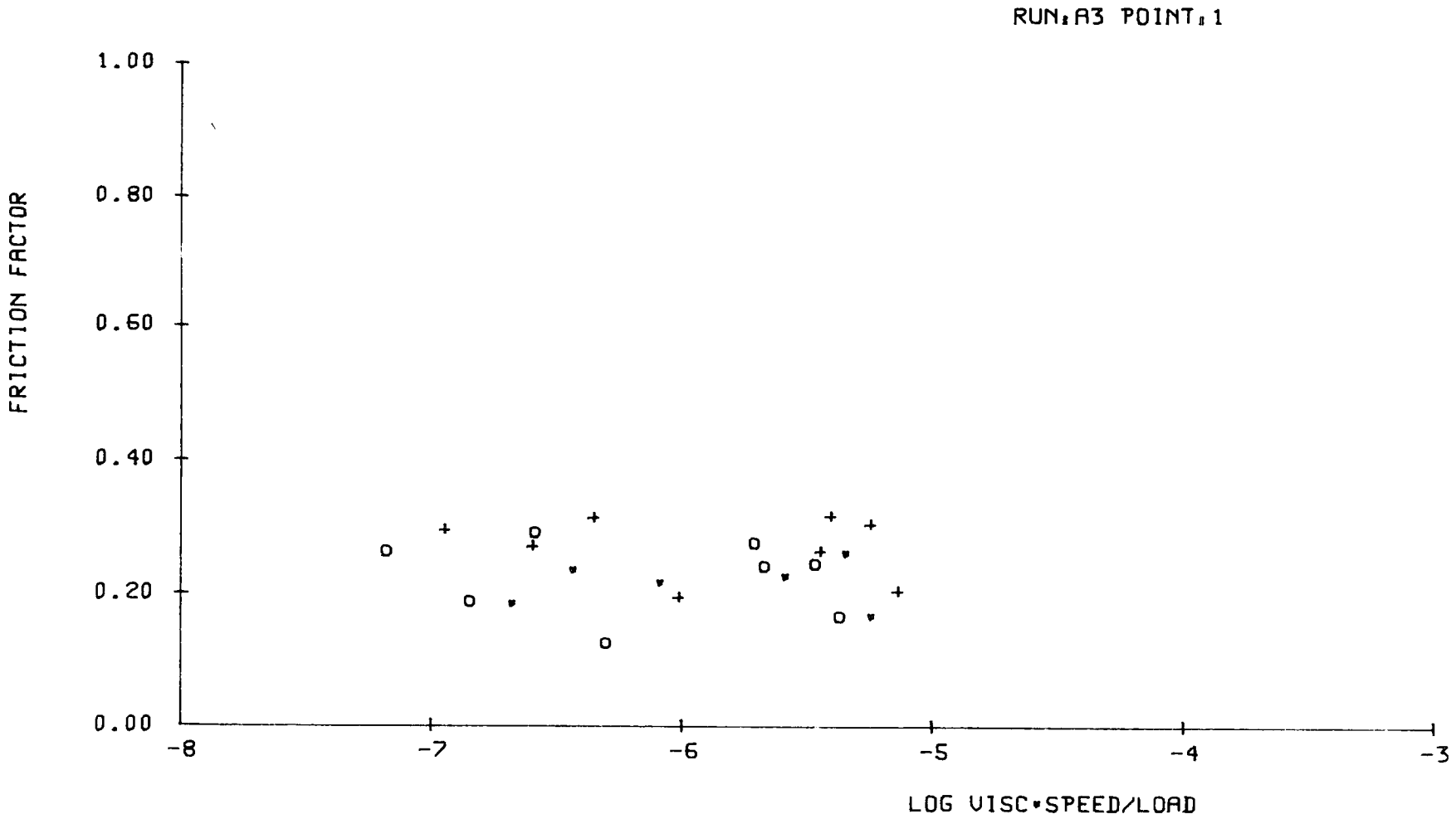

Figure 7.19

Joint A3: 3 mm layer lubricated with SCMC - point 1.

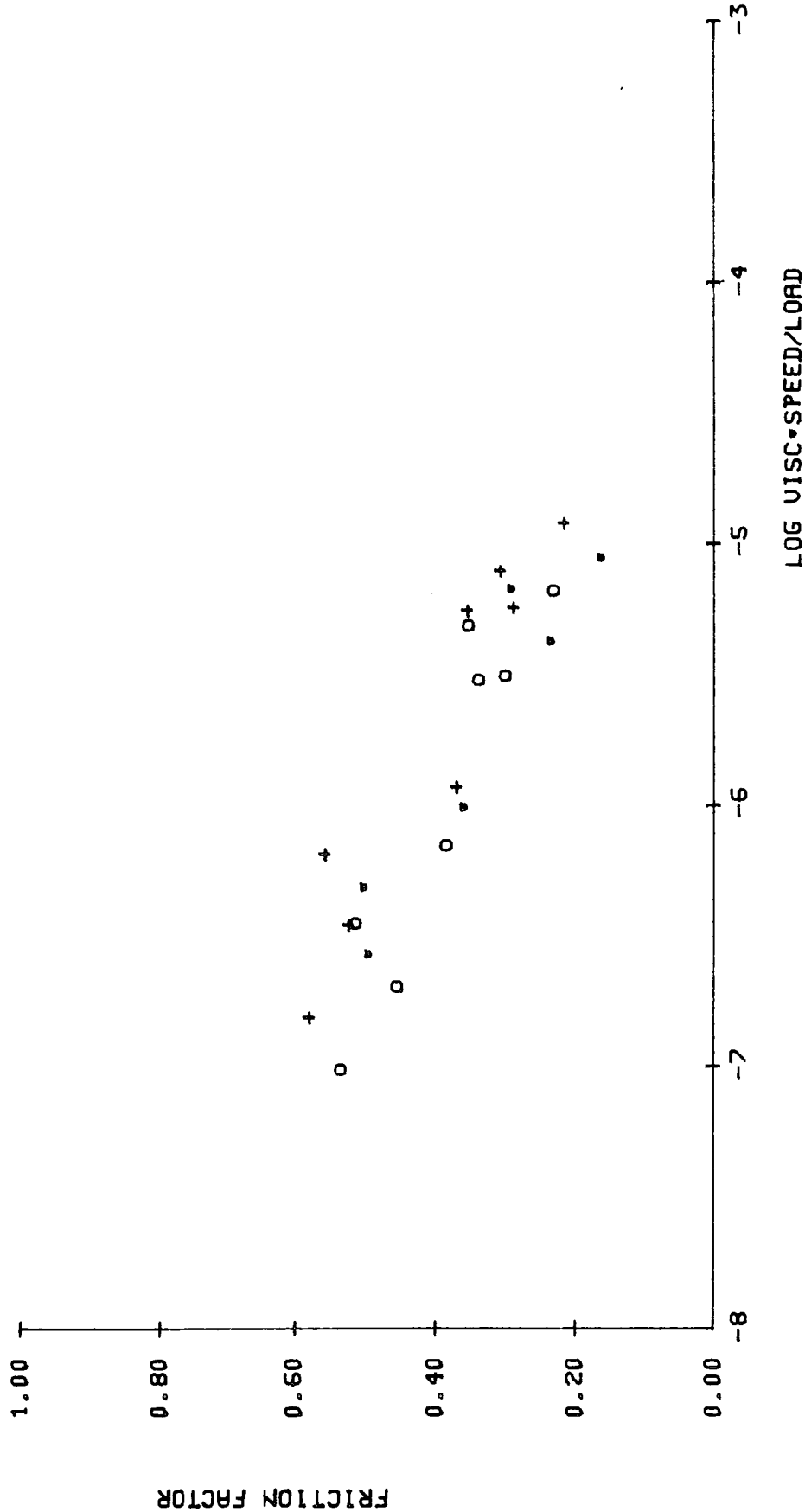

Figure 7.20

Joint A3: 3 mm layer lubricated with SCMC - point 2.

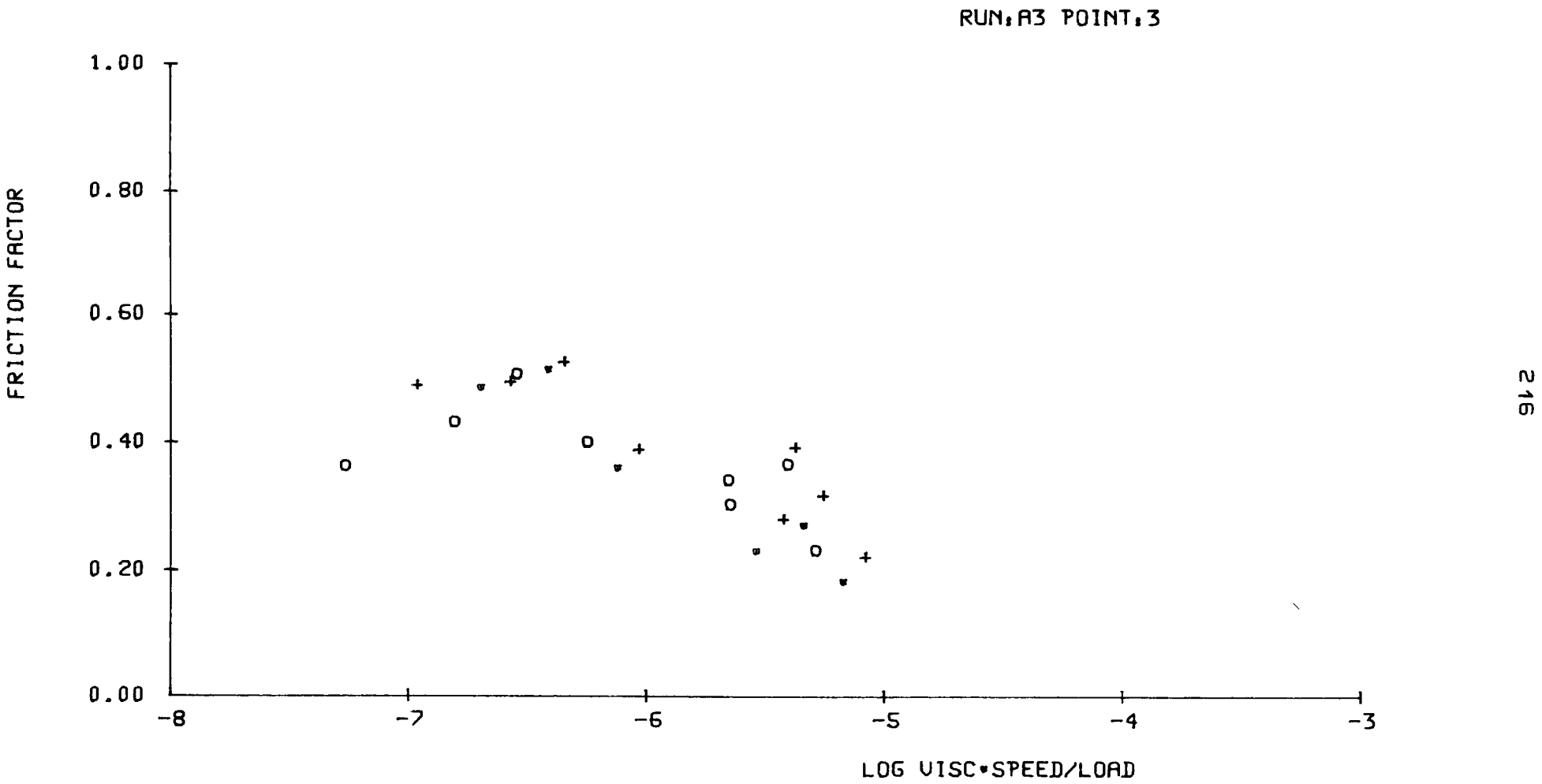

Figure 7.21

Joint A3: 3 mm layer lubricated with SCMC - point 3.

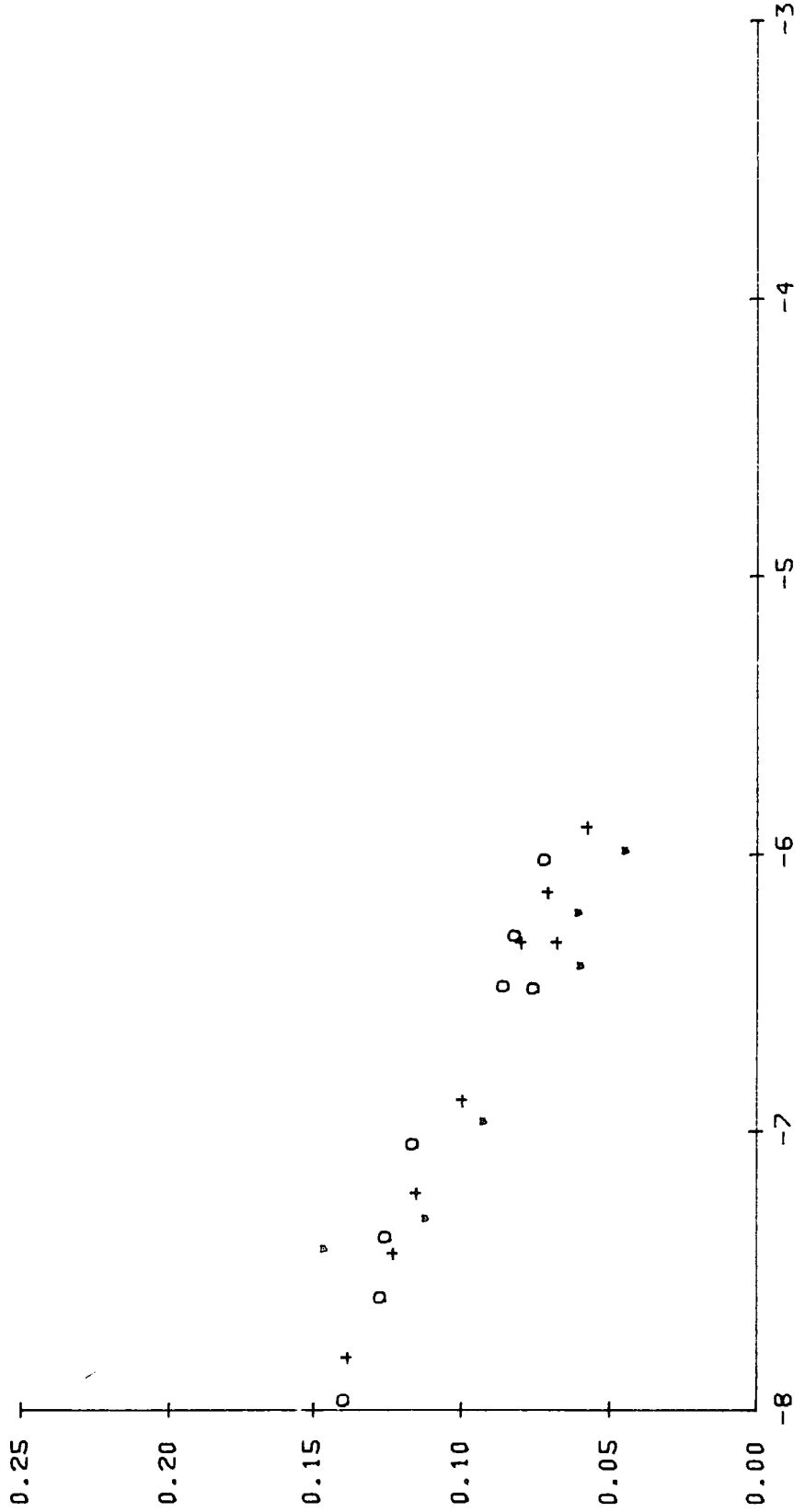

Figura 7.22

Joint A3: 3 mm layer lubricated with SCMC - point 4.

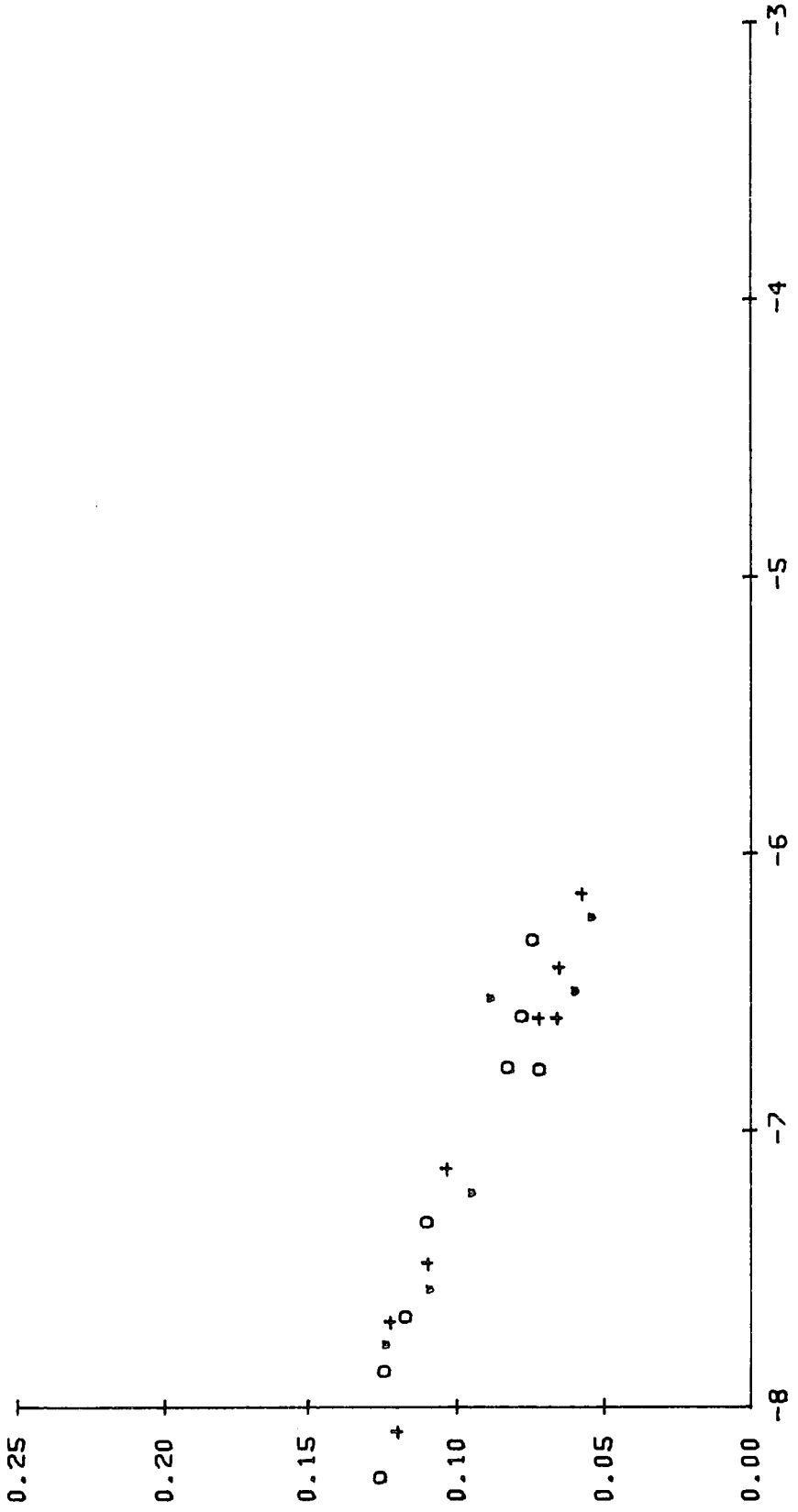

Figure 7.23

Joint A3: 3 mm layer lubricated with SCMC - point 5.

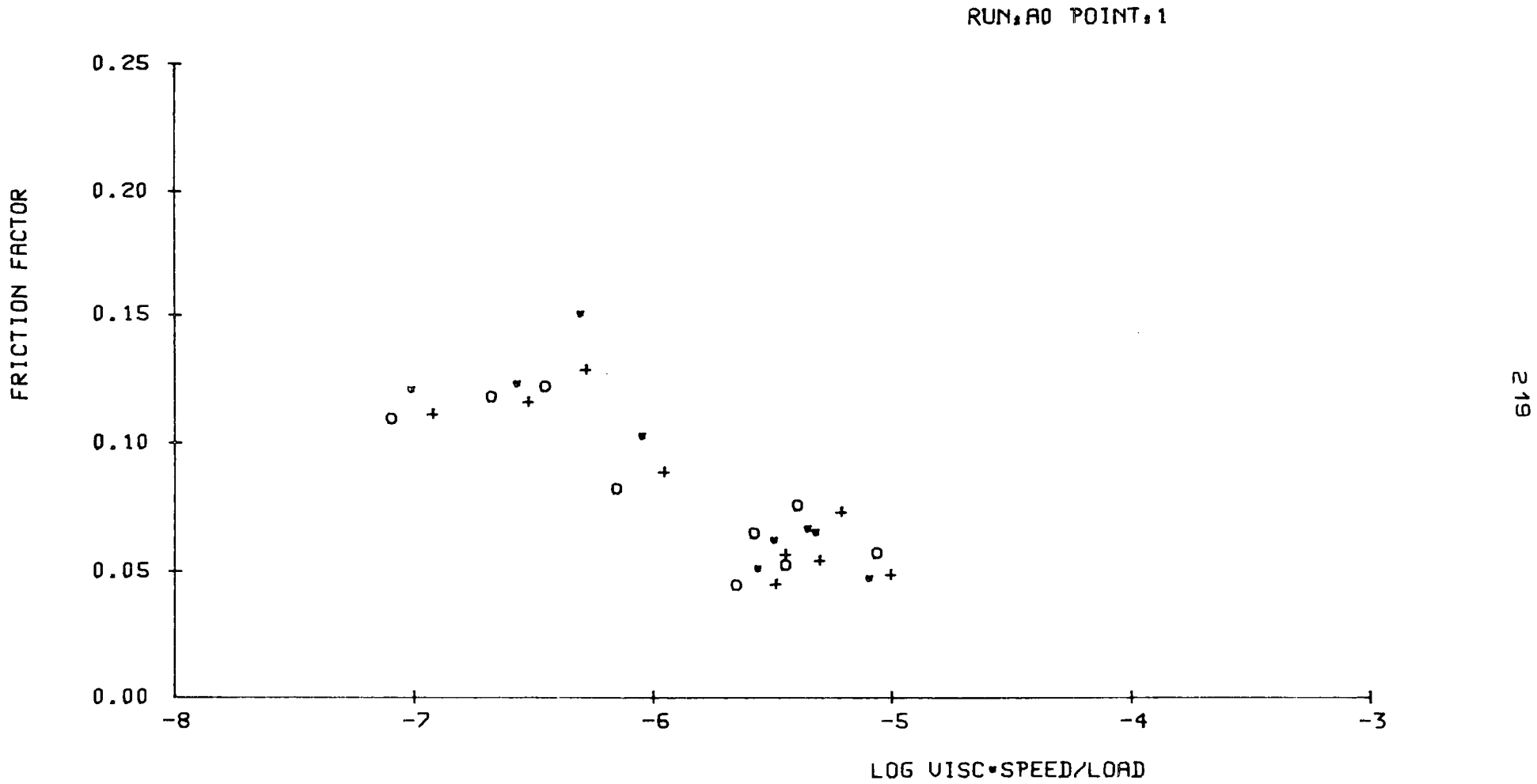

Figure 7.24

Joint A0: 0.5 mm layer lubricated with SCMC - point 1.

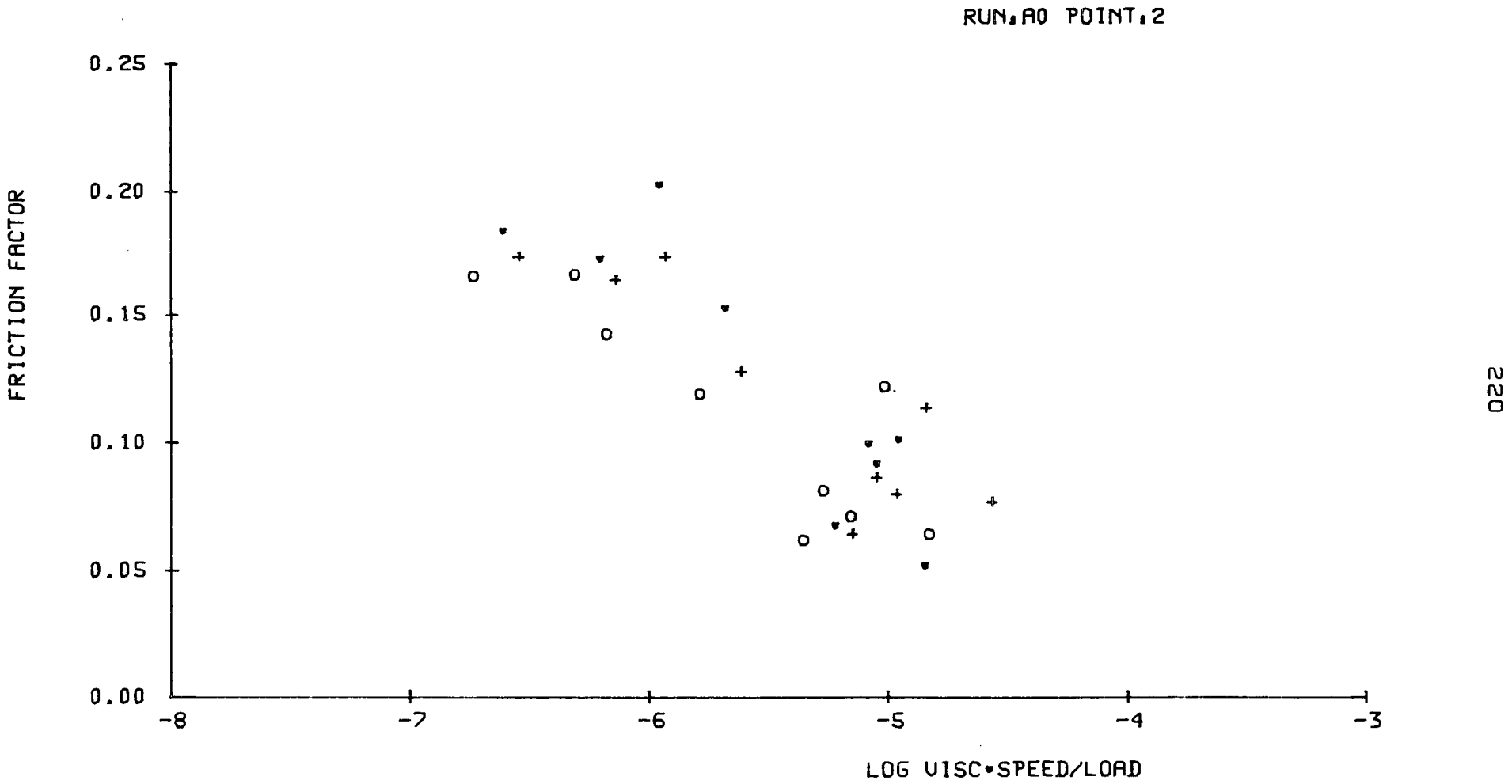

Figure 7.25

Joint A0: 0.5 mm layer lubricated with SCMC - point 2.

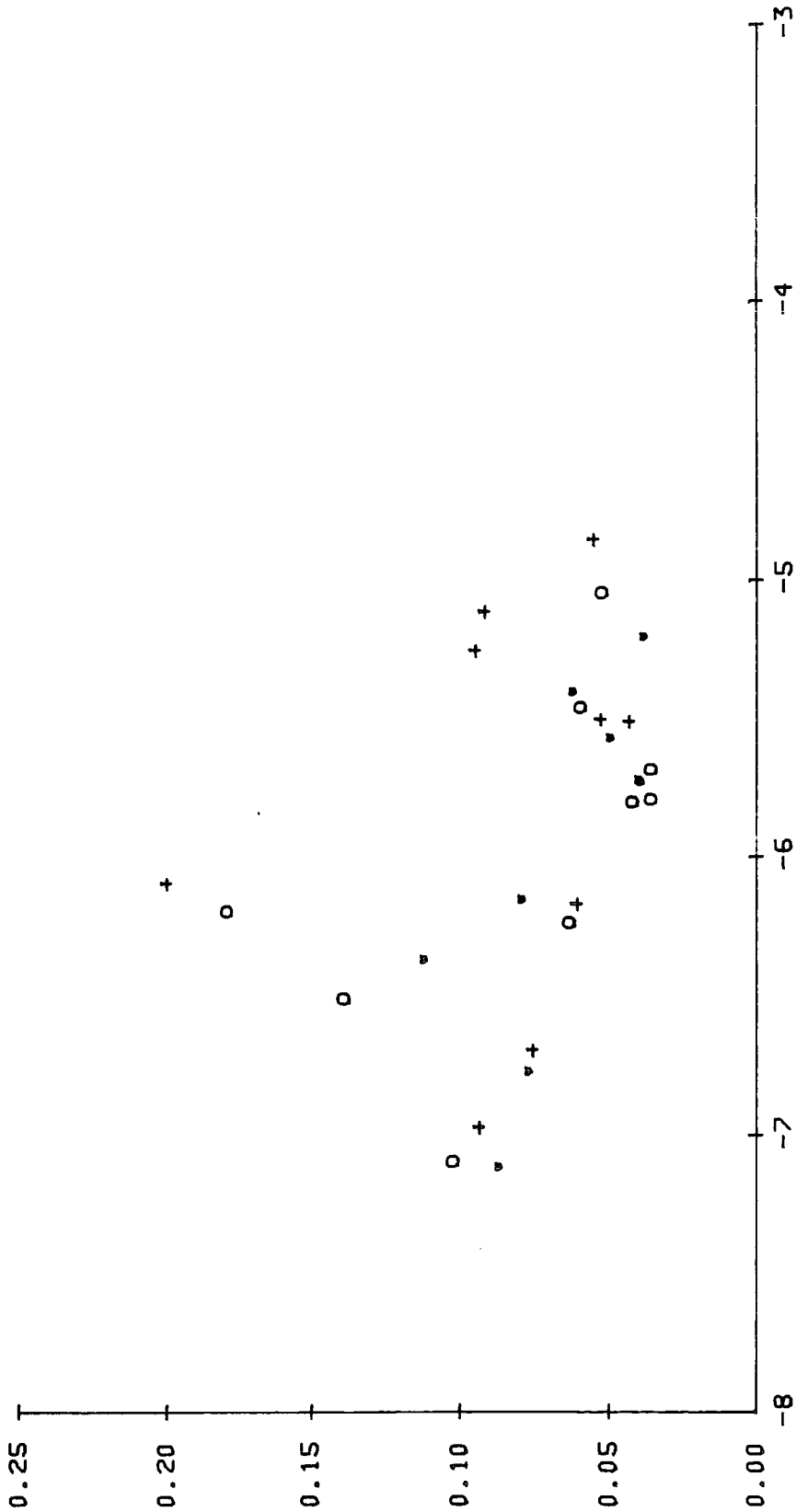

Figure 7.26

Joint A0: 0.5 mm layer lubricated with SCMC - point 3.

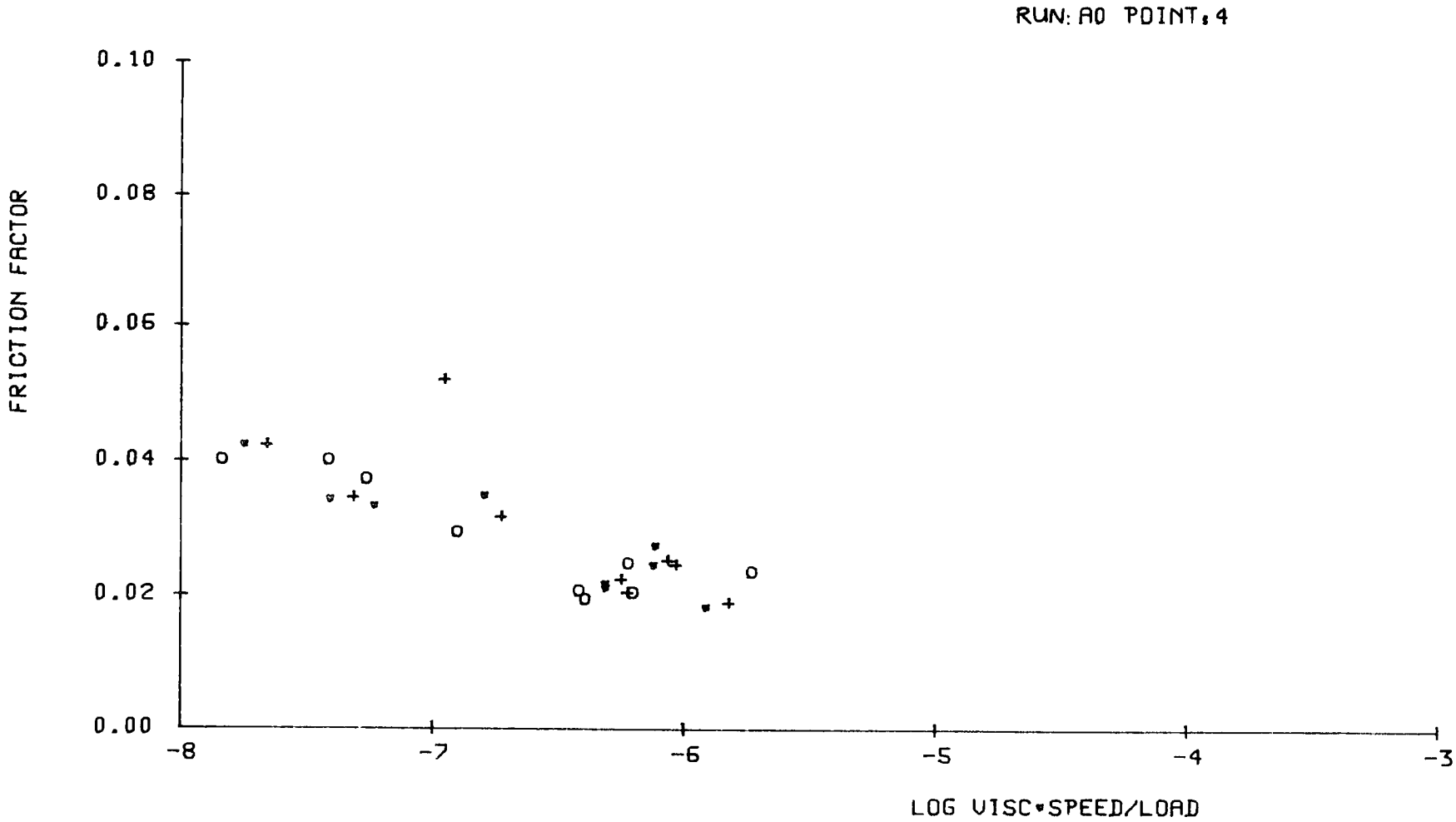

Figure 7.27

Joint A0: 0.5 mm layer lubricated with SCMC - point 4.

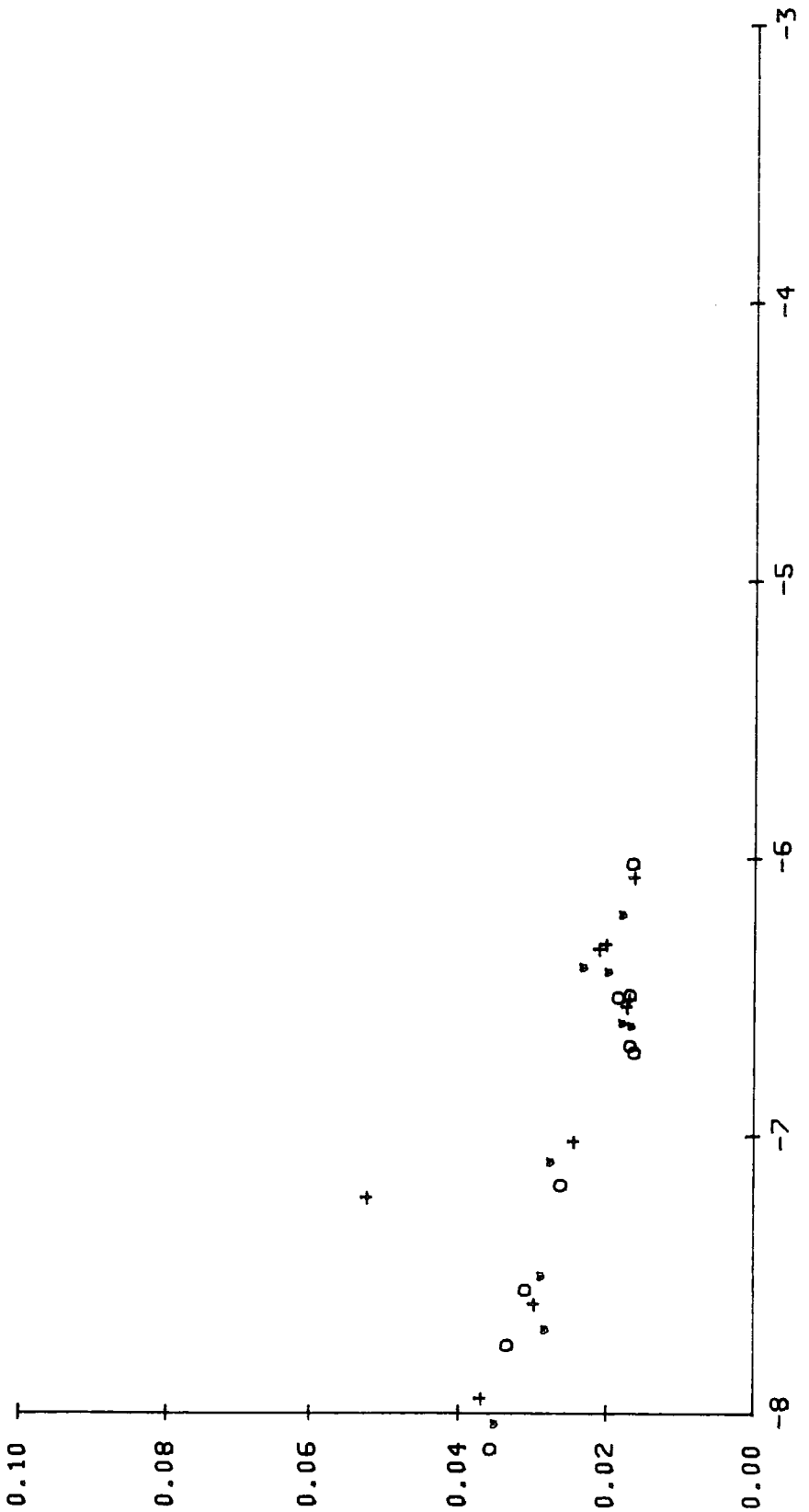

Figure 7.28

Joint A0: 0.5 mm layer lubricated with SCMC - point 5.

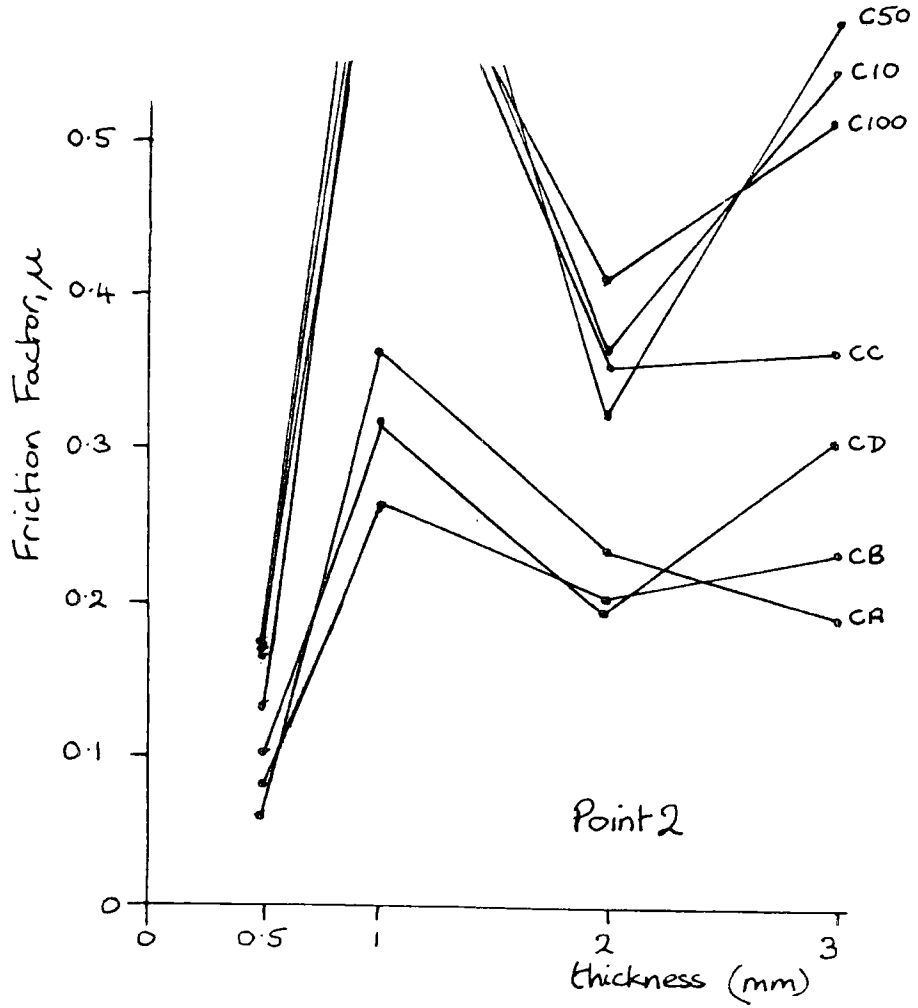

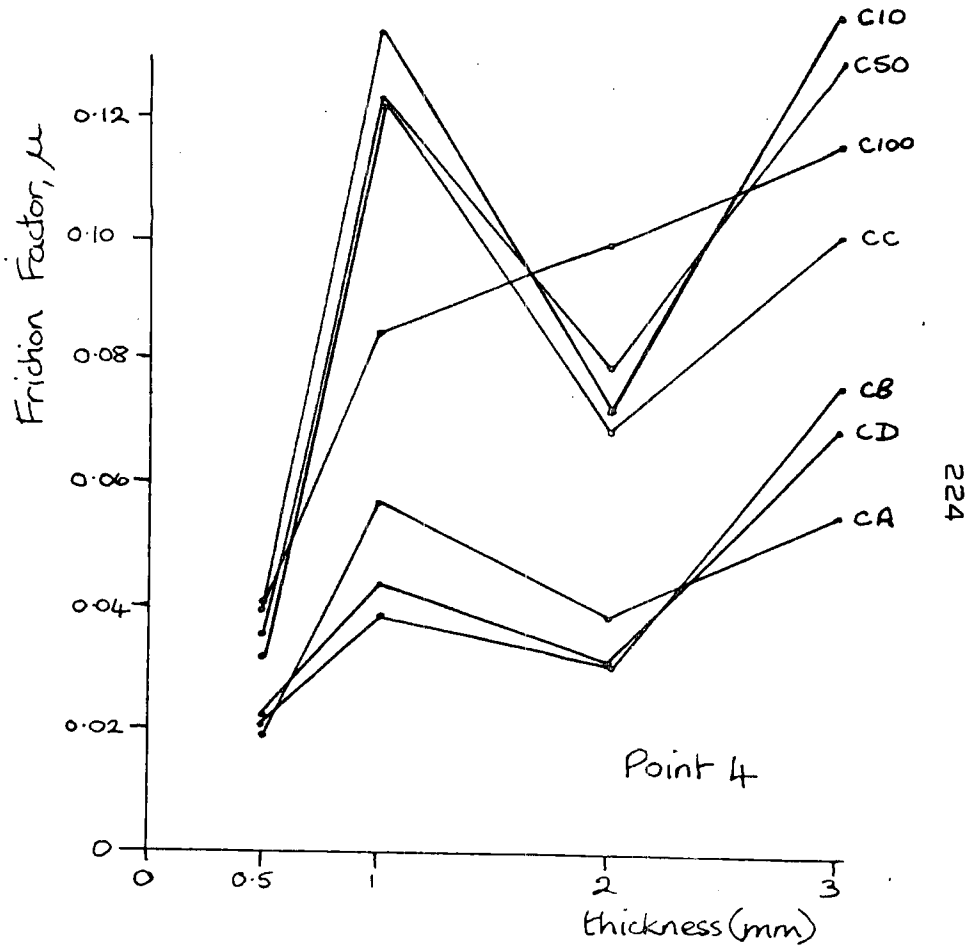

Figure 7.29

Variation of average friction factor with thickness of elastomer lining for points 2 and 4 lubricated with SCMC.

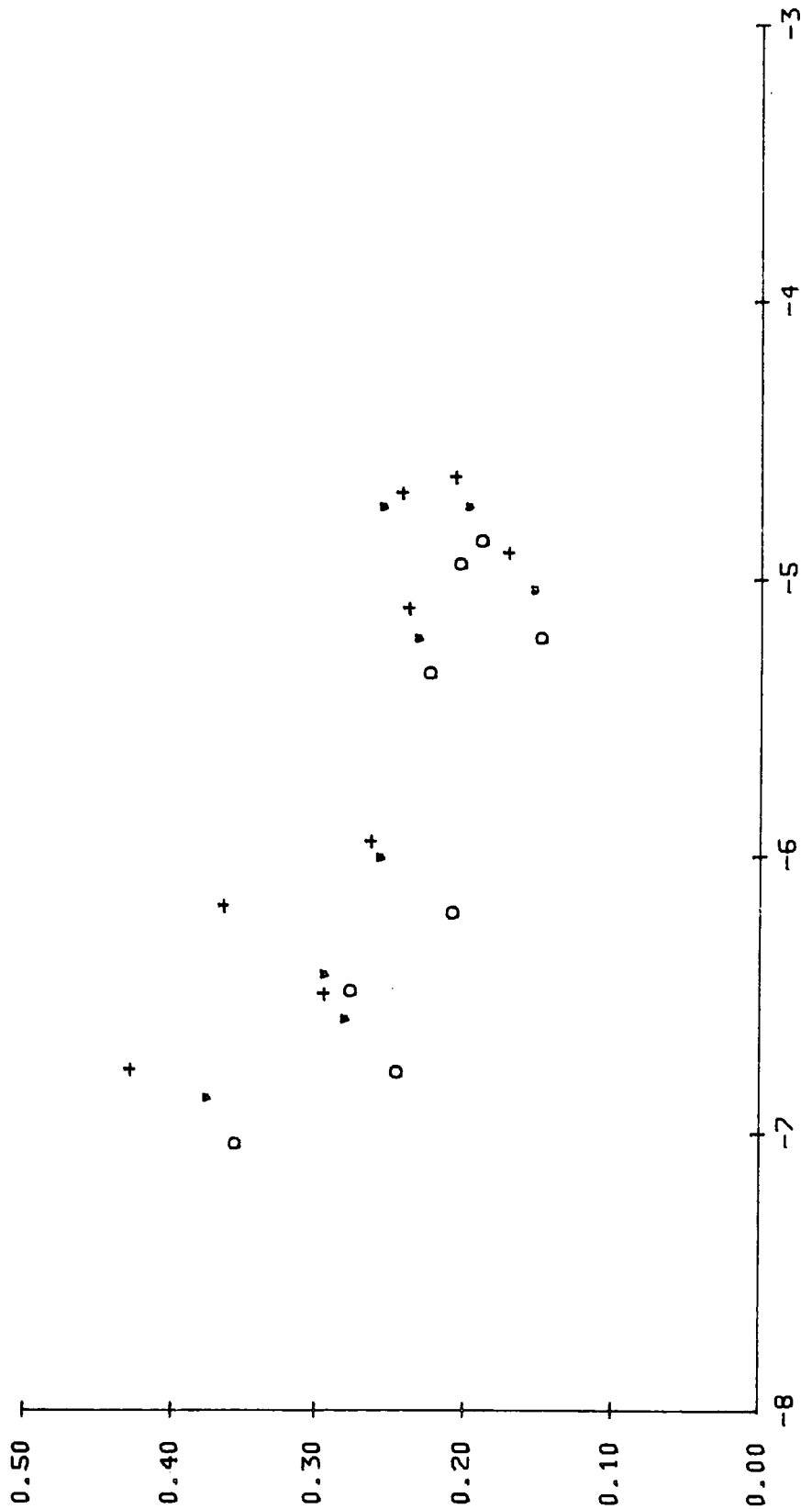

Figure 7.30

Joint Z1: 0.5 mm layer with increased clearance lubricated with SCMC - point 1.

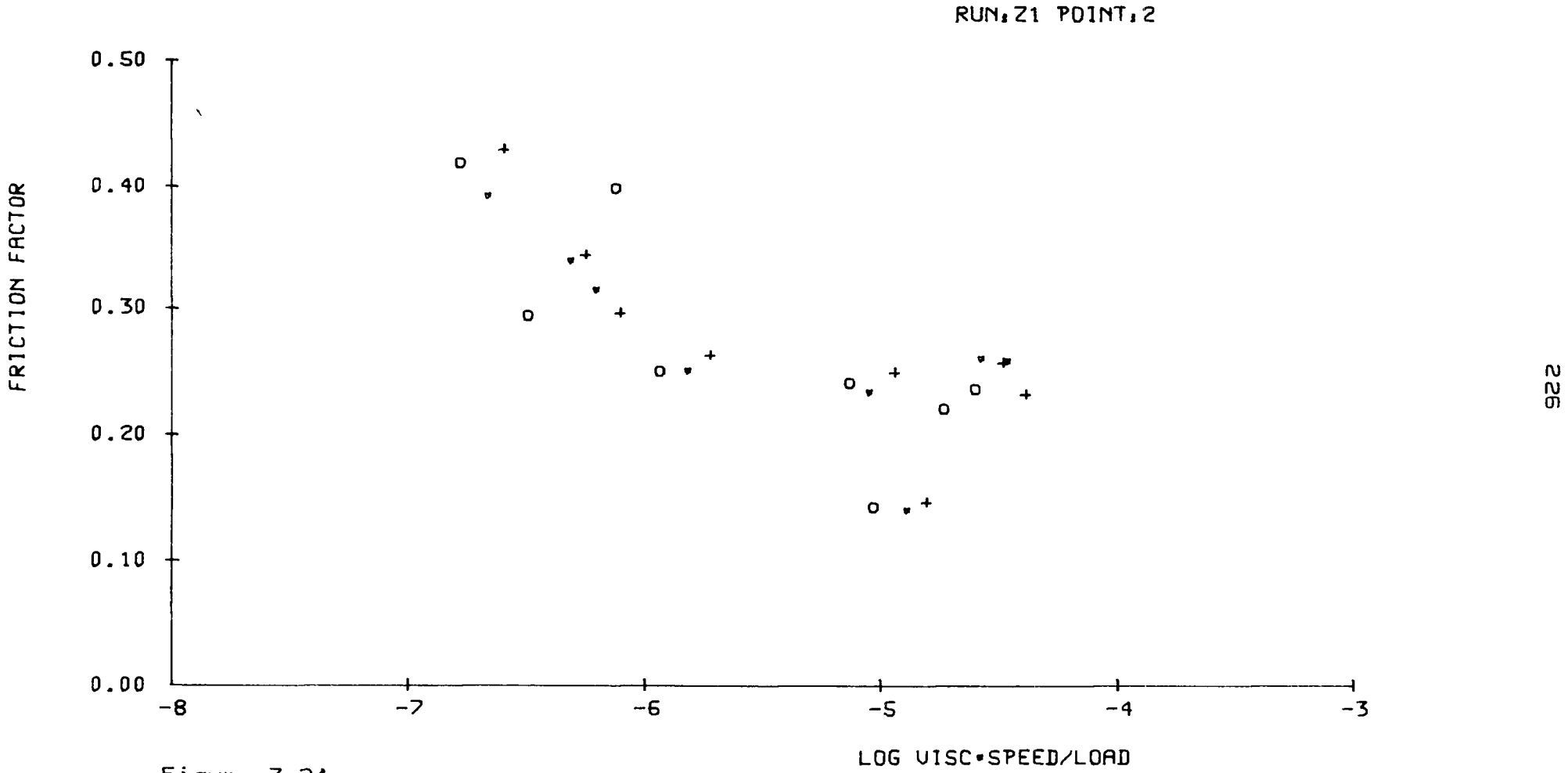

Figure 7.31

Joint Z1: 0.5 mm layer with increased clearance lubricated with SCMC - point 2.

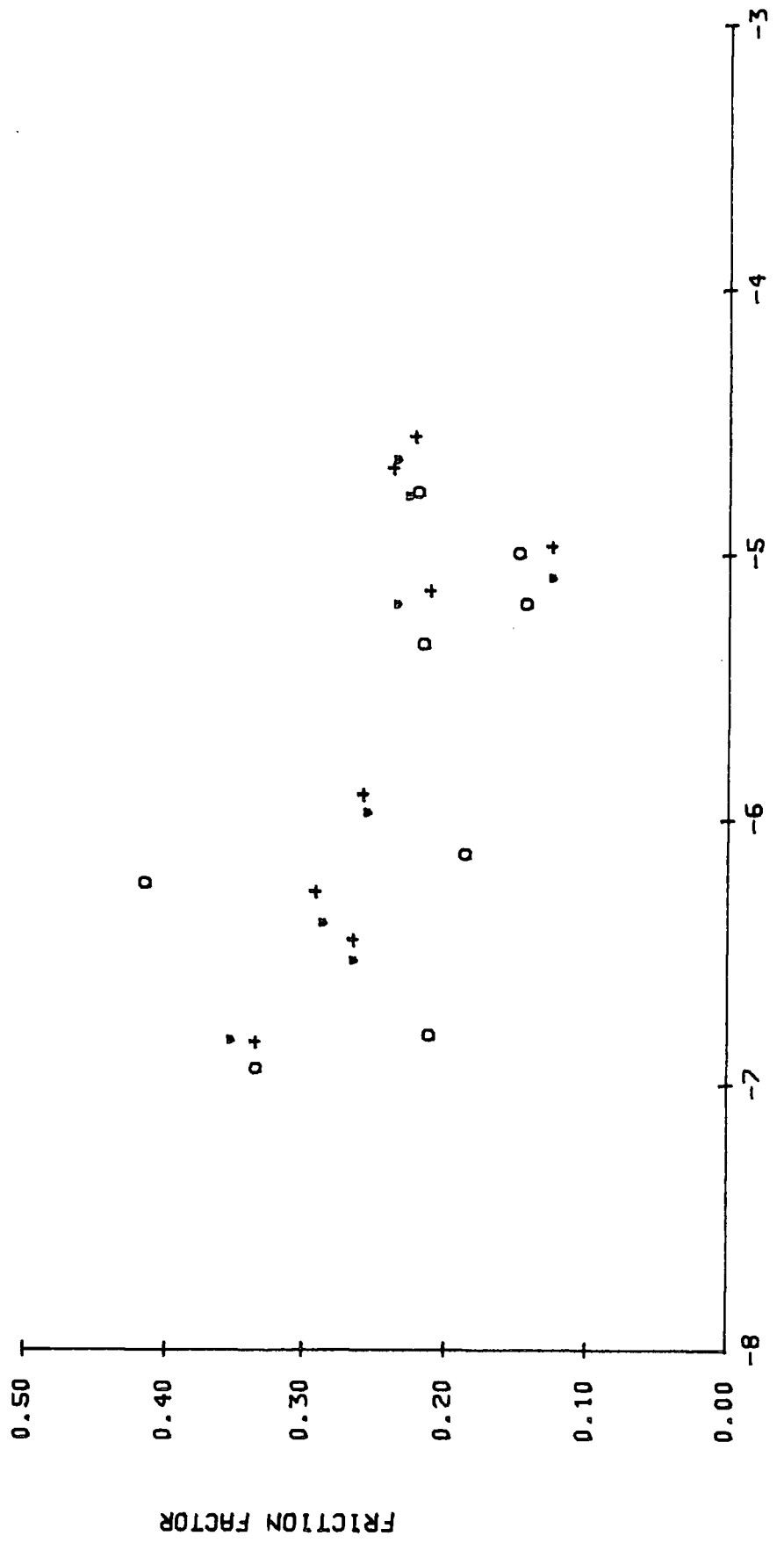

Figure 7.32

Joint Z1: 0.5 mm layer with increased clearance lubricated with SCMC - point 3.

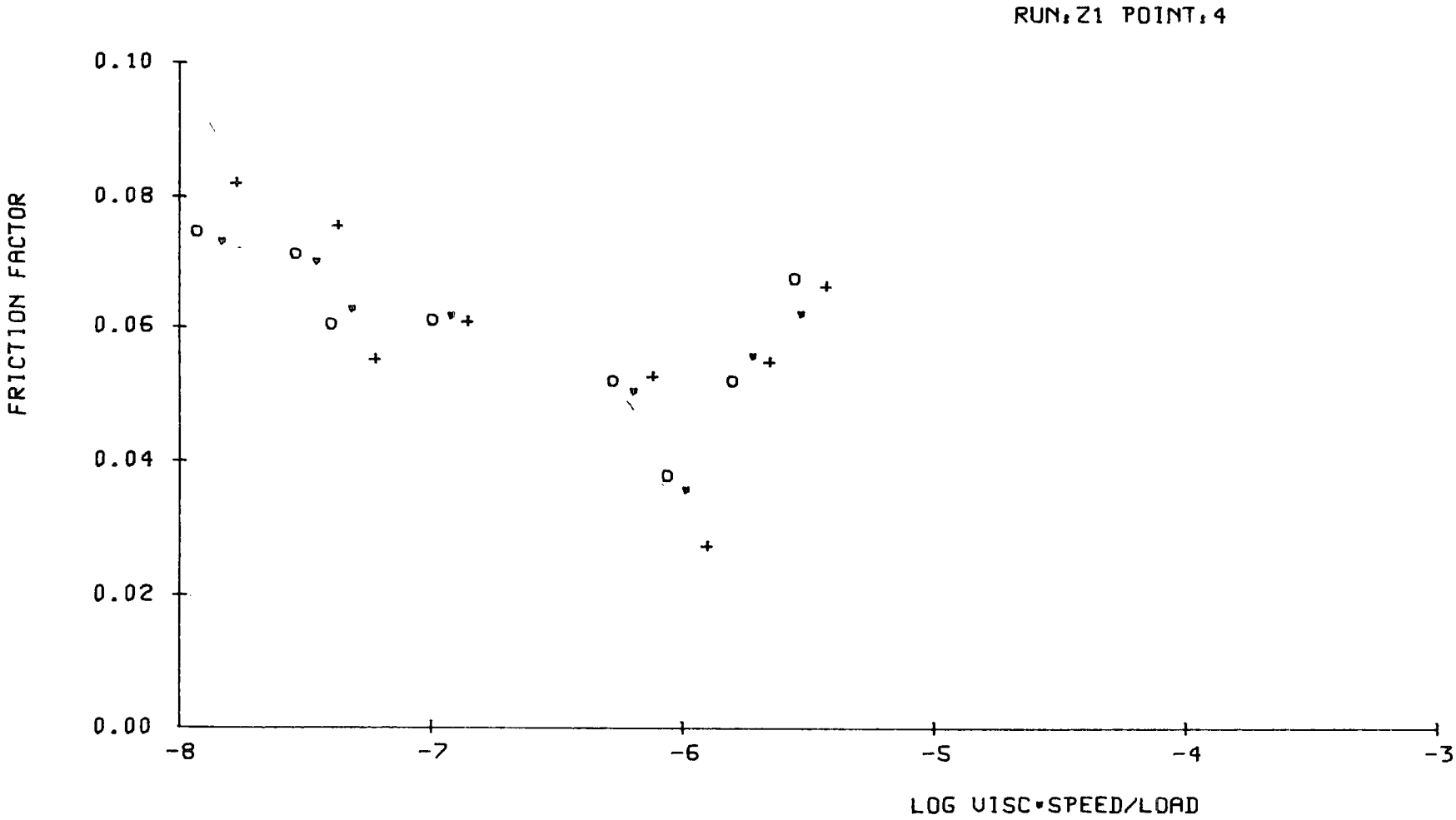

Figure 7.33

Joint Z1: 0.5 mm layer with increased clearance lubricated with SCMC - point 4.

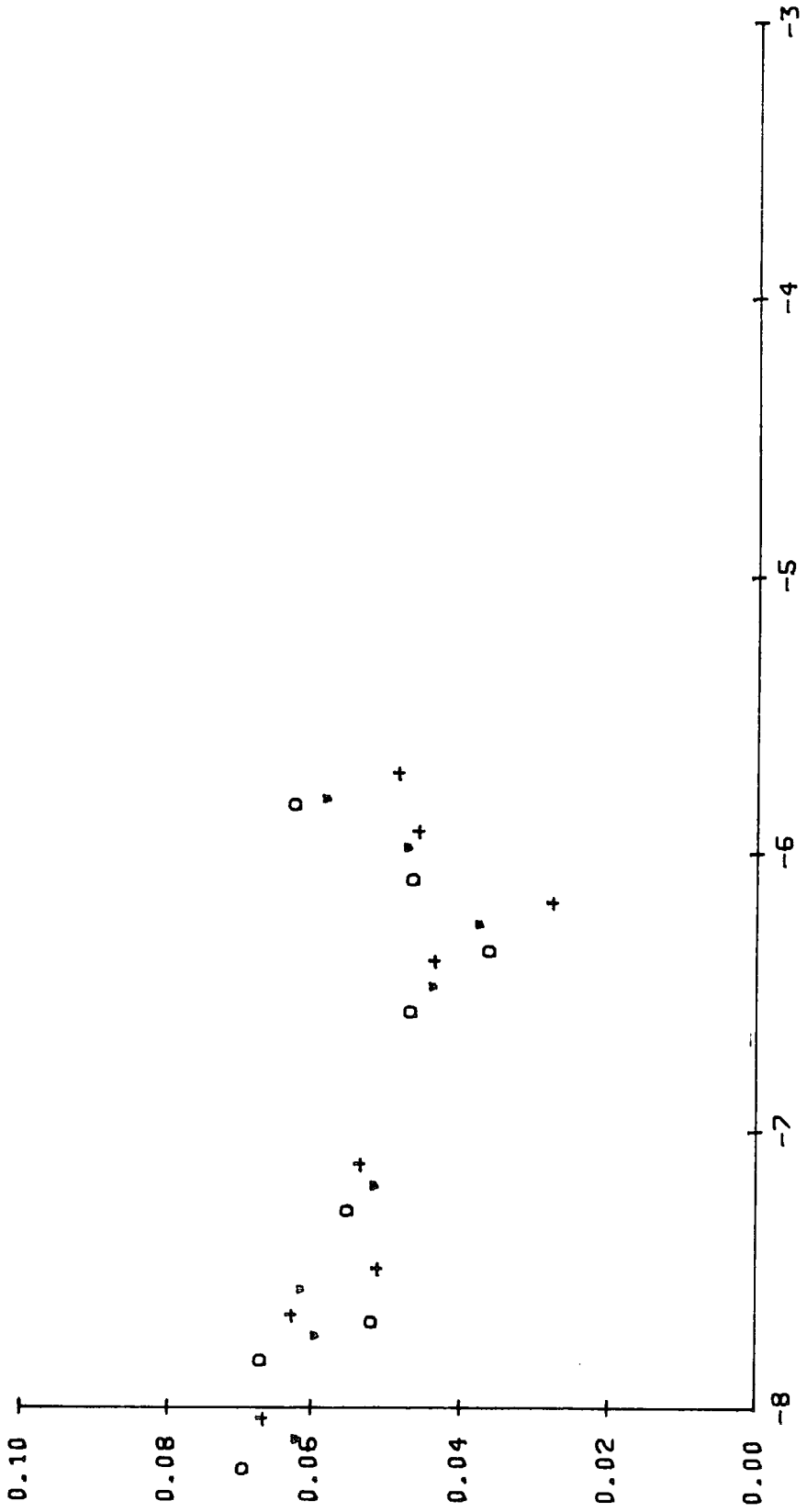

Figure 7.34

Joint Z1: 0.5 mm layer with increased clearance lubricated with SCMC - point 5.

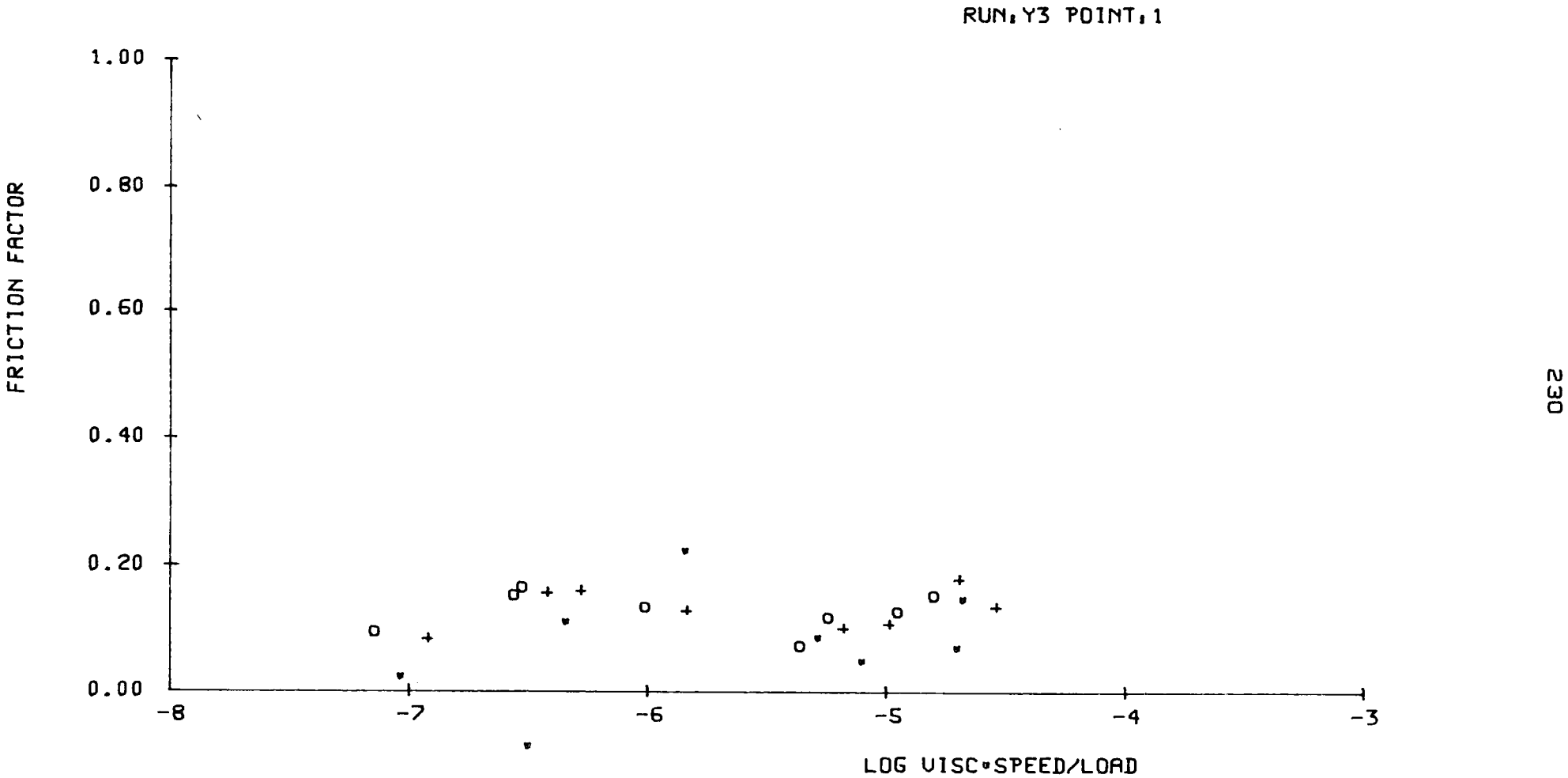

Figure 7.35

Joint Y3: 2.5 mm layer with increased clearance, lubricated with SCMC - point 1.

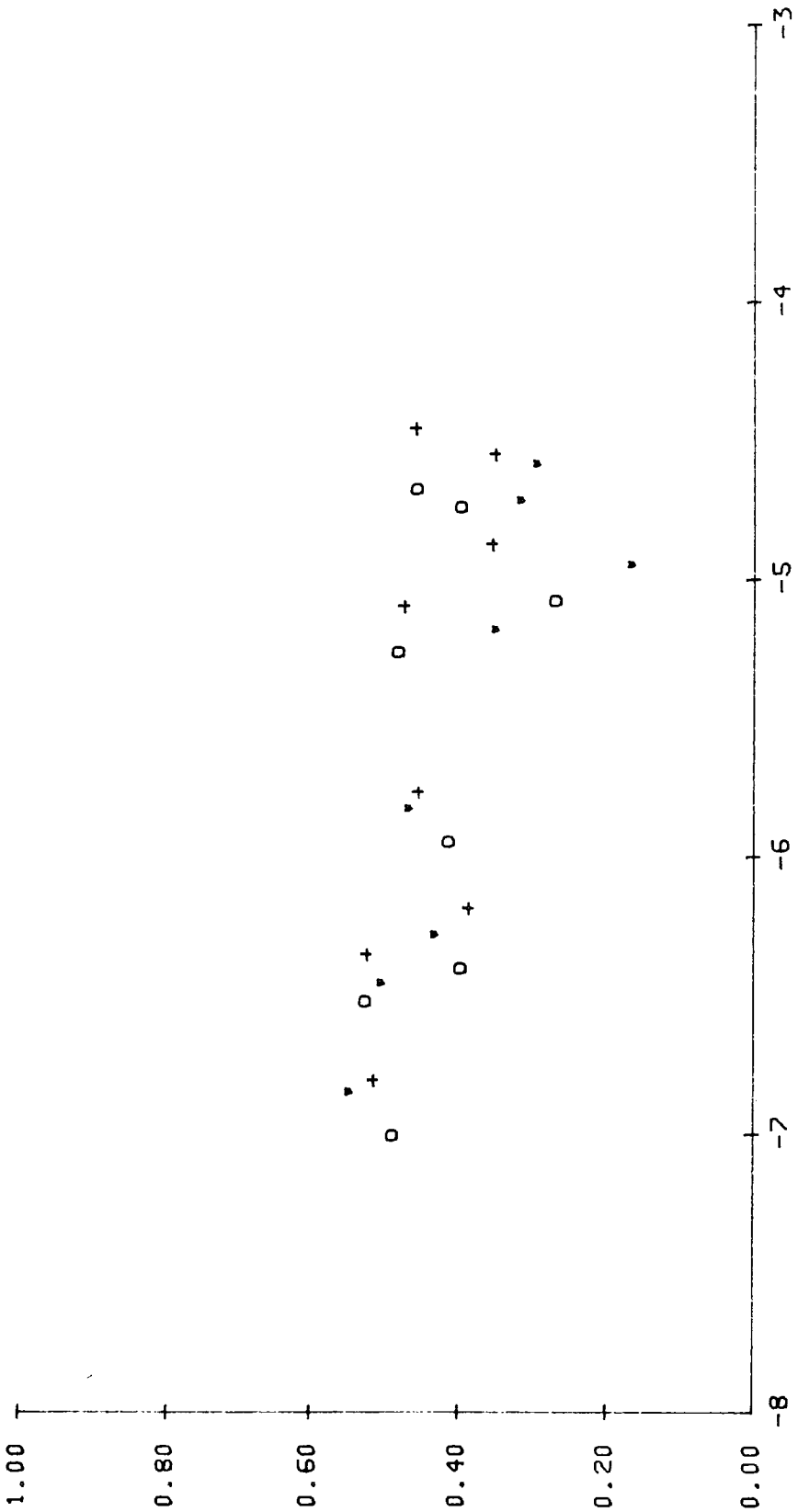

Figure 7.36

Joint Y3: 2.5 mm layer with increased clearance, lubricated with SCMC - point 2.

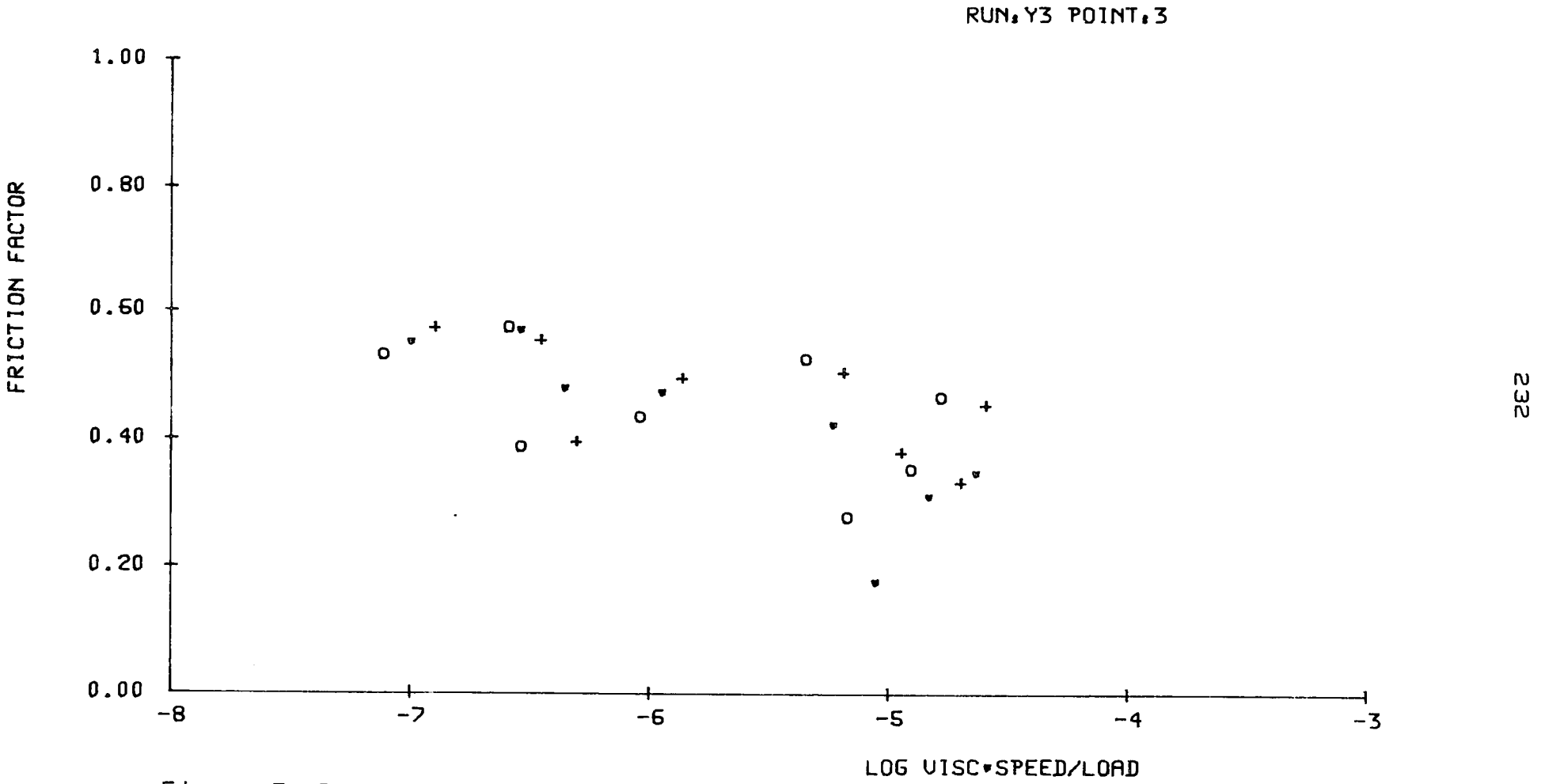

Figure 7.37

Joint Y3: 2.5 mm layer with increased clearance, lubricated with SCMC - point 3.

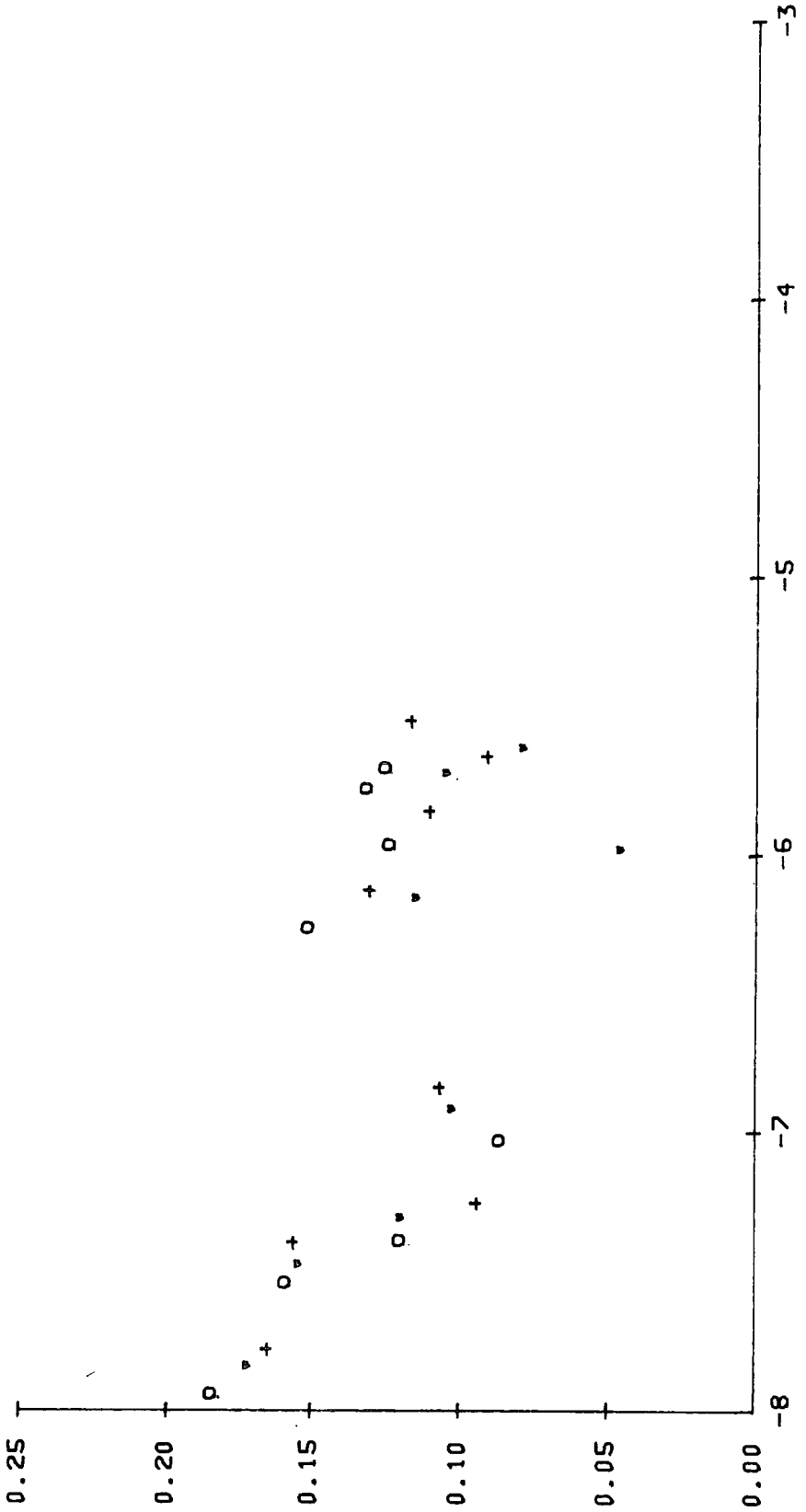

Figure 7.38

Joint Y3: 2.5 mm layer with increased clearance, lubricated with SCMC - point 4.

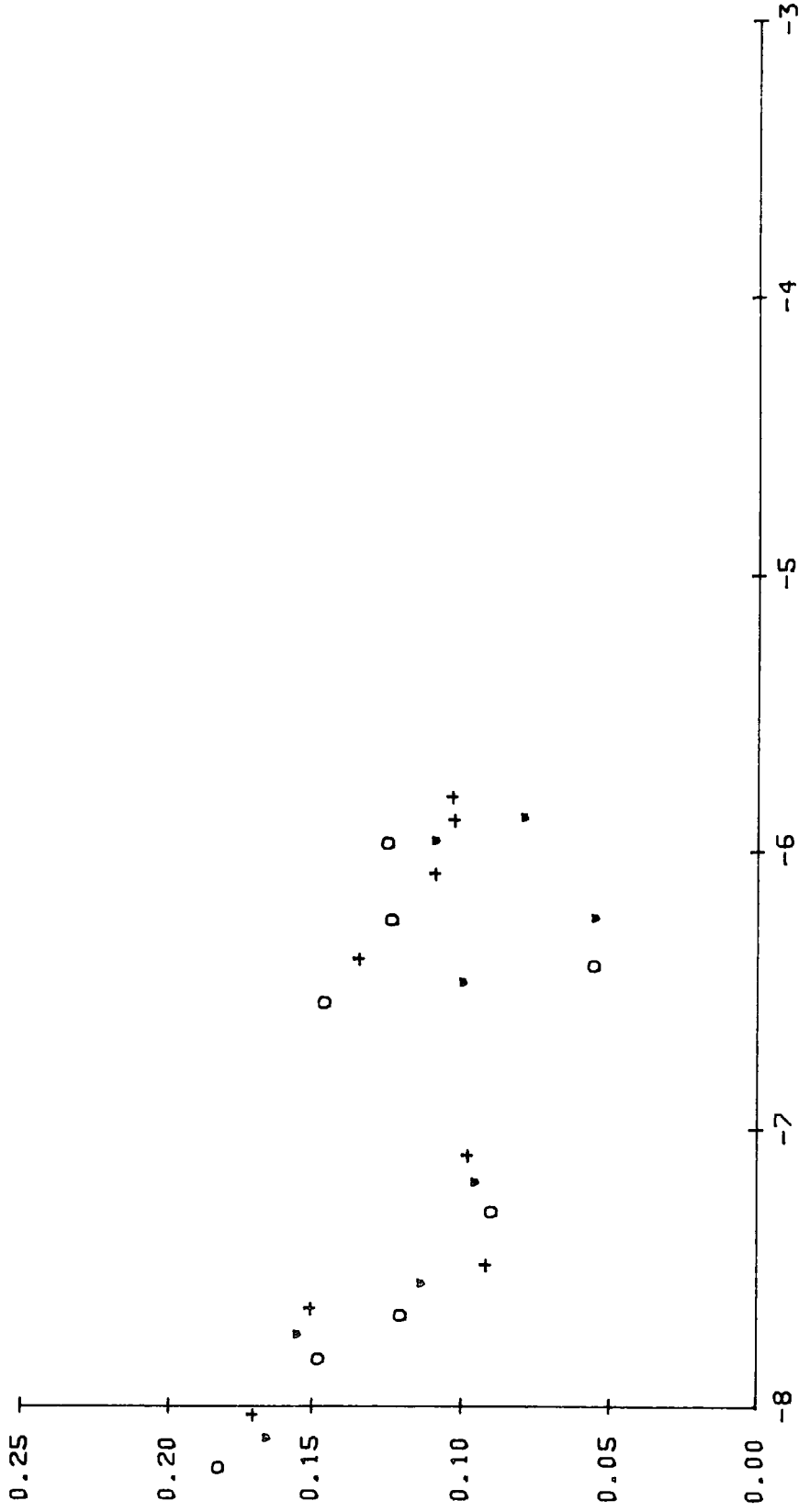

Figure 7.39

Joint Y3: 2.5 mm layer with increased clearance, lubricated with SCMC - point 5.

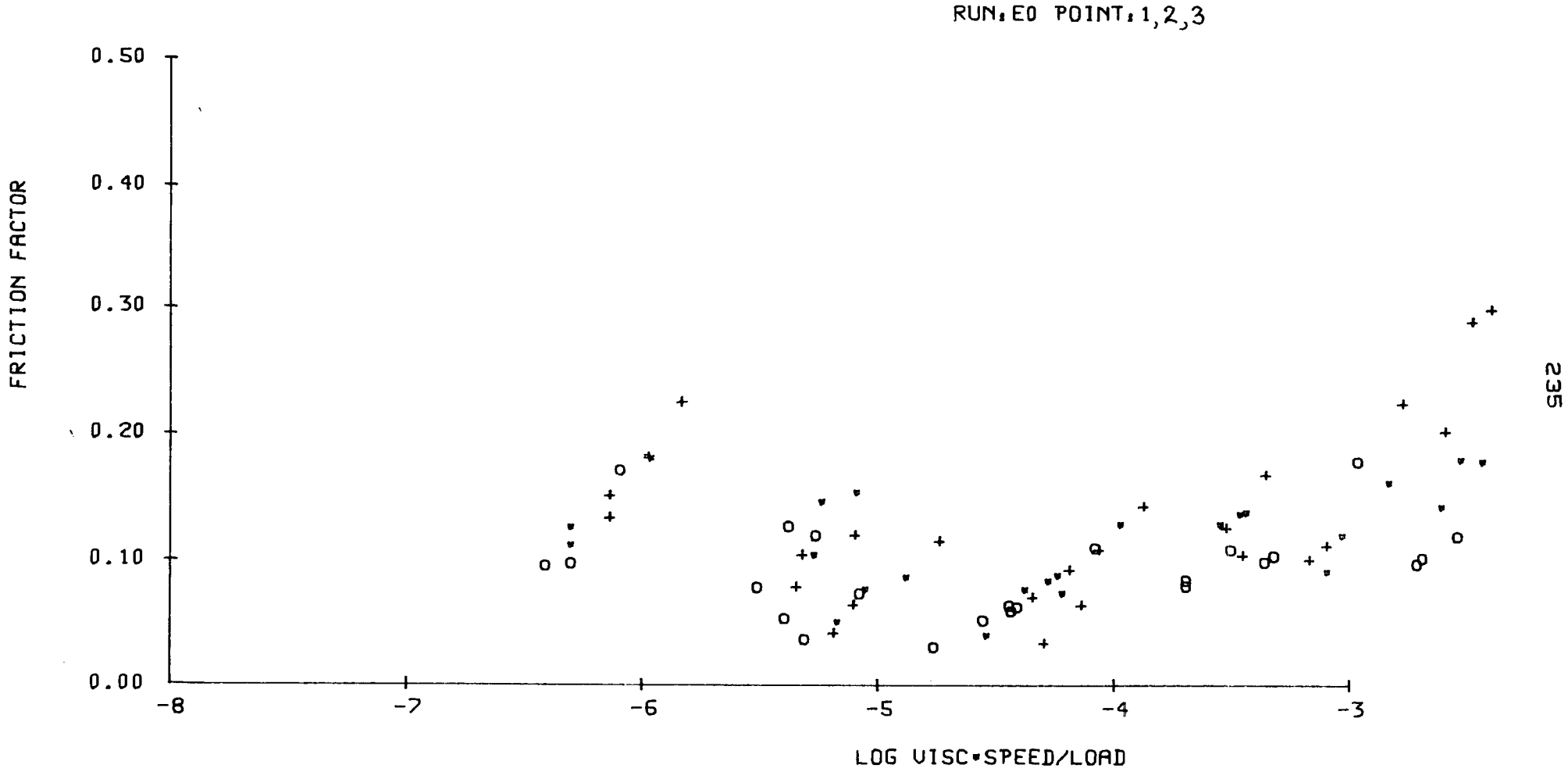

Figure 7.40

Joint E0: 0.5 mm layer lubricated with silicone fluids - points 1, 2 and 3.

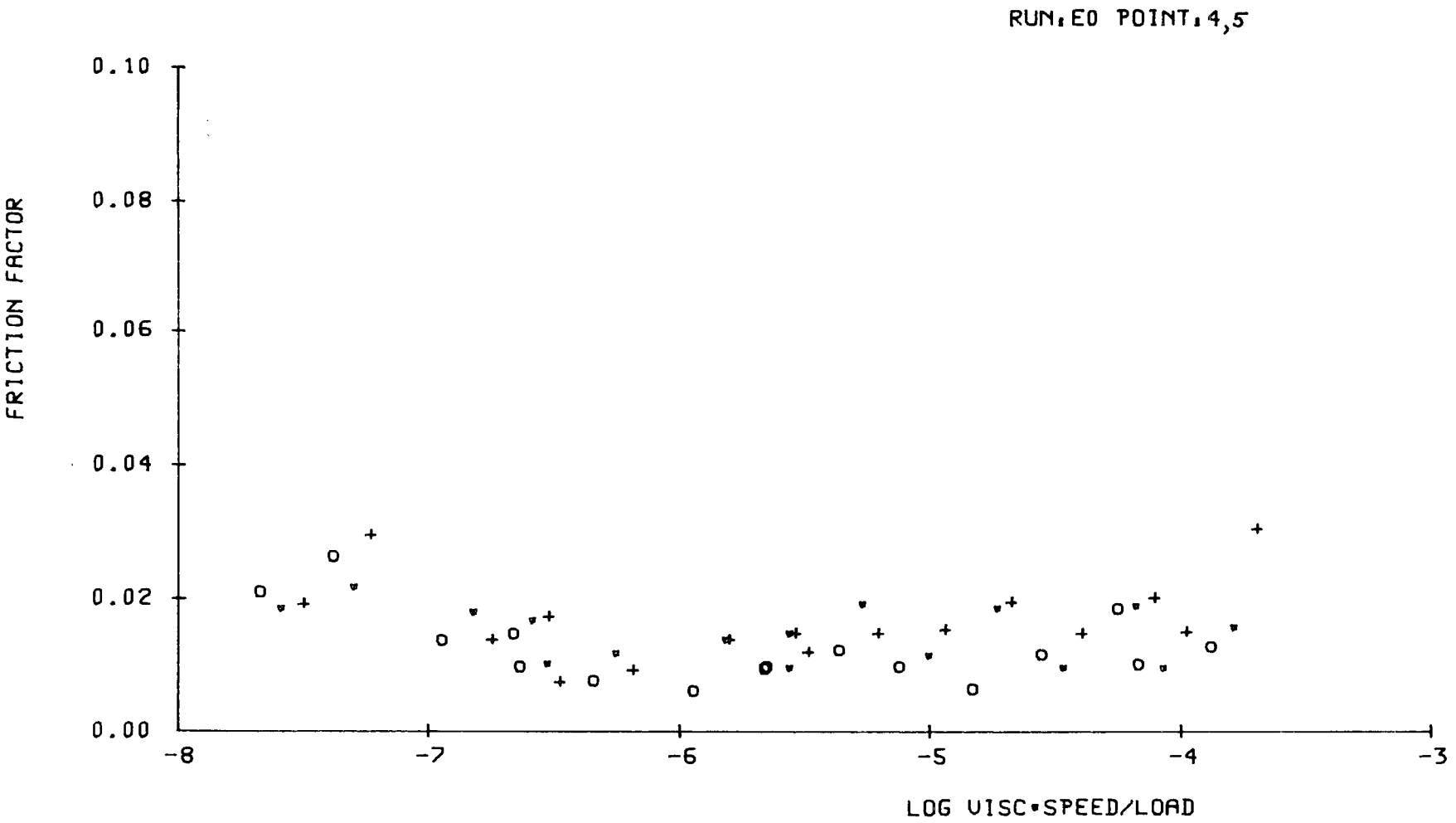

Figure 7.41

Joint E0: 0.5 mm layer lubricated with silicone fluids - points 4 and 5.

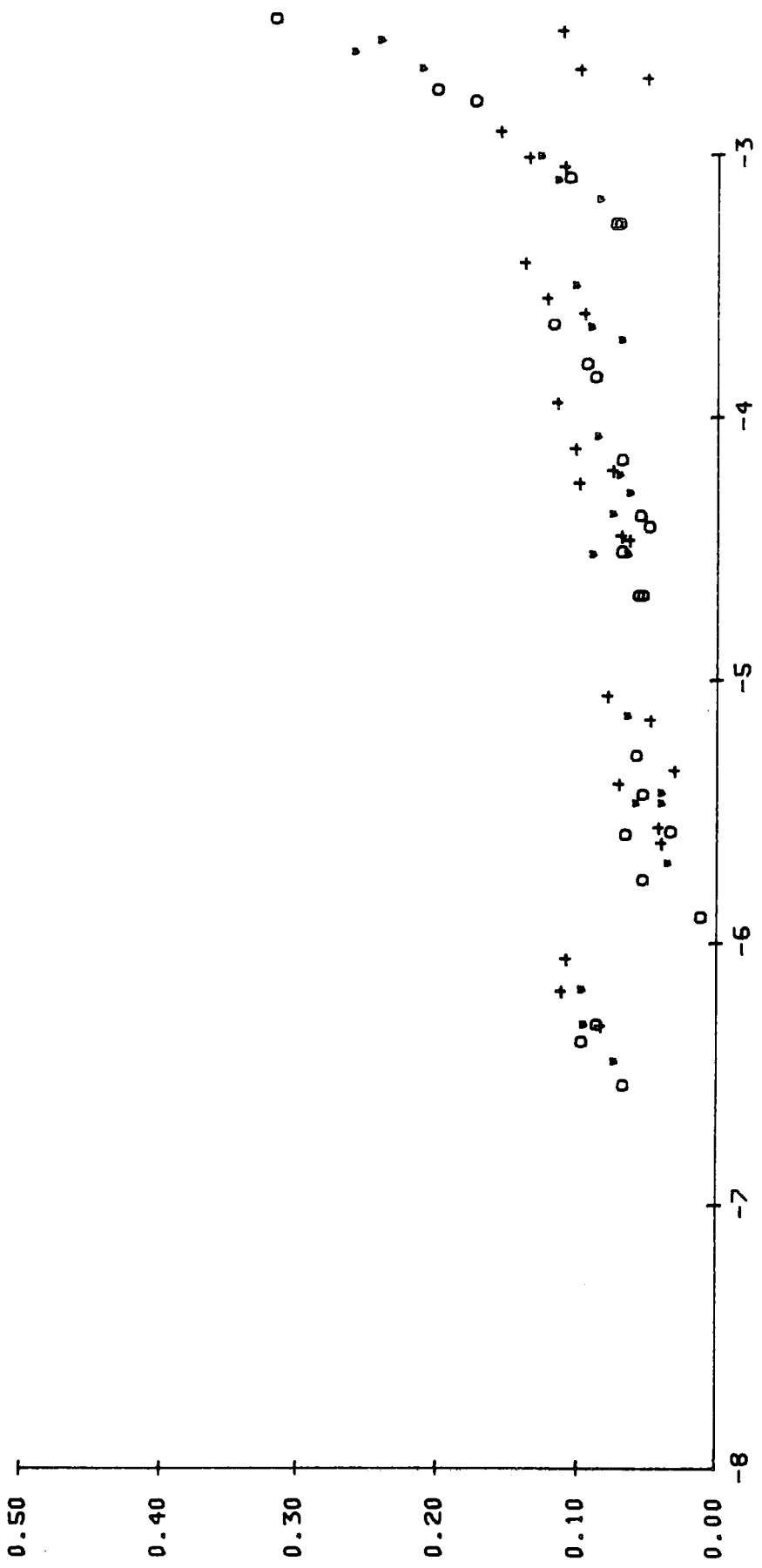

Figure 7.42

Joint C1: 1 mm layer lubricated with silicone fluids - points 1, 2 and 3.

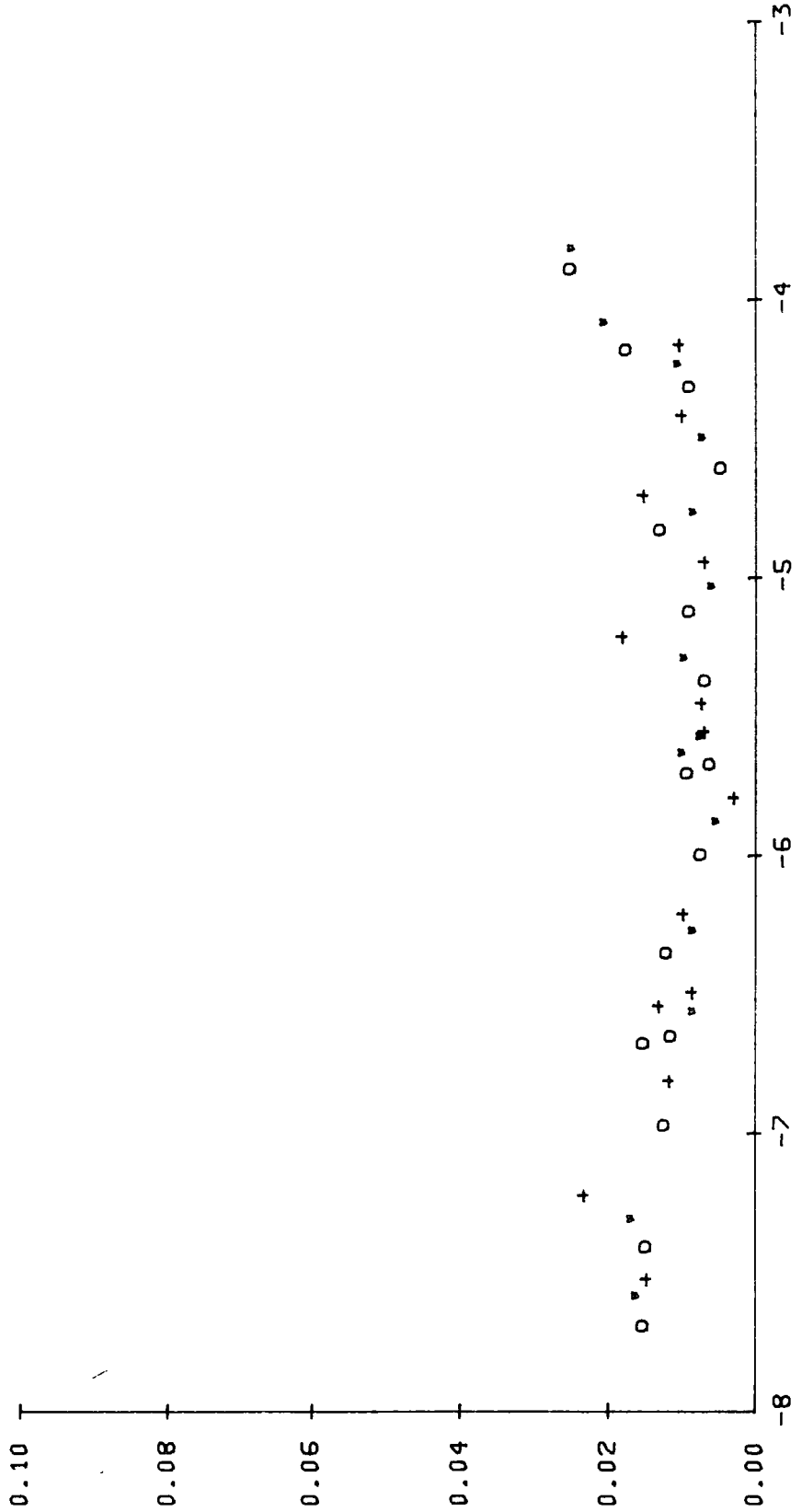

Figure 7.43

Joint C1: 1 mm layer lubricated with silicone fluids - points 4 and 5.

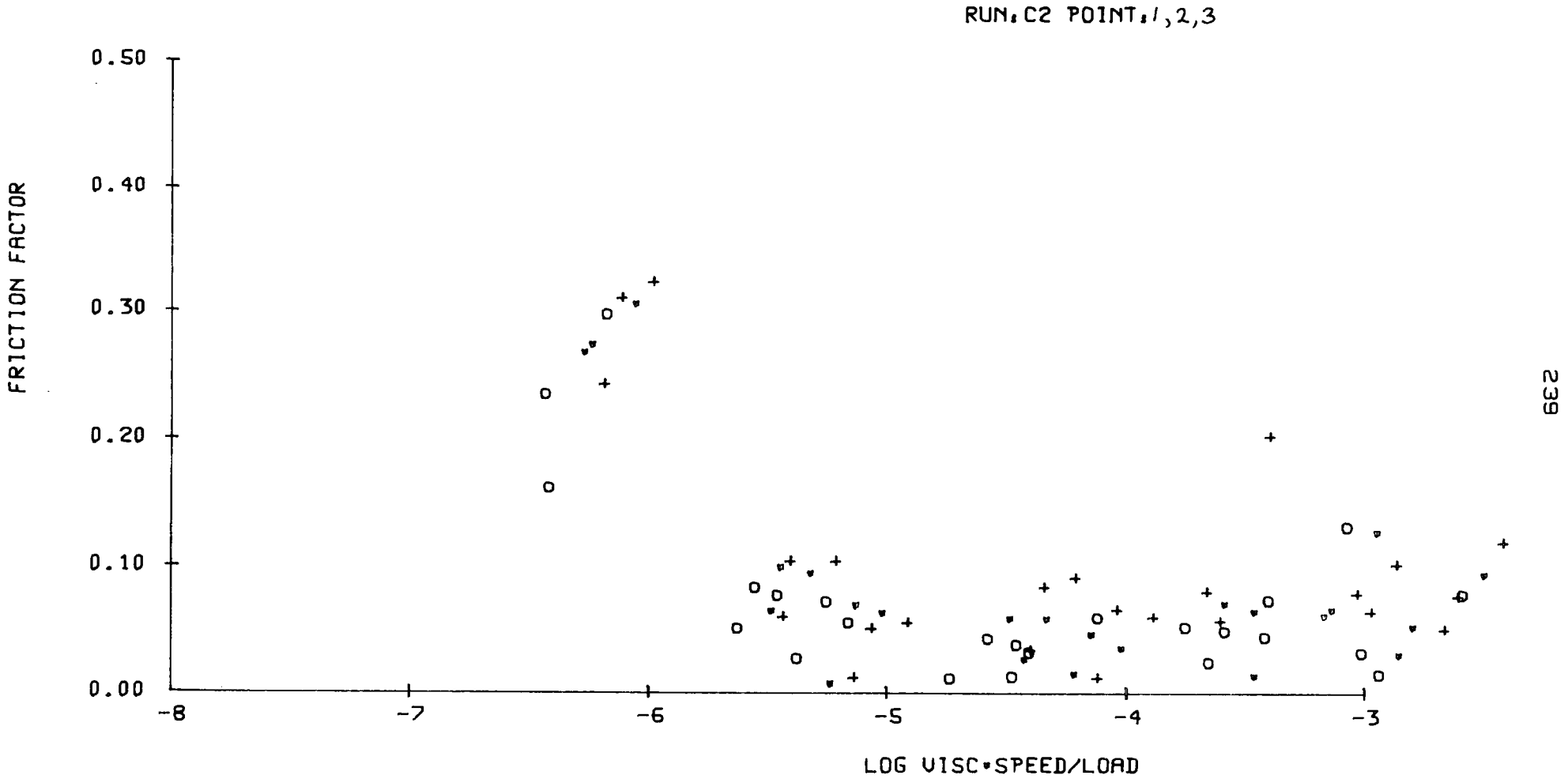

Figure 7.44

Joint C2: 2 mm layer lubricated with silicone fluids - points 1, 2 and 3.

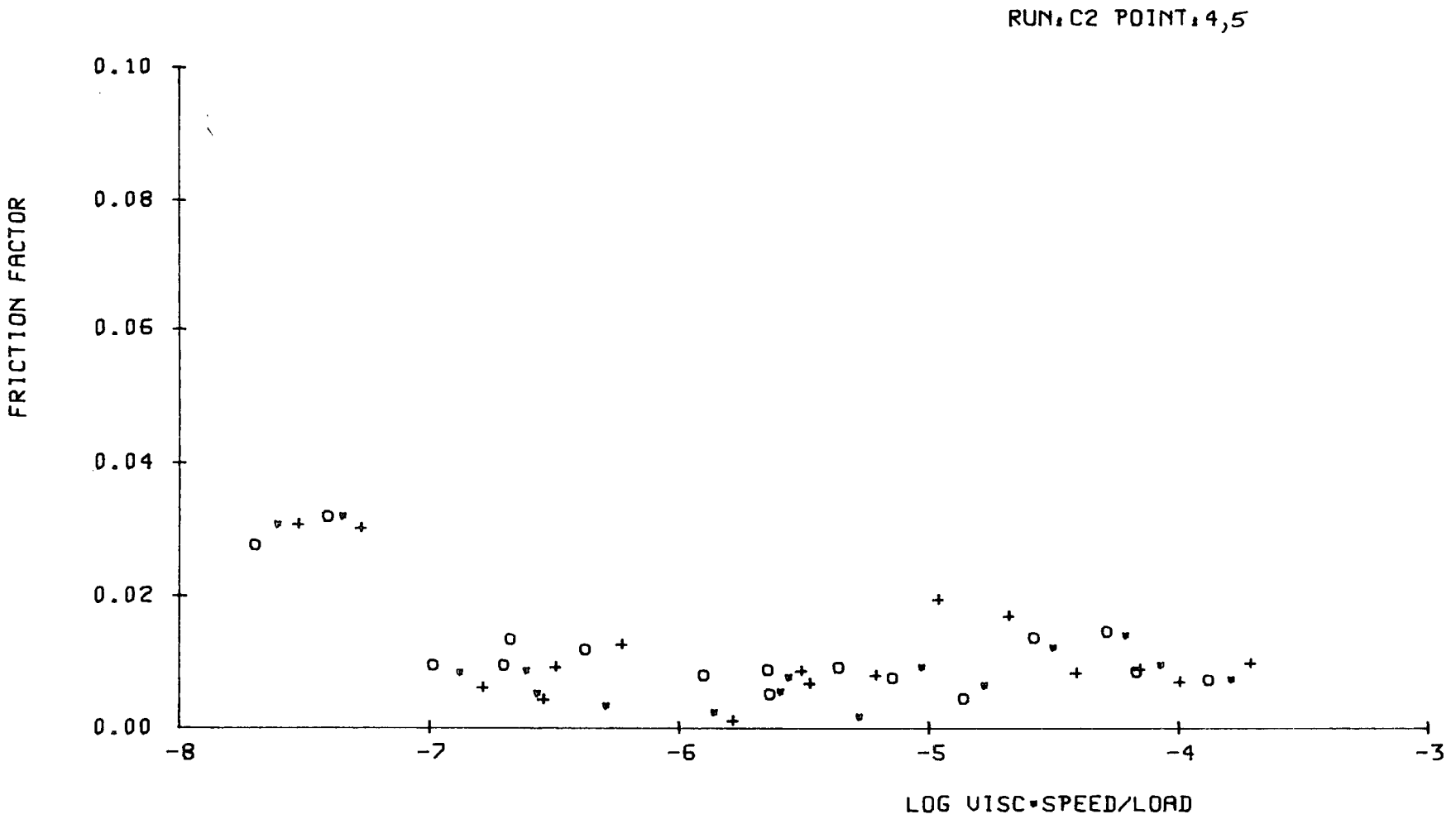

Figure 7.45

Joint C2: 2 mm layer lubricated with silicone fluids - points 4 and 5.

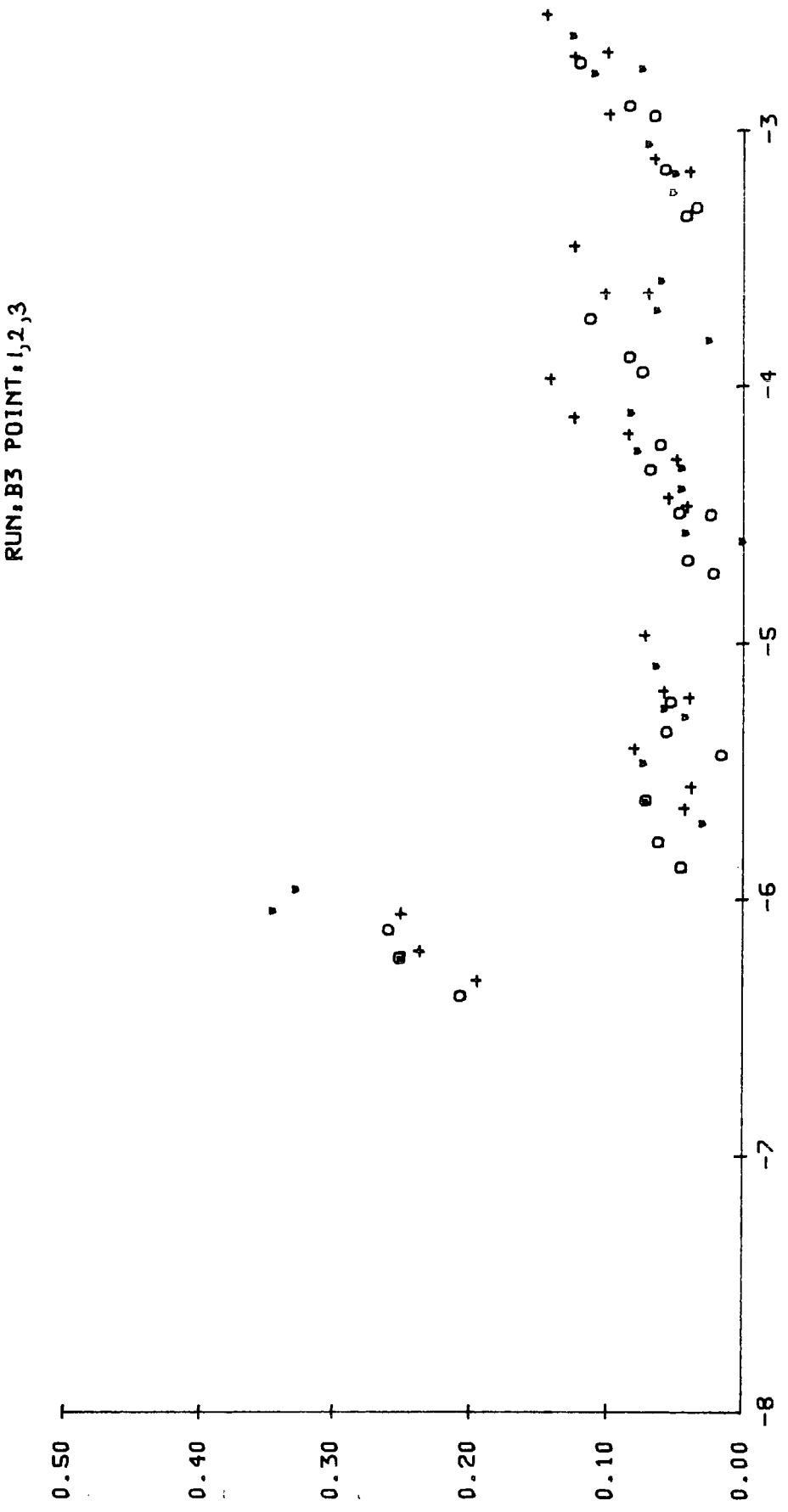

Figure 7.46

Joint B3: 3 mm layer lubricated with silicone fluids - points 1, 2 and 3.

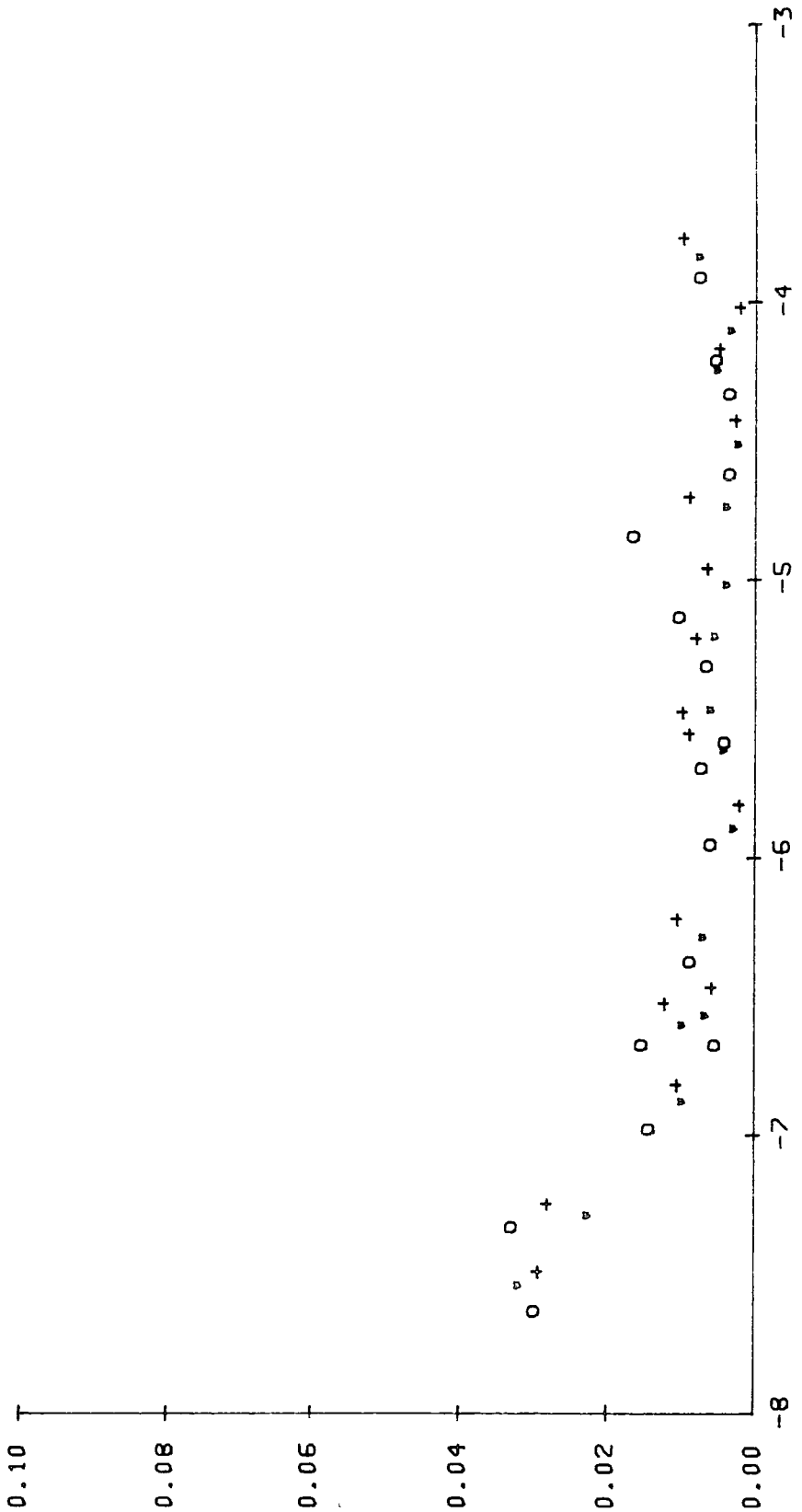

Figure 7.47

Joint B3: 3 mm layer lubricated with silicone fluids - points 4 and 5.

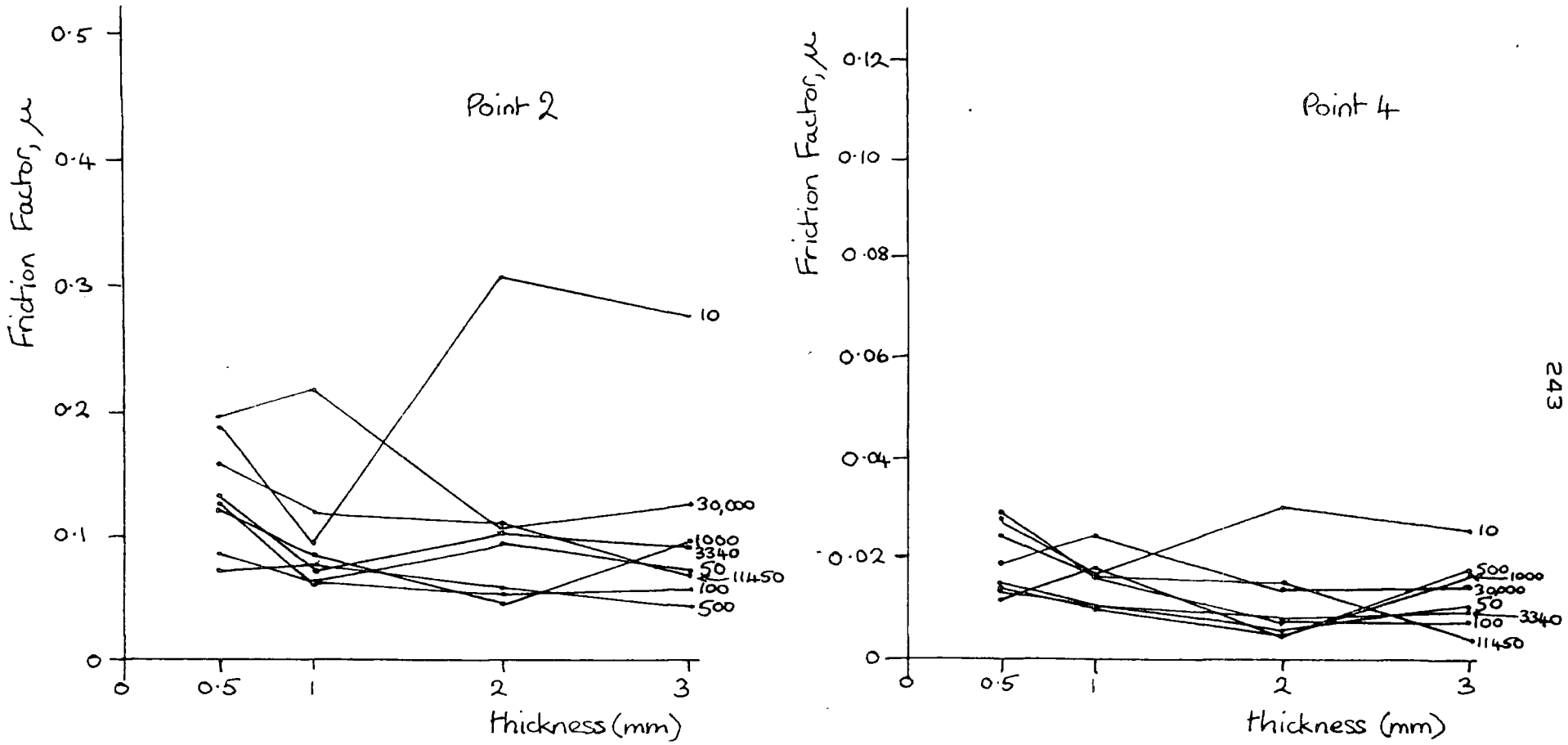

Figure 7.48

Variation of average friction factor with thickness of elastomer lining at points 2 and 4, lubricated with silicone fluids.

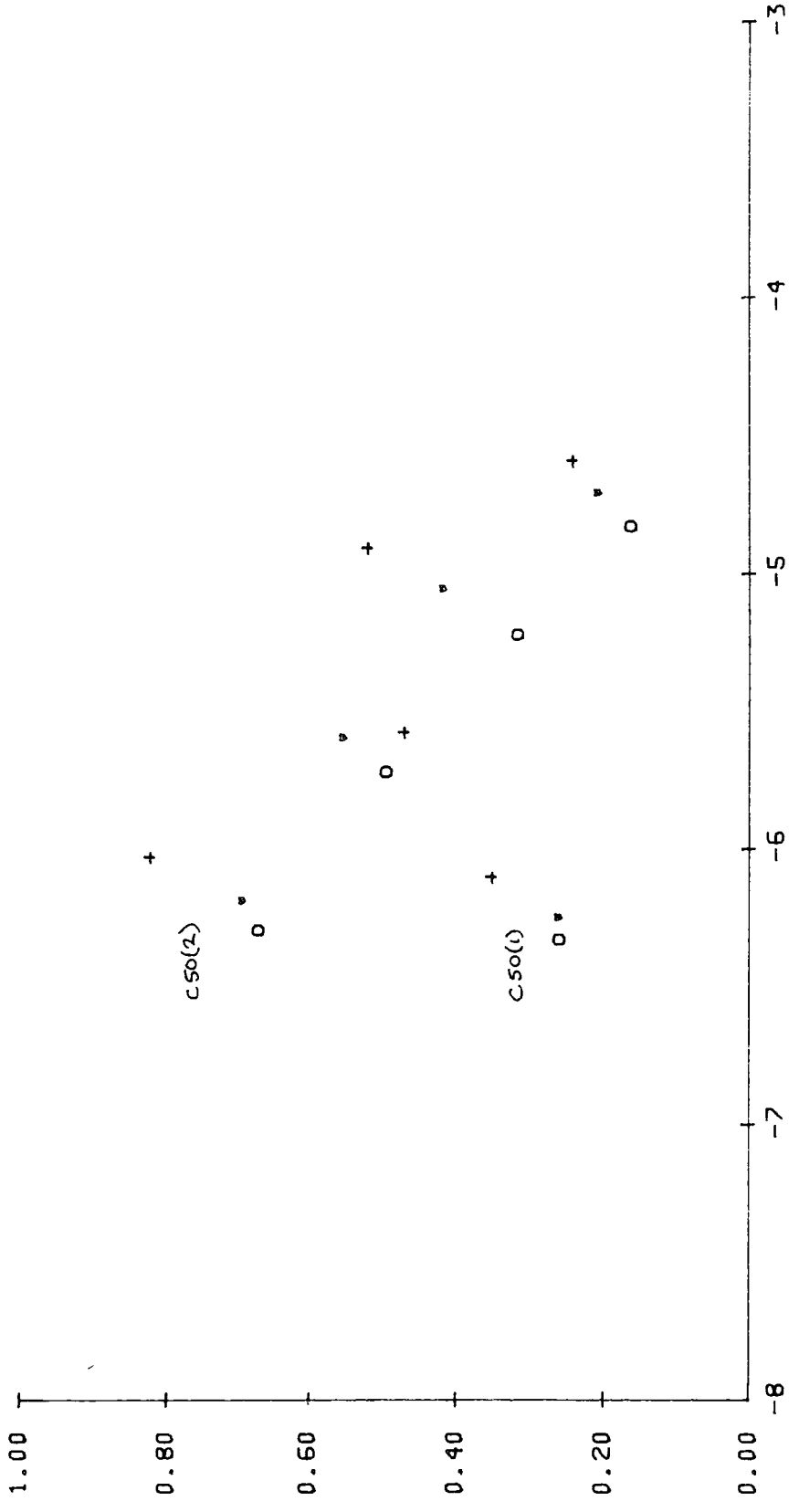

Figure 7.49

Joint D2: 2 mm layer soaked in silicone fluid but lubricated with SCMC - point 2.

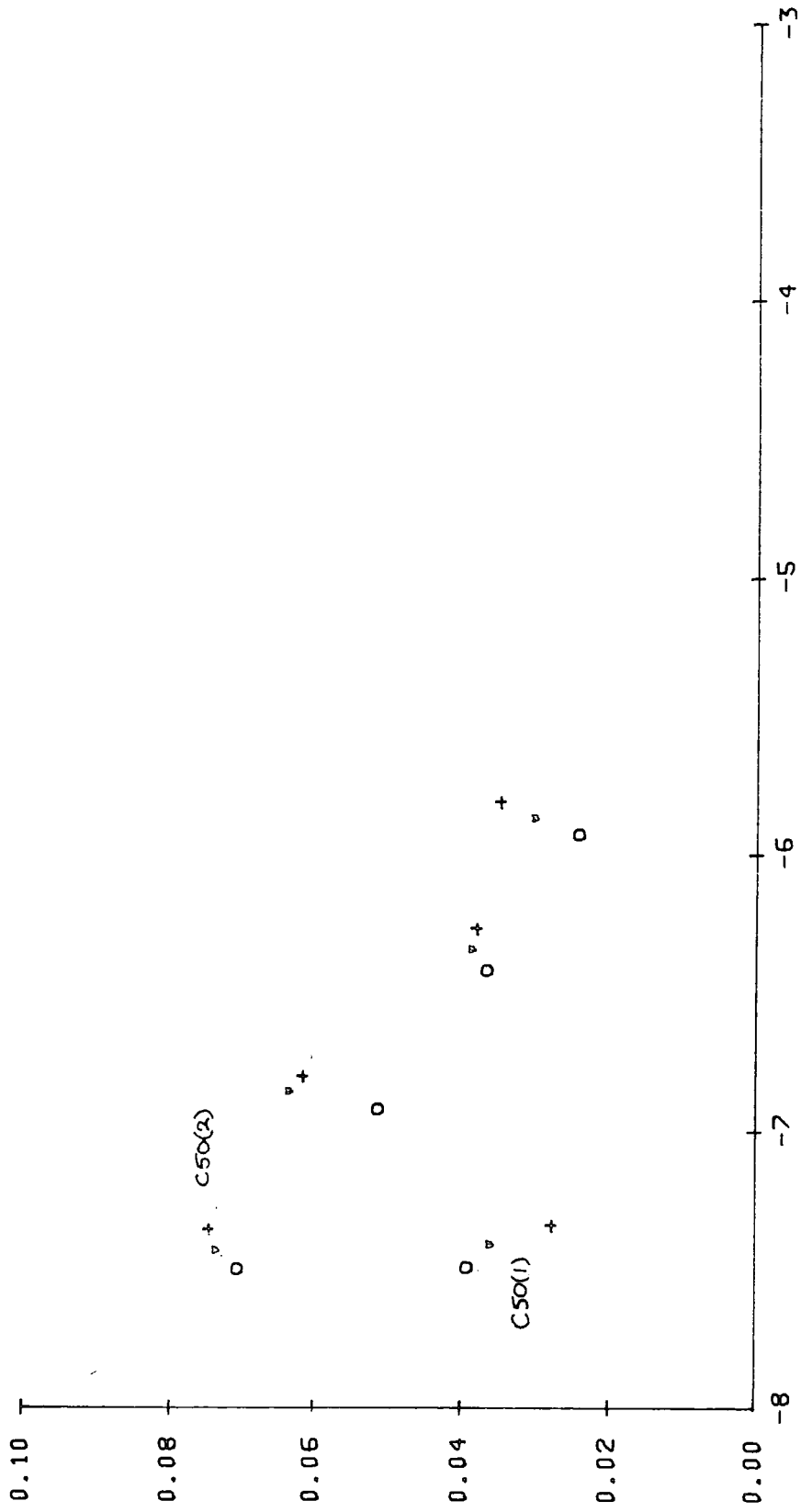

Figure 7.50

Joint D2: 2 mm layer soaked in silicone Fluid but lubricated with SCMC - point 4.

CHAPTER EIGHT

DISCUSSION

8.1 The hip-function simulator

Data collected from the hip function simulator needs to be interpreted in terms of the lubrication mechanisms acting in the joints and the relevance of this to the functioning of natural and artificial joints.

The data is relatively difficult to interpret since both the load and sliding speed varied throughout the cycle. On the other hand, this type of loading and sliding cycle is more likely to reproduce the effects found in the body than simpler models could.

There were some difficulties experienced with the use of the simulator. The main problem was ensuring that the joints, particularly the natural joints, were mounted centrally and at the correct height. The mounting procedure described in Chapter 4, worked adequately with practice and experience. The joint could be mounted centrally to an accuracy of 0.1 mm. For a load of 1500N, this could result in a maximum off-centre torque of 0.15Nm. However, by taking average values of frictional torque from the two halves of the cycle, this error could effectively be eliminated. The averaging technique produced an error since the load cycle was not exactly symmetrical, but this was very small, (of the order of 1 - 2% at most).

With one joint (H5), the results obtained were dependent on the order in which the tests were performed, ie the measured friction factors decreased as the tests progressed. This was thought to be due to a malfunction of the apparatus rather than a change in the joint itself.

Any plausible changes with time in a joint such as bio-chemical degradation or erosion of the cartilage would tend to increase rather than decrease friction factor. Also, at the end of the tests, the zero load position of the carriage was checked and found to have altered such that the measured loads would have been higher than the true loads. This drift in the zero reading of the load did not occur again and the explanation seems to be that the pressure of the compressed air supply to the simulator fell sufficiently for the regulator on the rig to be unable to maintain its set value.

8.2 Selection of analysis points through the cycle

Although a continuous record of load and frictional torque was obtained from the simulator tests, it was only practicable to analyse the data for a limited number of positions through the cycle. Five points were chosen in similar positions for each of the three speeds of oscillation commonly used for the tests (Figure 4.4). Point 2 was chosen as the position of maximum sliding speed. It was a low load, around 250N and corresponds to the swing phase. On either side of this point, the sliding speed was less and two points were chosen with

the same sliding speed, both still in the low load region. Point 1 occurred shortly after the high load had been removed, and whilst the sliding speed was increasing. Point 3, however, occurred while the sliding speed was decreasing, and after the low load had been maintained for a while. It was hoped that these two points although having the same values for load and sliding speed, would be helpful in an interpretation of lubrication mechanisms since their load and sliding speed histories were different.

Points 4 and 5 were in the highly loaded region (1500 - 1600N). Two points were chosen so that any effects of duration of loading could be observed. They were both taken before the carriage reversed its direction of motion since experience showed that the frictional trace did not always respond as rapidly as was expected to the reversal of the motion of the joint. This observation will be discussed later, but to use this region as one of the standard data points seemed further to complicate the analysis. Point 5 then, being just before the change in direction represents a slow sliding speed and point 4, a little faster.

8.3 Preliminary tests with a Charnley prosthesis

The results (Figures 6.1 - 6.3) obtained from the Charnley prosthesis lubricated with silicone fluids showed the curve typical of a mixed lubrication regime. The friction factor decreased as the viscosity of the lubricant increased. At the highest viscosities, the friction factor appeared

to reach a minimum. On Figure 6.1 this occurred at a value of $\eta u/L = 5 \times 10^{-4}$ m^{-1}. This minimum indicates the transition from mixed to full fluid film lubrication. The graphs show that when the amplitude of oscillation was increased, there was little change in friction factor and so the larger amplitude was used in subsequent tests since this corresponded more closely to the angle subtended during a walking cycle.

There was considerable difference between the curves obtained at high and low loads but as the sliding speeds were also different between the two positions, these tests cannot determine which variable was responsible for the effect.

The graphs obtained with a constant load throughout the cycle are interesting. The data from the five different points through the cycle varied only in sliding speed from point to point. Considering first the general shape of all the curves (Figures 6.4 - 6.8), the friction factors initially decreased, but reached an almost constant value at a viscosity of about 10^{-1} Pa s. (The data for point 1 is inexplicably erratic.) Below this value of viscosity, where the friction factors are decreasing, the results for the three loads used are separated with the friction factor decreasing as the load increases. This corresponds to the apparent variation of friction factor with load described earlier. Howver the constant value of friction factor obtained, appears to be independent of load.

This constant value does vary with position in the cycle, points 1 and 2 have the same value (around 0.015) whereas points 3, 4 and 5 are double that (around 0.03).

The results for the Charnley prosthesis with constant loading are very useful in interpreting other results. The friction factors obtained at points 1 and 2 were lower than at points 3, 4 and 5. For constant loading, the difference between these two groups is that the sliding speed was increasing at points 1 and 2 (where it reached a maximum) and was decreasing at points 3, 4 and 5.

Consider the prosthesis as a lubricated journal bearing where a hydrodynamic film acts (Figure 8.1). As the sliding speed increases, the offset , x, increases and the load, L, produces a torque, Lx, acting around the bearing centre. Hence in equilibrium

$$T_J - Lx = T_B$$

The greater the offset for a given load, the lower will be the value of T_B. It is the bearing torque, T_B, which is measured in the simulator. Hence an increasing sliding speed will cause a reduction in T_B, whereas a decreasing sliding speed will cause an increase in T_B. Also, applying this to the case of dynamic loading, as L increases, the offset , x, will decrease, but the product Lx still increases, resulting in a lower

value of T_B for a higher load - as observed throughout the present work.

8.4 Natural hip joints

Human hip joints were mainly used for testing the synovial fluid samples in the investigation of its constituent properties with regard to lubrication, but some tests were also run with synthetic lubricants to help in the interpretation of the synovial fluid results.

Due to the variability of biological specimens, it was not easy to compare results from one joint with another. Differences in friction factor between joints may be due to the overall geometry of the hip, to the surface condition and thickness of the cartilage and also to its compliance. Since some of these properties may change with time, all the lubricants tested on a joint which might be compared, were tested on the same day. Testing each group of lubricants in a random order ensured that the results could not be produced by one particular lubricant always following another. The traces themselves were only identified with a number corresponding to the order in which they were made. This ensured that any human bias was eliminated when taking measurements from them, since the expected results were not known. A separate list related the trace number to the experimental conditions.

Although measurements were taken from the traces at each of the five points described earlier, the results presented for the natural joints are mainly from points 2 and 4, chosen to be representative of a low load, high sliding speed and a high load, slow sliding speed. The variation of friction factor throughout the cycle will be discussed later.

8.5 Natural hip joints lubricated with silicone fluids.

Silicone fluids were chosen as one synthetic lubricant because they were available over a wide viscosity range, and their viscosity is independent of shear rate. Due to the possibility that they might affect the permeability of the cartilage or contaminate subsequent lubricants, since they are difficult to remove completely, they were always the last lubricant to be tested in a joint.

Two joints [H7, H9], were tested with silicone fluids, and the results presented in Figures 6.23 and 6.28. For both joints the data falls into two bands, one for points 1, 2 and 3, and the other for points 4 and 5. The only exception to this is point 1 for H9 which changes to the lower band for low values of viscosity. The low load, high sliding speed, data shows the rising characteristic of friction factor with $\eta u/L$ typical of full fluid film lubrication. Joint H7 shows a slight minimum around $\eta u/L = 10^{-5}\ m^{-1}$, but H9 remains constant below this value. Certainly neither joint displays the obviously mixed

lubrication mechanism as seen in the Charnley joint.

At the high loads and slower sliding speeds, the friction factor is lower, and it showed less variation with viscosity. In fact, for H9 there was no appreciable change at all. H7's friction factor did increase slightly at the higher viscosities. At high loads, which occur suddenly in the walking cycle, it is likely that there will be a substantial squeeze film effect in addition to the hydrodynamic mechanism acting. As the viscosity of the lubricant increases, the squeeze film time will increase and hence there will be a thicker film of lubricant separating the two surfaces than would be expected from a purely hydrodynamic effect. This may explain the constant value of friction factor at high loads irrespective of viscosity. The squeeze film thickness for synovial fluid in a typical joint has been estimated by Higginson [1977] to be of the order of 5×10^{-6} m after 0.5 s. This is longer than the time of application of the load during the simulator cycle, which for the slowest speed of oscillation used lasts for 0.25 s.

8.6 Natural hip joints lubricated with SCMC

Moving one stage closer to the rheology of synovial fluid, solutions of sodium carboxymethylcellulose in

water(SCMC) were used as a lubricant. These are shear-thinning. Homsy et al [1973] reported that they were able to produce solutions of SCMC which had very similar viscous properties to synovial fluid. They were interested in using SCMC solutions as a synthetic lubricant in human joints because experiments with an on/off loading cycle showed the initial friction when the load was first applied to be much reduced compared with that for a Newtonian lubricant.

The shear thinning properties of the SCMC solutions used can be seen in Figure 8.2, together with a typical curve for synovial fluid. It can be seen that the viscosity decreases rapidly at first, but the decrease is less marked as the shear rate increases. The viscosity values used were those obtained at the maximum shear rate measured, between 1600 and 1700 s^{-1}, depending on the size of cone used in the viscometer. However, this is obviously not correct since the shear-rate varies through the cycle of oscillation in the simulator. As the film thicknesses are not known, and could not be measured, the shear rate at any point is also unknown. An estimate can however be made using the surface roughness of the cartilage to provide a value for the distance apart of the two cartilage surfaces. Taking a value of 2×10^{-6} m for the separation of the two surfaces, at a typical maximum sliding speed of 20 mm s^{-1}, the shear rate becomes 10^{4} s^{-1}, at a slower

sliding speed, 2 mm s^{-1}, the shear rate for the same separation would be 10^3 s^{-1}. Both these values are in the region where the viscosity is almost constat therefore it seems reasonable to take the lowest value of viscosity recorded as a good approximation to the viscosity of the fluid at all five points analysed through the cycle. It must not be forgotten that the shear rate must fall close to zero at those places in the cycle where the carriage changes direction and hence the viscosity of the SCMC will be increased somewhat.

Three natural joints were tested in the simulator with SCMC solutions [Figures 6.19 and 6.20 - H6, Figures 6.21 and 6.22 - H7, Figure: 6.27 - H9). Looking first at the low load, faster moving points [1, 2 and 3), it can be seen that the friction factor decreases with increasing viscosity in a manner typical of mixed lubrication although the change in friction factor is only at most a reduction of 0.03. The results from points 1, 2 and 3 are separated, which must be a consequence of their different sliding speeds and histories. The high load results (points 4 and 5) also decrease slightly with increasing viscosity, but this reduction is very slight. The fact that the high load results and point 1 are again lower than for the other low loads implies that the squeeze film mechanism, helped by the elastic deformation of the cartilage surfaces under load, must be very important.

8.7 Natural hip joint lubricated with synovial fluid + hyaluronic acid

One joint, H9, was lubricated with synovial fluid enhanced with hyaluronic acid. As discussed in the previous section, the viscosity recorded at a shear rate of 1600 to 1700 s^{-1} was used in plotting the graphs of friction factor against $\eta u/L$. The data again split into two bands, and the results from point 1 again joined the high load data rather than the low load.

The results from points 2 and 3 are different from either of the synthetic lubricants. They form an almost constant band, with a slight minimum at $\eta u/L = 5 \times 10^{-6}$ m^{-1}. This corresponds to a viscosity of about 5×10^{-2} Pa s - a value which is possible for normal healthy fluid. Again the high load points [4 and 5] together with point 1 form a band of constant friction factor, below the low load results.

Figure 8.3 shows the approximate curves for the two synthetic lubricants together with the enhanced synovial fluid all for point 2 of H9, on the same axes. The curves correspond to a remarkable degree, considering how different the lubricants are from each other. The silicone fluids which are not water based, cannot be expected to react with the cartilage surfaces in the same manner as the synovial fluid, or the SCMC. The corresponding graph for the high loads is Figure 8.4. The agreement here is

even closer which is understandable since the value of $\eta u/L$ appears to affect the friction factor very little, if at all.

8.8 Synovial fluid treated with enzymes

The synovial fluid which was treated and used for lubrication tests in the simulator was pathological. This was the only fluid obtainable in a sufficient quantity to perform experiments with controls and also have enough fluid for viscometry and assay. It was felt that, although the fluid was less viscous than normal healthy fluid would have been, it was in fact closer to normal fluid than the bovine fluid which has often been used by other workers. The results from this section of the work could not be plotted in the same manner as the synthetic lubricants since the viscosity range available was so small. Also it was important to compare a digested fluid directly with its undigested, but similarly incubated control sample in order to remove any other variables from the experiment. For this reason, histograms were plotted showing the change in friction factor after digestion. A statistical analysis was performed on the results from each joint, using a two tail student - t test for paired data, to check whether the change in friction factor after digestion was significant.

8.9 Effect of hyaluronidase digestion of synovial fluid on friction factor

From the histograms (Figures 6.13, 6.15, 6.17, 6.18, 6.24 and 6.25) which have been plotted for points 2 and 4, representing the two extremes of loading and sliding conditions, it appears that the friction factor is increased by hyaluronidase digestion at point 2 but not at point 4. The student-t test confirmed this as the figures in Table 8.1 show. All the joints except H9 showed a significant difference at point 2 at the 5% level and most were better than this. H9 had very erratic friction factors, some of which were very high.

It is not surprising that the highly loaded point shows no significant difference since the results previously discussed show that the friction factor is almost constant at high loads whatever the viscosity or type of the lubricant. At point 2, the viscosity of the lubricant after digestion is decreased and the friction factor is increased. This means that the joint is operating in the mixed lubrication region or the full film region before digestion and mixed afterwards. The expression $\eta u/L$ for this data will typically have a value of 10^{-7} m^{-1} which, referring to Figure 8.3, is to the extreme left of the data plotted and hence in the mixed region. The viscosity of the synovial fluid thus plays an important role in lubrication at low loads. This viscosity is

provided by the hyaluronic acid chains in the fluid and is easily destroyed by the action of hyaluronidase.

It has been suggested [O'Kelly, 1977] that it may be the action of residual hyaluronidase in the synovial fluid which attacked the cartilage surfaces in the joint and for this reason increased the fricton factor. Any such action on the cartilage surfaces would not be reversible. Great care was taken in the present tests to avoid using the lubricants in any preconceived order, so that for some of the joints the sample treated with hyaluronidase was tested before its control. This removes the possibility that the effect of the hyaluronidase can be on anything other than the fluid itself.

8.10 Effect of trypsin digestion of synovial fluid on friction factor

The histograms showing the results for trypsin digestion [Figures 6.15, 6.18 and 6.24] indicate that the friction factor is sometimes increased and sometimes decreased after digestion by trypsin, particularly at point 2. The P values from the student-t test in Table 8.1 indicate that there is no significant difference in the two populations before and after digestion. The changes in friction factor must therefore be due simply to the inherent variability in the data obtained from the simulator. The trypsin digestion breaks up the protein chains in

the fluid, but the protein was not actually removed from the fluid. It is possible therefore that any beneficial effect the protein has on the lubricating ability of the fluid is still present after digestion. On the other hand, it has been suggested that the protein acts as a boundary lubricant in synovial fluid. At low loads it may play a role around the edges of the joint, in addition to the obvious viscosity dependent effect over the contact area. At high loads, where the friction factor is constant as $\eta u/L$ changes, conventional boundary lubrication alone would produce much higher friction factors than those recorded.

8.11 Effect of compliance of cartilage on friction factor

Since the lubrication mechanism acting in a joint may be influenced by the elasticity of the joint surfaces, the relationship between the compliance values of cartilage samples from the femoral head and the friction factors measured with Ringer's solution from each joint was investigated. Ringer's solution is the only lubricant to be used in all the joints (some of the synovial fluid samples were different from each other). Figure 8.5 shows that there was no obvious relationship between compliance and friction factor. Since the effective modulus of a thin soft elastic layer on a rigid base is dependent on the thickness of the soft layer, the compliance values were multiplied by the thickness of the cartilage and replotted, this time with the average value of friction factor for point 4 lubricated with

untreated synovial fluid, (H7 was therefore excluded, since there were no tests run on this joint with synovial fluid). A highly loaded part of the cycle, where a squeeze film mechanism may act, seemed to be the most likely circumstances to detect the effect of different cartilage properties. However, Figure 8.6 again shows no obvious correlation. This does not mean that the elasticity of the cartilage is irrelevant to the lubrication of the joints - the compliance values do not encompass a very wide range of values and the variation in friction factor observed between the joints may be due to the surface condition of the cartilage or the joint geometry rather than the compliance. Further discussion of the effect of compliance on friction factor appears in a later section on artificial joints.

8.12 Suggested lubrication mechanism through walking cycle

So far, the discussion has centred round the effect that a particular lubricant or mechanical property has on the friction factor. In this section, the lubrication mechanism through a walking cycle will be examined in the light of the information recorded for specific conditions.

Starting with the region where the load is small but the sliding speed is high, the results for synovial fluid with hyaluronic acid added indicate that for healthy fluid the lubrication can be full fluid film. However if the fluid is pathological and therefore less viscous,

the lubrication may become mixed. The viscosity of the lubricant is still important as was shown by the data for hyaluronidase digested fluid where the reduction of viscosity caused an increase in friction factor. It seems that healthy fluid in a healthy joint may lead to values of friction factor near the minimum of the curve for varying $\eta u/L$.

As the sliding speed reduces, from point 2 to point 3, the friction factor remains much the same. After application of the load, which occurs rapidly both in a natural walking cycle and in the simulator cycle, the friction factor is reduced and tends to remain constant regardless of viscosity of lubricant or changes in sliding speed (points 4 and 5). There are probably several contributing factors to the low friction under high load. The eccentricity effect discussed in section 8.3 may apply. The high sliding speeds in the low load region will have allowed the build up of a reasonably thick film of fluid by hydrodynamic action. With the application of load this film will be squeezed out from between the cartilage surfaces but the time for the film to reduce appreciably in thickness is considerably longer than the time of application of the load. The high load will also cause deformation of the cartilage surface which can reduce the heights of asperities and hence reduce the film thickness needed to ensure complete separation of the two surfaces. As the sliding speed reduces to zero,

the shear-rate must also decrease, which will increase the viscosity of the synovial fluid by a factor of about 10. (There will still be some shearing of the fluid caused by the squeeze film effect.) This increase in viscosity will help to maintain a full fluid film under the most adverse conditions - the full load and almost zero sliding speed. After the joint changes direction and the sliding speed starts to increase again, the friction remains low, even after removal of the load (point 1), but gradually increases. The low friction factor values often recorded for point 1 may be due to the time taken for the cartilage to recover its undeformed profile after the period of heavy loading.

This analysis of the lubrication mechanisms acting in a hip joint is in disagreement with the work of Radin, Swann and Weisser (1970) discussed in Chapter 3. They concluded that it was the protein component of synovial fluid which was totally responsible for the low coefficients of friction in human joints. This is not confirmed by the present work which demonstrates the dependence of the friction factor on the viscosity of the fluid, certainly for low loads. Their test method used a constant, heavy load, that is a similar arrangement to the experiment reported here with the Charnley joint lubricated with silicone fluids under constant loading. Little variation with viscosity of fluid was found under these conditions,

but they are not those generally experienced in human joints.

8.13 Choice of compliant linings

There were two main reasons for experimenting with prostheses which had a compliant lining in the acetabulum. One reason was to investigate further the possible effects of cartilage elasticity on the lubrication of natural joints. By using a prosthesis instead of a natural joint, it is possible to isolate the effect of changing a single variable. For instance, prostheses were manufactured with different thicknesses of compliant layers, but an otherwise similar geometry. Natural joints with differing thicknesses of cartilage would also differ in size and geometrical fit. The second reason for experimenting with compliant linings was to examine their behaviour with a view to using them in a prosthesis. Natural hip joints have an elastic layer, the cartilage, covering the bone ends to distribute stress and provide a suitable surface for low friction lubrication. Therefore, the possibility of using a compliant lining to reduce friction in a prosthesis seemed worth investigating.

An acetabular lining was chosen since it was relatively easy to mould and control the thickness. For simplicity and ease of analysis it was decided only to have one surface covered with elastomer. The geometry of the joint suggests that the elastomer/metal bond is less likely

to fail on a concave rather than a convex junction. For a given stress acting on the elastomer surface, the stress at the elastomer/metal junction will be greater for a convex surface, since its area is less than that of the elastomer surface. Conversely, for a concave surface, the stress at the interface will be reduced and therefore less likely to cause failure of the bond.

Thompson (1979) experimented with all three arrangements of compliant layers - the femoral head, the acetabulum and both - and found the double layer gave the lowest friction factor. All his results are however rather doubtful as he did not take averages from the two halves of the loading cycle and the asymmetry of the friction traces he obtained showed that the joint was not correctly aligned. He used the same simulator as in the present work, but it was rebuilt and the friction measuring carriage completely realigned before any of this present work was undertaken. Thompson used a Charnley head (22 mm diameter) in his work and found considerable deflection of the rubber layers due to the high stress level. This work was done using a McKee-Farrar head (diameter 35 mm), which meant that, for a similar load, the stress was reduced.

The elastomer used in the present tests was Sylguard 102. This is a transparent rubber which is cured at 75^{o}C. The Silcoset used by Thompson was not used here because although it had the advantage of curing at room temperature,

it was not transparent. Thompson had some difficulty in ensuring that no air bubbles were trapped in the elastomer when it was moulded since these were not visible until they caused the surface of the elastomer to break up during tests. A transparent elastomer circumvented this difficulty, since all the air bubbles could be eliminated before pouring the mix into the mould. Also the integrity of the compliant layer could easily be checked visually before mounting and testing.

8.14 Elastic modulus of compliant layers

With an artificial joint, it should be practicable to vary just one parameter at a time and therefore it was necessary to ensure that the cured elastomer had the same elastic modulus for each lining. The results in Table 7.1 give the measured values for the viscoelastic modulus calculated from measurements taken on slabs of elastomer from each mix. It is noticeable that the thinner slabs produced a higher modulus value than the thicker ones. This difference is obviously going to be more pronounced in the experimental acetabula, where the layer thickness (0.5 - 3.0 mm) is less. Waters (1965) has shown that for a non lubricated junction between indentor and elastomer (as in Clish's apparatus), the estimates of Young's modulus will be in excess of the true value by less than 5% provided:

$$\frac{t}{a_t} > 8$$

where t is the thickness of the sheet and a_t is the radius of the contact area of the indentation.

Now for the experiments on the slabs of elastomer, a_t had an average value of 3.7 mm, hence, for the greatest thickness used, 6.5 mm,

$$\frac{t}{a_t} = 1.8$$

The sheet was therefore not thick enough to give a true value of Young's modulus. Using Waters' empirical relationship between E_t and E_∞ :

$$E_\infty = E_t\left[1 - \exp\left(\frac{-0.41\ t}{a_t}\right)\right]^{3/2}$$

values of E_∞ were found for the different elastomer mixes. Appendix 2 contains greater detail of Waters' theory.

The differences in elastic modulus between the mixes are presumably due to differences in manufacture. The amount of curing agent added to the elastomer was measured to an accuracy of at least 1%. The product data sheet [Dow Corning, 1978] states that 'variations of up to 10% in the concentration of curing agent ... have little or no effect ... on the properties of the final cured part.' It may therefore have been the mixing or curing procedure which caused the variability.

It would have been possible to use Waters' relationship to find an effective modulus for the thin layers of elastomer bonded to the acetabular cups. However, the arrangement of the artificial joints may complicate the 'stiffness' actually found; the bond between metal and

elastomer and the confined space both contributing to deviations from the theoretical assumptions. The curves obtained during the Instron static loading tests (see Figure 7.3) demonstrate this effect. At the low loads the elastomer appears softer than at high loads. Presumably when the joint is initially loaded, the elastomer can deform but as the load increases, so the deformation is restricted by the reducing of the clearance and by the metal-elastomer bond. It would be expected that the thinner layers would be more restricted by the bond, and the thicker layers by the lack of space for the deformation to take place. The reduced 'stiffness' of the two layers with larger clearance emphasises the point that the apparent modulus of the elastomer layer is very much determined by the clearance in the joint.

8.15 Friction tests with compliant layers

In general the friction tests with the elastomer layers produced higher values of friction factor than had been expected from earlier trials (Thompson, 1979). This may be partly due to Thompson's misinterpretation of his frictional torque traces and partly due to his use of silicone fluids as lubricants. The results for silicone fluids in the present work were always lower than for SCMC. Since the silicone fluid interacted with the joints and changed their geometry, the results for silicone fluids and SCMC solutions will be discussed separately.

8.16 Compliant linings lubricated with SCMC

The detailed results of these tests were given in Chapter 7. Figure 8.7 shows a summary graph of the results for points 2 and 4 - typical low load, fast moving and high load, slow moving points. The friction factors decreased with decreasing thickness of compliant layer. The high load produced lower friction factors than low loads. As the viscosity of the lubricant was increased, the friction factor decreased. This is more marked for the low load points than for the high loads.

The same shear rate was used for all the points in the cycle for viscosity determinations, but as the sliding speed changes this is not necessarily valid. An estimate of the film thickness and hence the shear-rate can be obtained from the analysis of Higginson [1977] for a cylinder on plane geometry for a thin layer on a hard backing. The minimum film thickness is given by

$$h_{min} = \left(\frac{\eta u}{ER}\right)^{0.6} \left(\frac{w}{ER}\right)^{-0.2} R$$

For the artificial hip joints, we can take the following values:

$$R = 1.2 \text{ m}$$

$$E = 2 \times 10^{6} \text{ Pa}$$

$$\eta = 10^{-2} \text{ Pa s.}$$

Then for point 2 in the cycle where

$$w = 2 \times 10^{4} \text{ Nm}^{-1}$$

$$u = 0.02 \text{ ms}^{-1}$$

$$h_{min} = 3 \times 10^{-6} \text{ m}$$

and the shear rate is 7000 s^{-1}.

For point 4 in the cycle w is increased and u decreased:

$$w = 7.5 \times 10^{4}\ Nm^{-1}$$

$$u = 0.002\ m\ s^{-1}$$

$$h_{min} = 5 \times 10^{-7}\ m$$

and the shear rate is 4000 s^{-1}.

This order of magnitude calculation shows that for both points 2 and 4 in the cycle, the shear rate may be expected to be greater than $10^{3}\ s^{-1}$. At these high shear rates, the viscosity varies little and the use of the same value for the different points in the cycle therefore appears to be valid.

These rough calculations indicate a film thickness of 10^{-7} to 10^{-6} m for an elastohydrodynamic film caused by rolling/sliding. It is interesting to compare these values with the surface finish of the joint components. Figure 8.8 shows a Talysurf trace of the McKee-Farrar head used in these tests. Figure 8.9 shows traces obtained from the two brass plugs against which the elastomer was moulded for the compliant linings. The larger plug was used for those acetabula made with an increased clearance. Since the elastomer was moulded in contact with the brass, it should have faithfully reproduced the surface contours. Traces were not taken directly from the elastomer surface because of the increased difficulty of taking traces on a compliant surface, and because the

concave shape of the surface made the stylus movement much more complex. The Ra values for the components were

McKee-Farrar head 0.5 μm

Small brass plug 1.1 μm

Large brass plug 0.7 μm.

Therefore to separate the two surfaces completely in the joint would require a film thickness of about 2×10^{-6} m under zero load. At increased loads, the asperities on the elastomer surface would deform, so effectively reducing its Ra value and the thickness of fluid film needed to separate the surfaces. The previous calculation suggests that the required film thicknesses may be generated, provided the lubricant has a viscosity of at least 10^{-2} Pa s. However, with the particular materials and design used in the prostheses it appears that large scale deformation of the lining (rather than asperity deformation) considerably affects the friction factors obtained.

Since high friction factors had been observed with 0.25 mm radial clearance in the prostheses, it was decided to experiment with a larger clearance (0.5 mm). Thus the acetabular cups Z1 and Y3 were manufactured. It was at first thought that the high friction factors might be caused by a gripping effect around the equatorial region of the joint which would be alleviated by a larger clearance.

The results with an increased clearance were however even higher than those with normal clearance. Comparing the 'stiffnesses' of the acetabula with their friction factor ranking provides an explanation for this. Table 7.2 shows that the extra clearance produced prostheses which were less 'stiff' than the corresponding layer thicknesses with normal clearance. Since increasing layer thickness also reduces 'stiffness' and increases friction factor, this 'stiffness' appears to play an important part in the lubrication of the prostheses.

The anomalous results for the 1 mm thick layer, shown very clearly in Figure 7.29, where the friction factor was higher than would be expected from the general trend, has no real explanation. Two different layers were made and tested, both with the same high results, but the same steel base was used for each. The possibility that the base was misshapen and perhaps did not mount on the special jig in such a way that the cup was central cannot be disregarded.

8.17 Compliant linings lubricated with silicone fluids.

The individual results for each layer thickness have been brought together and the results for points 2 and 4 are displayed in Figure 8.10. The effect of layer thickness appears to be less than for joints lubricated with SCMC. The shape of the graph for point 2 suggests

that at the lowest viscosity [9.4 x 10^{-3} Pa s] the lubrication mechanism may be mixed, but as the viscosity of the lubricant is increased the friction factor falls to below 0.1 and then gradually increases again in the manner typical of full fluid film lubrication. The low values of friction factor at point 4 suggest that a full fluid film is operating here, doubtless helped by a squeeze film mechanism.

The composite graphs in Figure 7.48 show that the friction factor tends to decrease rather than increase with thickness of the compliant layer. The 'stiffness' of the joints as measured on the Instron still decreased with increasing thickness of lining after the soaking in silicone fluid [Figure 8.11]. This implies that the 'softer' the joint, the lower the friction factor. The exception is for the lowest viscosity silicone fluid [9.4 x 10^{-3} Pa s] [marked as '10' on the graph] which has an increasing friction factor with layer thickness. It appears then that this feature is perhaps characteristic of mixed lubrication and that if conditions are not suitable for a full film, they are made worse by the soft layer.

Care must be exercised in comparing the effect of layer thickness in the silicone lubricated prosthesis. The prostheses had all been soaked in fluid and swollen by a noticeable amount. This meant that the geometry of

the cups had changed and they would not all have the same clearance since the larger volume of elastomer would swell more. A rough investigation of this effect showed that the two thickest layers no longer had any clearance and were now an interference fit. The possibility that contact at the pole was not achieved even under high loads could not be discounted. Any comparison of the four swollen acetabula is therefore comparing changes in geometrical fit as well as layer thickness. These changes in the fit must affect the true contact area in the joint. With no contact between the bearing surfaces at the pole of the joint, a pool of lubricant will be trapped here and be able to act as a reservoir to maintain a fluid film.

8.18 Comparison of results from SCMC and silicone

There are two obvious differences between the tests with SCMC and silicone fluids as lubricants. In the first place, the friction factors for silicone fluids are less than for SCMC. However, the $\eta u/L$ values are higher for silicone fluids, since their viscosities were generally greater, and so comparing the graph of the SCMC and silicone results (Figures 8.7 and 8.10) shows that the results are approximately continuous. At point 2, the SCMC results provide the falling friction factor as the viscosity increases and the silicone results take the curve through its minimum and on to an increasing trend of friction

factor with viscosity, typical of full fluid film lubrication. The second difference is the effect of increasing the thickness of the lining on friction factor. With SCMC this increases the friction factor, whereas with silicone there is in general a reduction, though not as pronounced. The effect with SCMC was thought to be due to a lowering of the effective 'stiffness' of the joint as the thickness of compliant lining was increased. Figure 8.11 shows that the joints are softer after soaking in silicone fluid, and yet the friction factor is reduced. This must therefore be an effect either of the changed geometry and clearance in the joint or the interaction of the lubricant with the elastomer or a combination of both.

The effect of reducing clearance so that the joint halves were an interference fit was discussed in section 8.17 where it was explained how the lack of contact at the pole may increase the availability of lubricant for a full fluid film. It is unlikely that the soaked joint will 'weep' during lubrication tests in the manner suggested by McCutchen for the lubrication of natural joints. In a lubricated joint, under dynamic loading where the load is only applied for relatively short periods of time there will be little opportunity for the fluid to be expressed from the elastomer. This was borne out by the clearance tests in the swollen joints which were carried out after lubrication testing. One important

difference in the behaviour of the two lubricants is their ability to 'wet' the elastomer surface. Silicone fluid 'wets' the surface of silicone elastomer, but the SCMC does not do so to the same extent. Roberts [1971] noticed this effect when using water as a lubricant for silicone rubber spheres on glass sheets and he overcame it by adding detergent to the water. As this was not done in the present work it may have reduced the ability of the system to form a fluid film and hence increased the friction factor.

The lubrication test with SCMC on a joint which had been soaked in silicone provides some interesting extra evidence on the difference in the lubricants. After the first test, where the SCMC was obviously contaminated by surface absorbed silicone fluid, the friction factors became those typical of SCMC rather than silicone. This implies that it is not the swelling alone of the joint which affects the lubrication but is likely to be connected with the lubricant itself, very probabaly its 'wettability' on the compliant surface.

8.19 Comparison of results with theoretical model for the breakdown of Fluid Film lubrication

Medley et al [1980] have shown that the breakdown of Fluid Film lubrication for the sliding of an elastomeric surface over a metal sphere can be predicted by the

condition

$$\frac{R^{0.78}[\eta_o u)^{0.67}}{\sigma[E']^{0.45} F^{0.22}} \geqslant 0.902 \pm 0.335$$ for a full film to exist.

This is based on an isoviscous lubricant and so strictly could only be applied to the silicone fluids in the present work. Using typical values for point 2 and a viscosity of 10^{-3} Pa s, this factor becomes about 90 ie well above the critical value for a full elasto-hydrodynamic film. For a highly loaded point, it is necessary to consider the effect of pressure on viscosity, but since this is small at the pressures found in a joint, even for silicone fluids, the theory can still be applied and results in a value of approximately 10 for the factor - still well above the critical value for a full film.

8 .20 Squeeze films

It is unlikely during the highly loaded slow moving part of the simulator cycle that a fluid film can be maintained by an elastohydrodynamic action alone. The squeeze film mechanism, first suggested by Fein in 1967, must play an important role in maintaining a fluid film during the highly loaded parts of the cycle. The rough calcuations of film thickness produced by hydrodynamic action in the highly loaded part of the cycle produced a value of film thickness of 5×10^{-7} m for a viscosity of 10^{-2} Pa s. This is less than the Ra values for the surfaces. What film thickness does a similar calculation for squeeze film action produce?

Higginson [1977] uses a simple approximate formula to calculate the film thickness after a given time:

$$\frac{h}{R} \approx 2\left(\frac{P}{ER^2}\right)^{1/6}\left(\frac{\eta}{Et}\right)^{1/2}$$

As E is the equivalent elastic modulus, the approximation $E = 3 \times 10^6$ Pa will be used since thin layers are involved.

Using $R = 2.5$ m

$P = 1500$N

$\eta = 10^{-2}$ Pa s

$t = 0.5$ s

gives $h \approx 8 \times 10^{-5}$ m.

This is two orders of magnitude larger than for hydrodynamic action and certainly sufficient to maintain a fluid film.

Changing the clearance in the joint will alter the value of R. For 0.5 mm radial clearance, R becomes 6.3 m. The predicted film thickness is then 2.5×10^{-5} m, less than before, ie the closer the two surfaces conform, the better from a squeeze film point of view.

The sqeeze film action depends on the presence of a thick film between the two surfaces when the load is applied ie the low load part of the cycle, where the sliding speed is higher must act to draw fluid into the contact area. The calculations of the elastohydrodynamic factor in the previous section showed that the conditions were in the full elastohydrodynamic film region. Why then are

the recorded friction factors so high in the low load region for the compliant layers? The total friction factor is made up of 3 components:

$$\mu = \mu_c + \mu_h + \mu_f$$

where μ_c is due to contact between asperities

μ_h is caused by hysteresis effects in the elastomer

μ_f is the contribution from the fluid film.

If there were no fluid film in the low loaded part of the cycle, it seems improbable that it should appear in the highly loaded parts, yet in these parts the friction factor is low and must be fluid film . Perhaps in the low load region, μ_h makes a large contribution and we have also seen that the eccentricity present if the joint is considered as a journal bearing tends to reduce the measured friction factor at high loads.

8.21 Dependence of friction factor on position in the cycle

With both natural and artificial joints the dependence of the friction factor with position in the cycle has been noted. In particular, the low values of friction factor usually obtained at point 1 compared with point 3 which has nominally the same u/L value were particularly noticeable. The results for joints lubricated with silicone fluids, however, did not display this separation of friction factor values for points 1 and 3. One possible explanation is that although the sliding speeds were the same at the two points, the speed is increasing at point 1 and decreasing at point 3. The separation of the bearing surfaces may therefore be different so the lubricant

viscosity will be decreasing at point 1, rather than increasing as at point 3, and this may lead to a lower friction factor. As the viscosity of silicone is constant at all shear rates, the silicone tests would not be affected in this way.

An alternative explanation considers the deformation of the cartilage or elastomer, both on a macro and an asperity level. The highly loaded part of the cycle produces a high level of deformation. When the load is suddenly removed, the compliant layer will take a finite time to recover and hence the friction factor at point 1, just after the load has been removed, may remain low. In effect, this point will have a larger film thickness than would be predicted by consideration of the actual conditions at that time. As the compliant layer recovers, the friction factor rises. This effect would be much less noticeable with silicone fluids since the friction factors are never high.

The shear deformation of the elastomer and the finite time to cause it to reverse its direction may explain the lag of the friction trace when the carriage changes direction. Figure 8.12 shows that the friction trace does not change as rapidly as expected for hard surfaces.

Analysis of the lubrication mechanism in a hip joint is complicated by the changing sliding speeds and the dynamic

loading pattern, but there is evidence to show that both these conditions help to reduce the friction in the joint by maintaining a fluid film between the surfaces.

Reference	P for hyaluronidase		P for trypsin	
	Point 2	Point 4	Point 2	Point 4
H2	0.005	0.98	0.2	0.1
H3	0.05	0.2	0.5	0.02
H5	0.001	0.6	-	-
H6	0.005	0.3	0.5	0.7
H8	0.01	0.5	0.4	0.2
H9	0.2	0.6	-	-
Combined	0.05	-	-	-

Table 8.1

Results of Student-t test for hyaluronidase and trypsin digestion.

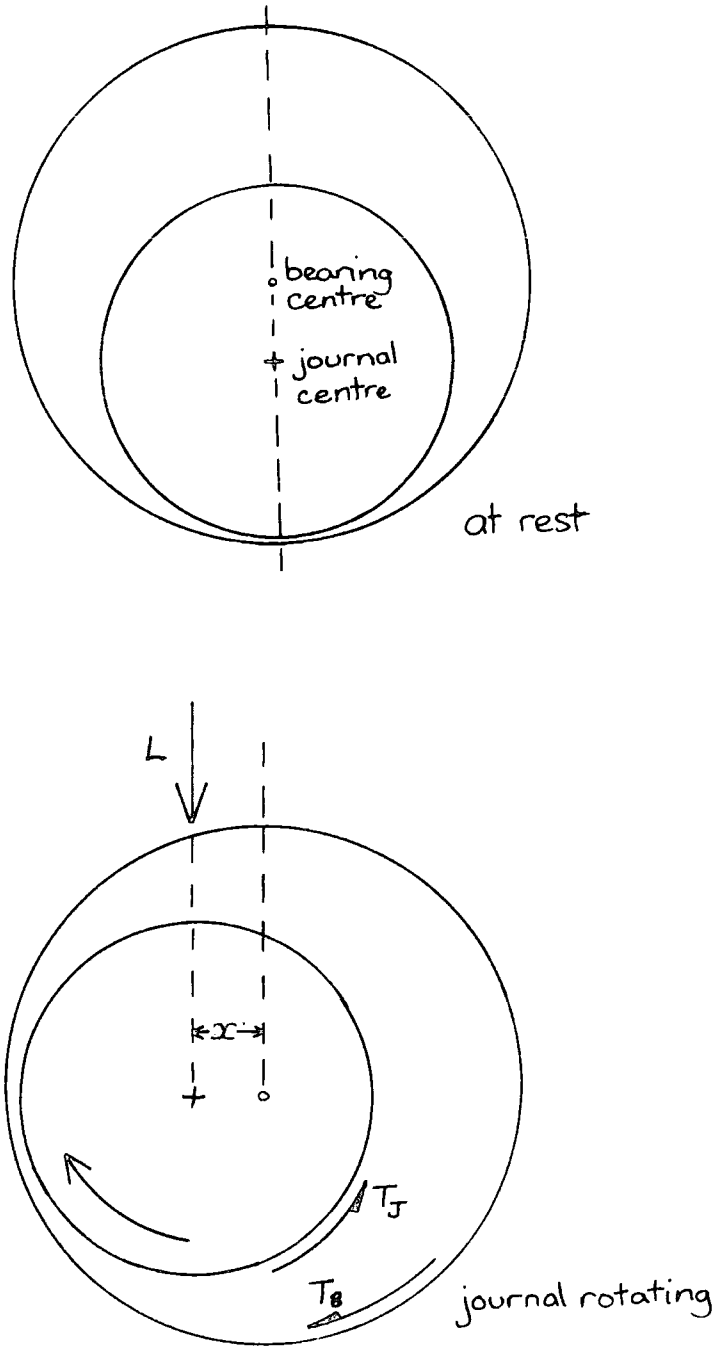

Figure 8.1

Effect of offset, x, of journal bearing on measured torque.

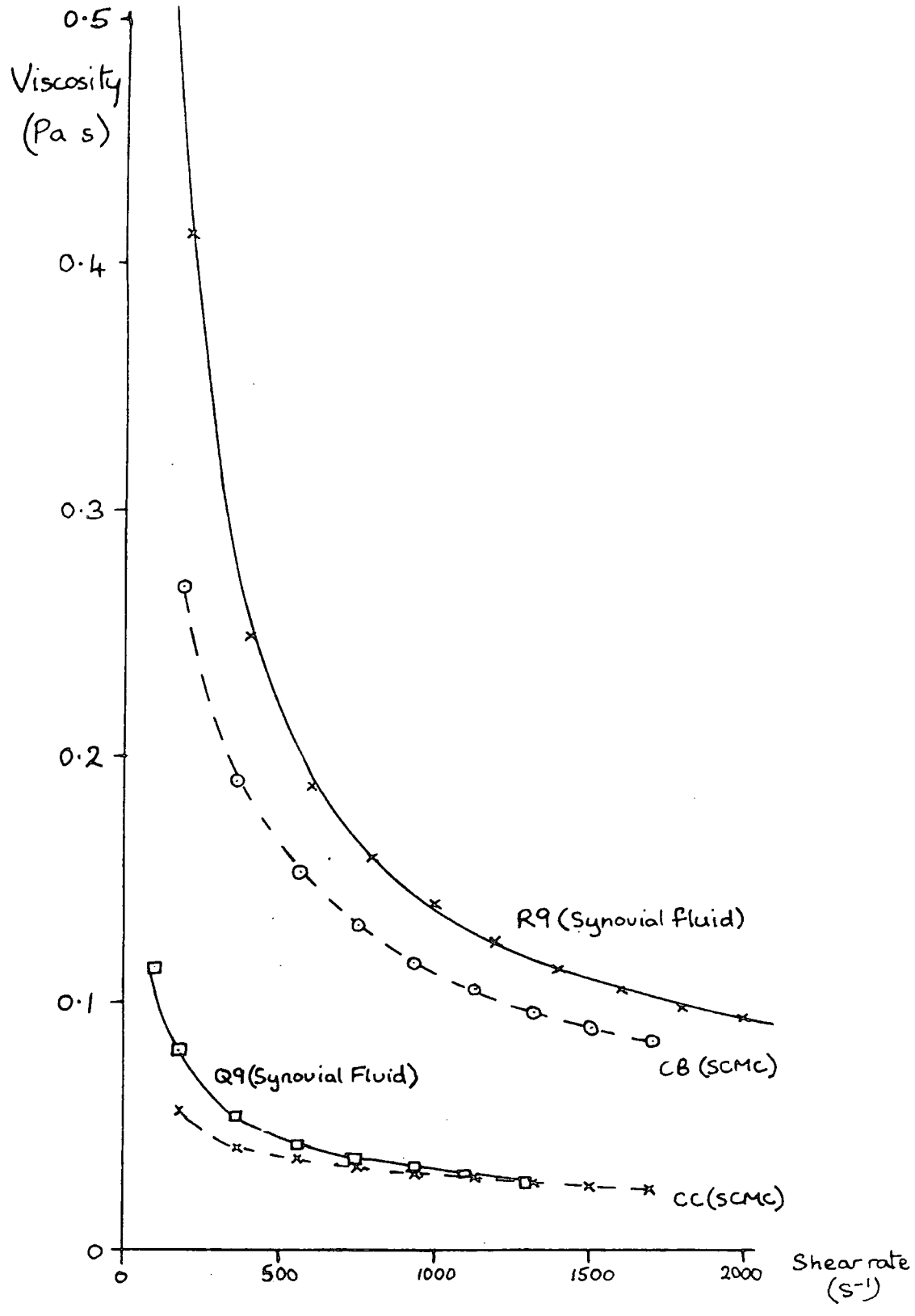

Figure 8.2

Dependence of viscosity on shear rate for samples of synovial fluid [with added hyaluronic acid] and SCMC.

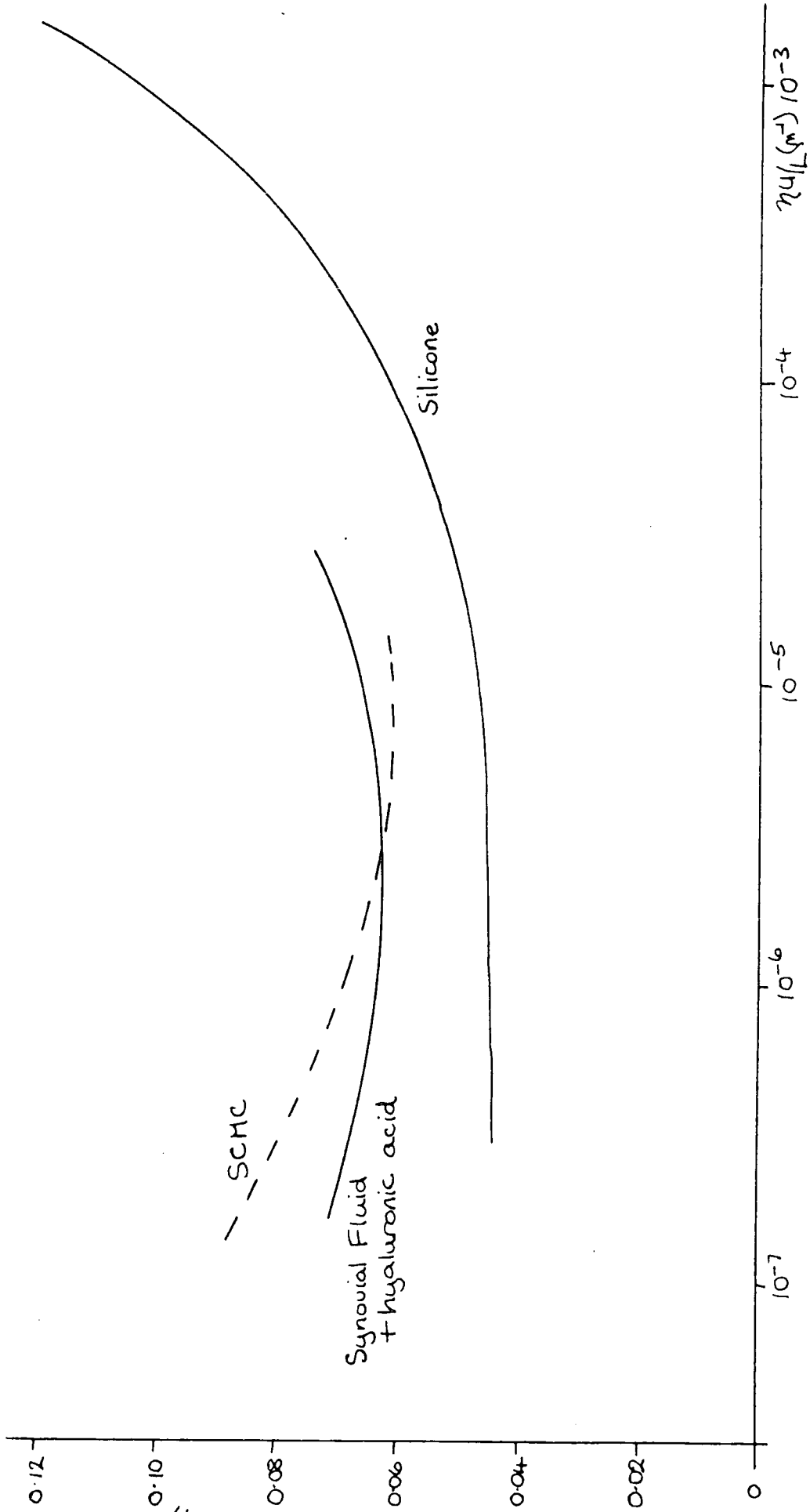

Figure 8.3

Summary of data from point 2 for various lubricants. Joint H9.

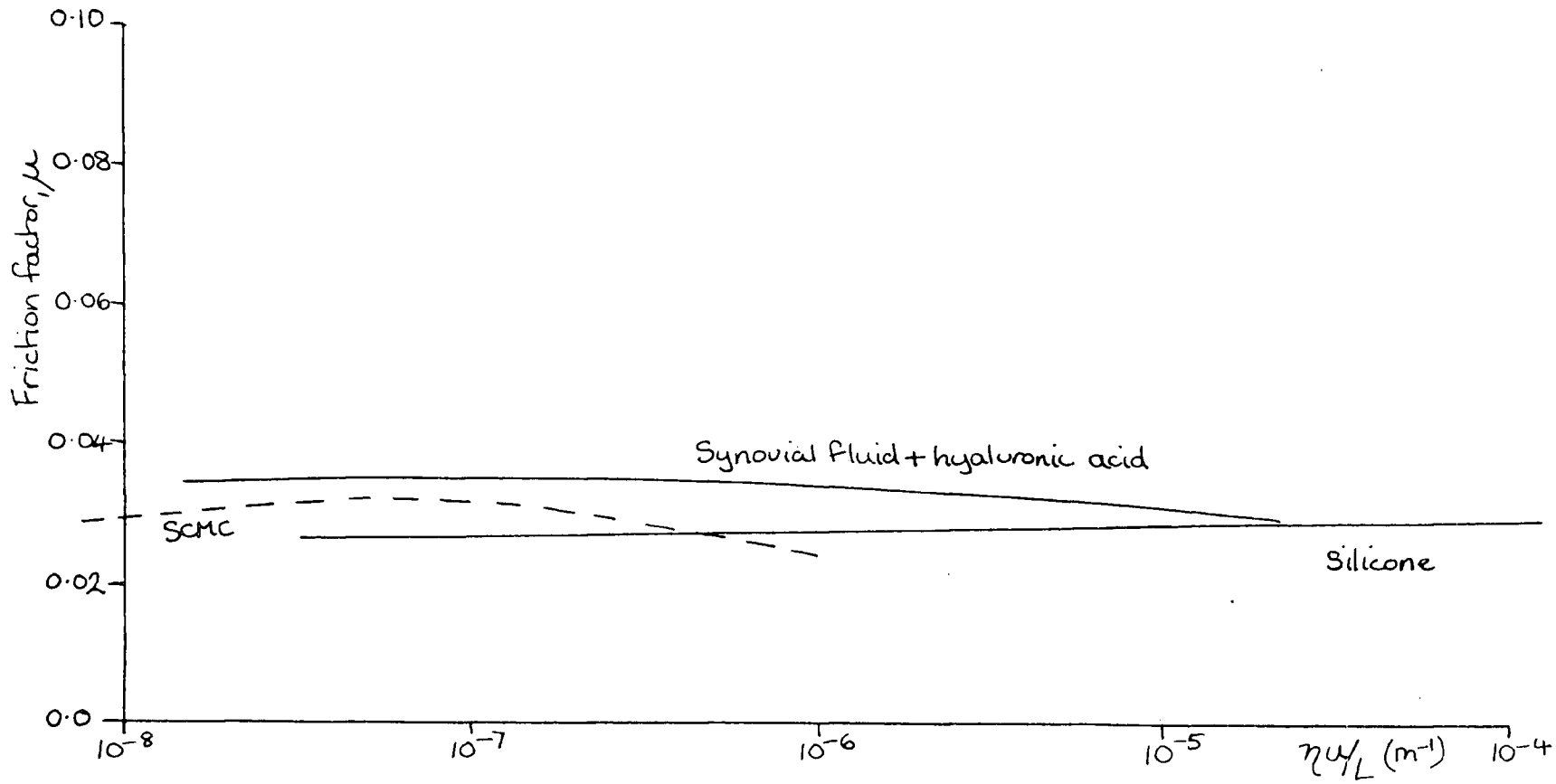

Figure 8.4

Summary of high load data for various lubricants. Joint H9.

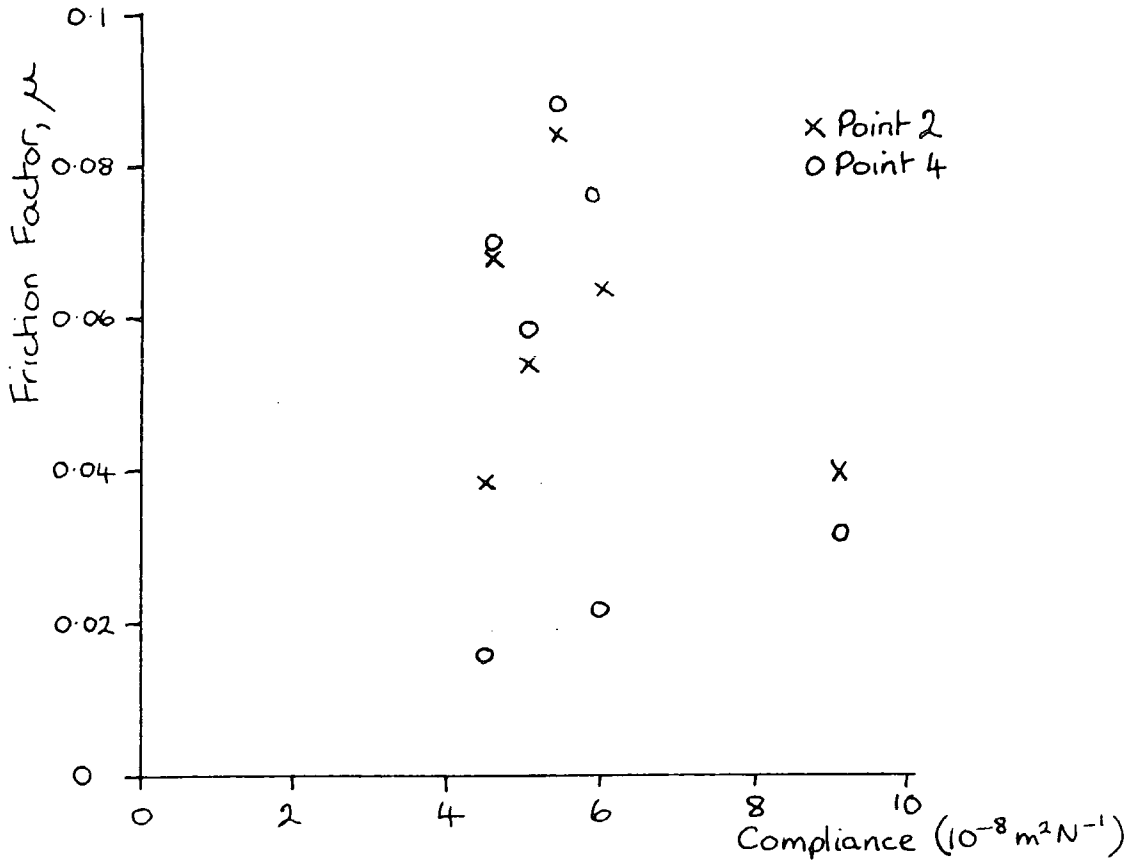

Figure 8.5

Dependence of friction factor on compliance of cartilage for natural joints lubricated with Ringer's solution.

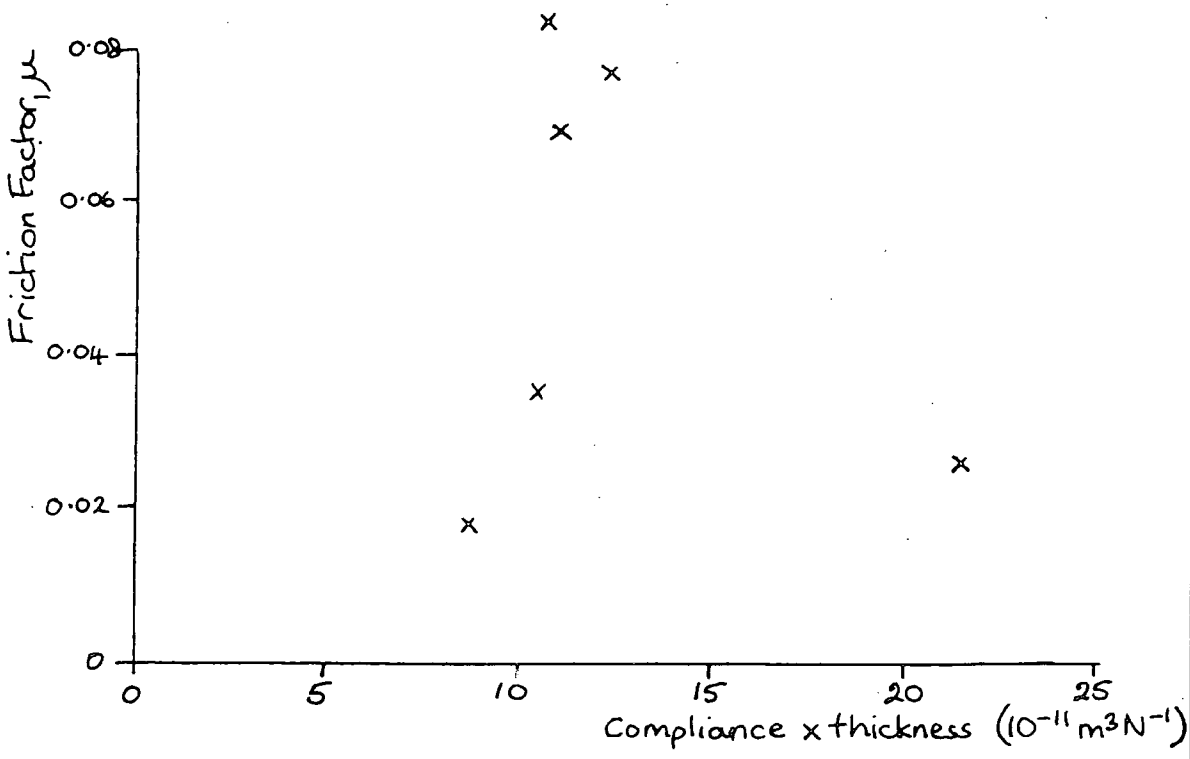

Figure 8.6

Dependence of friction factor on [compliance x thickness] of cartilage for natural joints lubricated with synovial fluid [point 4].

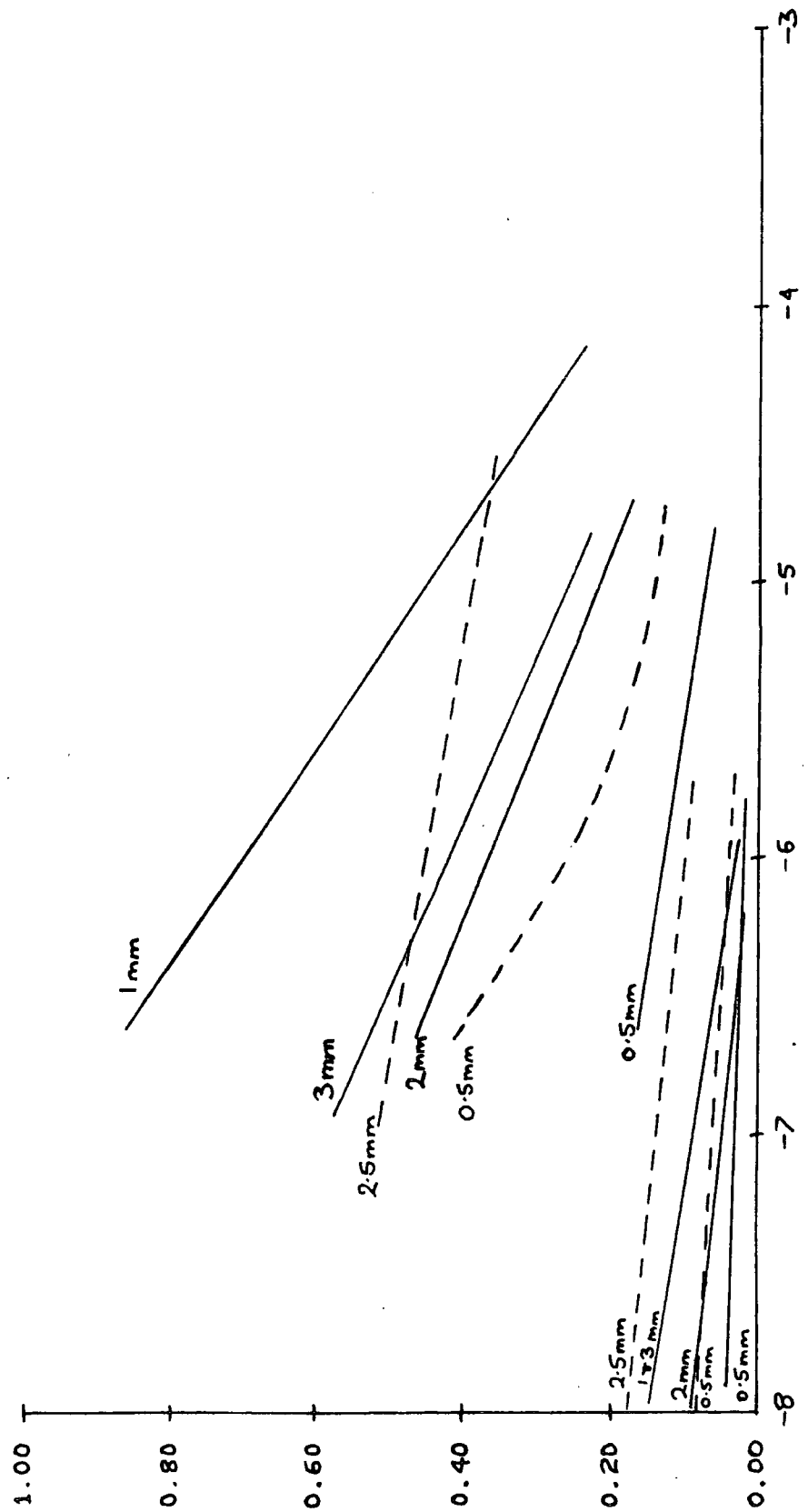

Figure 8.7

Summary graph for compliant layers lubricated with SCMC - points 2 and 4.
Dotted lines are for joints with increased clearance.

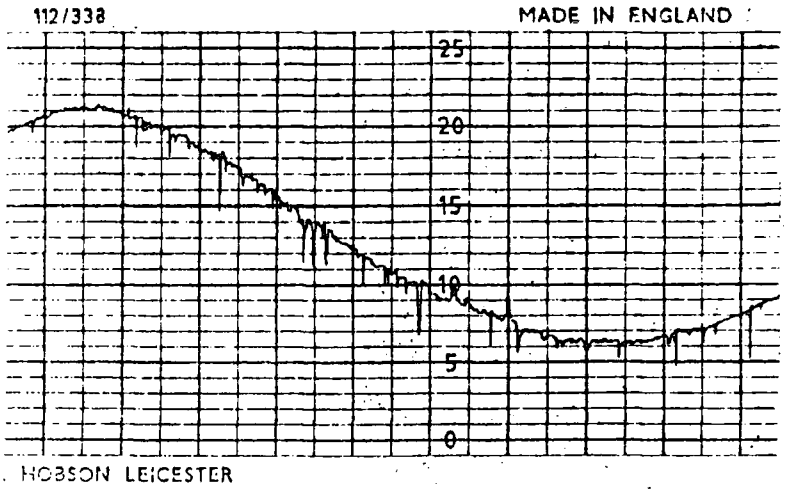

Figure 8.8

Talysurf trace of McKee-Farrar head vertical mag x 10,000 horizontal mag x 20.

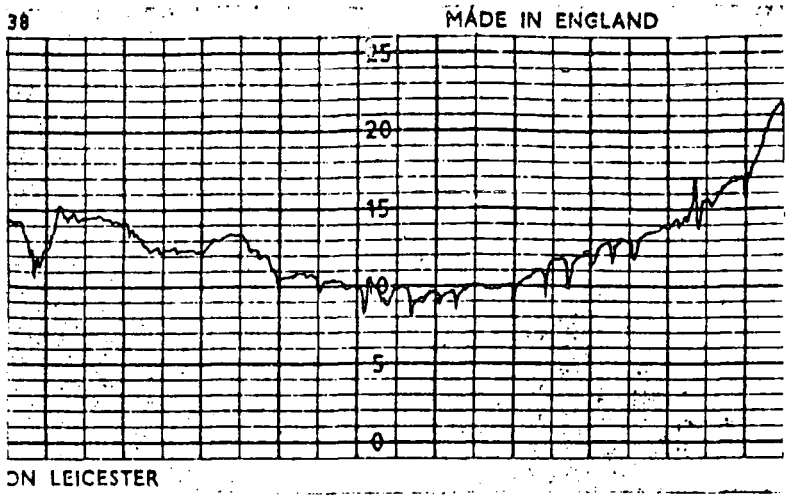

(a) Vertical mag x 2000 horizontal mag x 20

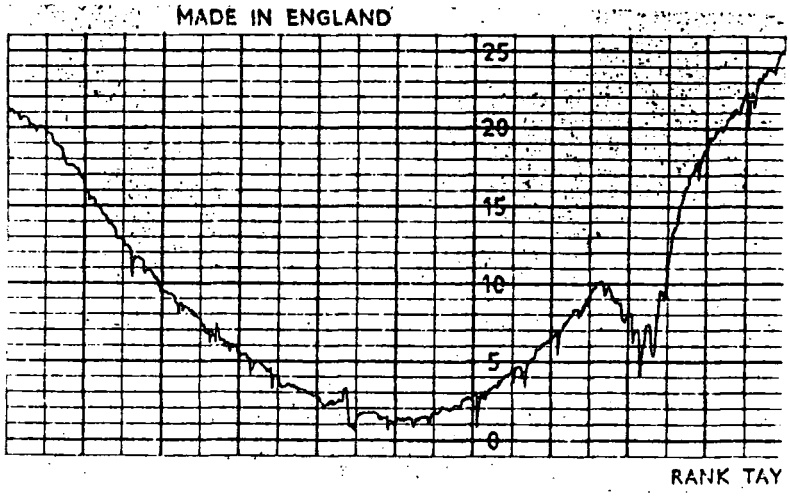

(b) Vertical mag x 5000 horizontal mag x 20

Figure 8.9 (a) and (b)

Talysurf traces of surface of brass plugs used for moulding compliant layers
(a) 0.50 mm radial clearance
(b) 0.25 mm radial clearance.

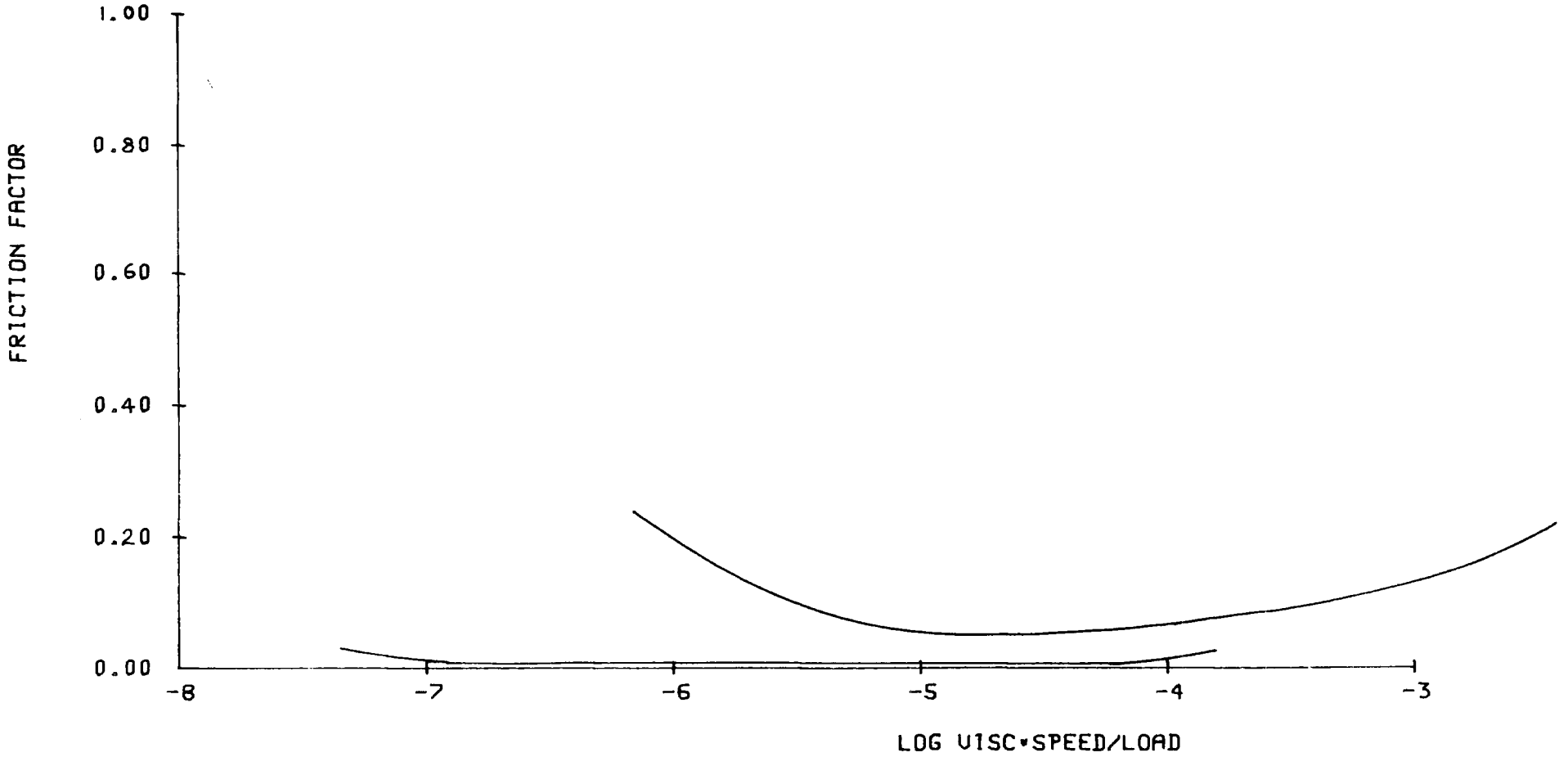

Figure 8.10

Summary graph for compliant layers lubricated with silicone fluids - points 2 and 4.

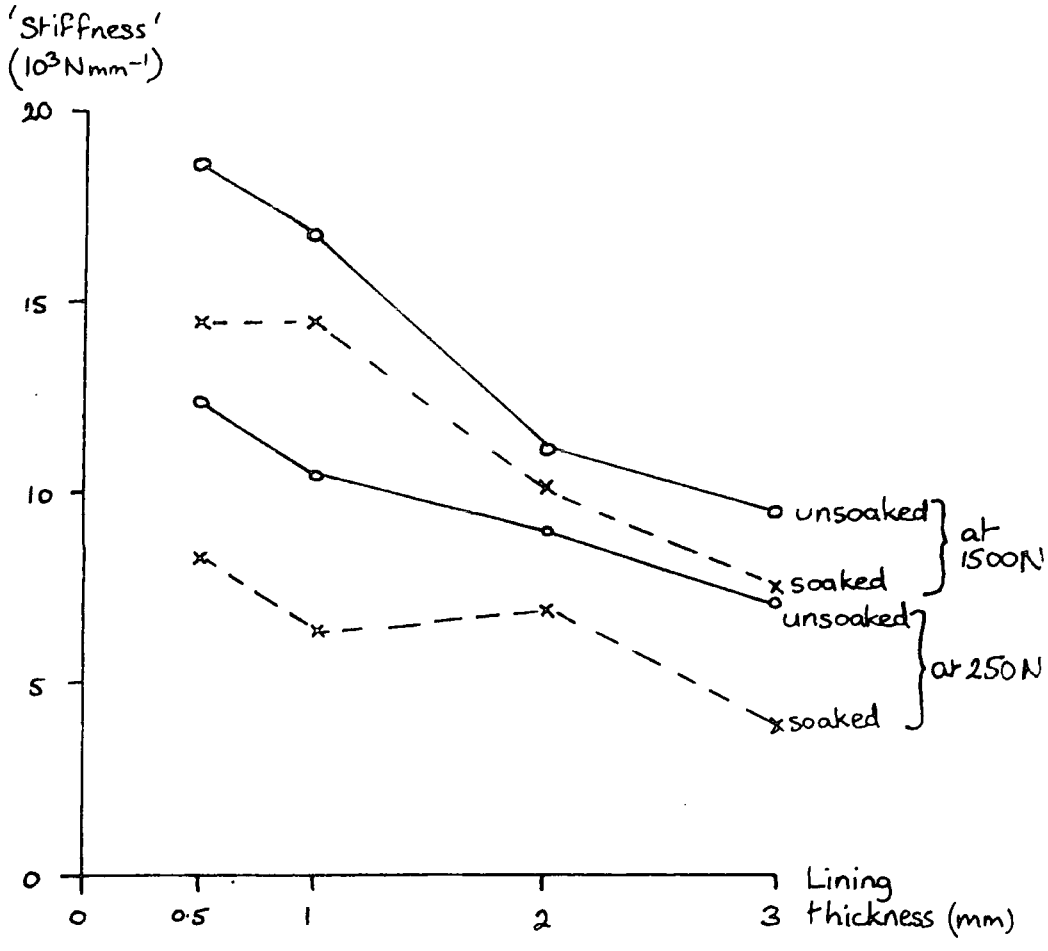

Figure 8.11

'Stiffness' of unsoaked and silicone fluid soaked acetabula against lining thickness.

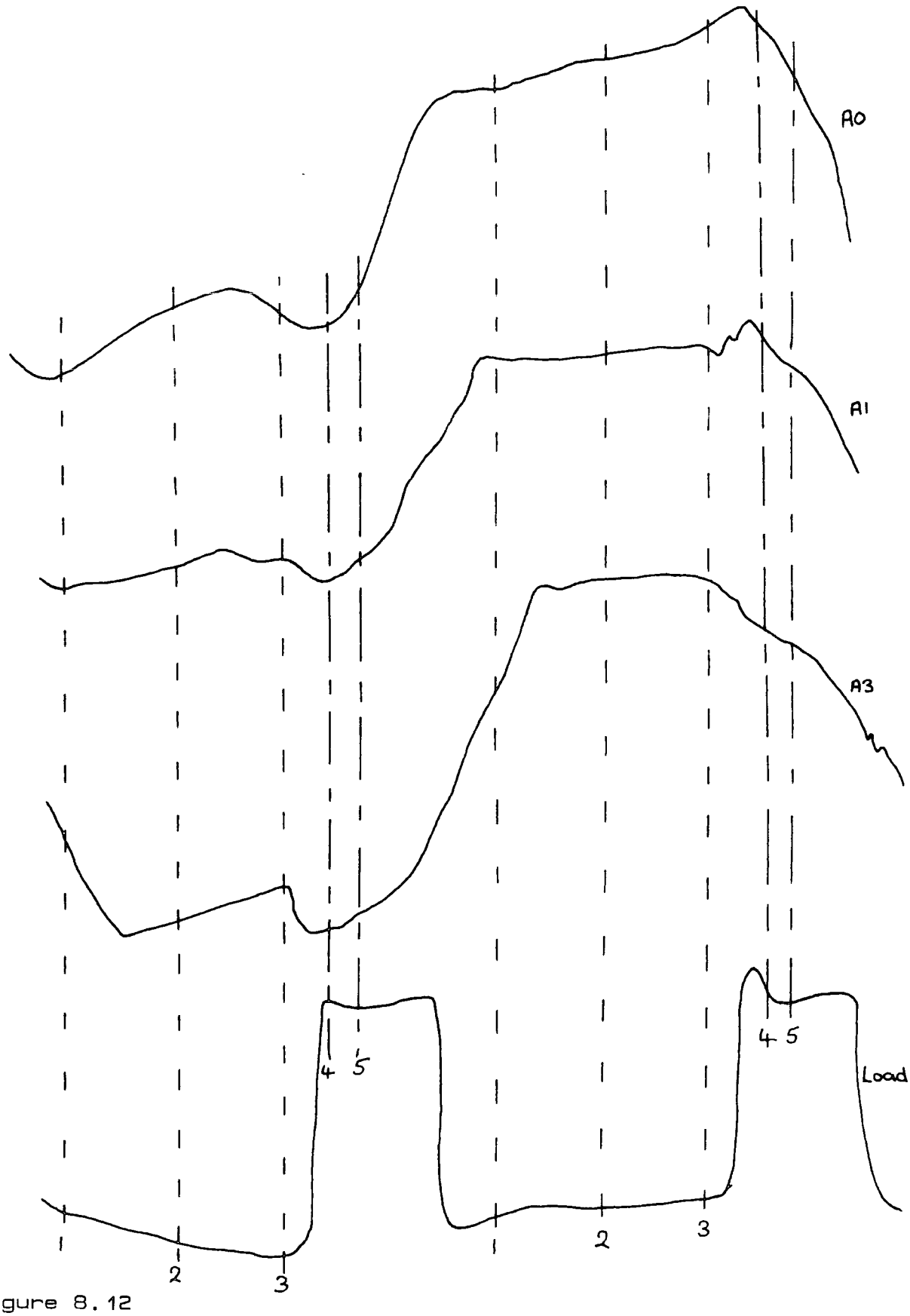

Figure 8.12

Typical traces obtained for frictional torque.

CHAPTER NINE

CONCLUSIONS

This work has shown that the hip function simulator can be used for testing both natural and artificial hip joints and their lubricants. The human hip joints were tested with both natural and synthetic lubricants.

The synthetic lubricants used with the human hip joints demonstrate the values of friction factor obtained over a wide range of viscosities. Silicone fluid, a Newtonian liquid, was used with viscosities from 9.4×10^{-3} Pa s up to 29.1 Pa s and the rising characteristic of friction factor with viscosity, typical of full fluid film lubrication was observed at viscosities above 0.1 Pa s. The SCMC solutions used had lower viscosities at high shear rates than the silicone fluids and consequently displayed a mixed lubrication mechanism in the low load region although at high loads the friction factor was almost constant. It appears that the combination of elasto-hydrodynamic, squeeze film and deformation effects at high loads lead to a friction factor almost independent of $\eta u/L$ for both natural joints and elastomeric lined prostheses.

The addition of hyaluronic acid to synovial fluid samples produced a range of lubricants for the human joints which appeared to demonstrate fluid film lubrication

for viscosities greater than 0.025 Pa s - a viscosity which is plausible for healthy fluid.

Digestion by hyaluronidase reduced the viscosity of the synovial fluid and also increased the friction factor at low loads. This may have been caused by a transition from fluid film to mixed lubrication as the viscosity became similar to that of water. At high loads, as expected, the digestion produced no significant difference in friction factor.

Trypsin digestion of the synovial fluid did not make any significant difference to friction factor. This implies that the protein content of the synovial fluid is not solely responsible for lubrication, and that the hyaluronic acid, acting as a viscosity-raiser, plays a very important role, certainly during dynamic loading.

The work with compliant linings showed that the thinner the lining, the lower the friction factors obtained when lubricated with SCMC. A thinner lining is also less compliant and future work should consider the use of less flexible elastomers.

Future work with compliant linings must attempt to resolve the problem of the high friction factors obtained with low loads. This may be improved by the use of a stiffer elastomeric layer, or, if the technology allows it, a

thinner layer. The interaction of the silicone elastomer and silicone fluid which produced low friction factors was interesting and work based on an elastomer permeable to a water based non-Newtonian lubricant such as SCMC could lead to new possibilities for prostheses.

In considering a programme of further work on the simulator a priority would seem to be to automate the data collection and analysis. A microcomputer could be used to record the load, displacement and frictional torque from a test in a digitized form and either process the results directly or combine them with results for other lubricants to produce graphs of the form used in this thesis. This would greatly reduce the tedium and enable the analysis to be performed at more points throughout the cycle.

A further refinement would be to use the computer to control the inputs to the simulator ie to control the oscillation speed and amplitude, and the load cycle applied to the joint. This would require a major alteration of the hydraulic circuit in the simulator, but it would be very advantageous to be able to specify a loading cycle in detail. As well as producing a more refined walking cycle, the simulator could then be used for other types of loading.

One of the advantages, however, of a simplified loading cycle is the use of the averaging technique to eliminate errors caused by off-centre loading. The problems of

mounting joints centrally (particularly natural joints) must be investigated if a more complex loading cycle is to be used.

APPENDIX 1

Results for hip joint H10 tested with synovial fluid and urate crystals

This joint was used for some preliminary tests to investigate the effect of the presence of urate crystals in synovial fluid. These crystals are deposited in joints in gouty conditions and it was wondered whether they would affect the friction factor obtained.

The joint was a 70 year old female hip in good condition. It had a diameter of 46 mm.

The urate crystals were obtained from Dr P Platt at the Department of Rheumatology, Royal Victoria Infirmary, Newcastle. Two suspensions of crystals in distilled water were made: the concentrations were 10.7 mg ml^{-1} and 28.7 mg ml^{-1}. The control samples of synovial fluid had 0.1 ml distilled water added to 1.0 ml fluid. The samples of fluid plus crystals had 0.1 ml of crystal suspension added to 1.0 ml synovial fluid. Figure A1.1 shows the results obtained for point 2 [low load] and point 4 [high load]. At high loads the friction factor was generally increased by the presence of the crystals whereas at the low load, only the higher concentration of crystals increased the friction factor; the lower concentration appeared to reduce it.

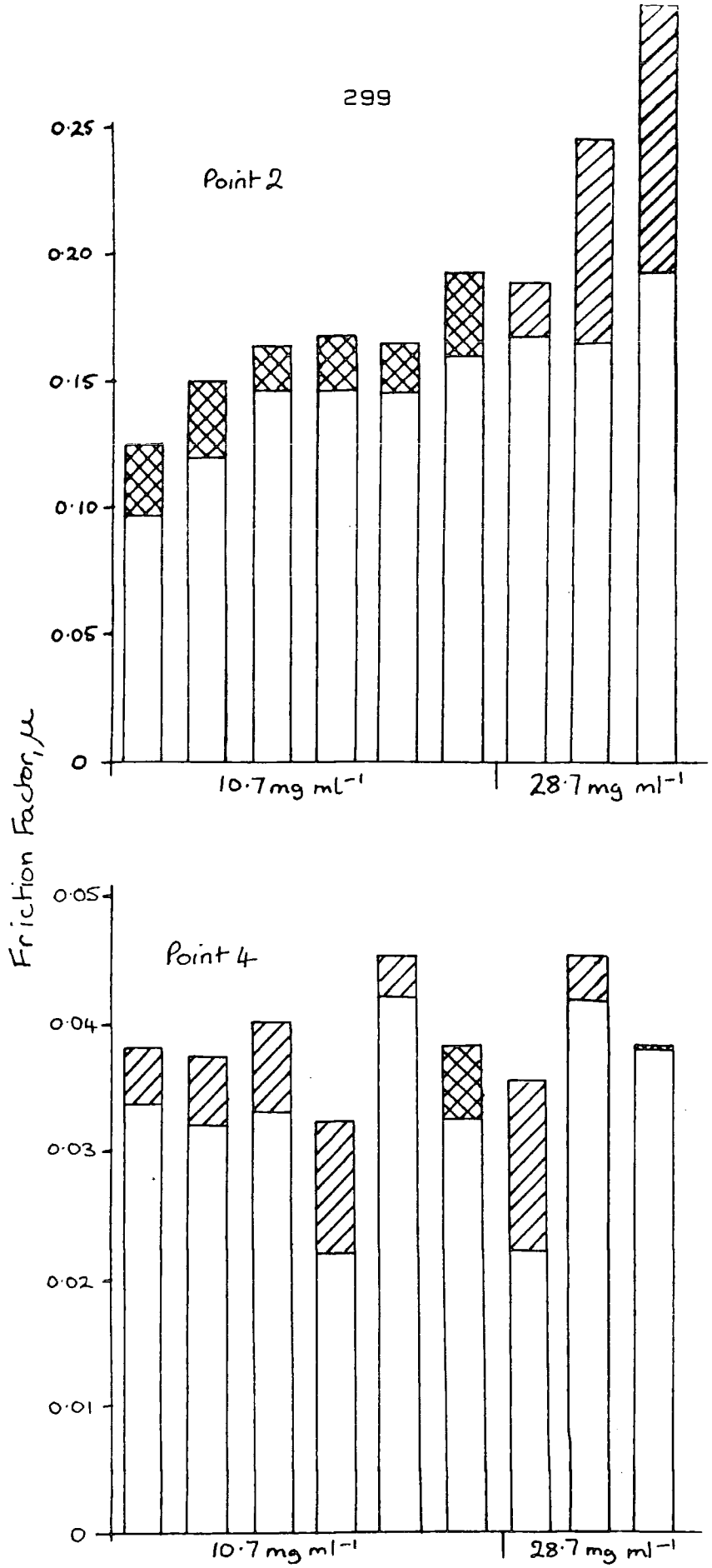

Figure A1.1

Joint H10. Lubricated by synovial fluid with and without the addition of urate crystals. Single hatching shows increase in friction factor after addition of crystals, cross hatching shows decrease.

APPENDIX 2

Effect of fininte thickness of elastomer sample on elastic modulus measured by an indentation method

Waters [1965] derived an empirical relationship for the increase in apparent elastic modulus found with indentation tests on thin samples of elastomer.

From the theory of contact of two spheres [Timoshenko and Goodier, 1951] it can be shown that, if one sphere is rigid and of radius R and the other elastic and of infinite radius,

the depth of indentation, $d_\infty = \left[\frac{81P^2}{256E^2R}\right]^{1/3}$ ... [1]

and the radius of contact, $a_\infty = R^{1/2} d_\infty^{1/2}$ ... [2]

Now if the plane elastic layer is only of depth t, the stress pattern will be distorted but can be assumed to be geometrically similar for any given ratio of t/a_t. Therefore equation [1] may be written as:

$$d_t = \left[\frac{81P^2}{256E^2R}\right]^{1/3} f\left(\frac{t}{a_t}\right) \quad \ldots [3]$$

where $f[t/a_t]$ is an unknown dimensionless function. Assuming that for small values of d_t, a_t is determined by d_t and R, equation [2] becomes:

$$a_t = R^{1/2} d_t^{1/2} \quad \ldots [4]$$

Plotting his data in the form $f[t/a_t]$ against t/a_t, Waters found that $f[t/a_t]$ was a universal function of the form:

$$f\left(\frac{t}{a_t}\right) = 1 - \exp\left[\frac{-At}{a_t}\right] \qquad \ldots [5]$$

where the constant A = 0.41 for a non-lubricated lower boundary. Substituting equations [4] and [5] in [3] gives

$$E_\infty = \frac{9PR}{16a_t^3}\left[1 - \exp\left[\frac{-At}{a_t}\right]\right]^{3/2} \qquad \ldots [6]$$

or, since

$$E_t = \frac{9PR}{16a_t^3} \qquad \ldots [7]$$

$$E_\infty = \left[1 - \exp\left[\frac{-At}{a_t}\right]\right]^{3/2} E_t \qquad \ldots [8]$$

This equation can be applied to the values of modulus obtained for the slabs of elastomer, using an average value of a_t. Table A2.1 shows the values calculated for E_∞ using the values of a_t for a total mass of 0.384 Kg loading the lens.

Joint reference	Slab thickness t [mm]	a_t [mm]	E_t [MPa]	E_∞ [MPa]
A0	3.5	3.7	2.63	0.48
A1	3.5	3.8	2.61	0.46
A2	6.5	4.2	1.72	0.55
A3	6.5	4.0	1.94	0.66
D0	6.5	4.0	2.00	0.68
Y3	6.5	4.0	2.08	0.71
Z1	6.5	3.9	2.14	0.75
D1	6.5	4.5	1.33	0.40

Table A2.1

Calculated values of E_∞ using Waters' empirical relation.

APPENDIX 3

Data collection and processing for artificial joints

Measurements taken from the traces obtained from the simulator were recorded on a data sheet, an example of which is shown in Figure A3.1. This was entered, along with other data from the same joint into a file, named for joint A2, JA2.DAT.

The program MU2.FTN, written in FORTRAN, read the data from the input file, processed it and output friction factor and $\eta u/L$ values for each lubricant into the output file MUA2.DAT. The graph plotting routine GA4.FTN requests the user to specify the joint and point number (1 - 5) required. It then selects the correct data from the appropriate output file, scales and plots it. The graphs are plotted with different symbols for the three speeds of oscillation.

D	34·9	·4983	&			A2
Lub	C10	·0028	Visc			
Speed	8	0·1	FSF			8
FA	16·5	28	24	26	28·5	
FB	26	26	30	37	35	
AL	10	6	4	42	40·5	
BL	8	8	8	41	41	
Speed	14	0·1	FSF			9
FA	28	20·5	29	33	33	
FB	19	25·5	24	23·5	27·5	
AL	9	7·5	8	41·5	41	
BL	9·5	6·5	3·5	44	43·5	
Speed	0	0·1	FSF			10
FA	27·5	28·5	22	27	28	
FB	24·5	25	26·5	33	31·5	
AL	9·5	5·5	3·5	37	36·5	
BL	8·5	8	8	41·5	41·5	

Figure A3.1

Data sheet for joint A2, lubricated with C10 [SCMC with viscosity of 0.0028 Pa s].

REFERENCES

Afoke N Y P, Byers P D, Hutton W C [1982]. A finite element study of the human hip joint. Eng in Med 11: 17 - 23.

Armstrong C G, Bahrani A S, Garner D L [1980]. Changes in the deformational behaviour of human hip cartilage with age. Trans ASME 102: 214 - 220.

Askew M J, Mow V C [1978]. The biochemical function of the collagen fibril ultrastructure of articular cartilage. J Biomech Eng 100: 105 - 115.

Barker S A, Bayyuk S H I, Brimacombe J S, Hawkins C F, Stacey M [1964]. The structure of the hyaluronic acid component of synovial fluid in rheumatoid arthritis. Clin Chim Acta 9: 339 - 343.

Barnett C H [1958]. Measurement and interpretation of synovial fluid viscosities. Ann Rheum Dis 17: 229 - 233.

Barnett C H, Cobbold A F [1962]. Lubrication within living joints. J Bone and Jt Surg 44B: 662 - 674.

Barrett A J [1972]. Hyaluronidase. In Dingle J T [ed] Lysosomes. A laboratory handbook. N Holland Pub Co.

Bennett A, Higginson G R [1970]. Hydrodynamic lubrication of soft solids. J Mech Eng Sci 12: 218 - 222.

Bitter T, Muir H M [1962]. A modified uronic acid carbazole reaction. Analy Biochem 4: 330 - 334.

Burck P J [1970]. Pancreatic secretory trypsin inhibitors. In Perlmann C E, Lorand L[eds] Enzymology XIX Academic Press 1970:907.

Chandra P [1980]. Synovial joint lubrication: A review. Nat Acad of Sci, India: Golden Jubilee Commemoration Vol.

Charnley J [1959]. The lubrication of animal joints. Symp on Biomech. London [I Mech E] 12 - 19.

Charnley J [1960a]. The lubrication of animal joints in relation to surgical reconstruction by arthroplasty. Ann Rheum Dis 19: 10 - 19.

Charnley J [1960b]. How our joints are lubricated. Triangle 4: 5: 175 - 179.

Clarke I C [1971]. Human articular surface contours and related surface depression frequency studies. Ann Rheum Dis 30: 15 - 23.

Clarke I C, Contini R, Kenedi R M [1975]. Friction and wear studies of articular cartilage: A scanning electron microscope study. J Lubn Tech July: 358 - 368.

Clish J [1979]. The effect of surface roughness on the coefficient of friction for a lubricated compliant material. M Sc thesis University of Durham.

Collins D H [1949]. The pathology of articular and spinal diseases. 74 - 115. Arnold, London.

Cooke A F, Dowson D, Wright V [1978a]. The rheology of synovial fluid and some potential synthetic lubricants for degenerate synovial joints. Eng in Med 7: 66 - 72.

Cooke A F, Dowson D, Wright V [1978b]. The pressure-viscosity characteristics of synovial fluid. Biorheology 15: 129 - 135.

Davies D V [1966 - 7] Properties of synovial fluid. Proc Inst Mech Eng 181: 3J: 25 - 29.

Davis W H, Lee S L, Sokoloff L [1978]. Boundary lubricating ability of synovial fluid in degenerative joint disease. Arthritis and Rheumatism 21: 7: 754 - 760.

Davis W H, Lee S L, Sokoloff L [1979]. A proposed model of boundary lubrication by synovial fluid: Structuring of boundary water. J Biomech Eng 101: 185 - 192.

Dintenfass L [1966 - 7]. Current status of joint lubrication. Proc Inst Mech Engrs 181: 3J: 142 - 145.

Dow Corning [1978]. Information about electrical/electronic materials. Bulletin 61-113A-01.

Dowson D [1966 - 7]. Modes of lubrication in human joints. Proc Inst Mech Engrs 181: 3J: 45 - 54.

Dowson D, Longfield M D, Walker P S, Wright V [1967]. An investigation of the friction and lubrication in human joints. Proc Inst Mech Engrs 182: 70.

Dowson D, Unsworth A, Wright V [1970]. Analysis of 'Boosted lubrication' in human joints. J Mech Eng Sci 12: 364 - 369.

Dowson D, Wright V [1972]. The lubrication of human joints. In Kenedi R M [ed] Proc Symp Perspectives in Biodmedical Eng 103 - 107. McMillan.

Dowson D [1979]. History of Tribology. 339. London, Longman.

Edwards J [1967]. Physical characteristics of articular cartilage. Proc Instn Mech Engrs 181: 3J: 16 - 24.

English T A, Kilvington M [1979]. In vivo records of hip loads using a femoral implant with telemetric output [a preliminary report]. Biomed Eng 1: 2: 111 - 115.

Fein R S [1966 - 7]. Are synovial joints squeeze film lubricated? Proc Inst Mech Eng 181: 3J: 125 - 128.

Freeman M A R [ed] [1979]. Adult articular cartilage. Pitman Medical.

Gaman I D C, Higginson G R, Norman R [1974]. Fluid entrapment by a soft surface layer. Wear 28: 345 - 352.

Gardner D L [1972]. The influence of microscopic technology on knowledge of cartilage surface structure. Ann Rheum Dis 31: 235.

Gore D [1981]. Mechanical properties of articular cartilage - variation with depth. Ph D thesis, University of Durham.

Gore T A, Flynn M, Stevens T [1979]. Measurement and analysis of hip joint movements. Eng in Med 8: 1: 21 - 25.

Gore T A [1980]. The kinematics of normal and pathological hip joints. Ph D thesis, University of Durham.

Gore T A, Higginson G R, Kornberg R E [1981]. Some evidence of squeeze-film lubrication in hip prostheses. Eng in Med 10: 2: 89 - 95.

Greenwald A S, O'Connor J J [1971]. The transmission of load through the human hip joint. J Biomech 4: 507.

Hamerman D, Schubert M [1962]. Diarthroidal joints, an essay. J Med 33: 555.

Higginson G R, Norman R [1974]. The lubrication of porous elastic solids with reference to the functioning of human joints. J Mech Eng Sci 16: 4: 250 - 257.

Higginson G R [1977]. Elastohydrodynamic lubrication in human joints. Proc I Mech E 191: 33: 217 - 223.

Higginson G R, Snaith J E [1979]. The mechanical stiffness of articular cartilage in confined oscillating compression. Eng in Med 8: 1: 11 - 14.

Holmes W F, Keefer C S, Myers W K [1935]. Anti-tryptic activity of synovial fluid in patients with various types of arthritis. J Clin Invest 14: 124 - 130.

Homsy C A, Stanley R F, King J W [1973]. 'Pseudosynovial fluids based on soduim carboxymethylcellulose' in Gabelnick H L, Litt M [eds] 'Rheology of biological systems' 278 - 298. Springfield, Illinois.

Jebens E H, Monk-Jones M E [1959]. On the viscosity and pH of synovial fluid and the pH of blood. J Bone Jt Surg 41B: 388 - 400.

Johnson G R, Dowson D, Wright V [1975]. A new approach to the determination of the elastic modulus of articular cartilage. Ann Rheum Dis 34: 116 - 117.

Jones E S [1934]. Joint lubrication. The Lancet 1: 1426 - 1427.

Jones E S [1936]. Joint lubrication. The Lancet 1: 1043 - 1044.

Kassell B, Radicevic M, Berlow S, Peansky R J, Laskowski M [1963]. The basic trypsin inhibitor of bovine pancreas. J Biol Chem 238: 10: 3274 - 9.

Kempson G E, Freeman M A R, Swanson S A V [1971]. The determination of a creep modulus for articular cartilage from indentation tests on the human femoral head. J Biomech 4: 239.

Kempson G E [1979]. Mechanical properties of articular cartilage. In Freeman M A R [ed] 'Adult articular cartilage'. Pitman Medical.

Kenyon D E [1980]. A model for surface flow in cartilage. J Biomech 13: 129 - 134.

Lamoureux L W [1971]. Kinematic measurements in the study of human walking. Bulletin of Prosthesis Res BPR 10 - 15 Spring: 3 - 84.

Lewis P R, McCutchen C W [1959]. Experimental evidence for weeping lubrication in mammalian joints. Nature 184: 1285.

Libby W F, Berger R, Mead J F, Alexander G V, Ross J F [1964]. Replacement rates for human tissue from atmospheric radiocarbon. Science 146: 1170.

Ling F F [1974]. A new model of articular cartilage in human joints. J Lubn Tech 449 - 507.

Linn F C [1967]. Lubrication of animal joints I. The arthrotripsometer. J Bone and Jt Surg 49-A: 6: 1079 - 1098.

Linn F C [1968]. Lubrication of animal joints II. The mechanism. J Biomech 1: 193 - 205.

Linn F C, Radin E L [1968]. Lubrication of animal joints III. The effect of certain chemical alterations of the cartilage and lubricant. Arthritis and Rheumatism 11: 5: 674 - 682.

Linn F C [1969]. Lubrication of animal joints. J Lubn Tech April: 329 - 341.

Little T, Freeman M, Swanson A [1969]. Experiments on friction in the human hip joint. In Wright V [ed] Lubrication and wear in joints. 110 - 114. Sector Pub Inc.

Longfield M D, Dowson D, Walker P S, Wright V [1969]. 'Boosted lubrication' of human joints by fluid enrichment and entrapment. Bio Med Eng November: 517 - 522.

McCall J G [1969]. Load deformation response of the micro-structure of articular cartilage. 39. In Wright V [ed], Lubrication and wear in joints. Sector, London.

MacConnaill M A [1932]. The function of intra-articular fibrocartilages with special reference to the knee and inferior radio-ulner joints. J Anatomy 66: 210 - 227.

McCutchen C W [1959]. Sponge-hydrostatic and weeping bearings. Nature 184: 1284.

McCutchen C W [1966 - 7]. Physiological lubrication. Proc Instn Mech Engrs 181: 3J: 55 - 62.

McCutchen C W [1972]. A note on weeping lubrication. In Kenedi R M [ed] Proc Symp Perspectives in Biomedical Eng. 109. McMillan.

Maroudas A [1966 - 7]. Hyaluronic acid flims. Proc Instn Mech Engrs 181: 3J.

Maroudas A, Bullough P G, Swanson S A V, Freeman M A R [1968]. The permeability of articular cartilage. J Bone Jt Surg 50B: 166 - 177.

Maroudas A [1979]. Physico-chemical properties. In Freeman M A R [ed] Adult articular cartilage. 157. Pitman, London.

Medley J B, Strong A B, Pilliar R M, Wong E W [1980]. The breakdown of fluid film lubrication in elastic-isoviscous point contacts. Wear 63: 25 - 40.

Meyer K, Smyth E M, Dawson M H [1939]. The isolation of a mucopolysaccharide from synovial fluid. J Biol Chem 128: 319 - 327.

Meyer K [1947]. The biological significance of hyaluronic acid and hyaluronidase. Physiol Rev 27: 3: 335.

Meyer K [1958]. The chemical structure of hyaluronic acid. Fed Proc 17: 1070.

Minns R J, Stevens F S [1976]. The collagen fibril organisation in human articular cartilage. J Anat 121: 437.

Mow V C [1969]. The role of lubrication in biomechanical joints. J Lubn Tech April: 320 - 8.

Muddeman J M [1980]. Lubrication of hip joints with soft layers using non-Newtonian fluids. Final year project, Department of Engineering, University of Durham.

Muir H, Bullough P, Maroudas A[1970]. The distribution of collagen in human articular cartilage with some of its physiological implications. J Bone Jt Surg 52B: 554.

Negami S [1964]. Dynamic mechanical properties of synovial fluid. M Sc thesis, Lehigh University, Bethlehem, Pennsylvania.

Ogston A G, Stanier J E [1950]. On the state of hyaluronic acid in synovial fluid. Biochem J 46: 364 - 376.

Ogston A G, Stanier J E [1952]. Further observations on the preparation and composition of the hyaluronic acid complex of ox synovial fluid. Biochem J 52: 149 - 156.

Ogston A G, Stanier J E [1953]. Some effects of hyaluronidase on the hyaluronic acid of ox synovial fluid and their bearing on the investigation of pathological fluids. J Physiol 119: 253 - 258.

Ogston A G, Sherman T F [1959]. Degradation of the hyaluronic acid complex of synovial fluid by proteolytic enzymes and by ethylenediaminetetra-acetic acid. J Biochem 72: 301 - 305.

O'Kelly J, Unsworth A, Dowson D, Jobbins B, Wright V [1977]. Pendulum and simulator for studies of friction in hip joints. In Dowson D, Wright V [eds] Evaluation of artificial joints. Biol Eng Soc London.

O'Kelly J, Unsworth A, Dowson D, Hall D A, Wright V [1978]. A study of the role of synovial fluid and its constituents in the friction and lubrication of human hip joints. Eng in Med 7: 2: 73 - 83.

O'Kelly J, Unsworth A, Dowson D, Wright V [1979]. An experimental study of friction and lubrication in hip prostheses. Eng in Med 8: 3: 153 - 159.

Paul J P [1966 - 7]. Forces transmitted by joints in the human body. Proc Instn Mech Engs 181: 3J.

Pigman W, Rizvi S [1959]. Hyaluronic acid and the ORD reaction. Biochem and Biophys Res Commun 1: 39 - 43.

Radin E L, Paul I L, Pollock D [1970]. Animal joint behaviour under excessive loading. Nature 226: 554 - 5.

Radin E L, Swann D A, Weisser P A [1970]. Separation of a hyaluronate-free lubricating fraction from synovial fluid. Nature 228: 377 - 378.

Radin E L, Paul I L, Swann D A, Schottstaedt E S [1971]. Lubrication of synovial membrane. Ann Rheum Dis 30: 322 - 325.

Radin E L, Paul I, Weisser P [1971]. Joint lubrication with artificial lubricants. Arth and Rheum 14: 126 - 129.

Radin E L, Paul I L [1972]. A consolidated concept of joint lubrication. J Bone Jt Surg 54-A: 3: 607 - 616.

Reynolds O [1886]. On the theory of lubrication and its application to Mr Beauchamp Towers' experiments. Phil Trans Roy Soc 177: 157.

Roberts A D [1971]. Squeeze films between rubber and glass. J Phys D: Appl Phys 4: 423 - 432.

Roberts B J, Unsworth A, Mian N [1982]. Modes of lubrication in human hip joints. Ann Rheum Dis 41: 217 - 224.

Ropes M W, Rossmeisl E C, Bauer W [1940]. The origin and nature of normal human synovial fluid. J Clin Invest 19: 795 - 799.

Ropes M W, Peabody R B, Bauer W, Robertson W B, Rossmeisl E C.[1947]. Synovial fluid mucin. Acta Med Scand Suppl 196: 700 - 744.

Rybicki E F, Glaeser W A, Strenkowski J S, Tamm M A [1979]. Effects of cartilage stiffness and viscosity on a nonporous compliant bearing lubrication model for living joints. J Biomech 12: 403 - 409.

Sandson J, Hamerman D, Schuster H, William L A [1962]. Isolation of hyaluronate protein from human synovial fluid. J Clin Invest 41: 1817 - 1830.

Sayles R S, Thomas T R.[1979]. Measurement of the surface microgeometry of articular cartilage. J Biomech 12: 257 - 267.

Scher I, Hamerman D [1972]. Isolation of human synovial-fluid hyaluronate by density-gradient ultracentrifugation and evaluation of its protein content. Biochem J 126: 1073 - 1080.

Silpananta P, Dunstone J R, Ogston A G [1968]. Fractionation of a hyaluronic acid preparation in a density gradient. Some properties of the hyaluronic acid. Biochem J 109: 43 - 50.

Swann D A, Radin E L [1972]. The molecular basis of articular lubrication 1. Purification and properties of a lubricating fraction from bovine synovial fluid. J Biol Chem 247: 24: 8069 - 8073.

Swann D A, Radin E L, Nazimiec M, Weisser P A, Curran N, Lewinnek G [1974]. Role of hyaluronic acid in joint lubrication. Ann Rheum Dis 33: 318 - 326.

Swann D A, Sotman S, Dixon M, Brooks C [1977]. The isolation and partial characterization of the major glycoprotein (LGP-1) from the articular lubricating fraction from bovine synovial fluid. Biochem J 161: 473 - 485.

Swanson S A V [1979]. Lubrication. In Freeman M A R [ed] Adult articular cartilage. 257. Pitman, London.

Tandon P N, Rakesh L [1981]. Effects of cartilage roughness on the lubrication of human joints. Wear 70: 29 - 36.

Tanner R I [1966]. An alternative mechanism for the lubrication of synovial joints. Phys Med Biol 11:1: 119 - 127.

Thomas T R, Sayles R S, Haslock I [1980]. Human joint performance and the roughness of articular cartilage. J Biochem Eng 102: 50 - 56.

Thompson J C [1979]. Frictional characteristics of artificial human hip joints with soft elastic layers. Ph D Thesis, University of Durham.

Timoshenko S, Goodier J N [1951]. Theory of elasticity. McGraw Hill, New York.

Unsworth A, Dowson D, Wright V [1975a]. The frictional behaviour of human synovial joints - Pt I: Natural joints. J Lubn Tech July: 369 - 376.

Unsworth A, Dowson D, Wright V, Koshal D [1975b]. The frictional behaviour of human synovial joints - Pt II: artificial joints. J Lubn Tech 377 - 382.

Unsworth A [1978]. The effects of lubrication in hip joint prostheses. Phys Med Biol 23: 2: 253 - 268.

Walker P S, Dowson D, Longfield M D, Wright V [1968]. 'Boosted lubrication' in synovial joints by fluid entrapment and enrichment. Ann Rheum Dis 27: 6: 512 - 520.

Walker P S, Sikorski J, Dowson D, Longfield M D, Wright V, Buckley T [1969a]. Behaviour of synovial fluid on surfaces of articular cartilage. A scanning electron microscope study. Ann Rheum Dis 28: 1.

Walker P S, Dowson D, Longfield M D, Wright V [1969b]. Rheological behaviour of human joints. Sonderdruck aus Rheologica Acta 8: 234 - 239.

Walker P S, Sikorski J, Dowson D, Longfield M D, Wright V [1970a]. Features of the synovial fluid film in human joint lubrication. Nature 225: 956 - 957.

Walker P S, Unsworth A, Dowson D, Sikorski J, Wright V [1970b]. Mode of aggregation of hyaluronic acid protein complex on the surface of articular cartilage. Ann Rheum Dis 29: 591 - 602.

Waters N E [1965]. The indentation of thin rubber sheets by spherical indentors. Brit J Appl Phys 16: 557 - 563.

Wilkins J F [1968]. Proteolytic destruction of synovial boundary lubrication. Nature 219: 1050 - 1051.

Wright V, Dowson D, Kerr [1973]. The structure of joints. Int Rev Connective Tissue Res 8: 105 - 125.